



Etudes des mécanismes associés à la qualité et la durabilité de la réponse vaccinale

Matthieu van Tilbeurgh

► To cite this version:

Matthieu van Tilbeurgh. Etudes des mécanismes associés à la qualité et la durabilité de la réponse vaccinale. Vaccinologie. Université Paris-Saclay, 2022. Français. NNT: 2022UPASQ052 . tel-04839405

HAL Id: tel-04839405

<https://theses.hal.science/tel-04839405v1>

Submitted on 16 Dec 2024

HAL is a multi-disciplinary open access archive for the deposit and dissemination of scientific research documents, whether they are published or not. The documents may come from teaching and research institutions in France or abroad, or from public or private research centers.

L'archive ouverte pluridisciplinaire **HAL**, est destinée au dépôt et à la diffusion de documents scientifiques de niveau recherche, publiés ou non, émanant des établissements d'enseignement et de recherche français ou étrangers, des laboratoires publics ou privés.

Etudes des mécanismes associés à la qualité et la durabilité de la réponse vaccinale

Study of quality and durability of vaccine immune response associated mechanisms

Thèse de doctorat de l'université Paris-Saclay

École doctorale n°569, Innovation thérapeutique, du fondamental à l'appliqué (IFTA)

Spécialité de doctorat : Immunologie

Graduate School : Santé et médicaments. Référent : Faculté de pharmacie

Thèse préparée dans l'unité de recherche **ImVA-HB (Université Paris-Saclay, Inserm, CEA)**
sous la direction de **Roger LE GRAND**

Thèse soutenue à Fontenay-aux-Roses, le 30 novembre 2022 par

Matthieu VAN TILBEURGH

Composition du Jury

Véronique GODOT	Rapporteure
Directrice de recherche, Professeure des universités, Université Paris-Est Créteil	
Rodolphe Thiebaut	Rapporteur
Professeur des universités-praticien hospitalier, Directeur de recherche, SISTM U 1219 INSERM, Université de Bordeaux	
Sylvie CHOLLET-MARTIN	Examinateuse
Professeure des universités – praticienne hospitalière, INSERM UMR996, Université Paris-Saclay	
Sabine RIFFAULT	Examinateuse
Directrice de recherche USC-EA3671, Université de Paris Saclay	
Hélène DUTARTRE	Examinateuse
Chargée de recherche Inserm U1111-CNRS-UMR5308-ENS de Lyon- University	
Roger LE GRAND	Directeur de thèse
Directeur de recherche, UMR1184, Université Paris-Saclay, CEA, Inserm, Fontenay-aux-roses	

Membres invités aux côtés du jury pour assister à la soutenance :

Pascal BLANC
PhD, SANOFI, Marcy l'Etoile
Pauline MAISONNASSE
PhD, CEA Fontenay-aux-roses

Invité

Invitée

REMERCIEMENTS

Tout d'abord, je voudrais remercier la Pr. Véronique Godot ainsi que le Pr. Rodolphe Thiébaut pour avoir pris le temps de rapporter cette thèse et de l'avoir enrichie de leurs commentaires.

Je voudrais également remercier la Pr. Sylvie Chollet-Martin, Mme Sabine Riffault et Mme Hélène Dutartre d'avoir accepté de faire partie du jury en tant qu'examinatrices.

Merci à Roger qui m'a accueilli au sein de l'unité et qui malgré sa position au sein du laboratoire a su se rendre disponible et trouver le temps de m'encadrer tout au long de cette thèse. Merci pour votre soutien et votre confiance pour ces 4 années.

A Pauline, pour m'avoir proposé ce stage de M2 où tout a commencé et pour avoir réussi à me convaincre que faire une thèse était dans mes capacités, merci ! Merci pour ton soutien, ta bonne humeur et tes conseils.

Merci à toute l'équipe de Sanofi ayant participé à ce projet. Merci pour vos conseils et votre aide sur la réalisation de cette étude et l'analyse. Je remercie tout particulièrement Pascal pour son implication dans la correction de ce manuscrit malgré l'urgence et les délais très courts.

TABLE DES MATIERES

REMERCIEMENTS	2
TABLE DES MATIERES	3
LISTE DES FIGURES.....	6
LISTE DES TABLEAUX.....	7
LISTE DES ABREVIATIONS	8
AVANT-PROPOS	10
A. INTRODUCTION.....	12
I. Orientation de la réponse vaccinale par l'immunité innée.....	12
1) La détection des pathogènes	12
2) La présentation antigénique : interactions de l'immunité innée et adaptative	15
3) Orientation de la réponse immunitaire par les cellules dendritiques	16
a) Les cellules dendritiques de la lignée myéloïde	17
i. Les cellules de Langerhans	17
ii. Les cDC1	18
iii. Les cDC2	19
iv. Les cellules dendritiques plasmacytoïdes (pDC)	20
v. Les cellules dendritiques dérivées des monocytes (moDC)	21
b) Les cellules dendritiques folliculaires (FDC)	23
4) Cibler les cellules présentatrices d'antigène pour orienter les réponses vaccinales..	24
a) Orientation de la réponse vaccinale par les adjuvants	24
b) Orientation de la réponse vaccinale en fonction des voies d'injection	25
II. Rôle des lymphocytes T CD4 dans l'orientation et la qualité des réponses vaccinales ..	25
1) Sélection, activation et migration des cellules T CD4 spécifiques	25
a) Circulation des cellules dans les ganglions.....	25
b) Interface innée/adaptatif : la synapse immunologique	27
2) Les différentes sous-populations de lymphocytes T CD4	29
a) Les lymphocytes auxiliaires de type 1 (Th1).....	30
b) Les lymphocytes auxiliaires de type 2 (Th2).....	31
c) Les lymphocytes auxiliaires de type 9 (Th9).....	32
d) Les lymphocytes auxiliaires de type 17 (Th17).....	32
e) Les lymphocytes auxiliaires de type 22 (Th22).....	32
f) Les lymphocytes auxiliaires régulateurs.....	33

g) Les lymphocytes T auxiliaires folliculaires (Tfh)	34
h) Plasticité des sous-populations de lymphocytes T CD4+	37
3) Maturation des réponses B : un mécanisme de haute interaction entre l'immunité innée et adaptative	38
4) Un rôle central dans les réponses vaccinales.....	40
III. Persistance de la réponse vaccinale : la mémoire adaptative	41
1) Génération de la mémoire adaptative.....	41
2) Les différentes sous-population de lymphocytes mémoires	42
3) Les modèles de différenciation des LT mémoires.....	45
a) Le modèle de différenciation linéaire	45
b) Le modèle de différenciation divergente.....	46
c) Le modèle de différenciation progressive.....	46
d) Compléments et variantes aux modèles.....	47
4) Paramètres influant sur la mise en place de la mémoire T	48
a) La fréquence des lymphocytes T mobilisés lors de la réponse immunitaire	48
b) L'existence de LT CD4+ mémoires spécifiques avant la rencontre avec le pathogène	48
c) La signalisation via le TCR.....	49
d) Rôle des molécules de co-stimulation.....	51
e) La signalisation par les cytokines	52
f) Épigénétique de la mémoire des LT CD4.....	53
g) Rôle de la phase de contraction.....	54
5) Paramètres de maintien et d'homéostasie de la mémoire des LT	55
6) Un rôle potentiel de la mémoire innée dans le maintien de réponses protectrices ..	57
IV. La biologie des systèmes comme outils d'exploration et de compréhension des mécanismes de la réponse vaccinale	57
1) La vaccinologie des systèmes.....	57
2) Application de la vaccinologie des systèmes pour améliorer et accélérer le design de candidat vaccin.....	59
B. PROJET DE RECHERCHE	62
I. Objectifs	62
II. Modèles expérimentaux	64
1) Modèle primate non humain (PNH).....	64
2) Modèles vaccinaux.....	66
a) ConM SOSIP.v7 comme plateforme vaccinale contre le VIH	66
b) Vaccin anti-Amaril ou vaccin contre le virus de la fièvre jaune : le « gold standard » de la vaccination.....	67

3) Technologies	70
a) Cytométrie de masse.....	70
b) Analyse et modèle statistique	71
C. RESULTATS	73
I. Innate cell markers that predict anti-HIV neutralizing antibody titers in vaccinated macaques	73
II. Identification de biomarqueurs précoce associés à la réponse neutralisante à long terme du vaccin contre le virus de la fièvre jaune	110
1) Caractérisation de la réponse LT CD4+ précoce.....	110
2) Analyses complémentaires	149
D. DISCUSSION ET PERSPECTIVES	150
I. Limites expérimentales	150
1) Le modèle PNH.....	150
2) La cytométrie de masse	150
3) Marquage in vivo de la prolifération cellulaire induite par les vaccins.....	151
4) Stimulation ex vivo avec le virus vaccinal vivant purifié	152
II. Discussion des données observées	152
III. Perspectives	157
BIBLIOGRAPHIE	160
ANNEXE.....	200

LISTE DES FIGURES

Figure 1: Impact de la vaccination sur la réduction de la mortalité contre les 10 pathogènes inclus dans le «Vaccine Impact Modelling Consortium (VIMC)».....	11
Figure 2: Orientation de la réponse adaptative par les cellules présentatrices d'antigènes.....	22
Figure 3 : Structure interne et circulation des cellules dans un ganglion lymphatique...	27
Figure 4 : Organisation de la synapse immunologique.	29
Figure 5 : Diversité des sous-populations de lymphocytes T CD4.....	30
Figure 6 : Schéma récapitulatif des différentes interactions intervenant dans la maturation des lymphocytes B par les Tfh.....	36
Figure 7 : Dynamique des processus de maturation et de sélection des cellules B au sein des centres germinatifs.	40
Figure 8 : Distribution des lymphocytes mémoire dans les différents tissus humain.	44
Figure 9 :Modèles de différenciation des cellules mémoires.....	47
Figure 10: Facteurs déterminants la différenciation des sous populations de cellules mémoires.....	50
Figure 11: Impact des cytokines sur la différenciation et le maintien des lymphocytes T CD4 mémoires.....	52
Figure 12: La vaccinologie des systèmes : de l'individu à la cellule.....	59
Figure 13: Pertinence des macaques cynomolgus comme modèles préclinique dans le cadre de la vaccination fièvre jaune.	65
Figure 14: Schéma du génome du virus de la fièvre jaune.	67
Figure 15: Schéma descriptif du processus d'atténuation du virus de la fièvre jaune sauvage (souche Asibi).	68
Figure 16: Schéma du cycle cellulaire du virus de la fièvre jaune.	69
Figure 17: Principe de fonctionnement de la cytométrie de masse.....	71
Figure 18: Schéma descriptif du mécanismes d'incorporation de la 5-Iodo-2'-deoxyuridine (IdU).....	111

LISTE DES TABLEAUX

Table 1 : Diversité des motifs de reconnaissance de motifs moléculaires (PRR) des pathogènes.....	15
---	----

LISTE DES ABREVIATIONS

APC: cellule présentatrice d'antigène	OLII: Organes lymphoïdes secondaires
BCR: récepteur des cellules B	PAMPs: motifs moléculaire associés aux pathogènes
cDC: cellule dendritique conventionnelle	PNH: primate non humain
CLR: récepteurs de type lectine-C	PRR: récepteurs de motifs moléculaires
CMH: complexe majeur d'histocompatibilité	RLR: récepteurs de type RIG-1
DC: cellule dendritique	SI: Synapse immunologique
DZ: zone sombre	SPADE: Spanning-tree Progression Analyses of Density-normalized Events algorithm
FDC: cellule dendritique folliculaire	Tcm: cellule T centrale mémoire
GC: centre germinatif	TCR: récepteur des cellules T
HEV: veinules endothéliales	Tem: cellule T effectrice mémoire
HLA: human leukocyte antigen	Temra: effecteur mémoire terminal
HMS: Hyper mutation somatique	Tfh: Lymphocytes T folliculaire
IC: Complexe immun	Th: lymphocyte T auxiliaire
LB: Lymphocyte B	TLR: Récepteurs de type Toll
LB: lymphocyte B	Treg: Lymphocyte T régulateur
LC: cellule de Langerhans	Trm: T résidente mémoire
LPS: lipopolysaccharide	Tscm: cellule T souche mémoire
LT: Lymphocytes T	VIH: virus de l'immunodéficience humaine
LTC: lymphocyte T CD8 cytotoxique	YFV: Virus de la fièvre jaune
LZ: zone claire	
MPLA: monophosphoryl lipide A	

La vaccination selon Louis Pasteur : « Inoculer des virus affaiblis ayant le caractère de ne jamais tuer, de donner une maladie bénigne qui préserve de la maladie mortelle. »

La vaccination selon le dictionnaire Larousse : Substance d'origine microbienne (microbes vivants atténués ou tués, substances solubles) qui, administrée à un individu ou à un animal, lui confère l'immunité à l'égard de l'infection déterminée par les microbes mêmes dont elle provient et parfois à l'égard d'autres infections.

La vaccination selon l'OMS : La vaccination est un moyen simple, sûr et efficace de se protéger des maladies dangereuses, avant d'être en contact avec ces affections. Elle utilise les défenses naturelles de l'organisme pour créer une résistance à des infections spécifiques et renforcer le système immunitaire.

AVANT-PROPOS

Depuis l'utilisation des premiers vaccins, les méthodes de développement n'ont cessé d'évoluer pour en améliorer la diversité, l'efficacité et la sécurité. De ce fait, aujourd'hui les vaccins représentent les produits de santé parmi les plus efficaces, les plus sûrs, simple d'utilisation et ayant l'impact sanitaire le plus important sur les populations. En effet, les vaccins ont incontestablement réduit l'incidence des maladies infectieuses telles que la poliomyélite, la rougeole ou la diphtérie, voire de les éradiquer comme ce fut le cas pour la variole. Avant la COVID-19, l'OMS estimait que 2 à 3 million de décès étaient évités chaque année grâce à la vaccination.

Aujourd'hui, la progression des vecteurs de maladie et de l'urbanisation favorise l'émergence (ou la réémergence) d'épidémies dont certaines pourraient être évitées par la vaccination (Figure 1). Lutter contre ces maladies implique donc une augmentation de la couverture vaccinale à travers le monde avec des vaccins existants mais également des efforts constants dans la recherche et le développement de nouveaux vaccins.

Cependant, la vaccinologie est confrontée à un fort taux d'échec dans le développement de nouveaux vaccins efficaces. En effet, dans une étude sur 2544 projets de vaccins entre 2000 et 2020, Lo *et al.* ont estimé à 39,6% la probabilité qu'un programme vaccinal soutenu par un industriel réussisse les essais cliniques ([Lo, Siah & Wong, 2020](#)). Ce nombre chute à 6,8% sans le soutien d'un industriel. Ce taux d'échec important repose, en partie, sur notre faible compréhension des mécanismes moléculaires et cellulaires à l'origine de la mise en place et de la persistance d'une réponse vaccinale efficace. Il apparaît donc primordial d'améliorer nos connaissances de la réponse immunitaire et des différents acteurs qui la composent pour accélérer le développement de vaccins contre les maladies infectieuses émergentes ou des endémies majeures telles que la malaria, le SIDA ou la tuberculose.

Au cours de cette thèse, nous allons essayer de compléter nos connaissances des mécanismes précoce de la réponse vaccinale et de mettre en lumière des éléments pouvant aider à accélérer le développement de nouveaux vaccins.

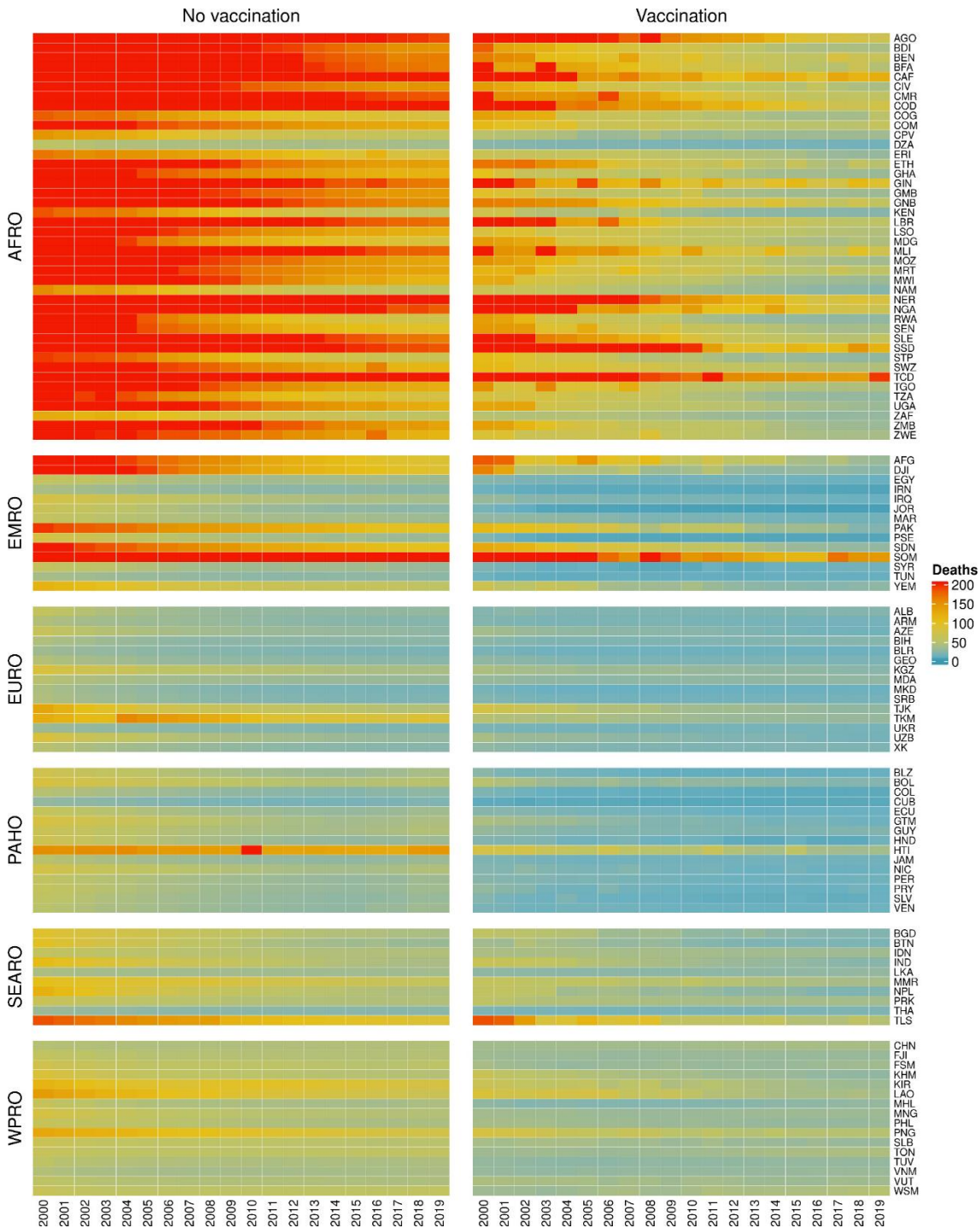


Figure 1: Impact de la vaccination sur la réduction de la mortalité contre les 10 pathogènes inclus dans le «Vaccine Impact Modelling Consortium (VIMC)». Comparaison de la mortalité moyenne prédictive par le VIMC pour 100 000 individus par habitants et par année sur la période 2000-2019 en cas de non vaccination ou de vaccination. Les 10 pathogènes inclus dans le VIMC sont l'hépatite B (HepB), Haemophilus influenzae type b (Hib), le papillomavirus humain (HPV), l'encéphalite japonnaise (JE), la rougeole, Neisseria meningitidis serogroup A (MenA), Streptococcus pneumoniae (PCV), rotavirus (Rota), la rubéole, and la Fièvre Jaune (YF). Les pays inclus dans cette étude sont ceux qui représentent la majorité des cas pouvant être évités par la vaccination et sont ordonnés selon les régions définies par l'OMS : African (AFRO), Eastern Mediterranean (EMRO), European (EURO), Pan American (PAHO), South-East Asian (SEARO), and Western Pacific (WPRO) regions. D'après (Toor et al., 2021).

A. INTRODUCTION

La mémoire est la capacité à recueillir, conserver et mobiliser une information.

Un vaccin doit permettre la mise en place d'une mémoire immunitaire dirigée contre ses composants antigéniques, lesquels sont dérivés d'un pathogène cible. La durabilité et l'efficacité sont deux paramètres critiques qui définissent la qualité d'un vaccin.

Les composants d'une formulation vaccinale, associés au calendrier vaccinal et à la voie d'immunisation contribuent au recrutement de nombreux acteurs moléculaires et cellulaires, de l'immunité innée et l'immunité adaptative qui modulent qualitativement et quantitativement la mémoire immunitaire.

I. Orientation de la réponse vaccinale par l'immunité innée

L'immunité innée est capable de percevoir le danger via l'expression de nombreux récepteur reconnaissant des motifs présents exclusivement sur les pathogènes. Elle est la première mobilisée à la suite de la pénétration d'un pathogène dans l'organisme. Elle comprend les barrières physiques protégeant l'organisme du milieu extérieur telles que la peau, les muqueuses ou la barrière hémato-encéphalique. Les cellules qui composent ces barrières (cellules épithéliales, kératinocytes) sont également impliquées dans l'induction de la réponse immune par le biais de production de médiateurs de l'inflammation et du recrutement des cellules du système immunitaire.

Le système immunitaire inné se compose également de cellules de la lignée myéloïde - les monocytes, les macrophages, les cellules dendritiques (DC, pour « dendritic cells ») et les granulocytes (éosinophiles, basophiles et neutrophiles) – ainsi que de cellules de la lignée lymphoïde comme les cellules NK (pour « Natural Killer ») et des cellules lymphoïdes innées.

1) La détection des pathogènes

Lors d'une infection ou d'une réponse vaccinale, le point de départ de la réponse immunitaire repose sur la détection de signaux de danger. Cette détection va être médiée

par des récepteurs spécifiques de motifs moléculaires (PRR, pour « pattern recognition receptor ») hautement conservés au sein de certaines classes de pathogènes (PAMP, pour « pathogen associated molecular pattern ») tels que le lipopolysaccharide (LPS) des bactéries à Gram négatives, le peptidoglycane composant la paroi des bactéries à Gram positive et négative ou encore les acides nucléiques (ADN ou ARN). En plus de la reconnaissance des pathogènes, certains PRR détectent les composés moléculaires associés aux cellules endommagées et/ou sénescentes (DAMPs, pour « Damages Associated Molecular Patterns »). L'engagement de multiples PRR permet l'intégration d'instructions spécifiques à chaque type de pathogène. La réponse immunitaire innée et son orientation sont prédéfinies et conduisent à l'activation des cellules de l'immunité, de la production de cytokines, de chimiokines, de médiateurs de l'inflammation et de chimiotaxie

La connaissance des PRR et de leur mécanismes d'action est déterminante pour en vaccinologie notamment pour le développement d'adjuvants. Les PRR peuvent être classifiés en cinq grandes catégories:

- Les récepteurs de type Toll (TLR, pour « Toll Like Receptor »), furent les premiers PRR identifiés ([Lemaitre et al., 1996](#)). Leur engagement conduit à la transcription de gènes impliqués dans la production de facteurs antiviraux et de l'inflammation ([Kumar et al., 2009](#)). Les TLR sont présents sur l'ensemble des cellules immunitaires innées et adaptatives, mais sont aussi présent sur des cellules non-immunitaires telles que les kératinocytes contribuant ainsi à l'homéostasie des tissus ([Lebre et al., 2007](#)). Les TLR se distribuent au niveau de différents compartiments cellulaires. Les TLR membranaire (TLR1, 2, 4, 5, 6 et 10) reconnaissaient les composants à la surface des pathogènes tels que le LPS ou le peptidoglycane. D'autres TLR sont localisés dans les endosomes et lysosomes (TLR3, 7, 8 et 9) et permettent la détection de composants microbiens intracellulaires, principalement les acides nucléiques ([Blasius & Beutler, 2010](#)).
- Les récepteurs de type NOD (NLR, pour « Nod Like Receptors) sont des récepteurs intracellulaires impliqués dans la reconnaissance de composés microbiens présents dans le cytoplasme. Leur engagement induit des médiateurs de l'inflammation. Les NLR les mieux documentés sont NOD1 détectant l'acide

diaminopimelique des bactéries à Gram négatives et NOD2 impliqués dans la reconnaissance du muramyl dipeptide ([Chamaillard et al., 2003; Girardin et al., 2003](#)).

- Les récepteurs de type lectine-C (CLR, pour « C-type Lectine Receptor) reconnaissent les carbohydrates présents à la surface des pathogènes bactériens ou fongiques ([de Quaglia e Silva et al., 2019; Feinberg et al., 2017; Taylor et al., 2007](#)).
- Les récepteurs de type RIG-1 (RLR pour « Rig-like receptor ») sont des récepteurs cytoplasmiques contenant un domaine hélicase permettant la détection des acides nucléiques et qui contribuent aux réponses antivirales ([Rehwinkel & Gack, 2020](#)).
- Récemment, un nouveau type de PRR a été décrit : les récepteurs absents des mélanomes de type 2 (ALR). Ces récepteurs sont impliqués dans la reconnaissance de l'ADN intracytoplasmique et contribuent à la régulation de l'apoptose ([Feng et al., 2019](#)).
- Enfin, en complément des PRR exprimés par les cellules, certains PRR sont également présents sous forme soluble retrouvées dans le sérum ([P. Zhang et al., 2015](#)). Les PRR solubles reconnaissent une large gamme de pathogènes et contribuent à leur élimination via un des fonctions telles que l'opsonisation ou l'activation du complément ou en interagissant directement avec les PRR cellulaires ([Jun & Lau, 2020](#)).

La reconnaissance des signaux de danger par ces récepteurs initie de diverses voies de signalisation, via des mécanismes de phosphorylation/déphosphorylation, lesquels aboutissent notamment à l'activation de facteurs de transcription tels que NF-kB et IRF-3, ou la cascade de signalisation conduisant à la formation de l'inflammasome. Ces processus conduisent à la production de cytokines inflammatoires, (e.g. la voie de l'IFN de type I) et au recrutement et à l'activation d'effecteurs de l'immunité innée ([D. Li & Wu, 2021; Tang et al., 2018](#)). Les différents types de PRR, leurs ligands, leur distribution ainsi que les voies de signalisation associées sont résumés dans le Tableau 1.

Tableau 1:Diversité des motifs moléculaires (PRR) des pathogènes reconnus par les PRR. La distribution cellulaire des PRR, le type de pathogène détecté et les voies de signalisation principales sont représentées. D'après (D. Li & Wu, 2021).

Items	PRR	Domains	Cellular distribution	PAMP	Sources	Signaling pathways
Toll-like receptors (TLRs)	TLR1 (TLR1-TLR2)	LRR domain-transmembrane	Mo, DC, Ma, Eo, Ba	Triacyl lipopeptide	Bacteria	Most TLRs: MyD88-dependent pathways; TLR3: TRIF-dependent pathways; TLR4: MyD88-dependent pathways and TRIF-dependent pathways
	TLR2 (TLR1-TLR2, TLR2-TLR6)	domain-TIR domain (extracellular to intracellular)	Mo, DC, Ma, Eo, Ba	Lipoteichoic acid Arabinomannan Peptidoglycan Zymosan Lipoprotein Pore protein	Bacteria Mycobacterium Bacteria Fungi Mycoplasma Neisseria	
	TLR3		Mφ, DC, IEC	dsRNA	Virus	
	TLR4 (MD-2/CD14)		Mφ, DC, Ma, Eo	Lipopolysaccharides Heat-shock proteins	Bacteria Host	
	TLR5		IEC	Flagellin	Bacteria	
	TLR6 (TLR2-TLR6)		Mo, DC, Ma, Eo, Ba	Lipoteichoic acid Peptidoglycan	Bacteria Bacteria	
	TLR7		pDC, Mφ, Eo	ssRNA Imidazoquinoline	Virus Artificially synthesized	
	TLR8		Mφ, N	ssRNA	Virus	
	TLR9		pDC, Eo, Ba	Non-methylated CpG DNA	Bacteria, Virus	
	TLR10 (human)		pDC, Eo, Ba	dsRNA	Virus	
Nucleotide-binding oligomerization domain-like receptor (NLRs)	TLR11 (mouse)		Mφ, DC	Profilin and related proteins	<i>Toxoplasma gondii</i>	
	TLR12 (mouse)		DC	Profilin and related proteins	<i>Toxoplasma gondii</i>	
	TLR13 (mouse)		Unknown	23s ribosomal RNA	Bacteria	
RIG-I-like receptors (RLRs)	NOD1	LRR domain-NBD-effector domains	IEC, cytosol of Mφ	iE-DAP	Gram negative bacteria	RIP2-TAK1-NF-κB pathways
	NOD2			MDP	Gram-negative bacteria, Gram-positive bacteria	
C-type lectin receptors (CLRs)	RIG-I	(RD)-CTD-DexD/H helicase domain-CARD	Cytosol	5'-triphosphorylated RNA, short-chain dsRNA	Virus	MAVS-TRAF6-NF-κB/TBK1 pathways
	MDA5			poly IC, long-chain dsRNA	Virus	
	LGP2			dsRNA	Virus	
Absent in melanoma-2-like receptors (ALRs)	Dectin-1	CTLD-ITAM	DC, Mφ	β-Glucan	Fungus	Tyrosine kinase-dependent and non-tyrosine kinase-dependent pathways
	Dectin-2			α-Mannan	Fungus	
Absent in melanoma-2-like receptors (ALRs)	ALRs	HIN-200-PYD	Cytosol	dsDNA	Bacteria	Inflammasome-pyroptosis

LRR leucine-rich repeat, TIR Toll/IL-1R domain, NBD nucleotide-binding domain, RD repressor domain, CTD C-terminal domain, CARD caspase activation and recruitment domain, CTLD C-type lectin-like domains, ITAM immunoreceptor tyrosine-based activation motif, PYD pyrin domain, Mo monocyte, DC dendritic cell, Ma mastocyte, Eo eosinophils, Ba basophils, pDC plasmacytoid dendritic cell, IEC intestinal epithelial cell, N neutrophil, dsRNA double-stranded RNA, ssRNA single-stranded RNA, iE-DAP γ-D-glu-meso-diaminopimelic acid, MDP muramyl dipeptide, MyD88 myeloid differentiation factor 88, TRIF TIR domain-containing adaptor protein-inducing interferon β, RIP2 receptor-interacting serine-threonine protein 2, TAK1 transforming growth factor-β-activated kinase 1, NF-κB nuclear factor κB, MAVS mitochondrial antiviral signaling protein, TRAF6 tumor necrosis factor receptor-associated factor, TBK1 TANK-binding kinase 1

2) La présentation antigénique : interactions de l'immunité innée et adaptative

Des cellules de l'immunité inné, dites cellules présentatrices d'antigène (APC), au premier rang desquels on trouve les DC, ont pour fonction de présenter des peptides endogènes ou exogènes apprêtés ou non aux lymphocytes B et T (LB et LT). La présentation des

antigènes aux cellules T implique les molécules du complexe majeur d'histocompatibilité (CMH) :

- Le CMH de classe 1 (CMH-I) permet la présentation de peptides aux LT CD8.
- Le CMH de classe 2 (CMH-II) permet la présentation de peptides aux LT CD4.

Chez l'Homme, les molécules du CMH sont aussi nommées molécules HLA (pour « Human Leukocyte Antigen »). La classe I du CMH comprend les molécules HLA-A, HLA-B et HLA-C, et la classe II du CMH les molécules HLA-DP, HLA-DQ et HLA-DR.

La cascade de signalisation amorcée par l'interaction d'un PRR avec son ligand induit une maturation synchronisée des APC. Cette maturation s'accompagne de changements phénotypiques via une augmentation de l'expression de CCR7 ([Förster et al., 1999; Ohl et al., 2004](#)), ainsi que la diminution de molécules d'adhésion. Ces changements favorisent la migration des APC depuis le site d'initiation de l'inflammation et permettent l'entrée des DC dans les organes lymphoïdes secondaires (OLII).

Les DC activées subissent des modifications morphologiques via une réorganisation de leur cytosquelette et perdent leur forme en dendrites caractéristiques. L'activation des APC va également induire une augmentation de l'expression des molécules du CMH ainsi que des récepteurs de co-stimulation. Cette augmentation de l'expression du CMH est concomitante d'une diminution de la capacité de prise en charge de l'antigène ([Tirapu et al., 2009](#)).

Les LT expriment à la membrane des récepteurs polymorphiques (TCR pour « T cell receptor »), capables de discriminer des peptides présentés par les APC du « non-soi ». L'activation des LT s'effectue via l'interaction entre le CMH d'une APC et le TCR spécifique de l'antigène. Toutefois, cette interaction seule n'est pas suffisante pour induire l'activation des cellules T et nécessite un ensemble de signaux « accessoires » prenant place au niveau de la synapse immunologique.

3) Orientation de la réponse immunitaire par les cellules dendritiques

Les mécanismes précoce suivant l'injection d'un vaccin tels que l'immunité innée, sont capitaux pour la mise en place de la réponse vaccinale. De nombreux acteurs cellulaires et moléculaires sont impliqués mais nous allons nous focaliser sur les DC et leur capacité

à activer et orienter la réponse adaptative par le biais de la présentation antigénique, tout particulièrement les lymphocytes T CD4 dits auxiliaires (Th pour « T-helper ») (Figure 2).

a) *Les cellules dendritiques de la lignée myéloïde*

Les DC, décrites pour la première fois par Steinman and Cohn, ont été identifiées comme les principales effectrices spécialisées dans la présentation des antigènes aux lymphocytes (Steinman & Cohn, 1973). Les DC sont présentes dans l'ensemble des tissus de l'organisme ce qui leurs permettent d'être au plus près des sites d'infection et sont caractérisées phénotypiquement par l'expression de HLA-DR. Les DC vont intervenir dans l'initiation et l'orientation des réponses immunitaires spécifiques et aussi contribuer aux processus de sélection négative des lymphocytes anti-soi dans le thymus ou à la différenciation de lymphocytes T régulateurs (Treg) (Banchereau & Steinman, 1998; Brocker et al., 1997; Darrasse-Jèze et al., 2009; Martín-Gayo et al., 2010). Plusieurs types de DC existent, chacun avec des fonctionnalités et un lignage propre : les DC conventionnelles (cDC) composé des cDC1 et cDC2, les cellules dendritiques plasmacytoides (pDC), le DC dérivées de monocytes et les cellules de Langerhans.

i. Les cellules de Langerhans

Les cellules de Langerhans (LC) sont les APC résidentes au sein l'épiderme et des couches kératinisées des muqueuses établissant des liens étroits avec les kératinocytes. Elles représentent donc les premiers acteurs de l'immunité innée mobilisés lors d'une rupture de la barrière cutanée ou muqueuse. Elles sont caractérisées par l'expression de CD207 (Tripp et al., 2004), ainsi que par l'expression de nombreux types de PRR dont les TLR1, 2, 3, 4, 5, 6 et 10 (Flacher et al., 2006; Schuler & Steinman, 1985). Les LC sont capables de migrer vers les ganglions lymphatiques et d'activer les réponses T. En effet, de nombreuses études ont mis en évidence la capacité des LC à induire des réponses Th1, Th2 et Th17 (Furio et al., 2009; Zaric et al., 2015), mais également les lymphocytes T folliculaires (Tfh) (Ndeupen et al., 2022). Les Th22 dont la production d'IL-22 stimule la prolifération et la production de composés antimicrobiens des kératinocytes en cas d'inflammation sont également induit par les LC (Boniface et al., 2005; Fujita et al., 2009). Furio et al. ont mis en évidence qu'en cas d'inflammation, les LC présentent une expression plus importante de molécules de co-stimulation (CD80/CD86) et une capacité

plus élevée à activer les lymphocytes Th1 et Th2 par comparaison aux DC du derme (Péguet-Navarro et al., 2010).

Outre l'induction des LT CD4+, les LC sont également impliqués dans l'induction de réponse T CD8 (Liard et al., 2012). De plus, Zaric et al. ont démontré qu'une déplétion des LC avant immunisation altère fortement la réponse cytotoxique (Zaric et al., 2015). Les auteurs ont également mis en évidence la capacité des LC à effectuer une présentation antigénique croisées par le CMH-I dont les mécanismes génétiques, particulièrement la diminution d'IRF4 sous l'action du TNF, ont été récemment décrits (Sirvent et al., 2020). L'activation des LT CD8+ est également favorisée par la production d'IL-15 par les LC (Banchereau et al., 2012).

En l'absence d'inflammation, les LC interviennent également dans l'homéostasie de l'épiderme par phagocytose des kératinocytes apoptotiques. Une migration vers les ganglions suite à l'internalisation de ces kératinocytes a été observée où les LC présentent alors les antigènes du soi et contribuent à la tolérance en promouvant l'activation des lymphocytes T régulateurs (Treg). Les LC sont également capables d'interagir directement avec les Treg, de produire de l'IL-10 et d'inhiber la production de cytokines pro-inflammatoire suite à la phagocytose des kératinocytes apoptotiques (Seneschal et al., 2012).

ii. Les cDC1

Les cDC1, originellement identifiées chez l'Homme par l'expression de CD141 sont présentes dans tous les types de tissus. Actuellement, cette population se caractérise phénotypiquement par l'expression de CADM1 et CLEC9A ainsi que par l'absence de CD11b et CD14. Le développement de ces APC dépend de nombreux facteurs de transcription tels que IRF8, PU.1 et BATF3 dont la balance intervient chez l'Homme et la souris, dans le contrôle de la différenciation des précurseurs myéloïdes de cDC (Carotta et al., 2010; Grajales-Reyes et al., 2015; Tamura et al., 2015).

L'activation des cDC1 est médiée principalement par les TLR3 et TLR10 bien qu'une expression des TLR1, 2, 6 et 8 ait été documentée (Hémont et al., 2013a; Jongbloed et al., 2010). La localisation endosomale du TLR3 et le rôle du CLR CLEC9A dans la détection des cellules nécrotiques (J. G. Zhang et al., 2012), reflètent une implication particulière des cDC1 dans la détection de la cytolysé associée aux pathogènes intracellulaire.

L'engagement puis l'internalisation de CLEC9A conduisent à une augmentation de l'expression de molécules de costimulation, telles que CD40 et CD80/CD86, (Colletti et al., 2016), ainsi qu'à la production d'IFN de type III, de cytokines pro-inflammatoires (IL-1b, IL-6, IL-23, and TNF α) et régulatrices (TGF β et IL-10).

La production d'IL-12 par les cDC1 contribue à l'orientation de la réponse immunitaire vers une réponse cytotoxique. Cette orientation promeut l'activation des cellules NK et la différenciation des LT Th1 (Jongbloed et al., 2010). La présentation croisée des antigènes aux LT CD8 par le CMH-I participe à cette orientation (Bachem et al., 2010; Haniffa et al., 2012; Jongbloed et al., 2010). Schreibelt et al. documenta chez l'Homme le rôle de CLEC9A dans la présentation croisée aux LT CD8. Ce mécanisme implique la reconnaissance par CLEC9A d'un complexe anticorps-antigène. Secondairement l'antigène est internalisé puis apprêté afin de permettre une présentation croisée via le CMH-I et le CMH-II (Schreibelt et al., 2012). Li et al. montra que ces mécanismes permettent l'induction d'une réponse humorale spécifique d'un antigène vaccinal chez les primates non humains (PNH) en s'affranchissant de l'usage d'adjuvants (J. Li et al., 2015). Une stratégie vaccinale ciblant CLEC9A sur les cDC1 permit l'induction d'une réponse anticorps forte et durable, ainsi que la formation de Tfh mémoire permettant la mise en place d'une réponse secondaire rapide même avec un vaccin ne contenant pas d'adjuvants (Kato et al., 2015). Cependant, l'utilisation de divers adjuvants en combinaison à des anticorps anti-CLEC9A permettrait de moduler l'orientation de la réponse adaptative vers différents profils auxiliaires LT CD4 (Joffre et al., 2010).

iii. Les cDC2

Chez l'Homme, les cDC2 sont caractérisées par l'expression du CD1c, de Fc ϵ RI et du CD172. Les cDC2 représentent la population de DC la plus abondante dans le sang et les organes lymphoïdes (Dziona et al., 2000; Sittig et al., 2016; Villani et al., 2017). A l'instar des cDC1, leur développement dépend de nombreux facteurs de transcription tels que GATA2, PU.1, IRF4, IRF8 ou ID2. Cependant, IRF4 semble être un facteur déterminant dans la différenciation en cDC2, chez l'Homme comme chez la souris (Bajaña et al., 2016; Schlitzer et al., 2013).

Les cDC2 expriment une large gamme de PRR (TLR, CLR, NLR et RLR) permettant ainsi la détection de nombreux types de pathogènes (Hémont et al., 2013b). Leur engagement

conduit à la production de cytokines pro-inflammatoires (TNF α , IL-1 β , IL-6, IL-8, IL-23) et régulatrices comme l'IL-10. Les cDC2 produisent peu d'IFN de type III ([Leal Rojas et al., 2017; Nizzoli et al., 2016](#)).

Les cDC2 sont des acteurs majeurs de l'orientation de la réponse LT CD4 impliquant la présentation de l'antigène apprêtée via le CMH-II ([Gao et al., 2013; Schlitzer et al., 2013; vander Lugt et al., 2014; J. W. Williams et al., 2013](#)). Yin *et al.* proposèrent une classification des cDC2 sur la base de l'expression du CD5 (Yin et al., 2017). Une première sous population exprime fortement le CD5 (CD5 hi), la seconde faiblement (CD5 lo) mais aussi des gènes associés aux monocytes ainsi que le CD14. Les auteurs ont documenté que les cDC2 CD5 hi et CD5 lo diffèrent fonctionnellement. Les cDC2 CD5 hi contribuent à l'orientation et la prolifération des LT Th2, Th17, Th22 et Treg. Les cDC2 CD5 lo sont quant à elles impliquées dans l'orientation Th1.

Les cDC2 permettent non seulement la mise en place des réponses LT CD4 et LT CD4 mémoire mais aussi la présentation antigénique croisée avec les LT CD8 ([Nizzoli et al., 2013; Segura, Durand, et al., 2013](#)). Cohn *et al.* ont démontré que la présentation antigénique via le CMH-I était équivalente à celle observée pour les cDC1. Ce mécanisme implique la prise en charge de l'antigène par un endosome précoce (Cohn et al., 2013). Nizzoli et al. ont démontré une capacité des cDC2 à produire de l'IL-12 et donc de potentialiser des réponses cytotoxiques (Nizzoli et al., 2013).

iv. Les cellules dendritiques plasmacytoïdes (pDC)

Les pDC se différencient à partir de précurseurs hématopoïétiques différents de ceux des cDC. On retrouve les pDC dans le sang et dans différents types de tissus. L'ontogénie des pDC requiert les facteurs de transcription tels que GATA2, E2-2 et IRF8 (Cisse et al., 2008; Murphy et al., 2016; Onodera et al., 2016). Phénotypiquement, les pDC sont caractérisées par l'expression des marqueurs CD123, CD303 et une expression du CD4 plus forte que sur les autres populations de DC. Inversement, l'expression de HLA-DR est faible et les marqueurs du lignage myéloïde tels que CD11b ou CD11c sont absents ([Jardine et al., 2013; G. Li et al., 2021](#)).

Après activation, l'expression du CMH-II et des molécules de co-stimulation augmentent. L'engagement des TLR7 et TLR9 des pDC va permettre l'expression des facteurs de transcription IRF7 et IRF8 et incidemment la production d'IFN de type I (IFN-I) (Bao & Liu,

2013). La grande capacité de production d'IFN- λ permet l'activation des cellules NK et des lymphocytes Th1.

Si les pDC sont capables de présentation antigénique à la fois aux LT CD4 et aux LT CD8, cette capacité est moindre comparée aux autres populations de DC (di Pucchio et al., 2008; Villadangos & Young, 2008). Néanmoins elles contribuent à l'orientation des réponses auxiliaires, en effet, de nombreuses fonctions ont été attribuées aux pDC, outre l'IFN- λ , elles sécrètent également diverses cytokines inflammatoires comme le TNF α , IP-10 ou l'IL-6.

L'orientation de la réponse adaptative par les pDC ne se limite pas uniquement à l'orientation vers la réponse cytotoxique. Les pDC sont aussi impliquées dans la tolérance et la régulation de la réponse immunitaire en promouvant la différenciation des lymphocytes T régulateurs (Martín-Gayo et al., 2010b; Moseman et al., 2004). Biswas et al. ont montré qu'un traitement à la rapamycine induirait chez la souris une prolifération des pDC laquelle favorisait la différenciation des Treg (Biswas et al., 2015).

Les pDC concourent également à la réponse humorale en contribuant au processus de différenciation des lymphocytes B (LB) en cellules sécrétrices d'anticorps via l'engagement de la molécule de costimulation CD70 ainsi que par la production d'IFN α et d'IL-6 (Bekeredjian-Ding et al., 2005; Jego et al., 2003; Shaw et al., 2010). En outre, Bekeredjian-Ding et al. ont également mis en évidence que la production d'IFN α augmente la sensibilité des LB aux ligands du TLR7, dont l'engagement renforce le processus de différenciation plasmocytaire. La production d'IFN α par les pDC contribue à l'augmentation de l'expression de molécules de co-stimulation (CD86, CD80, CMH-II) par les cellules B favorisant ainsi leur interaction avec les LT CD4 (Gujer et al., 2011).

v. Les cellules dendritiques dérivées des monocytes (moDC)

Les moDC, fréquemment décrites chez l'Homme et la souris dans des modèles d'inflammation, représentent une catégorie d'APC encore sujette à controverse quant à leur appartenance aux monocytes ou aux DC. Les moDC dérivent principalement des monocytes classiques et se présentent comme une population intermédiaire présentant des caractéristiques communes avec les DC.

En effet, elles se caractérisent par un phénotype proche de celui des cDC2 avec une expression de CD1c, CD172a, Fc ϵ RI et du facteur de transcription IRF4 associée au développement des cDC2, mais à l'instar des monocytes elles expriment aussi le CD11b (Shin & Greer, 2015). En terme de fonctionnalité, les moDC sont, tout comme les cDC2, capables d'effectuer une présentation antigénique via le CMH-I et le CMH-II ainsi que de sécréter des cytokines pro-inflammatoires (IL-1, IL-6, IL-12, IL-23, IFNg et TNFa) (Segura, Touzot, et al., 2013). Cependant, Chow *et al.* ont mis en évidence chez la souris une plus haute capacité des moDC à induire la polarisation des sous-populations Th1 et Th17 alors que les DC sont plus efficaces à induire la prolifération des Th et la production d'IL-2 (Chow *et al.*, 2016). Les moDC possèdent également une forte capacité de prolifération en cas d'inflammation, ainsi qu'une capacité de migration limitée et une forte capacité à recruter et activer les Th2 (Eguílez-Gracia *et al.*, 2016; Plantinga *et al.*, 2013).

Néanmoins, dans le contexte d'immunothérapie par injection de moDC apprêtées *ex vivo* leur efficacité est apparue réduite par comparaison aux stratégies employant des pDC ou des cDC2. Les études de Schadendorf *et al.* et Small *et al.* en sont le parfait exemple où la première, basée sur les moDC n'a pas réussi à démontrer une augmentation de la survie au cours d'essais cliniques de phase III contre le mélanome métastatique, à l'inverse de la seconde basée sur les DC naturelles (Schadendorf *et al.*, 2006; Small *et al.*, 2006).

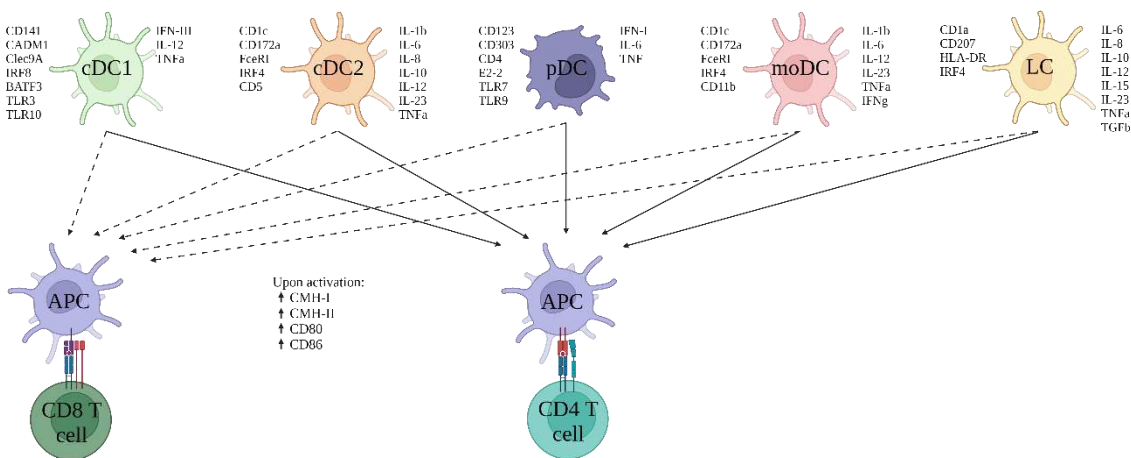


Figure 2: Orientation de la réponse adaptative par les cellules présentatrices d'antigènes. Les différentes sous populations d'APC sont représentées avec leur caractéristiques phénotypiques principales et leur production de cytokines.

b) *Les cellules dendritiques folliculaires (FDC)*

Les FDC sont présentes au sein de structures lymphoïdes des OLII et tertiaires (formés dans les tissus), les centres germinatifs (GC). Les GC sont des structures dynamique dans lesquels s'effectuent les processus de différenciation de maturation des LB naïfs en LB à mémoire et en plasmocytes (Aloisi & Pujol-Borrell, 2006). Contrairement aux cellules dendritiques hématopoïétiques, les FDC dérivent de cellules stromales (Jarjour et al., 2014; Krautler et al., 2012). L'ontogénie des FDC dépend de la production de TNF et de lymphotoxines par les cellules B (Mackay et al., 1997; Ngo et al., 1999). Réciproquement, la production de CXCL13 par les FDC contribue à la formation et au maintien des GC au sein des follicules via le recrutement des LB et les Tfh, lesquels expriment CXCR5, le récepteur de cette chimiokine (Ansel et al., 2000; Gunn et al., 1998; Ngo et al., 1999; S. M. Park et al., 2021). Se forme ainsi une boucle de rétrocontrôle positive favorisant la production de lymphotoxine par les LB qui à son tour stimule la production de CXCL13 (Ansel et al., 2000). Dans un modèle murin permettant l'ablation sélective des FDC, Wang et al. confirmèrent l'importance des FDC dans le maintien de l'architecture des GC.

La maturation des cellules B au sein des GC dépend également de contacts étroits avec les FDC médiés par la liaison des récepteurs d'intégrine ICAM1 et VCAM1. In vitro, ces récepteurs ont la capacité de retenir et de promouvoir la survie des LB en inhibant l'apoptose (Carrasco & Batista, 2006; Koopman et al., 1994). Cependant des études de microscopie ont mis en évidence que les cellules B au sein des GC sont très mobiles. Les interactions courtes observées suggèrent donc une autre fonction de ces récepteurs qu'une liaison stable entre FDC et LB.

Les FDC présentent aux LB l'antigène natif opsonisé par des anticorps et/ou des molécules du complément, soit sous forme de complexes immuns (IC pour « Immune Complex ») (L. L. Chen et al., 1978; Klaus & Humphrey, 1977). Cette présentation est médiée par les récepteurs au complément tels que CD21 et CD35 ainsi que les récepteurs aux portions Fc (pour « Crystallizable Fragment ») des anticorps comme CD23 et CD32 (FcγRIIb) (Allen & Cyster, 2008; Rozendaal & Carroll, 2007; Yoshida et al., 1993). Les IC sont stockés au niveau d'endosomes puis recyclés par les FDC (Heesters et al., 2013), délivrant ainsi graduellement les antigènes aux LB au sein des GC.

Ces IC vont contribuer à au processus de maturation du récepteur à l'antigène des LB (BCR pour « B cell receptor ») en favorisant les hyper mutations somatiques (HMS). Ainsi les LB dont le BCR aura acquis un avantage compétitif pour l'accès à l'antigène sera sélectionné positivement dans un processus, ci-après décris, faisant intervenir les Tfh (Aydar et al., 2005). Le CD32 est particulièrement impliqué dans ce processus (Yoshida et al., 1993). En effet, Van der Poel et al. ont montré qu'en l'absence de CD32, une sélection aberrante de cellules B se met en place au sein des GC, y compris des cellules de faible affinité (van der Poel et al., 2019).

Les FDC contribuent à l'homéostasie des GC via la production d'une protéine de liaison aux phosphatidylsérines, le Mfge8. Le rôle de Mfge8 dans les GC a été mis en évidence par Hanayama et al. et par la suite, Kranich et al. ont rapporté que les FDC produisent de grande quantité de Mfge8 s'accumulant au niveau des dendrites en contact permanent avec les cellules B (Hanayama et al., 2004; Kranich et al., 2008). Les LB apoptotiques cellules qui ont perdu leur affinité pour l'antigène présentent une augmentation de phosphatidylsérines à leur surface vont être très rapidement opsonisés par Mfge8 et stimuler le processus de phagocytose par les macrophages colonisant le follicule B. Les auteurs postulent que ce mécanisme contribue à l'élimination de clones LB potentiellement acquis un BCR auto-réactif.

4) Cibler les cellules présentatrices d'antigène pour orienter les réponses vaccinales

La caractérisation des différents mécanismes de détection des pathogènes par les cellules de l'immunité innée ont permis d'accroître notre compréhension des mécanismes d'action des vaccins existant. Cela a également permis de fournir des pistes pour le développement de nouveaux candidats vaccin avec une efficacité augmenté et plus durable.

a) Orientation de la réponse vaccinale par les adjuvants

Les adjuvants sont des composés de nature diverses tels que les minéraux (Alum), les dérivés microbiotiques (toxines, monophosphoryl lipide A (MPLA)...) ou encore des agonistes de PRR, ayant pour objectif de favoriser le recrutement d'effecteurs cellulaires et d'orienter la réponse immune. Ils exploitent les mécanismes de détection des

antigènes et/ou permettent une libération progressive de l'antigène par effet dépôt dans le but d'améliorer la qualité de la réponse vaccinale. A titre d'exemple, Calabro *et al.* ont mis en évidence la capacité du MF59, un adjuvant « huile dans eau » autorisé sur le marché, à induire la différenciation de monocytes en moDC et à favoriser la présentation antigénique (Calabro *et al.*, 2013). Les auteurs ont également mis en évidence la capacité du MF59 à augmenter la réponse anticorps et à activer et orienter une réponse T CD4 de type Th2.

b) *Orientation de la réponse vaccinale en fonction des voies d'injection*

La voie d'injection est également un facteur déterminant dans l'orientation de la réponse immunitaire. En effet, la distribution qualitative et quantitative des cellules de l'immunité, dont les APC, varie en fonction des tissus ce qui modulerait la prise en charge des antigènes et la vitesse de présentation aux LT (Rosenbaum *et al.*, 2020). Ols *et al.* montrèrent que la migration des APC vers les ganglions drainants varie en fonction de la voie d'immunisation employée. L'importance de la vascularisation des tissus dans la cinétique de diffusion de l'antigène dans l'organisme a été soulignée par les auteurs (Ols *et al.*, 2020). Certains tissus musculaires ou tissu adipeux présentent une vascularisation particulièrement riche. Enfin, comme évoqué précédemment, certaines cellules non immunitaires comme les kératinocytes interviennent dans la détection des pathogènes, l'induction de l'inflammation et le recrutement des cellules immunitaires. Adapter la voie d'injection au pathogène, permet également de favoriser la formation d'une réponse protectrice directement au niveau des sites d'infection. C'est particulièrement le cas des vaccinations via les muqueuses dont l'objectif serait de favoriser l'immunité collective en limitant le portage.

II. Rôle des lymphocytes T CD4 dans l'orientation et la qualité des réponses vaccinales

1) Sélection, activation et migration des cellules T CD4 spécifiques

a) *Circulation des cellules dans les ganglions*

La détection des pathogènes par les APC va induire leur activation et leur migration vers les ganglions lymphatiques drainants proches du site de contact avec l'antigène. Les ganglions lymphatiques sont des organes disséminés à travers l'organisme impliqués

dans l'interface entre l'immunité innée et adaptative, dans lesquels s'effectue la présentation antigénique.

Il s'agit de structures compartimentées, entourées par une capsule, comprenant le sinus subcapsulaire, le cortex, le paracortex (ou zone T) et la médulla. Le cortex contient les LB organisées en follicules denses, dans lesquels se forment des structures supplémentaires, les centres germinatifs, où vont s'effectuer la sélection et la maturation des LB (Figure 3). Un réseau de cellules stromales non lymphoïdes maintient la structure des ganglions. On dénombre trois types de cellules stromales, chacune avec une localisation et une fonction particulière : les cellules réticulaires fibroblastiques (FRC) et marginales (MRC) respectivement localisées dans la zone T et à la périphérie des follicules B, et enfin les FDC dans les follicules B.

L'entrée des APC dans les ganglions s'effectue par les vaisseaux lymphatiques afférents (via l'expression du CCR7) se déversant dans le sinus subcapsulaire avant de migrer vers le paracortex. L'entrée des lymphocytes B et T dans les ganglions se fait grâce aux veinules endothéliales (HEV) localisées dans le paracortex. Une régulation précise par le biais de chimiokines permet aux cellules de circuler au travers du réseau de cellules stromales et des différents compartiments des ganglions. Les APC et les LT vont répondre à un gradient de CCL19 et CCL21 ([Luther et al., 2000; Worbs et al., 2007](#)), fortement exprimé près des HEV, alors que les LB répondent majoritairement au CXCL13 produit par les FDC ([S. M. Park et al., 2021](#)). Enfin, la sortie du ganglion s'effectue par les vaisseaux lymphatiques efférents.

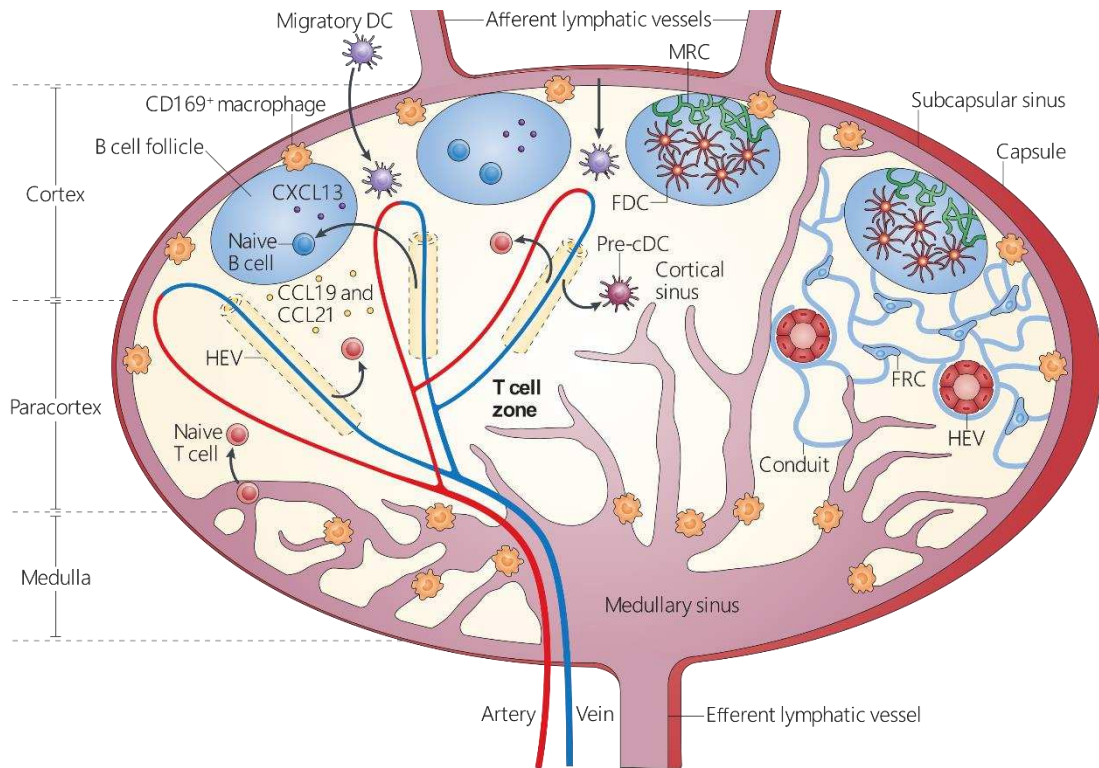


Figure 3 : Structure interne et circulation des cellules dans un ganglion lymphatique. FDC : cellules dendritique folliculaire. MRC : cellule réticulaire marginale. FRC : cellule réticulaire fibroblastique. HEV : veinule endothéliale D'après (Girard et al., 2012).

b) Interface innée/adaptatif : la synapse immunologique

Le mécanisme de reconnaissance de l'antigène via le récepteur des cellules T (TCR) est une étape clé marquant l'initiation de la réponse adaptative. La liaison entre le CMH des DC et le TCR des LT conduit à une réorganisation cellulaire donnant lieu à la formation et à la stabilisation d'une zone d'interaction : la synapse immunologique (SI) (Figure 4). Cette réorganisation est marquée par la formation d'une structure en trois couches concentriques avec une accumulation de TCR au niveau de la couche centrale (Grakoui et al., 1999; Monks et al., 1998). Une forte concentration d'intégrines et de leurs ligands comme LFA-1/ICAM-1 et LFA-3/CD2 est également retrouvée au niveau de la couche périphérique contribuant ainsi à la formation d'une interaction stable et prolongée. Enfin la couche distale se compose du récepteur CD45 (Barreiro et al., 2007). Au sein de la SI, l'induction de différents types de signaux déterminent l'activation des LT CD4, incluant le signal TCR, les signaux de co-stimulation et la signalisation par les cytokines.

De nombreuses études, résumées de manière approfondie par Heikrujam Thoihen Meitei *et al.* ont contribué à mettre en avant le rôle de la signalisation TCR dans la différenciation des LT CD4+ ([Meitei & Lal, 2022](#)). Ainsi, l'affinité du TCR pour l'antigène présenté par le CMH des APC, l'intensité du signal, de même que la durée de l'interaction avec le CMH donnent lieu à des cascades de signalisation et des changements transcriptomiques intervenant dans l'activation et la différenciation des LT CD4+. Par exemple, van Panhuys *et al.* ont mis en évidence que la différenciation des Th1 était préférentiellement associée à une forte stimulation TCR et à l'inverse, Gottschalk *et al.* ont observé l'induction de FoxP3, un facteur de transcription impliqué dans la différenciation des LT régulateurs (Treg), en cas de signal TCR faible ([Gottschalk et al., 2010](#); [VanPanhuys et al., 2014](#)).

Le deuxième signal nécessaire à l'activation des LT CD4+ mobilise les molécules de co-stimulation au niveau de la SI contribuant à l'amplification du signal induit par le TCR. Parmi elles, on retrouve notamment le CD28, un récepteur appartenant à la superfamille des immunoglobulines exprimé par les LT et ses ligands, CD80/CD86, exprimés par les APC suite à leur activation. L'interaction avec le CD28 intervient dans l'induction de la voie NF-kB et la production d'IL-2 ([Kong et al., 2011](#); [Nagai & Azuma, 2019](#)).

D'autres molécules de co-stimulation déterminent également le devenir des cellules T telles que le couple CD70/CD27 respectivement exprimé par les DC et les T CD4 ([Hendriks et al., 2000](#); [van Oosterwijk et al., 2007](#)), et le couple CD40/CD40L. Ces deux couples ont démontré leur rôle dans l'amplitude et l'orientation des réponses primaires ainsi que dans la génération de la mémoire ([M. MacLeod et al., 2006](#)).

En compétition avec le CD28, CD80/CD86 interagissent également avec le récepteur inhibiteur « checkpoint » CTLA-4. La liaison de ce récepteur avec CD80 induit un signal, plus fort que celui induit par CD28, inhibant la transduction du signal TCR et les réponses T dépendantes de CD28 telles que la production d'IL-2 ([Pentcheva-Hoang et al., 2004](#); [Vogel et al., 2015](#)). Le couple PD-1/PDL-1 exprimé respectivement par les LT et les DC, constitue également un signal de co-stimulation inhibiteur de l'activation des cellules T.

Enfin, parallèlement à la signalisation TCR et aux molécules de co-stimulation, l'action des cytokines et chimiokines produites par les DC va également induire des signaux

supplémentaires afin d'orienter la différenciation de la cellule T impliquée dans une SI (Meitei & Lal, 2022).

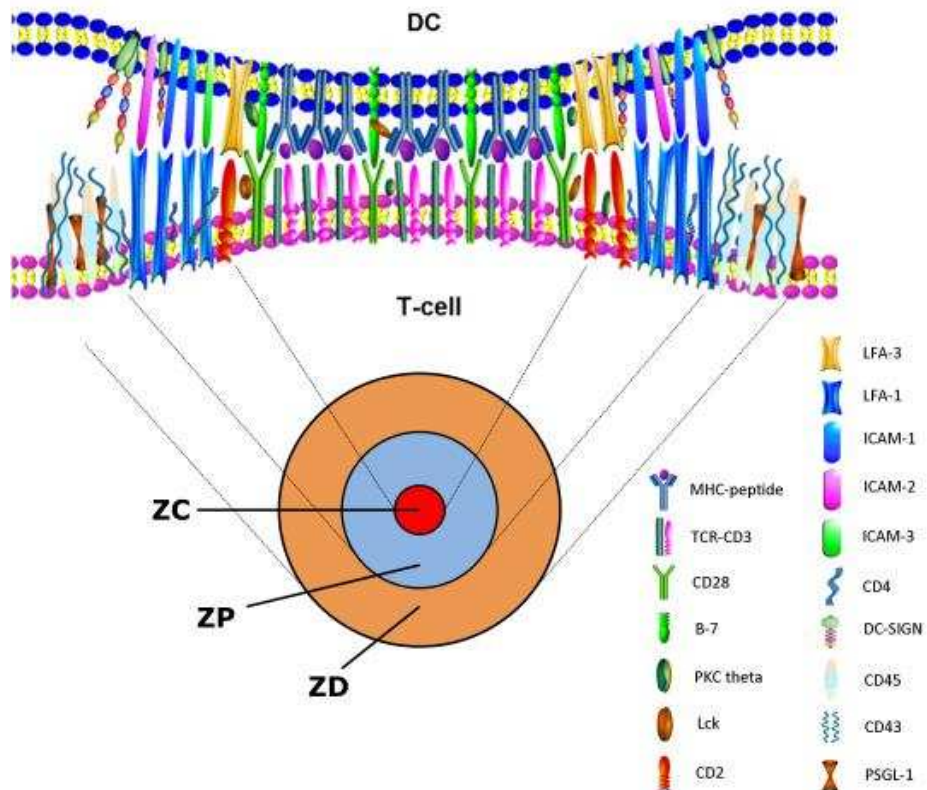
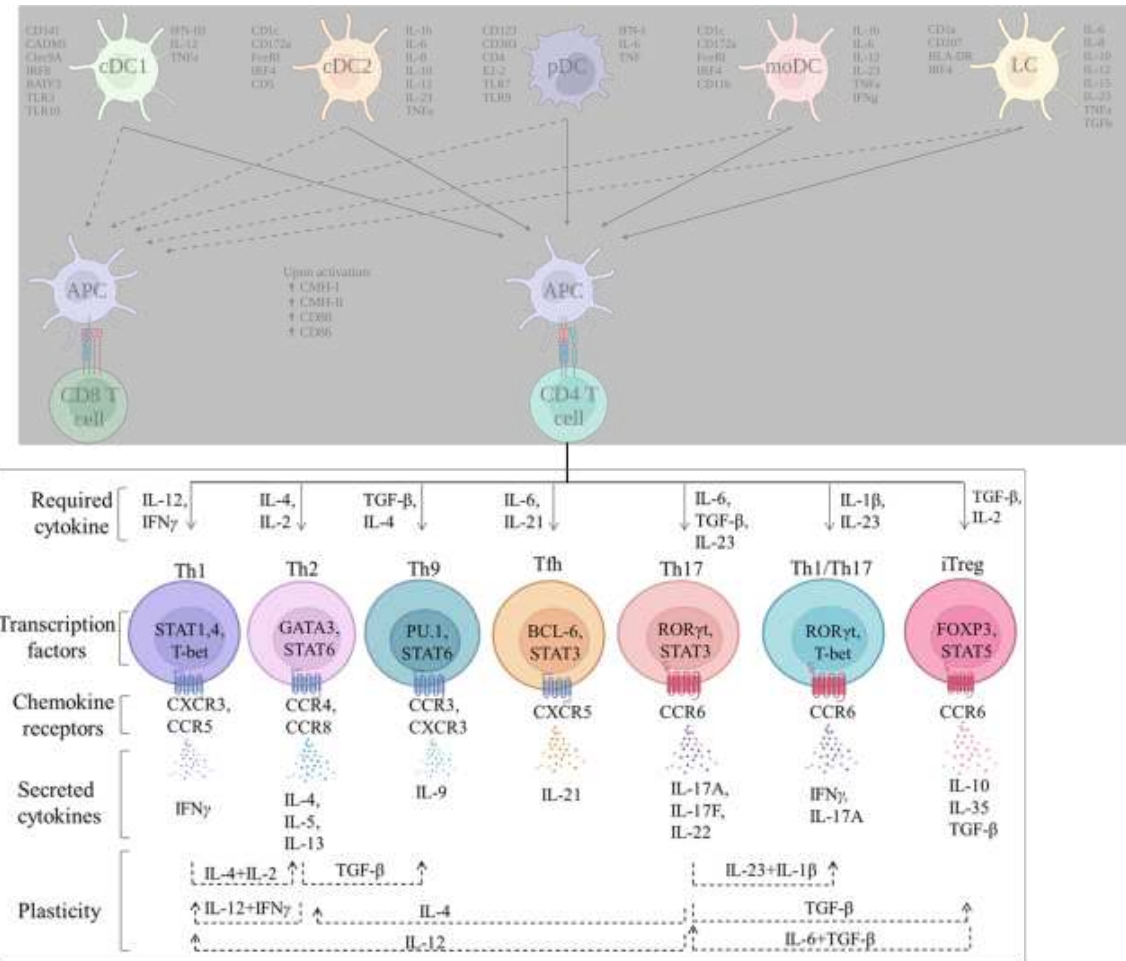


Figure 4 : Organisation de la synapse immunologique. La structure et les interactions des molécules de costimulation sont représentées. ZC : zone centrale. ZP : Zone périphérique. ZD : Zone distale. D'après (Tai et al., 2018).

2) Les différentes sous-populations de lymphocytes T CD4

Les LT CD4+ auxiliaires reconnaissent par leur TCR les peptides présentés dans le contexte du CMH-II. Les LT CD4 spécifiques de l'antigène sont activés en fonction de l'environnement cytokinique et de l'engagement de corécepteurs. Ces LT Th représentent une population très hétérogène impliquée dans l'orientation de la réponse immunitaire et la mémoire immunitaire (Figure 5).



a) Les lymphocytes auxiliaires de type 1 (Th1)

Les Th1, dont la différenciation s'effectue principalement sous l'influence des cytokines IFN γ et IL-12, orientent vers un type de réponse immunitaire dite « cellulaire » laquelle cible principalement les pathogènes intracellulaires (Paul & Seder, 1994; Trinchieri et al., 2003). Ces Th1 supportent notamment l'activation des LT CD8 cytotoxiques (LTC), des cellules NK ou des macrophages. L'intensité du signal médié par le TCR contribue à l'orientation vers le phénotype Th1. Un signal fort promeut la différenciation des LT naïfs en Th1 (Pfeiffer et al., 1995; VanPanhuyse et al., 2014).

Phénotypiquement, les LT Th1 sont caractérisés par l'expression des récepteurs CXCR3 et CCR5, et par l'expression des facteurs de transcription STAT4 et T-bet. T-bet contrôle entre autres l'expression de cytokines de type 1 comme l'IFN γ et l'IL-12 (Lighvani et al.,

2001; Lugo-Villarino et al., 2003). Ces dernières sont impliquées dans les actions microbicides des cellules NK, des macrophages ainsi que dans l'activation des LTC. T-bet ainsi que l'action autocrine de ces cytokines contribuent au maintien du profil Th1 des LT CD4+ via une inhibition des gènes associés à la production de l'IL-4 et une répression du facteur de transcription GATA3, chacun contribuant à une orientation vers le profil Th2 décrit ci-après (Djuretic et al., 2007; Hwang et al., 2005; Szabo et al., 2003).

b) *Les lymphocytes auxiliaires de type 2 (Th2)*

Le rôle des Th2 fut particulièrement documenté dans la réponse immunitaire dirigée contre les pathogènes extracellulaires tels que les bactéries ou les parasites. L'expression des marqueurs CCR4, CR8 et CTRH2 permettent de discriminer phénotypiquement les Th2 (Bonecchi et al., 1998; Mikhak et al., 2009; Watanabe et al., 2020). L'action combinée des cytokines IL-4 et IL-2 contribue à la différenciation des LT CD4+ naïfs en Th2 via l'expression de deux facteurs de transcription : STAT6 et GATA3 (Cote-Sierra et al., 2004; Zhu et al., 2003; Zhu & Paul, 2008). L'IL-6 a également été décrit comme inducteur de Th2 et inhibitrice des Th1 (Diehl et al., 2000a). A l'instar de T-bet capable de réprimer la différenciation vers le profil Th2, GATA3 intervient dans l'inhibition de la différenciation en Th1 en réprimant le facteur de transcription STAT4 ainsi que la transcription de l'IFNy (Diehl et al., 2000b; Usui et al., 2003). La différenciation des Th2 serait associée à un signal TCR « faible » (Yamane & Paul, 2013). En effet, une interaction TCR-CHM-II « forte » déclencherait une cascade de signalisations aboutissant à l'inhibition de la transcription de GATA3. GATA3 coordonne également la transcription des cytokines caractéristiques des Th2 : l'IL-4 et l'IL-13 (Luckheeram et al., 2012; Swain et al., 1990; Zheng & Flavell, 1997). Ces deux cytokines contribuent à la commutation isotypique permettant la production d'IgG1 et d'IgE.

Les Th2 ont été également décrits comme secrétant les cytokines IL-5, IL-10 et TNF α . L'IL-10, cytokine anti-inflammatoire et immunosuppressive, contribuerait au maintien du profil Th2 en exerçant une action répressive sur la production d'IFNy par les LT Th1 (Fiorentino et al., 1991).

c) *Les lymphocytes auxiliaires de type 9 (Th9)*

L'action conjointe des cytokines IL-4 et TGF β promeut la différenciation des LT, naïfs ou Th2, vers le profil Th9. Le facteur de transcription PU.1, en coordination avec GATA3, STAT6 et IRF4 est caractéristique des LT Th9 (Kaplan, 2013; Staudt et al., 2010).

Les Th9 produisent essentiellement l'IL-9 mais également l'IL-10 et l'IL-21 (C. Tan et al., 2010). Les Th9 sont impliqués dans l'induction de l'inflammation. Ces cellules ont également été associées avec des réactions auto-immunes et allergiques (Jones et al., 2012; Yao et al., 2011). Le transfert adoptif de Th9 dans des modèles murins de mélanome ou de cancer des poumons a permis de documenter leur potentiel antitumoral (Purwar et al., 2012).

d) *Les lymphocytes auxiliaires de type 17 (Th17)*

Les Th17 ont été décrits comme contributeurs majeurs dans la défense contre les bactéries et les champignons (Puel et al., 2011). Ils sont caractérisés par l'expression des récepteurs CCR4, CCR6 et IL-23R ainsi que par les productions d'IL-17a, IL-17f, IL-21 et IL-22 (Acosta-Rodriguez et al., 2007; Ivanov et al., 2006; C. O. Park et al., 2017; Zhou et al., 2007). Leur différenciation est promue par l'action conjointe de l'IL-6 et du TGF β ainsi que par l'expression des facteurs de transcription RORgt et STAT3 (McGeachy et al., 2007; Xu et al., 2007). L'IL-23 contribue également à la différenciation des Th17, cependant, la différenciation médiée par cette cytokine a souvent été associée à un profil pathologique (Ghoreschi et al., 2010; Langrish et al., 2005). RORgt est impliqué dans la production des cytokines IL-17a et IL-17f. L'IL-17 contribue au recrutement des cellules immunitaires au site d'infection, en particulier les neutrophiles (Kolls & Lindén, 2004; H. Park et al., 2005). Ce mécanisme est amplifié via la production de cytokines pro-inflammatoires comme l'IL-6 et l'IL-8.

La cytokine IL-21 a été décrite comme contribuant au maintien de l'orientation Th17 en promouvant l'expression du récepteur à l'IL-23 et du facteur de transcription RORgt (Lexberg et al., 2008; Stritesky et al., 2008).

e) *Les lymphocytes auxiliaires de type 22 (Th22)*

Les LT Th22 ont initialement été associés aux LT Th17 avant d'être décrits comme une population distincte de LT CD4 (Acosta-Rodriguez et al., 2007). Ils sont caractérisés par

la production d'IL-22, d'IL-13, de TNF α , ainsi que par l'absence de sécrétion d'IFN γ , IL-4 et IL-17. Phénotypiquement ces LT expriment CCR4, CCR6 et CCR10. Ce dernier récepteur est impliqué dans la migration vers la peau (Duhen et al., 2009; Eyerich et al., 2009; Trifari et al., 2009).

Les mécanismes de différenciation des ces cellules est encore mal documenté. Cependant l'IL-6, le TNF α et le facteur de transcription AhR semblent contribuer à ce processus (Duhen et al., 2009; Trifari et al., 2009). T-bet a également été décrit comme permettant le maintien du phénotype et la production de cytokines par les Th22 (Barnes et al., 2021).

f) *Les lymphocytes auxiliaires régulateurs*

Les lymphocytes auxiliaires régulateurs (Treg) sont des cellules spécialisées dans le contrôle de la réponse immunitaire et incidemment au maintien de l'homéostasie. Ils sont caractérisés par l'expression du facteur de transcription FoxP3 et du marqueur CD25 (IL-2Ra). Le facteur de transcription STAT5, en permettant la transcription de FoxP3, contribue à la différenciation des LT en Treg (Burchill et al., 2007; R. Wang & Huang, 2020). L'affinité du TCR intervient dans la formation de Treg. Ainsi une faible interaction entre le TCR et un complexe CMH-II-peptide, soit du fait d'une faible affinité du TCR, soit d'une stimulation trop courte, favoriserait l'expression de FoxP3 et l'augmentation de la différenciation en Treg (M. S. Turner et al., 2009).

Deux grandes populations de Treg ont été décrites : les Treg naturels (nTreg) et les Treg inducibles (iTreg). Les nTreg proviennent du thymus, présentent une expression constitutive de FoxP3 et sont impliqués dans le contrôle de l'activation des cellules naïves dans les organes lymphoïdes secondaires (Weiss et al., 2012). A l'inverse, les iTreg se développent à partir des LT CD4+ activés exposés au TGF β au niveau des OLI. Les nTreg se différencient des iTreg par l'expression de la neuropilin 1 (Nrp1) et du CD31 (Booth et al., 2010; Weiss et al., 2012; Yadav et al., 2012). Les iTreg interviennent dans le contrôle de la réponse immunitaire à la périphérie en réprimant l'action des cellules effectrices. Ainsi ces cellules contribuent au contrôle de l'immunité contre les microorganismes commensaux ainsi qu'aux mécanismes de tolérance orale.

Les Treg秘ètent les cytokines immunomodulatrices TGF β , IL-10 et IL-35 (Fujio et al., 2010). Ils peuvent également moduler la réponse immunitaire via l'expression de

molécules membranaires tels Lag3 et CTLA4. Le TGF β produit par les Treg exerce aussi une action autocrine en stimulant la prolifération, de même que l'expression de FoxP3. L'IL-10 contribue au contrôle de la réponse cellulaire et de l'inflammation en inhibant la sécrétion de médiateurs de l'inflammation et en diminuant la présentation antigénique (Haller et al., 2017; McBride et al., 2002). L'IL-35 intervient également dans le contrôle de l'inflammation, l'inhibition des Th17 et en réduisant l'activité des APC. Son action favorise la sécrétion d'IL-10 et de TGF β et soutien la prolifération des Treg (C. Hou et al., 2016).

Plusieurs populations de iTreg n'exprimant pas constitutivement le facteur Foxp3 ont été décrites : Les Th3, le Tr1 et les iTr35. Chacune de ces populations est caractérisée par la sécrétion d'une cytokine dominante. Ainsi, les Th3, produisent principalement du TGF β et peu d'IL-10. Inversement, les Tr1(Groux et al., 1997) produisent de fortes quantités d'IL-10 et peu de TGF β et les iTr35 produisent essentiellement de l'IL-35 (Collison et al., 2010).

Enfin, Grossman et al. ont rapporté que les Treg peuvent aussi moduler la réponse immunitaire par cytolysse via la production de granzyme B et de perforine (Grossman et al., 2004). Ces Treg ont par la suite été particulièrement observés dans le cas de cancers mais également dans le contrôle de l'inflammation (Loebbermann et al., 2012; Sun et al., 2020).

g) *Les lymphocytes T auxiliaires folliculaires (Tfh)*

L'activation, puis les processus de prolifération, de maturation et de différenciation des lymphocytes B dans les organes lymphoïdes secondaires sont régulés par une population de lymphocytes T : les LT auxiliaires folliculaires ou Tfh (pour « follicular helper ») (Schmitt et al., 2014). Les Tfh sont principalement localisés au sein des ganglions lymphatiques au niveau des follicules B. Ils contribuent au bon fonctionnement des GC, structures dynamiques dans lesquels se met en place, entre autres, la mémoire immunitaire. Les Tfh fournissent aux LB des signaux solubles et membranaires permettant d'orchestrer les processus de maturation, de sélection, et différenciation des lymphocytes B. Au sein des GC, le BCR va subir le processus des hyper mutations somatiques (HMS) au niveau génique modifiant ainsi l'affinité pour l'antigène, et de commutation isotypique. Les Tfh

orientent le destin des clones LB lesquels se différencieront soit en LB à mémoires, soit en plasmocytes à longue durée de vie (Cannons et al., 2010; Okada et al., 2018).

Les Tfh sont caractérisés par l'expression du facteur de transcription Bcl-6 impliqué dans l'expression d'un certain nombre de marqueurs phénotypiques caractéristiques : CXCR5 et CCR7, impliqués dans la migration vers les GC, ou ICOS, PD-1, SAP et CD40L, intervenant dans l'interaction et l'immuno-modulation des LB par les Tfh (Bauquet et al., 2009; Cannons et al., 2010; Choi et al., 2011; C. Wang et al., 2011). Ces marqueurs contribuent également à la définition de l'état d'activation des Tfh et de leur capacité « hepler ». De plus, l'expression différenciée de ces marqueurs permet l'identification et le suivi des Tfh dans les différents compartiments des ganglions avec une expression de CD57 observée par les Tfh des GC (Wong et al., 2015). Un autre facteur de transcription, Maf, est caractéristique de cette population par son rôle direct dans la production de l'IL-21, la cytokine effectrice des Tfh (Kroenke et al., 2012). Les facteurs de transcriptions STAT3 et STAT4 interviennent également dans la différenciation des Tfh (Crotty, 2014; Padhan et al., 2021) et à l'inverse, l'expression de STAT5 et un fort signal IL-2 vont contribuer à inhiber la différenciation des Tfh (Ballesteros-Tato et al., 2012; Johnston et al., 2009).

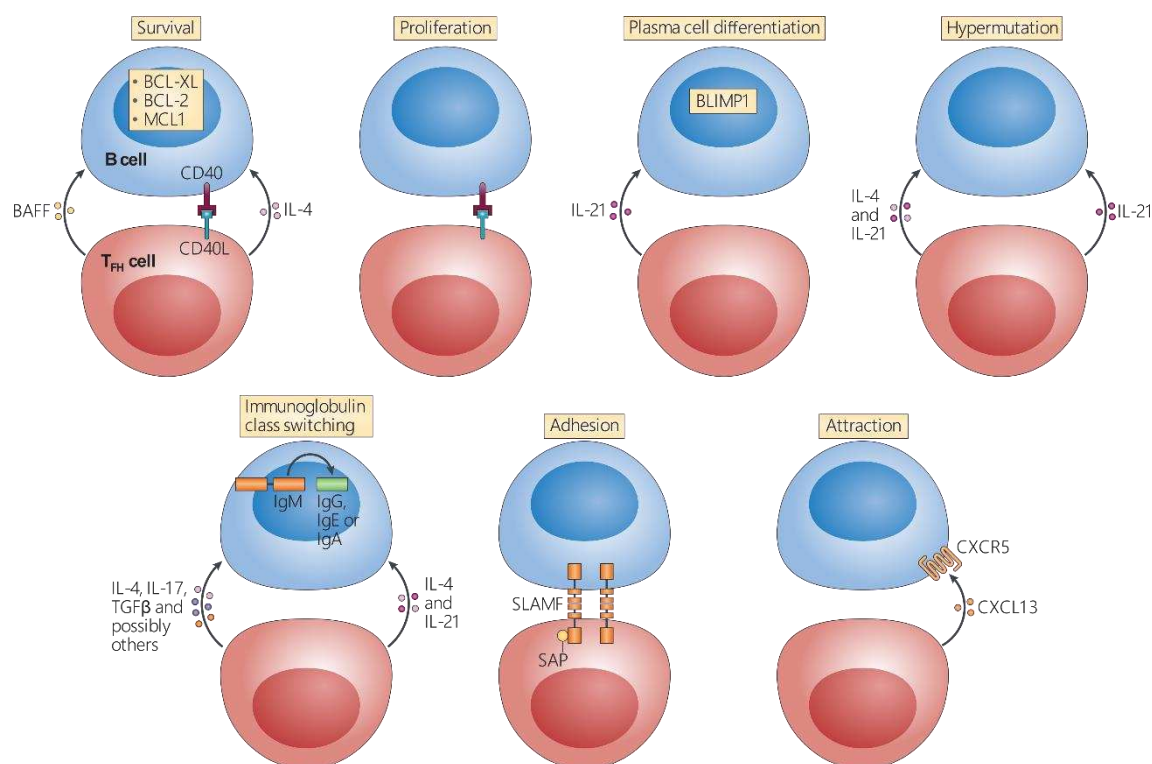
La différenciation des Tfh dépend d'une multitude de processus complexes provenant de l'interaction de marqueurs de co-stimulation avec les APC, les LB, les FDC mais également sous l'action de cytokines telles que l'IL-6 et l'IL-21. Les Tfh sont aussi caractérisés par un TCR de haute affinité dont les stimulations continues avec l'antigène permettent leur maintien (Fazilleau et al., 2009). Choi et al. ont également mis en évidence qu'une faible expression de CD25 combinée à une forte signalisation ICOS peut conduire à la différenciation des Tfh (Choi et al., 2011).

La maturation des cellules B et des réponses humorales repose sur des contacts étroits de différentes natures avec les Tfh via l'engagement des molécules de costimulation telles que ICOS/ICOSL ou CD40/CD40L. La protéine SAP contribue à la stabilisation des interactions entre Tfh et LB au niveau de liaison des protéines SLAM (Cannons et al., 2006).

L'action des Tfh est médiée par la production des cytokines IL-21 et IL-4, déterminantes dans la différenciation des LB en plasmocytes, dans la commutation isotypique, ainsi que

dans la maturation d'affinité des anticorps par les HMS. La production de CXCL13 par les Tfh est impliquée dans la migration des cellules dans les follicules B et l'organisation des GC. Enfin, BAFF est également un facteur clé dans la régulation des cellules B par les Tfh (Mackay & Browning, 2002). BAFF va intervenir dans la survie, l'homéostasie et la tolérance des LB mature et des plasmocytes via les récepteurs BR3 et BCMA (O'Connor et al., 2004; Schiemann et al., 2001). BAFF intervient également dans la régulation des Tfh en promouvant ou inhibant leur expansion en fonction des récepteurs BR3 et BCMA (Coquery et al., 2015).

Outre son action sur la différenciation des LB, l'IL-21 revêt un rôle capital dans l'action des Tfh par une stimulation autocrine via le récepteur de l'IL-21 (IL-21R). En effet, cette cytokine favorise la prolifération et impacte le phénotype des Tfh en tant que co-stimulateur du signal TCR (Vogelzang et al., 2008). Les différentes fonctions des Tfh dans la maturation des réponses B sont résumées dans la figure 6.



Il a également été observé que, suivant le type d'infection, les Tfh sont capables d'exprimer des facteurs de transcription et de produire des cytokines associées aux Th1,

Th2, Th17 ou Treg. L'expression de ces marqueurs de Th définissent ainsi des sous-populations de Tfh (Tfh1, Tfh2, Tfh17 et Tfr) intervenant dans l'orientation de la réponse anticorps (Akiyama et al., 2016; Hale & Ahmed, 2015).

Toutefois, l'action des Tfh n'est pas exclusivement cloisonnée au GC. En effet, certaines études ont mis en évidence une sortie du GC des Tfh et des Tfh mémoires vers la périphérie. Ces Tfh circulants présentent de grandes capacités fonctionnelles sont également associés à la production d'anticorps y compris d'anticorps neutralisants à large spectre dans le cas du VIH, par exemple (Locci et al., 2013; Morita et al., 2011). Cependant, les Tfh circulants présentent des différences phénotypiques avec leurs homologues du GC dont une diminution de l'expression de Bcl6, CXCR5 et PD-1 ainsi qu'une expression de CCR7 plus élevée. Les Tfh sont également retrouvés au sein des tissus autres que les ganglions drainants, tels que les GC des OLIII au niveau des plaques de Peyer, où ils interviennent dans la maturation des réponses B et la production d'IgA dans le tube digestif (Tsuji et al., 2009).

h) Plasticité des sous-populations de lymphocytes T CD4+

Depuis la caractérisation des premières cellules auxiliaires, l'amélioration des techniques et des stratégies d'analyse ont permis de lever le voile sur le dogme Th1/Th2 et ainsi de mettre en évidence une grande diversité de fonction et de populations au sein du compartiment T CD4+. Cependant, de nombreuses études ont également mis en évidence qu'au cours d'une réponse immunitaire, cette classification des T auxiliaires n'était pas figés mais présentait au contraire une importante plasticité. Ainsi, selon les conditions de stimulation, cette plasticité permet à un certain type de T auxiliaires d'acquérir et/ou de changer de fonctionnalité (Figure 5).

Par exemple, il a été démontré que sous l'influence combinée d'IFNy et d'IL-12, les Th2 sont capables de se différencier en Th1 mais également qu'une stimulation par le TGF β entraîne une plasticité des Th2 vers les Th9 (Tsuji et al., 2009; Veldhoen et al., 2008). Cependant, la transition Th1/Th2 semble favoriser les cellules dont le niveau de polarisation par l'expression des marqueurs caractéristiques (T-bet et IFNy pour les Th1 ou GATA3 et IL-4 pour les Th2) est faible (Hegazy et al., 2022; Martinez-Sanchez et al., 2018).

Cette plasticité cellulaire a aussi été observée pour des Treg pouvant générer des Tfhs au sein des plaques de Peyer (Tsuji et al., 2009). De manière similaire, Hirota et al. ont démontré que dans les plaques de Peyer chez la souris, des Th17 pouvaient se différencier en Tfhs impliqués dans la maturation et la production d'IgA par les cellules B (Hirota et al., 2013). De plus, Martinez-Sánchez et al. et Xu et al. ont également souligné le rôle du TGFβ et de l'IL-6 dans la plasticité des Th17 vers un phénotype Tfhs, ainsi que dans la plasticité des Treg à induire Th17 et Tfhs (Martinez-Sánchez et al., 2018; Xu et al., 2007).

Cette plasticité du compartiment T CD4+ représente donc un avantage certain dans la lutte contre les pathogènes permettant l'adaptation permanente des réponses effectrices en fonction des besoins. Toutefois, plusieurs études ont également montré que cette plasticité peut aussi être négativement impliquée dans l'évolution de maladie auto-immune (Meitei & Lal, 2022). C'est particulièrement le cas pour l'arthrite rhumatoïde où il a été observé une conversion des Treg FoxP3+ en Th17 contribuant ainsi à l'aggravation de l'inflammation (Komatsu et al., 2013). Ou encore dans le cas de l'infection par HTLV-1 (human T-lymphotropic virus type 1) où s'opère une conversion des Treg en Th1 suite à des changements transcriptionnels conduisant à la perte d'expression de FoxP3 (Araya et al., 2014).

3) Maturation des réponses B : un mécanisme de haute interaction entre l'immunité innée et adaptative

Suite à la reconnaissance d'un antigène par le BCR, les LB activés vont migrer vers la zone T des ganglions où la première interaction avec des Tfhs spécifiques du même antigène détermine l'entrée du LB soit dans une réponse extra-folliculaire ou soit dans un processus de maturation d'affinité au sein d'un GC. Dans les deux cas, l'interaction avec Tfhs peut induire la commutation isotype du BCR passant de IgM+ aux autres types d'anticorps (IgG, IgA, IgE).

Qi et al. ont démontré qu'en cas d'interaction courte, une réponse extra-folliculaire se met en place, caractérisée par la différenciation du LB en plasmocyte à courte durée de vie producteur d'anticorps de faible affinité. De plus, bien que les GC soient associés à la formation de la mémoire B, il a été mis en évidence une différenciation d'une fraction de LB indépendante des T et n'ayant pas subi de commutation isotypique (IgM+) en cellule

mémoire à long terme (Blink et al., 2005; Kaji et al., 2012; J. J. Taylor et al., 2012). Les mécanismes à l'origine de ces observations sont encore mal compris mais certaines études ont suggéré qu'une affinité forte du BCR pour l'antigène favoriserait cette différenciation rapide T-indépendante (Chan et al., 2009; Paus et al., 2006; Schwickert et al., 2011).

Comme évoqué précédemment, la maturation d'affinité des LB ainsi que la différenciation en plasmocytes à longue durée de vie et en cellules mémoires dans les GC nécessitent d'importantes interactions avec des FDC, des TfH et des macrophages. La migration des précurseurs B vers le GC requiert une augmentation de l'expression de Bcl6, la détection de CXCL13 (produit principalement par les FDC) par le CXCR5 ainsi que l'expression de S1PR2 qui favorise la rétention des LB dans les GC (Green et al., 2011; Kitano et al., 2011). A l'inverse, les TfH ne sont pas confinés au sein des GC mais au contraire sont très mobiles, pouvant ressortir du GC avant d'y retourner, migrer vers un autre follicule ou même gagner la périphérie pour y acquérir un phénotype mémoire. Shulman et al. ont mis en évidence cette circulation par microscopie bi-photonique chez la souris en suggérant que cette circulation permet de diversifier l'aide fourni par les TfH aux cellules B (Shulman et al., 2013).

Ces processus de maturation interviennent au sein de deux structures composant les GC : la zone sombre ou « dark zone » (DZ), une zone dense en LB, et la zone claire ou « light zone » (LZ), moins dense en LB et riche en FDC, TfH et macrophages (Figure 7).

Les LB impliqués dans la voie GC dépendante vont subir une prolifération intense et subir les HMS dans la DZ avant de migrer vers la LZ. A l'intérieur de la LZ, la sélection des LB de haute affinité intervient suite à l'interaction avec les FDC présentant les antigènes sous forme de IC et les TfH fournissant les signaux d'aide. Les mécanismes précis de sélection des cellules B sont encore peu élucidés mais semblent impliquer le récepteur inhibiteur CD32 au niveau des FDC (Qin et al., 2000; van der Poel et al., 2019). Ravetch et al. ont également proposé un modèle basé sur la compétition du BCR avec CD32 exprimé par les LB : si le signal BCR dépasse le signal inhibiteur de CD32 alors cela déclenche l'expression de facteur de survie. En revanche s'il n'est pas suffisant, le signal induit par CD32 déclenche l'apoptose des LB de faible affinité qui seront éliminé par les macrophages (Ravetch & Nussenzweig, 2007). Après sélection, les cellules B peuvent se

différencier en cellules B mémoires ou plasmocytes à longue durée de vie, sortir du GC et du ganglion pour gagner la périphérie.

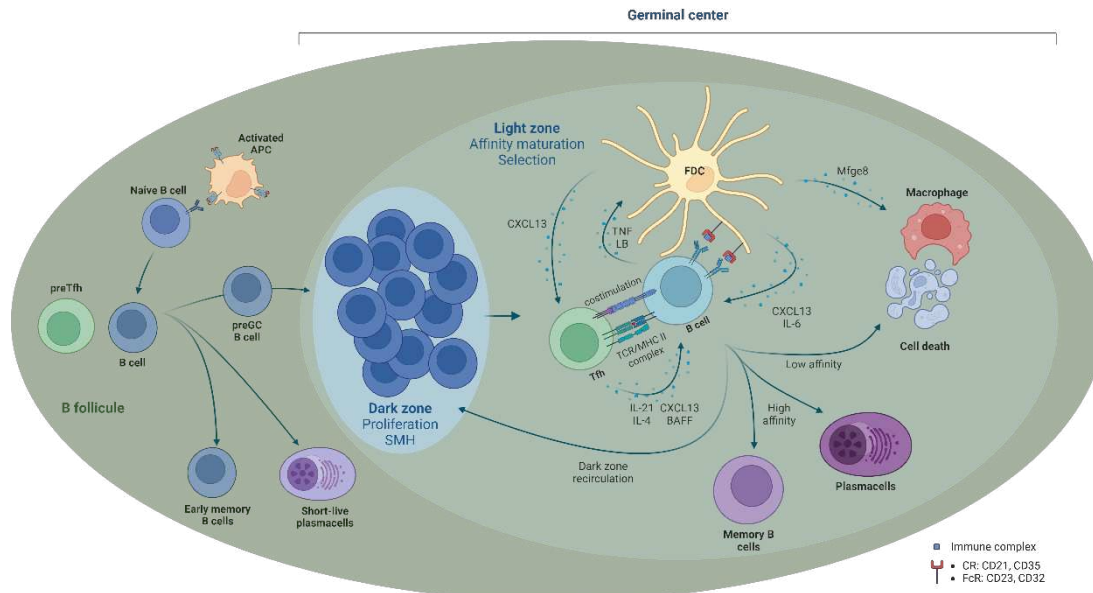


Figure 7 : Dynamique des processus de maturation et de sélection des cellules B au sein des centres germinatifs. APC : cellule présentatrice d'antigène. FDC : cellule dendritique folliculaire. CR : récepteur au complément. FcR : récepteur au partie Fc des anticorps. SMH : hypermutation somatique.

Bien que le rôle des cellules T dans la maturation des cellules B au sein des GC soit considéré comme le mécanisme principal contribuant à l'induction de cellules B mémoires et de plasmocytes à longue durée de vie, une activation des cellules B indépendante des LT existe. Cette réponse T-indépendante, implique des antigènes riches en motifs répétés comme les polysaccharides des bactéries ou des virus. Récemment des études ont mis en évidence les réponses T indépendantes étaient également capable d'induire la formation de GC et d'aboutir à la formation de cellules B mémoire et de plasmocytes à longue durée de vie (Liao et al., 2017a; Liu et al., 2022).

4) Un rôle central dans les réponses vaccinales

De par les différentes sous-populations et leurs fonctions impliquées dans l'orientation et la régulation de la réponse immune, les T CD4+ ont une position centrale dans la qualité des réponses vaccinales.

Galli *et al.*, Nayak *et al.*, ont montré que l'amplitude de la réponse T CD4+ induite respectivement par des vaccins contre la grippe H5N1 et H1N1, permet de prédire la persistance de la réponse anticorps neutralisantes (Galli *et al.*, 2009; Nayak *et al.*, 2013). Similairement, Bentebibel *et al.* ont corrélé l'abondance d'une population de cTfh ICOS+ CXCR3+ CXCR5+ avec l'augmentation de la réponse anticorps préexistante suite à l'injection d'un vaccin trivalent contre la grippe (Bentebibel *et al.*, 2013). Diverses études en « vaccinologie des systèmes » ont également mis en évidence l'association des LT CD4+ avec diverses composantes de la réponse vaccinale (Gorini *et al.*, 2020; J. Hou *et al.*, 2017). Notamment, Gorini *et al.* ont démontré que la vaccination Canarypox ALVAC-SIV recombinant chez des macaques rhésus induit une plus forte mobilisation des Th1 par rapport aux Th2 et que cette mobilisation corrèle avec les monocytes et un risque diminué d'acquérir le SIVmac251.

L'implication des LT CD4+ dans la qualité des réponses vaccinales a été récemment souligné par des études sur le rôle des LT CD4 mémoires préexistant à la vaccination (Campion *et al.*, 2021; Elias *et al.*, 2022). Elias *et al.* ont notamment montré que les LT CD4+ mémoires préexistant contre l'hépatite B permettent une induction plus rapide et plus ample d'anticorps mais également l'induction d'une réponse T CD4+ plus robuste.

III. Persistance de la réponse vaccinale : la mémoire adaptative

1) Génération de la mémoire adaptative

Comme évoqué précédemment, la première rencontre avec un pathogène ou une immunisation déclenche la mise en place d'une réponse primaire décomposée en plusieurs phases initiées par l'activation des LT CD4+ naïfs par les APC suivies par une phase de prolifération intense, de différenciation des cellules spécifiques et de la migration vers les sites d'infection. Une fois le pathogène éliminé, la phase de contraction marquée par une mort cellulaire par apoptose des cellules activées contribue à un retour à la normale et au maintien de l'homéostasie. Bien que la majorité des cellules activées vont être éliminées lors de la phase de contraction, une partie des cellules se différencie et perdure dans l'organisme pendant plusieurs années formant ainsi le compartiment mémoire. Lors d'une nouvelle infection par le même pathogène, une réponse secondaire

amplifiée se met en place, caractérisée par une activation plus rapide, plus intense et par des fonctions améliorées des cellules mémoires ([M. K. L. MacLeod et al., 2010](#); [Richer et al., 2013](#)). Ces propriétés résultent de divers phénomènes de maturations cellulaires mais également d'un seuil d'activation plus faible et moins dépendant des signaux de co-stimulation comparé aux cellules naïves.

A la différence des cellules naïves, les cellules mémoires possèdent une capacité de survie accrue et se caractérisent par une persistance à très long terme. En effet, des LT CD4+ mémoires spécifiques de la variole ont pu être détectées jusqu'à 83 ans après une infection ([Hammarlund et al., 2010](#)). Les cellules mémoires contribuent à la défense de l'organisme en circulant dans la périphérie et également dans les tissus. Cette distribution au plus proche des sites d'infection permet une activation plus rapide entraînant également une phase de prolifération plus intense. Les phénomènes d'amplification sont également liés aux capacités effectrices améliorées des cellules mémoires obtenues suite à des réarrangements génétiques. Ainsi les cellules mémoires, une fois activées, sécrètent des cytokines et d'autres molécules effectrices plus vite en plus grande quantité. Une multiplicité accrue des fonctions a également été observée.

Enfin, de la même manière que la réponse primaire, la phase de contraction élimine les cellules activées lors de la réponse secondaire alors qu'une partie des cellules spécifiques contribue à enrichir le compartiment mémoire.

2) Les différentes sous-population de lymphocytes mémoires

Les LT mémoires sont bien souvent identifiés à l'aide des marqueurs CD45RA, CD45RO et le récepteur de migration vers les ganglions lymphatiques CCR7. Les niveaux d'expression de ces marqueurs, combinés à des marqueurs d'activation, de migration ou à des capacités de prolifération ont ainsi permis l'identification de plusieurs sous populations de cellules mémoires : les centrales mémoires (Tcm), les effectrices mémoires (Tem), les effecteurs mémoires terminaux (Temra), les cellules souches mémoires (Tscm) et les cellules mémoires résidentes (Trm).

Les Tcm et les Tem, les premières populations mémoires identifiées, sont caractérisées par une expression de CD45RA- et de CD45RO+ mais présentent des profils opposés pour des marqueurs de migration ou d'homing tels que CCR7 et CD62L. Les Tcm ont

également conservé une forte capacité de prolifération après un second contact avec l'antigène alors qu'une prolifération intense est moins susceptible d'être observée pour les Tem. Le profil d'expression caractéristique des Tcm (CD45RA- CD45RO+ CCR7+ CD27+ CD62L+) est très similaire à celui des cellules naïves. Elles expriment le CD45RA (CD45RA+ CD45RO- CCR7+ CD27+ CD62L+) mais n'expriment pas les récepteurs de migration nécessaires à l'entrée dans les tissus à l'inverse des Tem qui peuvent migrer dans les tissus inflammés ([Masopust & Schenkel, 2013](#)). En conséquence, les cellules naïves et les cellules Tcm sont principalement restreintes à une circulation dans le sang et les organes lymphoïdes.

Par la suite, une population phénotypiquement et fonctionnellement proche des cellules naïves a été identifiée et décrite pour la première fois comme étant des Tsm par Zang *et al.* ([L et al., 2011](#); [Y. Zhang et al., 2005](#)). Ces cellules, expriment le CD45RA ainsi que de forts niveaux de molécules de co-stimulation (CD27/CD28) et de récepteurs de migration vers les ganglions tels que CD62L et CCR7. Elles diffèrent cependant des cellules naïves par l'expression des récepteurs de mort cellulaire CD95 et du marqueur mémoire CD122.

A l'inverse des Tem productrices de cytokines effectrices, les Tcm produisent uniquement de l'IL-2 ([L et al., 2011](#); [Sallusto et al., 2004](#)). Cependant, il a été démontré que les Tcm et les Tscm sont capables de produire d'autres cytokines effectrices telles que l'IFNy et le TNF mais avec des amplitudes différentes ([Sathaliyawala et al., 2013](#)). Les Tem produisent une importante quantité d'IFNy et de TNF et une plus faible quantité d'IL-2 alors qu'à l'inverse, les Tcm et les Tscm ont une plus forte production d'IL-2 et une expression d'IFNy et de TNF plus limitée.

Alors que l'expression de CD45RA a été associée à un phénotype peu différencié, il a été observé une réexpression du CD45RA par certaines cellules mémoires, les Temra. Les Temra sont une population hétérogène parmi les LT CD4+ dont la proportion varie entre individus ([Burel et al., 2017](#); [Tian et al., 2017](#)). De manière générale, ces cellules sont caractérisées par une baisse d'expression des molécules de co-stimulation CD27 et CD28, suggérant un état de différenciation avancée, ainsi qu'une augmentation de la cytotoxicité marquée par l'expression de CX3CR1, et de la production de molécules effectrices telles que la perforine et le granzyme B ([Weiskopf et al., 2015](#)).

Un dernier type de cellules mémoires, les Trm, caractérisées par leur localisation dans les muqueuses ou la peau et leur capacité de recirculation très réduite a également été identifié ([Schenkel & Masopust, 2014](#)). A la différence des cellules circulantes, les Trm ont un niveau plus élevé d'expression de CD69, qui intervient dans la dégradation du récepteur S1PR1 impliqué dans la recirculation des cellules, agissant donc comme un marqueur promouvant la rétention des cellules dans les organes ([Cyster & Schwab, 2012](#); [Shiow et al., 2006](#)). Les Trm et particulièrement les LT CD8+, sont caractérisées par l'expression du récepteur de résidence dans les tissus CD103. Ces cellules mémoires sont parmi les premières à intervenir lors d'une réinfection par leur capacité de réponse plus rapide et leur localisation au plus près des sites d'infection ([Mueller & Mackay, 2015](#)). Les Trm représentent la population mémoire la plus abondante et Sathaliyawala *et al.* ont pu mettre en évidence que la distribution des cellules mémoires et leurs capacité de production de cytokines varie en fonction des tissus ([Sathaliyawala et al., 2013](#)) (Figure 8).

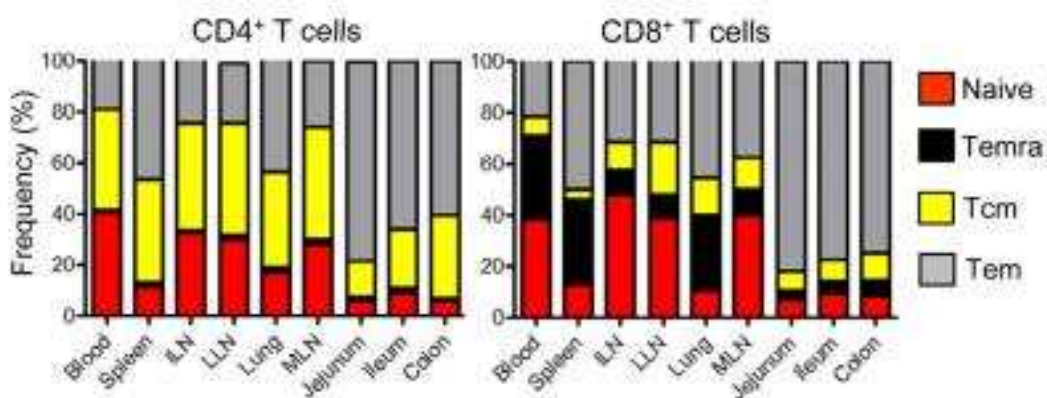


Figure 8 : Distribution des lymphocytes mémoire dans les différents tissus humain. Les cellules naïves sont définies par un phénotype CD45RA+ CCR7+, les Tcm CD45RA-CCR7+, les Tem CD45RA- CCR7- et les Temra CD45RA+ CCR7-. D'après ([Sathaliyawala et al., 2013](#)).

De la même manière, Gebhardt *et al.* ont mis en évidence des différences de distribution et de motilité entre les Trm CD4+ et les Trm CD8+ de la peau. Les Trm CD4+ sont plus mobiles et sont plutôt localisés dans le derme alors que les Trm CD8+ sont localisées dans l'épithélium et ont une mobilité restreinte ([Gebhardt et al., 2011](#)). L'origine des Trm est encore mal comprises mais récemment, Matos *et al.* ont établi que les Tcm sont les

précurseurs de Trm les plus compétents. Ils entrent dans la peau en plus grand nombre que les Tem et ont la capacité de générer plus de Trm (Matos et al., 2022).

Des études de prolifération et de différenciation des cellules mémoires ont mis en évidence que les Tcm et les Tscm constituaient un état intermédiaire entre les LT naïfs et les Tem par leur capacité de prolifération intense et leur importante plasticité. En effet, les Tcm ainsi que les Tscm ont gardé la capacité de générer différents effecteurs selon les signaux reçus (L et al., 2011; Pepper et al., 2011).

Cela a permis d'établir la graduation : naïve > Tscm > Tcm > Tem > Temra, où chaque population est capable de se différencier en n'importe quelle population plus avancée dans la maturation de la mémoire.

3) Les modèles de différenciation des LT mémoires

L'identification des différentes populations de cellules mémoires a soulevé de nombreuses questions quant à leur origine et leur évolution au cours d'une réponse primaire. Cette partie s'intéresse aux différents modèles de différenciation des cellules mémoires qui ont été proposés (Figure 9).

a) *Le modèle de différenciation linéaire*

Le modèle de différenciation linéaire représente le modèle le plus simple pour expliquer la formation de cellules mémoires. Il part du principe qu'une cellule naïve, après activation par l'antigène, subit une différenciation unidirectionnelle en cellules effectrices puis progressivement poursuit sa différenciation en cellules mémoires sous l'action de la signalisation TCR (Ahmed et al., 2009; Kaech et al., 2003).

Toutefois ce modèle suppose un passage effecteur/mémoire au cours de la phase de contraction ce qui implique qu'un mécanisme détermine l'orientation des effecteurs vers la mort ou la persistance. Kaech et al. ont proposé que le niveau de CD127 (IL-7Ra) exprimé par les effecteurs déterminait la différenciation en cellules mémoires. Plus récemment, des études épigénétiques portées sur les méthylations spontanées de l'ADN supportent ce modèle de différenciation (Ladle et al., 2016; Youngblood et al., 2017). Cependant, ce modèle présente des limites et n'explique pas l'émergence de populations mémoires telles que les Tscm qui présentent un phénotype peu différencié.

b) *Le modèle de différenciation divergente*

Le modèle divergent suppose qu'une cellule naïve peut donner forme à la fois à des cellules effectrices et de cellules mémoires par le biais d'une division asymétrique après activation. Ce seraient ces divisions asymétriques précoces qui détermineraient le devenir des cellules filles avec une distribution de facteurs de différenciation inégale. Ce phénomène a été démontré par Chang *et al.* en suivant la répartition des TCR après les premières divisions, dont les rôles dans la génération de la mémoire sera abordé ultérieurement (Chang et al., 2007). De plus, une étude réalisée chez la souris a montré que le transfert d'une cellule spécifique était capable de générer une grande diversité de cellules effectrices et de cellules mémoires (Stemberger et al., 2007).

c) *Le modèle de différenciation progressive*

Comme son nom l'indique, ce modèle suppose que la génération des populations effectrices et mémoires après activation d'une cellule naïve dépend de phénomènes de maturation progressifs. En effet, un certain nombre d'études ont, par exemple, observé un impact de la stimulation antigénique sur la différenciation cellulaire des populations effectrices et mémoires. Ainsi, une stimulation courte favorise le développement de Tcm alors qu'une stimulation plus longue induit la différenciation d'effecteurs et d'effecteurs mémoires.

Dans le cas des LT CD8+, le rôle des cytokines inflammatoires a également été mis en évidence par Richer *et al.* dans l'augmentation de la signalisation TCR conditionnant ainsi la différenciation des cellules effectrices et mémoires (Richer et al., 2013).

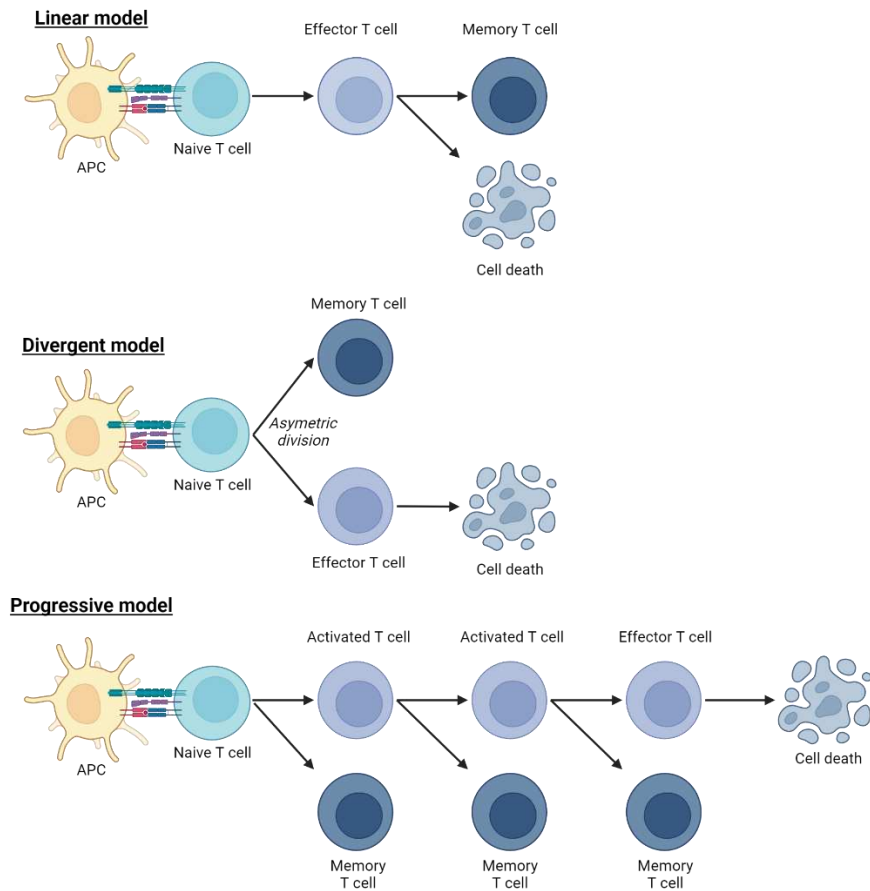


Figure 9 :Modèles de différenciation des cellules mémoires.

d) Compléments et variantes aux modèles

Les différentes études réalisées sur les cellules mémoires ont établi que de nombreux facteurs intervenaient sur leur génération, leur différenciation ainsi que sur leur persistance. Parmi ces facteurs, certains permettent d'élargir la définition et la compréhension des voies de différenciation des cellules mémoires et mettent en évidence une plasticité qu'il est parfois difficile d'imputer à un modèle en particulier. Par exemple, la génération de cellules effectrices n'est pas uniquement assurée par la différenciation des cellules naïves. En effet, les Tcm sont capables d'effectuer une réversion à un phénotype effecteur après stimulation (Lanzavecchia & Sallusto, 2002). Messi *et al.* ont également observé des différences épigénétiques déterminantes dans l'induction des Tcm et des Tem (Messi *et al.*, 2003). Toutefois, certaines études ont démontré que ces modifications de l'ADN n'étaient pas permanentes ce qui suggère qu'une réversion d'un phénotype mémoire à un autre est possible selon les conditions.

Ces différents mécanismes suggèrent également que des interventions différencieront au cours de la réponse immunitaire pourraient orienter le devenir potentiel d'une cellule en cellule mémoire. Ainsi, il est probable que les phénomènes de maturation de la mémoire résultent d'une combinaison de différents modèles de différenciation dont l'induction repose sur un ensemble de signaux.

4) Paramètres influant sur la mise en place de la mémoire T

Hammarlund *et al.* ont mis en évidence la capacité de LT CD4+ mémoires à perdurer dans l'organisme plus de 80 ans après une exposition à un pathogène ([Hammarlund et al., 2010](#)). Cela suppose la mise en place de mécanismes particuliers dans la génération, la différenciation et le maintien à long-terme des cellules mémoires. Dans cette partie, nous allons aborder divers facteurs intervenant dans la formation de la mémoire immunitaire pouvant amener à une telle persistance.

a) *La fréquence des lymphocytes T mobilisés lors de la réponse immunitaire*

Le nombre de cellules mobilisées en réponse à un agent pathogène influence les fonctions et le phénotype des cellules T mais également la formation de la réponse mémoire ([Kwok et al., 2012; Moon et al., 2007; Whitmire et al., 2008](#)). Polonsky *et al.*, ont montré que le nombre de LT CD4+ spécifiques mobilisés lors de la réponse intervient dans leur différenciation. Une forte densité de cellules spécifiques est aussi impliquée dans la différenciation d'une plus grande proportion de Tcm. Ces cellules conservent ce phénotype à au cours du temps après un transfert adoptif de LT CD4+ activés *in vitro* ([Polonsky et al., 2018](#)).

b) *L'existence de LT CD4+ mémoires spécifiques avant la rencontre avec le pathogène*

Outre la proportion de cellules mobilisées lors de la réponse immunitaire, il a été montré que l'existence et le nombre de LT CD4+ spécifiques, y compris des LT CD4+ mémoires, précédent la rencontre avec le pathogène est également susceptible d'influencer la qualité de la réponse immune et donc la formation du pool de cellules mémoires. En

effet, il a été mis en évidence que la formation de LT CD4+ mémoires spécifiques ne nécessite pas obligatoirement une première rencontre avec le pathogène mais peut également être détectée chez des individus naïfs. L'induction de ces cellules repose probablement sur des phénomènes de cross-réactivité des antigènes (Campion et al., 2014; Mateus et al., 2020; Su et al., 2013; Su & Davis, 2013).

Le rôle de ces LT CD4+ mémoires préexistant a été observé dans le cas d'études des vaccins Influenza, VIH mais également dans le cas du vaccin contre l'hépatite B où la présence de ces LT CD4+ mémoires a été associée avec une induction plus rapide d'anticorps à une réponse T CD4+ plus intense après la vaccination (Campion et al., 2021; Elias et al., 2022; Nienen et al., 2019).

c) *La signalisation via le TCR*

Comme mentionné précédemment, le signal TCR est primordial pour l'activation et la différenciation des LT CD4+ en Th mais est également déterminant dans la différenciation des cellules T en cellules mémoires.

En effet, Solouki et al. et Mercado et al. ont rapporté qu'une interaction du TCR, une intensité du signal et une affinité à l'antigène réduite des LT CD8+ sont associées au développement des cellules mémoires (Mercado et al., 2000; Solouki et al., 2020). Pareillement, Snook et al. ont démontré que la différenciation des LT CD4+ mémoires et Tfh était associée à un signal TCR faible et que la force du signal régule les fonctions des cellules mémoires via la transcription de NFAT et NFkB. Ces facteurs de transcription ont tous deux un impact sur la production de cytokines et l'expression de récepteur à l'IL-2 (Snook et al., 2018). La force du TCR régule aussi la production de cytokines par les effecteurs qui vont avoir un impact sur le développement des cellules mémoires (Solouki et al., 2020). Le rôle des cytokines, particulièrement de l'IL-2, dans la différenciation des cellules mémoires sera traité ultérieurement. Les travaux de Fiege et al. supportent également la différenciation des cellules mémoires avec une faible stimulation du TCR dans le cas de la formation de Trm dans les poumons (Fiege et al., 2019). En revanche, ils ont observé que la signalisation TCR n'impact pas le phénotype ou la persistance à long terme des Trm.

La détermination des phénotypes effecteurs ou mémoires apparaît donc fortement liée à la signalisation TCR dont l'intensité croissante permet détermine le devenir de la cellule naïve (Figure 10). Ainsi une stimulation insuffisante maintiendra le phénotype naïf, une augmentation du signal donnera lieu à la formation de Tscm, de Tcm suivie des Tem et une intensité forte donnera lieu à la formation de LT effecteurs ([Raeber et al., 2018](#)).

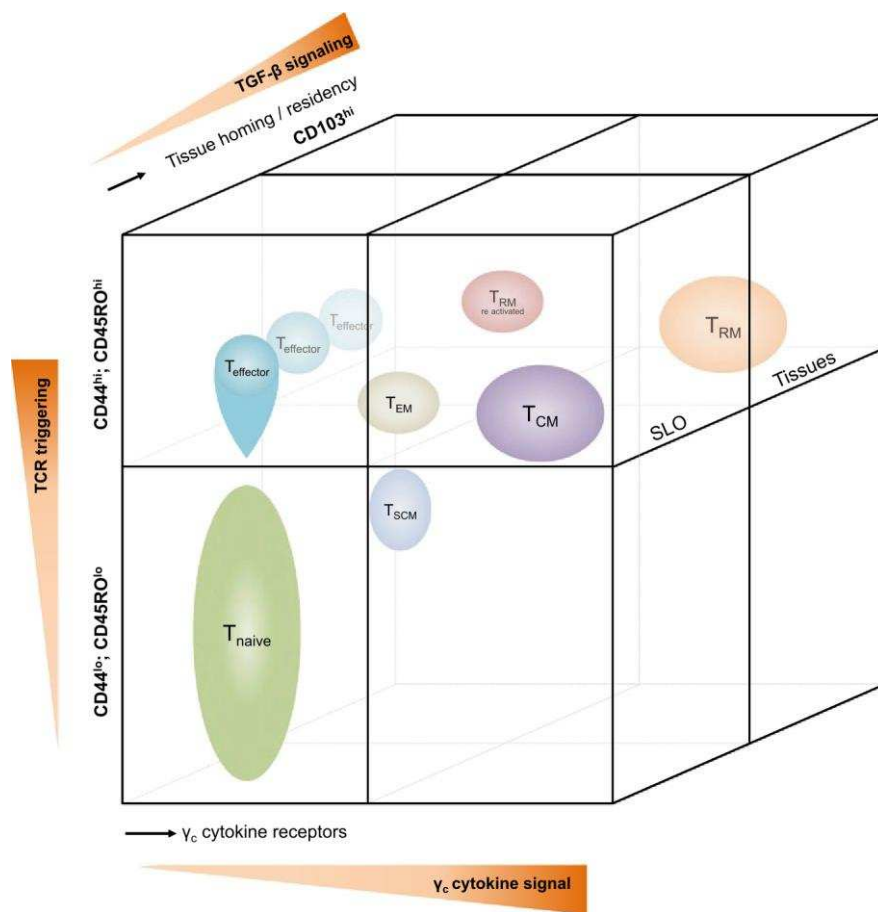


Figure 10: Facteurs déterminants la différenciation des sous populations de cellules mémoires. Les récepteurs de cytokines γ_c comprennent par exemple les récepteurs à l'IL-2 (CD122 : IL-2R β), l'IL-7 (CD127), l'IL-15 (IL-15R α) ou IL-21 (IL-21R α). SLO : Organe lymphoïde secondaire. D'après ([Raeber et al., 2018](#)).

Cependant, dans le cas des LT CD4+, des études suggèrent qu'un TCR de haute affinité est plus enclin à promouvoir l'expansion des LT spécifiques, augmentant ainsi le réservoir potentiel de cellules mémoires. A l'inverse, une faible affinité du TCR serait impliquée dans la génération de LT mémoires à courte durée de vie ([Whitmire et al., 2008](#); [M. A. Williams et al., 2008](#)). Obst *et al.* et McKinstry *et al.* ont mis en évidence que la

différenciation des LT CD4+ naïfs en cellules mémoires nécessite une exposition prolongée avec l'antigène (McKinstry et al., 2014; Obst et al., 2005). Cette opposition dans les observations suggère le fait que la signalisation TCR seule n'est pas suffisante pour définir et induire la différenciation des cellules mémoires.

d) *Rôle des molécules de co-stimulation*

Parallèlement au signal TCR, les molécules de co-stimulation interviennent dans la plasticité des populations T CD4+, l'orientation et la qualité des réponses ainsi que dans la génération de la mémoire immunitaire.

Parmi ces co-stimulations, on retrouve notamment l'interaction de CD28 avec les récepteurs CD80/CD86 exprimés par les APC. Cette interaction est à la base d'une sensibilité accrue des LT CD4+ avec le CMH-II nécessaire à l'expansion clonale et la génération des cellules mémoires. Elle induit également la transcription d'IL-2 et de facteurs de survie augmentant la prolifération et la survie des cellules (Pagán et al., 2012; Parry et al., 2003).

Similairement, MacLeod et al. ont démontré que l'amplitude des réponses primaires et la formation de la mémoire étaient dépendantes de l'interaction avec le CD40 (M. MacLeod et al., 2006). Bloquer l'interaction CD40/CD40L réduit la magnitude des réponses primaires et donc la formation de la mémoire. Koguchi et al. et Casamayor-Palleja et al. ont mis en évidence un stockage de CD40L par les cellules mémoires qui interviendrait dans les capacités d'activation plus rapides lors d'une réponse secondaire (Casamayor-Palleja et al., 1995; Koguchi et al., 2007, 2012).

Enfin, l'interaction du CD27 avec le CD70 exprimé par les APC est aussi un facteur déterminant de la génération des cellules mémoires. En effet, le traitement de souris avec des anticorps anti-CD70 induit une baisse d'expression d'IL-2 par les cellules effectrices ainsi qu'une baisse de l'expression de CD127 (IL-7Ra) induisant une altération de la génération de la mémoire (McKinstry et al., 2014). Ainsi, le signal de co-stimulation CD27/CD70 supporte la génération des cellules mémoires en augmentant la production d'IL-2 par les cellules effectrices (Figure 11).

Les différents signaux induits par le signal TCR et les molécules de co-stimulation induisent des activations ou inhibitions transcriptionnelles des cytokines régulant la plasticité et le devenir des cellules T (Solouki et al., 2020).

e) La signalisation par les cytokines

L'IL-2 a été identifié comme un paramètre clé dans la génération des cellules mémoires à long terme. En effet, l'IL-2 joue un rôle capital dans la prolifération et la survie des effecteurs cellulaires mais en son absence, ils subissent une phase de contraction rapide (Figure 11). Cette survie cellulaire médiaée par l'IL-2 entraîne une augmentation de l'expression de CD127, le récepteur de l'IL-7 impliqué dans le maintien du phénotype mémoire (McKinstry et al., 2014).

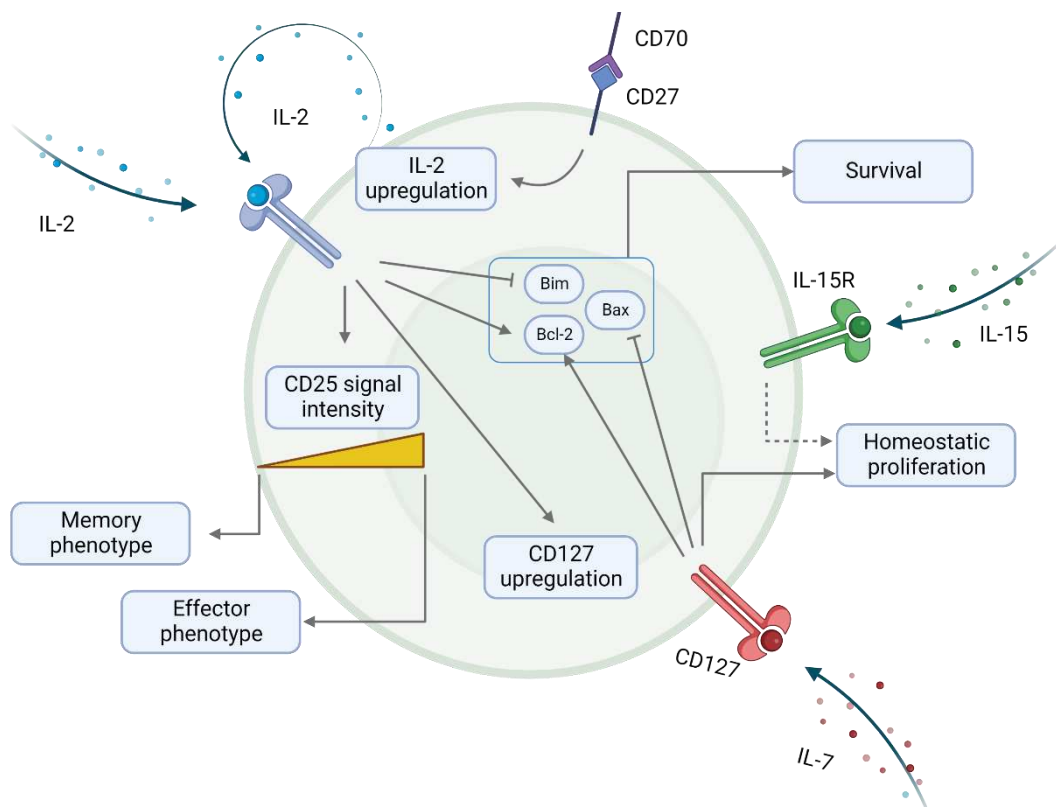


Figure 11: Impact des cytokines sur la différenciation et le maintien des lymphocytes T CD4 mémoires.

En conséquence, l'expression du CD25 (sous unités α du récepteur à l'IL-2) intervient lui aussi comme un facteur clé dans la génération des cellules mémoires. Dans un modèle

de souris déficientes en CD25, Pepper *et al.* ont observé que la différenciation des Th1 effecteurs mémoires et des Tfh centraux mémoires est associée respectivement à une forte ou une faible expression du CD25 (Pepper *et al.*, 2011). Cette différenciation dépendante de CD25 a également été observée plus récemment par Snook *et al.* qui ont pu établir un lien de prédiction entre l'expression du CD25 et le nombre de cellules T mémoires (Snook *et al.*, 2018). Ils ont cependant observé que les cellules mémoires dérivant d'effecteurs CD25^{lo} ou CD25^{hi} étaient capables de répondre similairement après stimulation.

f) Épigénétique de la mémoire des LT CD4

En réponse aux différents stimuli, les cellules T naïves s'engagent dans une voie d'activation et de différenciation conditionnée par des cascades de signalisations donnant lieu à l'expression ou à la répression de gènes. Ces régulations génétiques sont dictées par l'ouverture ou fermeture de la chromatine contrôlée par les histones permettant ainsi l'accès aux gènes devant être exprimés. En conséquence, de nombreuses études se sont concentrées sur les mécanismes génétiques associés à la différenciation des effecteurs ainsi qu'aux modifications épigénétiques intervenant dans le passage et au maintien du phénotype mémoire.

Malgré leur rôle central dans les réponses immunitaires, beaucoup d'études sur l'épigénétique de la mémoire ont été réalisées au sein des LT CD8+. Ainsi il a été mis en évidence une dynamique de méthylation et de déméthylation des gènes des LT CD8+ naïfs, conduisant à une différenciation en cellules mémoires à longue durée de vie (Ladle *et al.*, 2016; Youngblood *et al.*, 2017). Akondy *et al.* ont également identifié une persistance à long terme des modifications épigénétiques des cellules T CD8 mémoires puisque des gènes effecteurs associés à une ouverture de la chromatine ont été observés plusieurs années après la vaccination contre la fièvre jaune (Akondy *et al.*, 2017).

Toutefois, un nombre croissant d'études sur les mécanismes génétiques associés aux LT CD4+ contribuent à une plus grande compréhension de la plasticité de ce compartiment cellulaire. Par exemple, des hyperacétylation de l'histone H3 au niveau des loci *Ifng* et *Il4* des LT CD4 ont été observées permettant le maintien des fonctions Th1 et Th2 au sein des cellules mémoire. Le maintien des fonctions Th2 est indépendant du signal IL-4 (Messi *et al.*, 2003; Yamashita *et al.*, 2004). Messi *et al.* ont également pu mettre en

évidence des différences épigénétiques entre les populations mémoires avec une acétylation des gènes de cytokines pour les cellules effectrices mémoires alors que les cellules centrales mémoires présentent des gènes de cytokines hypoacétylés.

Plus récemment, de multiples signatures génétiques liées à la différenciation ainsi qu'à la persistance à long terme des LT CD4+ mémoires ont été identifiées chez la souris. Parmi ces gènes on retrouve notamment l'expression de gènes intervenant dans l'inhibition de la prolifération et de l'apoptose mais également dans la réparation de l'ADN ([Song et al., 2020](#)).

En outre, il a été montré que ces modifications épigénétiques sont également à la base de mécanismes évolutifs tel qu'observé chez les singes verts africains. En effet, des méthylations de l'ADN au niveau du locus *Cd4* ont été associés à une diminution de l'expression de ce gène et une acquisition de fonctions cytotoxiques chez les LT CD4+ mémoires, conférant ainsi une résistance naturelle au virus de l'immunodéficience simienne ([Rahmberg et al., 2022](#)).

g) Rôle de la phase de contraction

Lors d'une réponse immunitaire, l'élimination des pathogènes déclenche une réduction de l'activité des cellules effectrices et marque le point de départ de la phase de contraction. Cette phase est caractérisée par une apoptose cellulaire intense induite soit par l'engagement des récepteurs de mort cellulaire soit par absence de signalisation externe par les cytokines.

Jay *et al.* ont mis en évidence une augmentation de l'expression du facteur de transcription pro-apoptotique Bim, intervenant dans l'élimination des cellules Th1 de faible affinité ([Jay et al., 2013](#)). Ce mécanisme permet une sélection des clones avant une différenciation en cellules mémoires.

La baisse de la dose d'antigène au cours de la contraction a également été identifiée comme facteur initiateur de la réduction d'activité des cellules effectrices. Cela se traduit par le biais d'une diminution de l'engagement du TCR dont l'intensité du signal est également un facteur clé dans la différenciation des cellules mémoires ([Dalai et al., 2011; Sadegh-Nasseri et al., 2010; Snook et al., 2018; Solouki et al., 2020](#)).

5) Paramètres de maintien et d'homéostasie de la mémoire des LT

En l'absence d'antigène, les cellules mémoire basculent dans un état quiescent et persistent sur de longues périodes dans l'attente d'une nouvelle rencontre avec l'antigène. La persistance et le maintien à long terme des cellules mémoires constitue un des objectifs primordiaux de la vaccination. De nombreuses questions sont encore sans réponse quant aux mécanismes régissant le maintien et l'homéostasie des cellules mémoires.

De nombreuses études ont souligné l'importance de la moelle osseuse en tant que haut lieu de persistance de la mémoire à long terme via un autorenouvellement permanent et une recirculation constante des cellules mémoires (Baliu-Piqué et al., 2018). Des études fonctionnelles ont également souligné une proportion plus importante de cellules mémoires polyfonctionnelles au sein de la moelle osseuse (Herndler-Brandstetter et al., 2011). Cependant, la majorité des cellules T mémoires n'est pas stockée dans la moelle osseuse mais dans les tissus non-lymphoïdes (Sathaliyawala et al., 2013), ce qui soulève la question du type de cellules mémoires qui persistent dans la moelle osseuse. Okhrimenko et al. ont apporté une réponse à cette question en démontrant une spécificité de la moelle osseuse pour la maintenance des cellules mémoires spécifiques des pathogènes systémiques (Okhrimenko et al., 2014).

Parmi les mécanismes de maintien les mieux documentés, on retrouve la dépendance de la signalisation par l'IL-7 et l'IL-15, produite par l'environnement des cellules mémoires (Figure 11). L'implication de ces deux cytokines a été récemment soulignée *in vitro* par Yurova et al. dans la régulation de l'apoptose cellulaire induite par l'activation (Yurova et al., 2020). La fixation de l'IL-7 sur son récepteur, le CD127 (IL-7Ra), favorise la survie en augmentant l'expression de Bcl2 et en diminuant celle de Bax, respectivement des facteurs anti et pro-apoptotiques (Khaled et al., 2002; Kondrack et al., 2003; J. C. Li et al., 2003). Toutefois, bien que l'importance de l'IL-7 ait été démontrée pour les deux grandes populations de cellules T, le rôle de l'IL-15 ne semble pas indispensable pour les LT CD4+ comparé aux LT CD8+, possiblement en raison d'une plus faible expression du récepteur à l'IL-15 (CD122) par les LT CD4+ (J. T. Tan et al., 2002; X. Zhang et al., 1998). Nolz et Harty ont observé des mécanismes épigénétique favorisant la survie des LT CD8

mémoires en permettant l'augmentation de l'expression de gènes associé à l'IL-15 ainsi qu'à leur migration dans les tissus producteurs d'IL-15 ([Nolz & Harty, 2014](#)).

L'impact de la signalisation TCR sur l'homéostasie des LT mémoires demeure controversé. En effet, McKinstry *et al.* ont suggéré que la signalisation TCR influencerait la génération et la persistance des LT CD4+ mémoires ([McKinstry et al., 2014](#)). A l'inverse Fiege *et al.* ont démontré que la signalisation TCR n'impactait pas le maintien à long terme de Trm dans les poumons ([Fiege et al., 2019](#)). Cependant, dans cette étude, les auteurs se sont focalisés sur les LT CD8+ or il a été rapporté que cette population n'est pas dépendante de la stimulation antigénique pour induire la persistance, contrairement aux LT CD4+.

Initialement les cellules mémoires ont été définies comme capables de persister même en l'absence d'antigènes mais des expositions répétées dans des zones endémiques contribuent à renforcer le stock de cellules mémoires spécifiques. Certaines cellules telles que les FDC étant capables de stocker des antigènes pour la maturation d'affinité des cellules B, cela soulève la question d'un mécanisme similaire ou d'une persistance et/ou d'une réactivation de l'antigène, impliqué dans le maintien de la mémoire.

Récemment, une étude de Song *et al.* s'est concentrée sur l'identification de ces mécanismes de persistance à long terme des LT CD4+ mémoires chez la souris ([Song et al., 2020](#)). Les auteurs ont notamment mis en évidence un profil d'expression de gènes dès l'activation des LT CD4+ qui perdure au niveau des cellules mémoires impliquant : l'inhibition de l'apoptose, ainsi qu'une augmentation de la capacité des cellules à répondre aux dommage de l'ADN mais également en réduisant la prolifération et l'activation. De nouveaux marqueurs de surface associés aux cellules mémoires ont également été identifiés tels que CD99, CCR10 et Itga3, également retrouvés chez l'Homme. Enfin, les auteurs ont mis en évidence une transition au sein des cellules mémoires T CD4 du métabolisme du glucose vers celui des lipides.

Les mécanismes identifiés par cette étude élargissent notre compréhension de la persistance de la mémoire T CD4 et apportent ainsi de nouvelles pistes pour le design de nouveaux vaccins.

6) Un rôle potentiel de la mémoire innée dans le maintien de réponses protectrices

Traditionnellement, la définition de la mémoire immunitaire repose sur la persistance à long terme de la protection contre un pathogène via la formation d'un compartiment de cellules spécifiques. Toutefois, un nombre croissant d'études ont mis en évidence des modifications au niveau des cellules innées leur conférant des capacités de réponse améliorées aux pathogènes. Cela a notamment été démontré dans le cas de la vaccination BCG où l'immunisation par un vaccin est capable de fournir une protection croisée contre d'autres vaccins ([Arts et al., 2018; Goodridge et al., 2016](#)). En tenant compte de ces phénomènes innés, Netea *et al.* ont ainsi proposé une nouvelle définition de la mémoire immunitaire comme tout changement du système immunitaire après une infection ou vaccination menant à une réponse améliorée en cas de réinfection ([Netea et al., 2019](#)). Ces aspects ne sont pas traités dans notre document mais ouvrent de nouvelles perspectives pour la modulation de la réponse vaccinale.

IV. La biologie des systèmes comme outils d'exploration et de compréhension des mécanismes de la réponse vaccinale

1) La vaccinologie des systèmes

L'administration d'un vaccin se caractérise par une multitude de réactions en chaîne et d'interactions complexes du système immunitaire à différentes échelles.

Dans une étude transcriptomique sur l'influence du polymorphisme génétique sur la réponse vaccinale, Poland *et al.* ont été parmi les premiers à aborder l'intérêt des technologies à haut débit dans la caractérisation des interactions du système immunitaire au cours de la vaccination. Ils ont également évoqué le terme de « vaccinologie prédictive » ([Poland et al., 2007](#)), par la suite appelé « vaccinologie des systèmes ».

Un des objectifs principaux de la vaccinologie des systèmes consiste à identifier des signatures vaccinales caractéristiques qui diffèrent statistiquement entre les individus immunisés et non-immunisés. Les premières études de vaccinologie des systèmes employaient majoritairement des profils transcriptomiques dans leurs modèles de prédiction. Plus récemment, les paramètres étudiés se sont diversifiés, incluant de

nouvelles données moléculaires telles que les cytokines ou des métabolites mais également le phénotype et les dynamiques des populations cellulaires.

En associant différentes technologies telles que le séquençage, la protéomique, la métabolomique, la cytométrie ou encore l'imagerie corps entier avec de puissantes approches bio-informatiques et statistiques, la vaccinologie des systèmes vise à identifier des biomarqueurs et signatures pouvant être utilisés pour établir des modèles prédictifs de la réponse vaccinale (Figure 12).

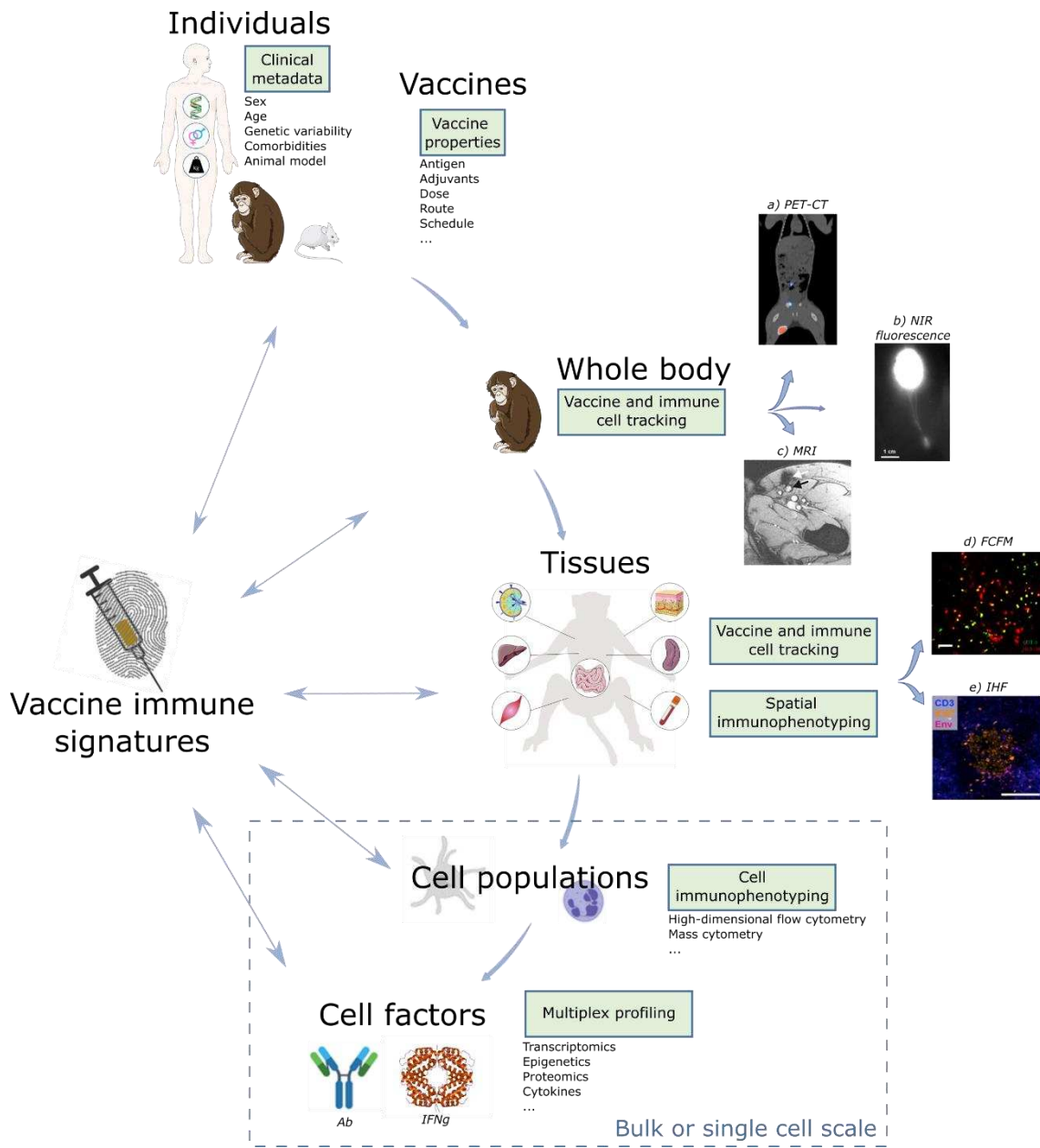


Figure 12: La vaccinologie des systèmes : de l'individu à la cellule. Intégration de techniques à différentes échelles pour aider à définir et comprendre des signatures vaccinales. D'après (Van Tilbeurgh et al., 2021).

2) Application de la vaccinologie des systèmes pour améliorer et accélérer le design de candidat vaccin

De nombreux vaccins actuels ont été développés sans connaître les mécanismes sous-jacents de l'efficacité et de la protection, aujourd'hui partiellement identifiés grâce à des analyses rétrospectives.

L'analyse des réponses anticorps a largement été employée pour évaluer l'efficacité des vaccins et a souvent permis l'identification de biomarqueurs prédictifs induits au cours de la première semaine suivant l'activation (S. Li et al., 2014). Cependant, bien que ces réponses peuvent être considérées comme des corrélats de protection fiables pour des pathogènes stables, leur utilisation est remise en cause pour des pathogènes présentant une grande diversité ou des vaccins dont la protection est médiée par la réponse cellulaire. Les réponses anticorps peuvent être générées selon des voies dépendantes ou indépendantes des LT suggérant que d'autres biomarqueurs pourraient corrélérer avec la protection (Liao et al., 2017b).

Ce point a d'ailleurs été souligné par Chaudhury et al. dans le cas d'un modèle vaccinal contre la malaria dans laquelle l'étude des anticorps ne permet pas d'identifier des différences de réponse entre les différentes formulations vaccinales (Chaudhury et al., 2018). Ils ont cependant identifié des signatures cytokiniques (IL-4 et IL-6) comme étant des variables importantes entre différents tissus. Dans leur étude sur le vaccin contre la fièvre jaune, Querec et al. ont identifié une signature transcriptomique précoce, incluant notamment la protéine du complément C1qB, prédictive de la réponse T CD8+ spécifique (T. D. Querec et al., 2009). Les auteurs ont donc mis en évidence l'intérêt de la vaccinologie des systèmes pour prédire d'autres caractéristiques que la réponse anticorps, importante pour les vaccins à médiation cellulaire.

Les réponses vaccinales sont également dépendantes de nombreux facteurs. En effet, la composition des vaccins, en particulier les immunogènes et les adjuvants, ou les voies d'injection, influencent la dynamique des paramètres immunitaires, modifiant ainsi les signatures vaccinales (S. Li et al., 2014). Comprendre ces signatures permettrait de favoriser le développement de vaccins efficaces. À titre d'exemple, dans un modèle de vaccination contre la grippe avec ou sans l'adjuvant MF59, Nakaya et al. ont mis en avant une signature transcriptomique et LT CD4+ particulière pour le vaccin adjuvanté (Nakaya et al., 2016). Par ailleurs, Hagan et al. ont démontré que des variations du microbiote intestinal influencent la réponse vaccinale, devenant donc une source potentielle de biomarqueurs (Hagan et al., 2019). L'utilisation de la vaccinologie des systèmes intègre donc de plus en plus de facteurs susceptibles d'influencer la qualité d'une réponse

vaccinale et permet une comparaison profonde de ces modalités contribuant ainsi à élargir les connaissances des mécanismes associés à la protection.

Enfin, certaines études soulignent l'intérêt de la vaccination personnalisée avec notamment l'identification de signatures prédictives de la réponse vaccinale avant immunisation ([Suloway et al., 2005](#); [Tsang et al., 2014](#)). Pogorelyy *et al.* ont également mis ce concept en avant en identifiant des répertoires TCR spécifiques différents chez des jumeaux homozygotes vaccinés contre la fièvre jaune ([Pogorelyy et al., 2018](#)).

Bien que souvent plus complexes, les études de vaccinologie des systèmes apparaissent comme prometteuses pour l'identification de nouveaux marqueurs clés des réponses vaccinales. Appliquer de telles approches aux modèles précliniques représente un grand intérêt dans l'identification de biomarqueurs prédictifs. En effet, identifier des signatures d'efficacité vaccinale permettrait de déterminer dès les étapes précoces de développement si un candidat vaccin a le potentiel d'induire une réponse efficace et donc de réduire le temps et les coûts de développement. De plus, identifier de tels biomarqueurs dans des modèles précliniques, en particulier les PNH, permettrait de faciliter la transposition des résultats chez l'Homme permettant ainsi d'améliorer nos connaissances des mécanismes de protection et d'accélérer le développement de vaccins.

Dans une revue présentée en annexe, nous avons traité de manière plus exhaustive l'utilisation de la vaccinologie des systèmes et l'éventail de technologies qu'elle utilise pour explorer la réponse vaccinale dans le but d'améliorer le design de nouveaux candidats vaccins.

B. PROJET DE RECHERCHE

I. Objectifs

L'amélioration de notre connaissance des multiples interactions survenant entre les différents acteurs moléculaires et cellulaires de la réponse immunitaire nous ont permis d'accroître notre compréhension des réponses induites par les vaccins actuels et de mettre en évidence des cibles potentielles pour le design de vaccins futurs.

La réponse anticorps est particulièrement importante dans la vaccination. Nous nous sommes donc intéressé aux facteurs précoce qui modulent cette réponse. Si l'importance de l'immunité innée dans l'induction et l'orientation des réponses adaptatives, notamment celle du compartiment T CD4, est communément admise, les mécanismes précoce déterminants la qualité de la réponse humorale sont encore mal compris. Il en va de même pour leur implication dans les mécanismes de persistance de la mémoire qui sont encore controversés.

L'identification et la caractérisation des nombreuses sous-populations T auxiliaires a permis d'établir le rôle central des LT CD4+ dans l'orientation et la régulation de la réponse effectrice. Néanmoins, une question concernant l'identification des mécanismes génétiques, fonctionnels et phénotypiques permettant de différencier les populations de LT CD4+ spécifiques à court terme et mémoire à long terme reste encore sans réponse. L'implication des LT CD4+ dans la persistance de la protection, humorale ou cellulaire, est également sous-documentée. Enfin, La majorité des études sur la persistance de la mémoire ont été conduite sur les LT CD8+ mais comme nous venons de le voir, certaines études soulignent des mécanismes de maintien de la mémoire différents entre les LT CD8+ et les LT CD4+.

Notre projet vise à fournir des éléments permettant d'accroître nos connaissances des mécanismes précoce déterminants la qualité des réponses humorales, leurs fonctionnalités et leur durabilité dans le cadre de la vaccination.

Dans un premier temps nous avons abordé la thématique de la qualité de la réponse humorale dans un modèle de vaccination VIH. En effet, le défi dans cette infection repose sur l'induction d'anticorps neutralisants à large spectre pour palier à la grande diversité

du VIH, mais également d'anticorps avec de puissantes fonctions effectrices. Nous avons essayé de comprendre comment les modulations de la réponse innée précoce par des voies d'injections et des adjuvants avec des propriétés d'adressage et de stimulation des APC différentes pouvait impacter la réponse neutralisante. Pour cela nous avons étudié l'amplitude de la réponse anticorps, les capacités de neutralisation et à induire la cytotoxicité cellulaire dépendante des anticorps (ADCC). A l'aide du modèle de vaccination contre le VIH chez des PNH nous essayons de répondre aux questions :

- Quels sont les populations cellulaires innées mobilisées par la vaccination en fonction de la voie et de l'adjuvant ?
- Quel impact de ces populations sur la qualité de la réponse anticorps ?
- Quels sont les biomarqueurs innés précoces de la réponse humorale ?

Dans un second temps nous avons cherché à explorer les mécanismes précoces de la réponse T CD4+ impliqués dans la durabilité de la réponse anticorps en utilisant le vaccin contre la fièvre jaune (YFV) comme modèle d'étude chez les PNH. En effet, une seule injection confère une protection à vie avec un titre anticorps protecteur détectable plusieurs décennies. Avec ce modèle nous avons cherché à répondre aux questions :

- Quelles sont les populations LT CD4+ mobilisées par la vaccination et quelle est leur persistance ?
- Quelles sont les caractéristiques des cellules spécifiques ? Quelles sont leurs fonctions ? Comment évolue le compartiment spécifique au cours du temps ?
- Quel est l'impact de la réponse T CD4+ précoce sur l'induction et la persistance de la réponse humorale ?
- Quels sont les biomarqueurs précoces de la réponse T CD4+ associés à la persistance de la réponse humorale ?

Pour répondre à ces différentes questions nous avons employé un large panel de techniques d'exploration de la réponse immunitaire incluant la réponse humorale pour en déterminer l'amplitude, la capacité de neutralisation, la fonctionnalité et la persistance. A l'aide de la cytométrie de masse nous avons caractérisé les réponses

systémiques innée et adaptatives induites par les différents vaccins. Enfin nous avons réalisé un dosage des cytokines plasmatique dans le but d'étudier son impact sur la qualité de la réponse adaptative et la persistance des anticorps.

II. Modèles expérimentaux

1) Modèle primate non humain (PNH)

Bien que la vaccinologie des systèmes ai pour objectif final de développer des modèles de prédiction d'efficacité vaccinale chez l'Homme, employer cette approche dans les modèles animaux permet de tester plusieurs hypothèses au stade préclinique. Ces approches permettent notamment d'intégrer des temps très précoces de prélèvements ainsi que des données obtenues par des prélèvements tissulaires. Les modèles de PNH, de par leur proximité phylogénétique avec l'Homme et leur capacité à reproduire la physiopathologie humaine constituent des modèles de prédilection en vaccinologie (Bjornson-Hooper et al., 2022). La vaccinologie des systèmes appliquée à des modèles PNH permet ainsi l'identification de biomarqueurs et le développement de modèles prédictifs plus facilement transposables à l'Homme.

Pour ce projet, nous avons choisi le modèle du macaque cynomolgus (*Macaca fascicularis*) originaire de l'île Maurice. L'introduction des macaques cynomolgus sur l'île Maurice est relativement récente (environ 500 ans) à partir de quelques dizaines d'individus ce qui a eu pour conséquence de limiter la diversité génétique de l'espèce. Cela se caractérise notamment par un polymorphisme restreint, particulièrement au niveau du CMH, favorisant l'homogénéité des observations faite lors des études sur ces animaux (Ogawa & Vallender, 2014).

Les macaques cynomolgus reproduisent la dynamique de la réponse immunitaire ainsi que la pathologie humaine à la fièvre jaune (Bryant et al., 2007; Monath, 2001; Moreno et al., 2013) ou au SIV (Cavarelli et al., 2021; le Grand et al., 2016). Une étude comparative entre le model du macaque cynomolgus et l'Homme réalisée au CEA en collaboration avec Sanofi Pasteur, a non seulement démontré que la souche sauvage et vaccinale du YFV reproduisent la dynamique de réponse anticorps neutralisante contre YFV observée

chez l'Homme (Figure 13). De la même manière, par une approche transcriptomique l'équipe a décrit la similarité des réponses impliquant des gènes liés à la réponse IFN ou encore à l'activation des DC suite à la vaccination (Figure 13C).

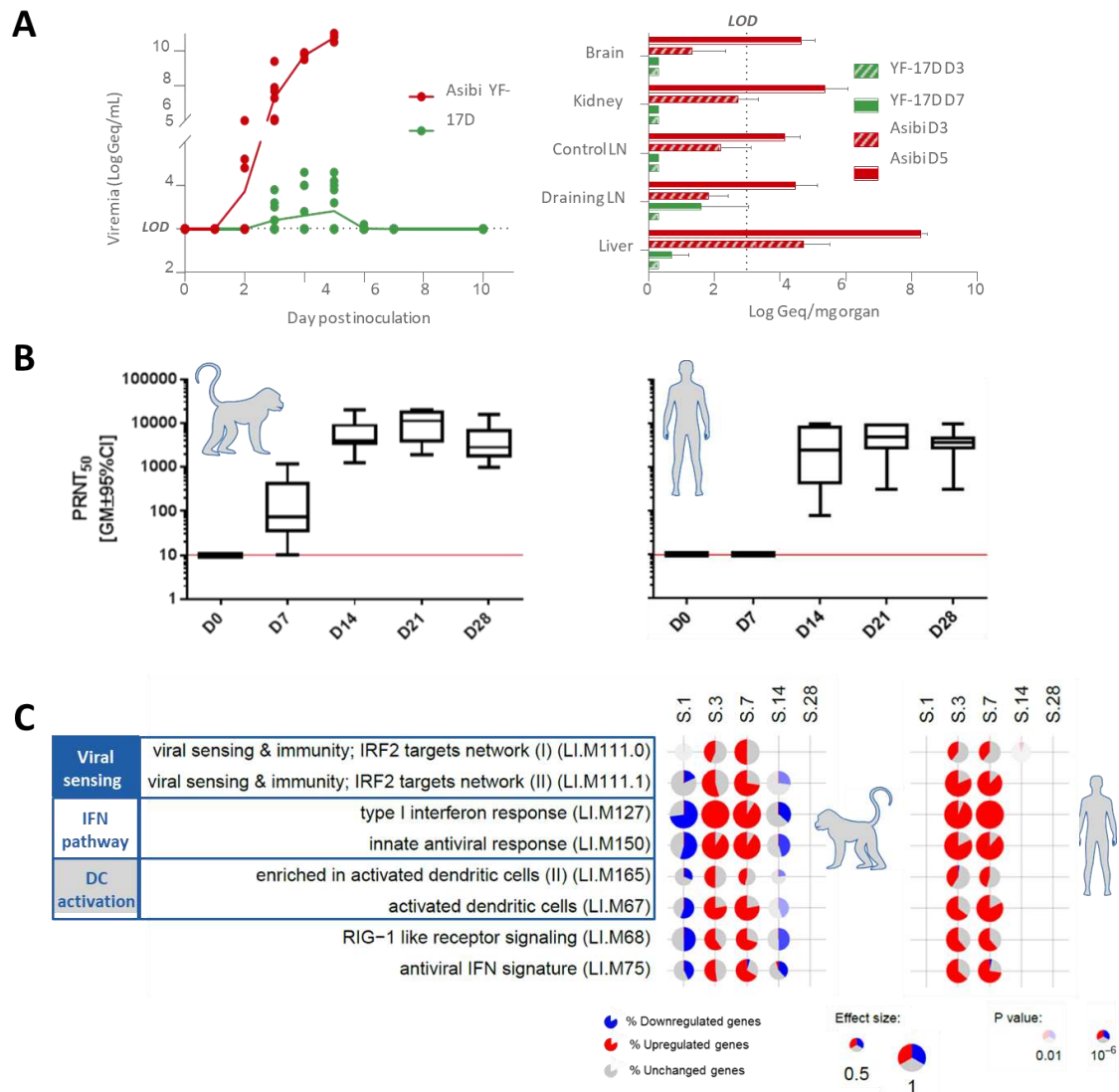


Figure 13: Pertinence des macaques cynomolgus comme modèles préclinique dans le cadre de la vaccination fièvre jaune. (A) : Charge viral chez le macaque cynomolgus après inoculation du YFV sauvage (souche Asibi) ou vaccinal (YF-17D). Comparaison entre le macaque cynomolgus et l'Homme du titre en anticorps neutralisants (B) et de la réponse transcriptomique (C) suite à une inoculation du YFV. D'après Mantel et al. in preparation.

2) Modèles vaccinaux

a) *ConM SOSIP.v7 comme plateforme vaccinale contre le VIH*

Les protéines SOSIP sont des glycoprotéines trimériques développées pour mimer la glycoprotéine d'enveloppe du VIH (Env). L'évolution des protéines SOSIP est marquée par une succession de mutations de la séquence d'acides aminés ayant pour objectif de favoriser l'exposition d'épitopes d'anticorps neutralisants et d'anticorps neutralisants à large spectre ([Sanders & Moore, 2017](#)). Certaines de ces mutations telles que la substitution Ile559P, permettent l'insertion d'un pont disulfure entre les sous-unités gp120 et gp41 ([Binley et al., 2000](#)), stabilisant ainsi la protéine dans une forme de préfusion. De manière similaire, une substitution A316W va permettre de limiter l'exposition d'épitopes non neutralisants en masquant la boucle V3 ([de Taeye et al., 2015](#)).

Afin de favoriser l'induction d'une grande diversité d'anticorps neutralisants ou d'anticorps neutralisants de large spectre, la protéine SOSIP utilisée dans notre étude a été développée à partir de séquence consensus du groupe M. Cette SOSIP, appelé ConM SOSIP.v7 a démontré chez le lapin et le modèle macaque une forte capacité à induire des réponses neutralisantes ([Sliepen et al., 2019](#)).

Nous avons utilisé ce vaccin pour étudier l'impact des voies d'injection et des combinaisons des adjuvants sur la réponse anticorps et les marqueurs précoces associés.

Pour étudier l'immunité innée en réponse à la vaccination VIH et son impact sur la qualité de la réponse humorale, les ConM SOSIP.v7 ont été administrées à trois groupes de six macaques cynomolgus selon des modalités différentes.

Nous avons vu précédemment que la colonisation en APC des tissus était en mesure d'induire des réponses vaccinales différentes aussi nous avons choisi d'injecter les vaccins par les voies intramusculaire et intradermique, appliquées pour la majorité des vaccins. De la même manière, les adjuvants sont eux aussi capables d'influencer la réponse vaccinale ainsi, un agoniste du TLR4, le monophosphoryl-lipide A (MPLA) et une émulsion de squalène (SQ) similaire à l'adjuvants commercial MF59 ont été sélectionné pour leur capacité à induire de forte réponse humorale. Les trois vaccins se présentent avec les formulations suivantes :

- ConM SOSIP.v7 + Injection intramusculaire + MPLA
- ConM SOSIP.v7 + Injection sous-cutanée + MPLA
- ConM SOSIP.v7 + Injection intramusculaire + SQ

Chaque vaccin est administré selon une stratégie « prime-boost » en trois injections avec la deuxième et la troisième effectuées respectivement, 8 et 28 semaines après le prime.

b) Vaccin anti-Amaril ou vaccin contre le virus de la fièvre jaune : le « gold standard » de la vaccination

Le vaccin contre la fièvre jaune commercialisé aujourd’hui est un vaccin vivant atténué (souche YFV-17D-204), développé en 1937 par Max Theiler à partir du virus sauvage, souche Asibi. Il est composé d’une capsid icosaédrique et d’un ARN viral simple brin de polarité positive d’environ 11000 nucléotides (Figure 14).

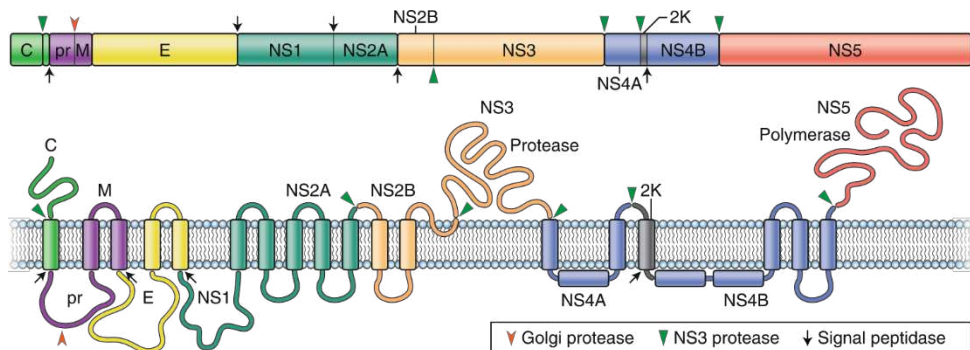


Figure 14: Schéma du génome du virus de la fièvre jaune. Le génome viral se compose d'un cadre ouvert de lecture ou « Open Reading Frame (ORF) » codant une polyprotéine qui, après clivage par des protéases cellulaires et virales, va former trois protéines structurales : capsid (C), prémembranaire/membranaire (prM) et d'enveloppe (E) et sept protéines non-structurales (NS1 à NS5). D'après (Pierson & Diamond, 2020).

La souche vaccinale a été atténuée par passages successifs au sein de cellules de macaques rhésus puis sur des cellules d’embryons de poulet dépourvus de tissus nerveux (Figure 15). Ces passages successifs ont respectivement permis de réduire le tropisme viscéral et d’induire une perte du neurotropisme de la souche virale chez l’Homme conférant ainsi l’innocuité de ce vaccin vivant.

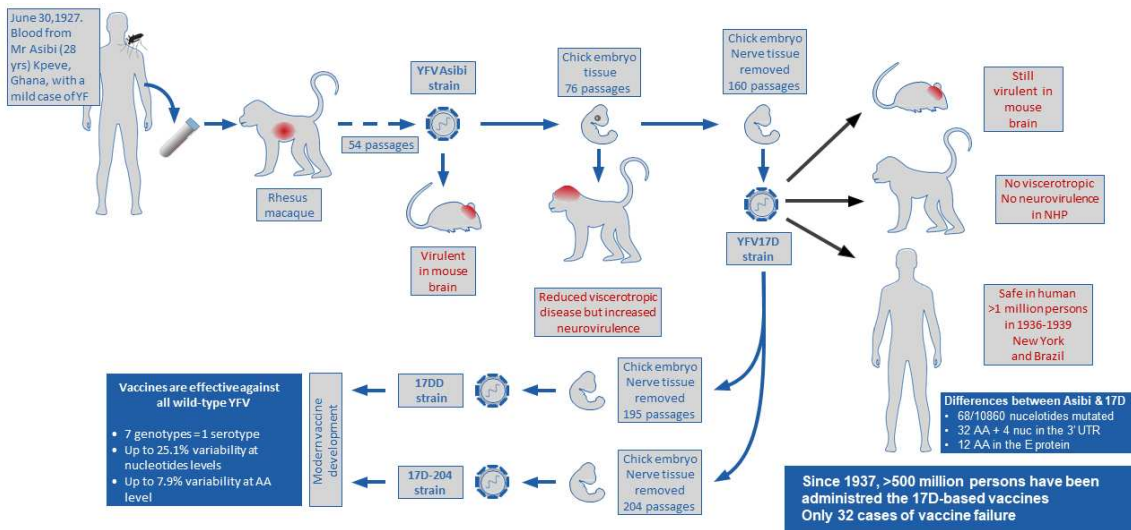


Figure 15: Schéma descriptif du processus d'atténuation du virus de la fièvre jaune sauvage (souche Asibi). D'après (Barrett & Teuwen, 2009; Plotkin et al., 2017; Theiler & Smith, 1937; Watson & Klimstra, 2017).

Le vaccin fièvre jaune se caractérise par une grande immunogénicité mobilisant l'ensemble des compartiments immunitaire avec:

- une signature antivirale marquée de l'immunité innée (production d'IFN-I)
- une production précoce d'anticorps neutralisants conférant une protection dans les 10 jours suivant l'injection et capable de persister plusieurs décennies.
- une mobilisation importante et une polyfonctionnalité de LT CD4+ avec un pic deux semaines après injection
- une forte mobilisation d'effecteurs cellulaire NK et LT CD8+, la dernière pouvant persister plusieurs semaines après vaccination

Bien que réduite par rapport à la souche sauvage, la souche vaccinale est capable de se répliquer chez l'Homme mais également chez le macaque selon le cycle présenté dans la figure 16.

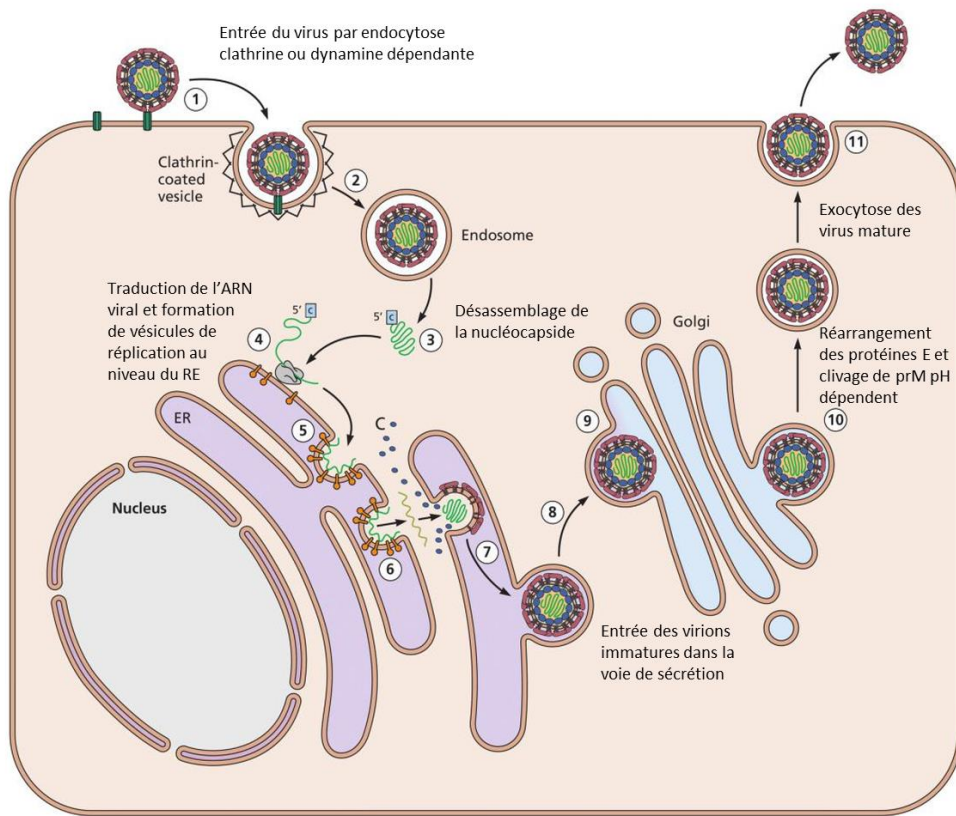


Figure 16: Schéma du cycle cellulaire du virus de la fièvre jaune. ER : Réticulum endoplasmique. (Principles of Virology, 4th Edition, 2 Vol Set by S. Jane Flint, Lynn W. Enquist, Vincent R. Racaniello, Glenn F. Rall, Anna Marie Skalka)

Pour ce projet, nous avons choisi d'utiliser un autre vaccin YFV (souche 17D), inactivé au β -priopiolactone et adjuvanté par de l'hydroxyde d'aluminium (Alum), décrit par Thomas Monath. Bien qu'incapable de se répliquer et de présenter des antigènes viraux tels que les protéines non-structurales, contrairement à la souche vaccinale du Stamaril, ce vaccin permet d'induire des anticorps neutralisants chez différents modèles animaux y compris chez des macaques rhésus (Monath et al., 2010) et la réponse anticorps neutralisante et l'efficacité sont inférieures au vaccin Stamaril.

Nous avons utilisé ces vaccins comme modèles pour comparer les signatures T CD4+ précoce associées à la persistance de la réponse anticorps neutralisante.

Cette partie du projet a été organisée selon un design expérimental proche aux études de T. Monath (Monath et al., 2010, 2011), avec un emploi de la même dose pour le vaccin inactivé. Cependant, les injections du vaccin inactivé ont été injectées en sous-cutanée

pour utiliser la même voie que pour le Stamaril®, et pour faciliter la récupération et l'étude des ganglions drainants, les injections ont été réalisées dans la zone inguinale.

Dix-huit macaque cynomolgus ont été répartis en deux groupes de neuf animaux injectés par le Stamaril ou le vaccin inactivé. Les neuf macaques cynomolgus de chaque groupe ont été utilisés pour étudier dans le sang la mise en place de la réponse T CD4+ à des temps précoces, ainsi que la persistance de la mémoire avec des prélèvements à des points tardifs. Le schéma vaccinal du groupe inactivé impliquant un rappel 28 jours après la primo-injection, les individus de ce groupe ont été immunisés en premier. Les individus du groupe Stamaril ont reçu une unique immunisation qui a été synchronisée avec le rappel du groupe inactivé.

Une étude de la réponse mémoire dans les organes lymphoïdes secondaires impliquant des prélèvements lourds pouvant altérer le court de la réponse immune, seul trois macaques cynomolgus de chaque groupe ont été sélectionné pour effectuer des prélèvements de ganglions lymphatiques et de moelle osseuse. Le choix de ces organes pour étudier la réponse fièvre jaune spécifique repose dans leur implication avec la formation et la persistance de la mémoire.

3) Technologies

Au cours de ce projet, diverses techniques ont été mises en œuvre, incluant notamment un marquage *in vivo* de la prolifération cellulaire induite par les vaccins grâce à un analogue de la thymidine, des technologies de phénotypage complexe par cytométrie de masse, et des méthodes de détection multiple de cytokines dans les fluides biologiques. Des outils bio-informatiques ont également été mobilisés pour permettre l'étude et la caractérisation de l'induction et de la persistance de la réponse neutralisante ainsi que de la mémoire immunitaire

a) Cytométrie de masse

La cytométrie de masse, combinaison de la cytométrie en flux et de la spectrométrie de masse, permet une caractérisation phénotypique étendue des cellules immunitaire, grâce à une détection simultanée de près de 50 marqueurs. Cette technologie est basée sur le couplage des anticorps de marquage avec des isotopes de métaux lourds appartenant principalement à la classe des lanthanides (Bendall et al., 2012; Ornatsky et al., 2010). La

détection par le cytomètre étant basée sur la masse et le temps de vol des différents éléments après une ionisation dans un plasma d'argon (Figure 17), elle s'affranchit donc des problèmes de superposition des spectre d'émissions des fluorochromes utilisés en cytométrie en flux.

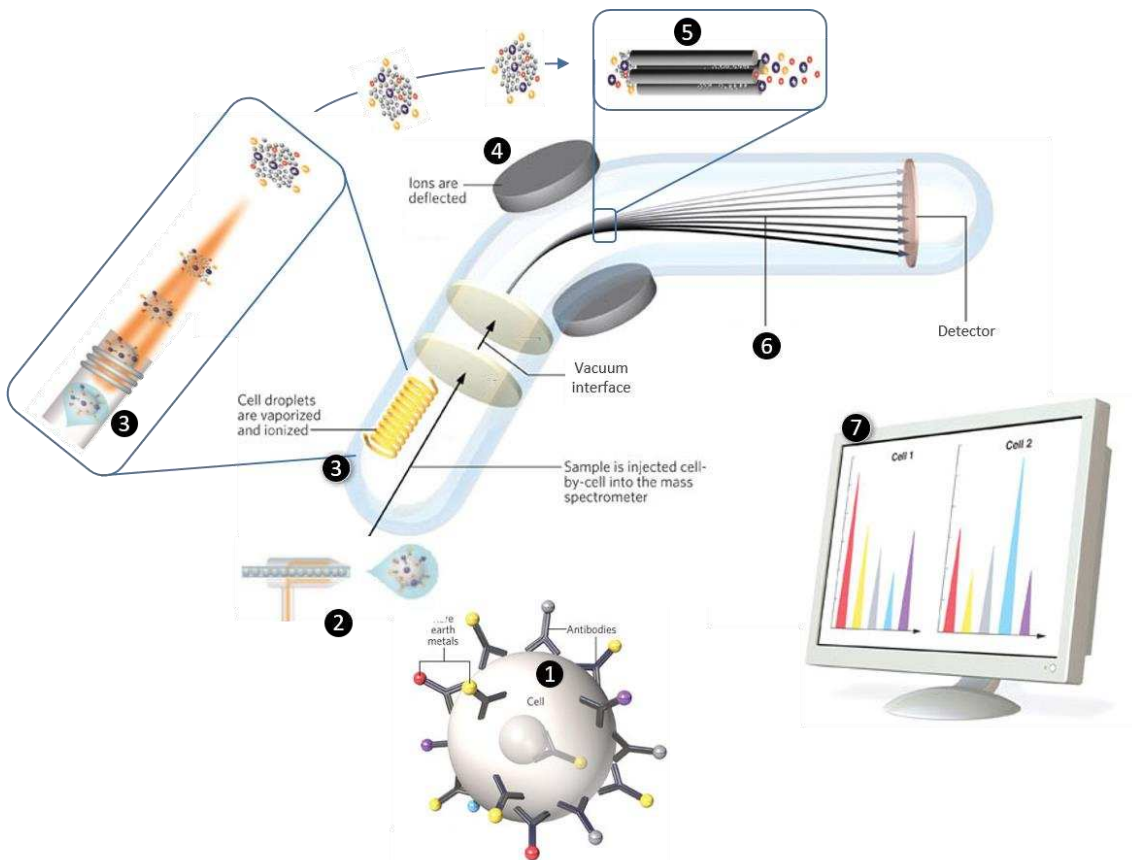


Figure 17: Principe de fonctionnement de la cytométrie de masse. Suite au marquage par des anticorps couplés à des métaux lourds de la classe des lanthanides (1), les cellules sont aérosolées par un nébuliseur (2). Les cellules incluses dans les gouttelettes sont ensuite dirigées une à une dans le plasma où elles vont être ionisées et former un nuage d'ions (3). Le déflecteur (4) va orienter le nuage d'ion correspondant à chaque cellule vers un quadrupole permettant d'éliminer du nuage d'ions tous les éléments avec une masse faible (5). Les ions lourds sont ensuite séparés en fonction de leur masse et de leur temps de vol jusqu'au détecteur (6). La quantité de chaque isotope pour chaque cellule sera mesurée par le détecteur puis les données seront converties en fichier FCS pour analyse (7).

b) Analyse et modèle statistique

Pour l'analyse des données de cytométrie de masse et de ses nombreux paramètres, l'algorithme SPADE « Spanning-tree Progression Analyses of Density-normalized Events algorithm » et son pipeline d'analyse SPADEVizR développé par Gautreau *et al.* (Gautreau *et al.*, 2017) ont été sélectionné. Contrairement aux analyses bidimensionnelles classiques, ce type d'analyse permet d'explorer les données de manière non-supervisée.

Cette analyse repose sur la hiérarchisation de l'hétérogénéité cellulaire offre la possibilité d'identifier de nouvelles sous-populations cellulaires, modélisées par un arbre où chaque point, ou « cluster » représente un groupe de cellules phénotypiquement similaires. De plus, SPADE possède une étape de « downsampling » ayant pour but de diminuer le nombre de cellules intervenant dans la création des clusters. Cette étape permet de favoriser l'identification et l'enrichissement en populations rares de l'arbre par rapport aux populations à fortes densités.

C. RESULTATS

I. Innate cell markers that predict anti-HIV neutralizing antibody titers in vaccinated macaques

Dans cette étude, nous avons employé le modèle du macaque cynomolgus pour caractériser la réponse innée précoce un jour après chacune des trois injections de la protéine ConM SOSIP.v7, associée à différents adjuvants et injectées par différentes voies d'immunisation.

Bien que nous n'ayons observé aucune différence significative entre les adjuvants, nous avons en revanche observé que la voie intramusculaire induisait des réponses anticorps de meilleure qualité que la voie sous-cutanée. En effet, la voie sous-cutanée induit de plus faibles niveaux d'IgG, présentant une faible capacité de liaison au Fc_YRIIIa et les anticorps neutralisants n'ont pu être détectés qu'après la troisième injection pour certains animaux.

Nous avons pu mettre en évidence par cytométrie de masse la grande diversité des DC et monocytes ainsi que des phénotypes intermédiaires des populations innées induites par la vaccination. Nous avons montré que l'adjuvant à base de mono-phospho-lipide A (MPLA) induit une plus forte mobilisation des monocytes que le squalène (SQ) et que cet effet est amplifié lorsque qu'il est administré par la voie intramusculaire.

L'analyse cinétique des différentes populations de monocytes et cellules dendritiques a permis de définir des signatures cellulaires précoces, spécifiques de chaque vaccin, et pouvant être définies par un panel restreint de marqueurs caractéristiques. Ces signatures ont également permis de générer des hypothèses sur l'origine des différences de qualité de réponse anticorps avec notamment une signature cDC1, associée aux réponses Th1 et cellulaires, pouvant expliquer la plus faible qualité de la réponse anticorps induite par le vaccin MPLA-SC. À l'inverse une signature cDC2-moDC apparaît associée à l'induction des réponses humorales observées pour le SQ-IM.

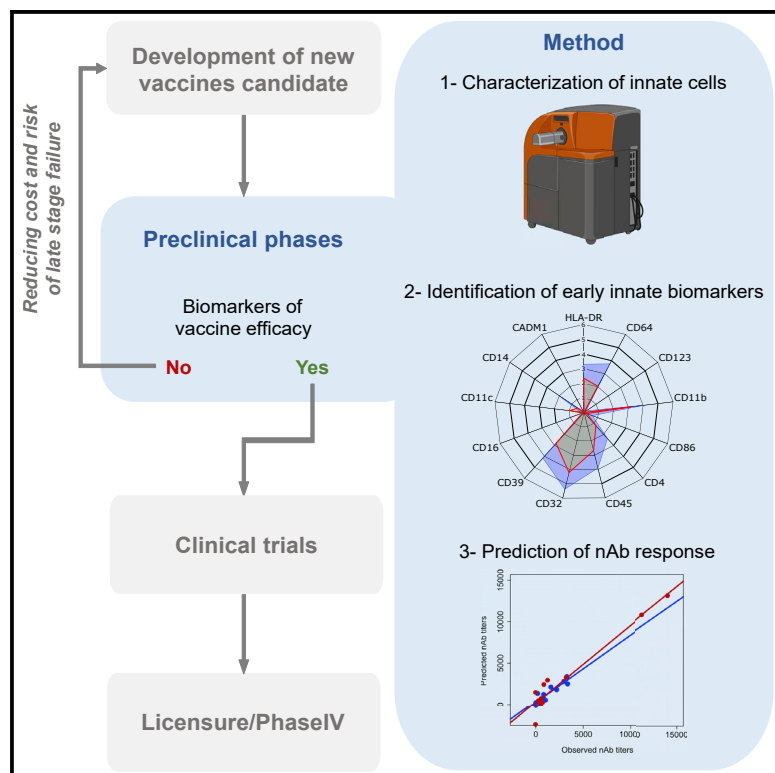
Ces signatures cellulaires ont été intégrées dans un modèle prédictif de la qualité de la réponse anticorps. Nous avons ainsi démontré qu'il est possible chez le macaque

cynomolgus, de prédire la qualité de la réponse anticorps spécifique uniquement à l'aide de la réponse myéloïde précoce.

Ces résultats obtenu dans le cadre du consortium européen « European AIDS Vaccine Initiative 2020 » (EAVI2020) ont été publié dans Cell Reports Medicine (Tilbeurgh et al., 2022). Un grand merci à l'ensemble des collaborateurs ayant participé à la réalisation de ce projet.

Innate cell markers that predict anti-HIV neutralizing antibody titers in vaccinated macaques

Graphical abstract



Authors

Matthieu Van Tilbeurgh,
Pauline Maisonnasse,
Jean-Louis Palgen, ..., Gabriella Scarlatti,
Rogier W. Sanders, Roger Le Grand

Correspondence

roger.le-grand@cea.fr

In brief

Van Tilbeurgh et al. use mass cytometry to identify innate cell signature predictive of neutralizing antibody response in a non-human primate model. They highlight that better understanding early immune mechanisms may be of great help to design new vaccine candidates.

Highlights

- HIV-Env SOSIP trimers induce neutralizing antibodies in cynomolgus macaques
- Vaccine-induced innate cells changes are characterized using mass cytometry
- Adjuvant and route of immunization influence early innate signatures in vaccinated NHP
- Early innate cell signatures predict neutralizing antibody levels

Article

Innate cell markers that predict anti-HIV neutralizing antibody titers in vaccinated macaques

Matthieu Van Tilbeurgh,¹ Pauline Maisonnasse,¹ Jean-Louis Palgen,¹ Monica Tolazzi,² Yoann Aldon,³ Nathalie Dereuddre-Bosquet,¹ Mariangela Cavarelli,¹ Anne-Sophie Beignon,¹ Ernesto Marcos-Lopez,¹ Anne-Sophie Gallouet,¹ Emmanuel Gilson,⁴ Gabriel Ozorowski,⁵ Andrew B. Ward,⁵ Ilja Bontjer,⁶ Paul F. McKay,³ Robin J. Shattock,³ Gabriella Scarlatti,² Rogier W. Sanders,^{6,7} and Roger Le Grand^{1,8,*}

¹Université Paris-Saclay, Inserm, CEA, Center for Immunology of Viral, Auto-immune, Hematological and Bacterial Diseases (IMVA-HB/IDMIT), 92265 Fontenay-aux-Roses, France

²Viral Evolution and Transmission Unit, Division of Immunology, Transplantation and Infectious Diseases, IRCCS Ospedale San Raffaele, 20132 Milan, Italy

³Imperial College London, Faculty of Medicine, Department of Infectious Disease, London, UK

⁴Life & Soft, 28 rue de la Redoute, 92260 Fontenay-aux-Roses, France

⁵Department of Integrative Structural and Computational Biology, The Scripps Research Institute, La Jolla, CA 92037, USA

⁶Department of Medical Microbiology and Infection Prevention, Amsterdam University Medical Centers, Location AMC, University of Amsterdam, 1105 AZ Amsterdam, the Netherlands

⁷Department of Microbiology and Immunology, Weill Medical College of Cornell University, New York, NY 10021, USA

⁸Lead contact

*Correspondence: roger.le-grand@cea.fr

<https://doi.org/10.1016/j.xcrm.2022.100751>

SUMMARY

Given the time and resources invested in clinical trials, innovative prediction methods are needed to decrease late-stage failure in vaccine development. We identify combinations of early innate responses that predict neutralizing antibody (nAb) responses induced in HIV-Env SOSIP immunized cynomolgus macaques using various routes of vaccine injection and adjuvants. We analyze blood myeloid cells before and 24 h after each immunization by mass cytometry using a three-step clustering, and we discriminate unique vaccine signatures based on HLA-DR, CD39, CD86, CD11b, CD45, CD64, CD14, CD32, CD11c, CD123, CD4, CD16, and CADM1 surface expression. Various combinations of these markers characterize cell families positively associated with nAb production, whereas CADM1-expressing cells are negatively associated ($p < 0.05$). Our results demonstrate that monitoring immune signatures during early vaccine development could assist in identifying biomarkers that predict vaccine immunogenicity.

INTRODUCTION

HIV-1 is responsible for a pandemic of more than 37 million people and continues to spread at a rate of >1.7 million new infections every year.¹ It is widely acknowledged that a protective vaccine would be the most effective means to reduce HIV-1 spread and ultimately eliminate the pandemic. Despite decades of research, we do not yet have a vaccine capable of protecting people from HIV-1 infection or halting disease progression. Developing new strategies for HIV vaccines requires a long-term effort challenging the investment in the designing of immunogens and immunization modalities while reducing the risk of failure in the late stages of development.

Vaccine development failure may result from our poor understanding of immune mechanisms of protection following immunization as only a few immune parameters are assessed during efficacy trials. Seeding studies from R.P. Sekali and B. Pulendran have revealed system biology as a promising and power-

ful exploration tool,^{2,3} taking advantage of wide multiplexed data, allowing a deep understanding of cellular and molecular partners implicated in immune responses. Systems vaccinology has been applied to multiple vaccine approaches, including yellow fever, HIV, influenza and recombinant vesicular stomatitis virus-Zaire Ebola virus (rVSV-ZEBOV) vaccines, and to identify adjuvant immune signature.³⁻⁷ Tsang et al. even described host blood parameters, predicting before immunization the capacity to respond to influenza vaccine.⁸ Thus, systems vaccinology may contribute to reduce vaccine development failure by identifying markers that predict protective immunity at the early stages of preclinical animal model studies and clinical trials.^{9,10}

Studies in animal models are critical in vaccine development. Non-human primates (NHPs) are particularly relevant because of the close phylogenetic relationship with humans, resulting in a very similar organization of the respective immune systems, allowing testing immunogenicity without requiring

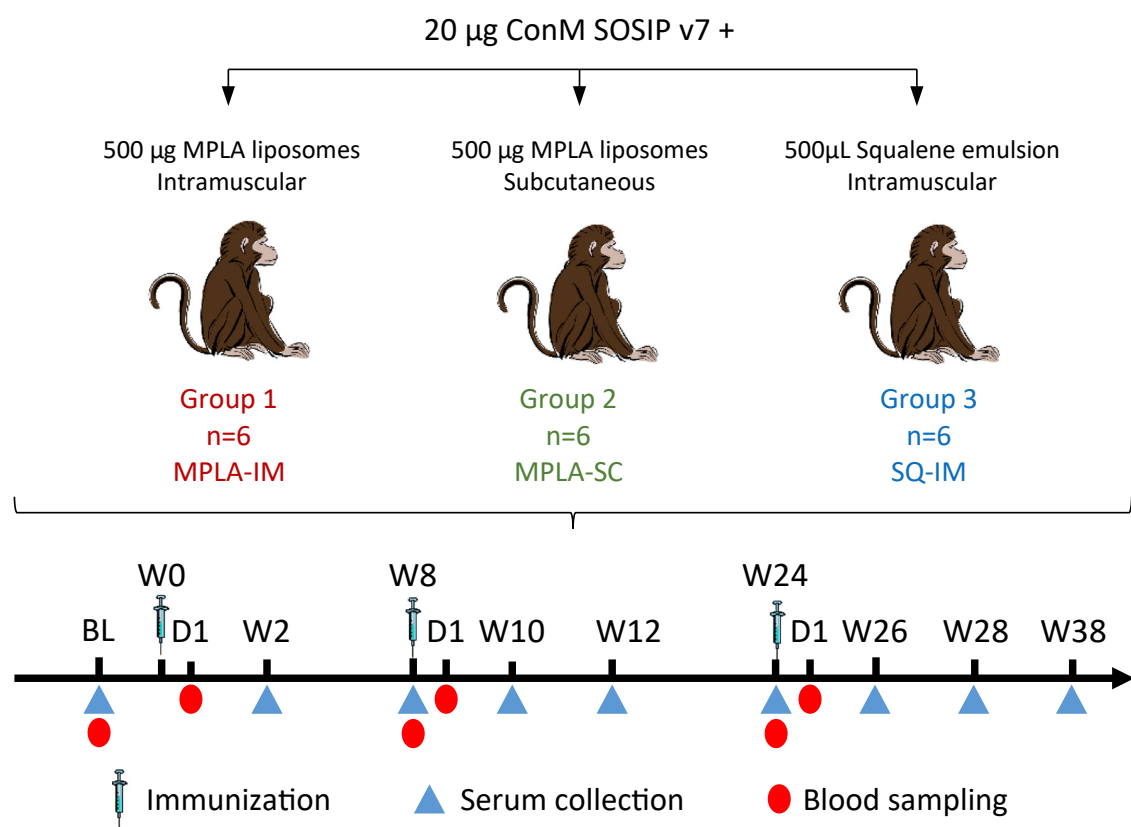


Figure 1. Experimental design

Three groups of six cynomolgus macaques received three immunizations of ConM SOSIP.v7 vaccine adjuvanted either with MPLA liposomes or squalene emulsion and were injected by the intramuscular (IM) or the subcutaneous (SC) route, at week (W)0, W8, and W24. Blood samples were collected before and 24 h after each immunization. Serum was collected before each immunization and then every 2 weeks to quantify Ag-specific IgG, nAb, and Fc_γR-binding titers.

adaptation of the candidate vaccine to the species. Cynomolgus and rhesus macaques are widely used in the development of an HIV vaccine, because simian immunodeficiency virus (SIV) and simian-human immunodeficiency virus (SHIV) challenge models also recapitulate most of the features of HIV infection and acquired immunodeficiency syndrome (AIDS) in humans.^{11,12}

Innate immunity is one of the first players in shaping the vaccine-induced immune responses, and molecular and cellular changes immediately following vaccine injection may help to identify markers predicting the orientation, durability, and efficacy of the adaptive response. Such predictive signals would be particularly useful to accelerate the selection of the most promising vaccine candidates at early developmental stages.

Here, we demonstrate in cynomolgus macaques that subsets of myeloid cells, characterized by mass cytometry and appearing in blood very early following the injection of native-like trimeric HIV-1 envelope SOSIP (Env) immunogens,^{13,14} differ depending on the given adjuvant and immunization route. Moreover, we identified a set of cell markers that correlates with vaccine-induced neutralizing antibody (nAb) activity that could be used to develop models that predict the quality of the vaccine response.

RESULTS

The humoral response to an HIV SOSIP Env vaccine is influenced by both the injection route and the adjuvant

We characterized the vaccine-induced response in three groups of six cynomolgus macaques to a stabilized Env derived from a consensus sequence of HIV-1 group M (ConM SOSIP.v7) that we previously reported to induce strong nAb responses in rabbits,^{15,16} which is being evaluated in phase 1 trials in humans (NCT03816137, NCT03961438, NCT04046978). We assessed the impact of subcutaneous (SC) or intramuscular (IM) immunization in combination with squalene emulsion (SQ) or mono-phosphoryl-lipid A liposome (MPLA) adjuvants (Figure 1). The adjuvants were shown not to compromise the conformational integrity of the ConM SOSIP.v7 trimers (Figure S1).

Animals immunized IM with MPLA (Group 1) or SQ (Group 3) showed similar levels of ConM-specific IgG ($838,307.004 \pm 2.163$ and $1,622,973.717 \pm 1.737$ area under the curve [AUC], respectively [geometric mean \pm geometric SD]) and nAb titers ($22,610.1922 \pm 2.642$ and $18,488.409 \pm 2.268$ AUC, respectively), with peaks at 2 weeks after the first and second boost (week (W) 10 and 26, respectively), suggesting that both adjuvants are as effective by the IM route (Figures 2A–2D and S2). In both groups, ConM-specific IgG levels remained high after

Cell Reports Medicine

Article

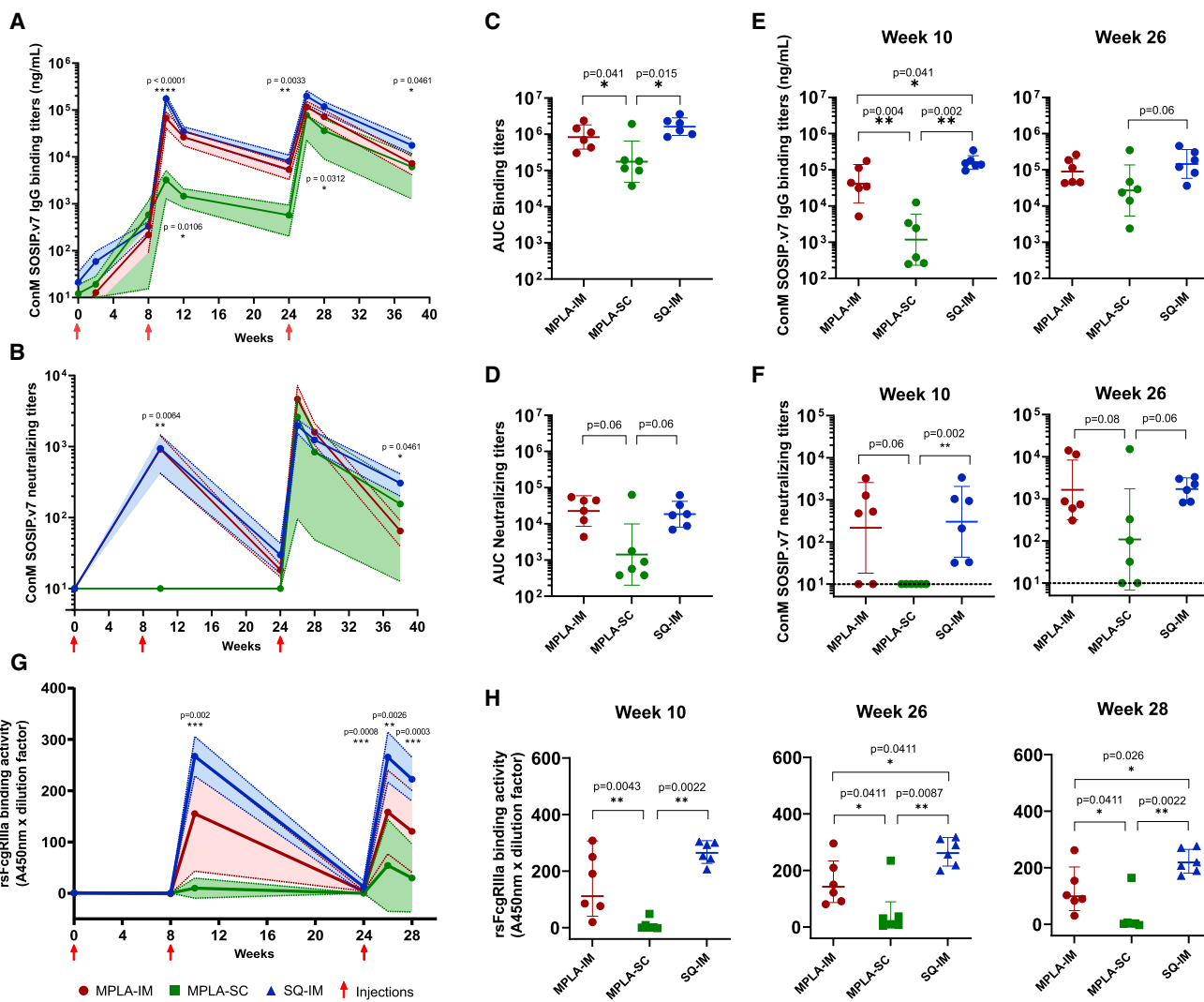


Figure 2. Antigen-specific humoral response in macaques' serum following ConM SOSIP.v7 immunizations

ConM SOSIP.v7 IgG binding (A) and nAb (B) titers. The geometric mean titers and geometric SD of each group are displayed in red (MPLA-IM), green (MPLA-SC), and blue (SQ-IM). Significant differences between groups ($n = 6$) were assessed with a Kruskal-Wallis test, and p values < 0.05 are displayed. (C) and (D) display the area under the curve (AUC) from W0 to W38 for ConM SOSIP.v7 IgG binding and nAb titers, respectively. Comparison of ConM SOSIP.v7 IgG binding (E) and nAb titers (F) at the peaks of IgG production (weeks 10 on the left and 26 on the right). (G) rsFc γ RIIIa binding profile of Ag-specific IgG following SOSIP ConM immunizations. The geometric mean titers and geometric SD of each group are displayed. (H) Comparison of rsFc γ RIIIa binding activity geometric mean between vaccines. Pairwise comparison was made using the Mann-Whitney test ($n = 6$) to compare AUCs, Ab titers, and rsFc γ RIIIa binding activity at the different time points. p values < 0.05 are shown. Immunizations (weeks 0, 8, and 24) are indicated by red arrows.

reaching a peak 2 weeks after each boost, while nAb titers dropped after the first (16.288 ± 1.716 and 20.246 ± 2.461 ng/mL, respectively) and to a lesser extent after the second boost (41.296 ± 2.906 and 202.250 ± 2.945 ng/mL, respectively). In contrast, MPLA-SC immunization (Group 2) induced significantly lower ConM-specific IgG levels (1421.370 ± 7.028 AUC) compared with MPLA-IM and SQ-IM immunizations ($p = 0.041$ and $p = 0.015$, respectively, Figure 2C), especially at W10 (Figure 2E). Neutralization to conM was observed in the MPLA-SC group only after the third immunization with heterogeneous nAb titers. Notwithstanding, neutralizing titers tended to be lower in the

MPLA-SC group despite two animals displaying equivalent titers to the lowest and highest of the IM groups (Figure 2F). Heterologous neutralization against the highly neutralization-sensitive 93MW965.26 (MW965) pseudotyped virus (PSV) at W28 was also assessed. Neutralization of MW965 was 10- to 100-fold lower than that of ConM, but similar trends were observed between groups (Figure S3).

We then compared Fc γ -receptor IIIa (Fc γ RIIIa) binding characteristics of ConM SOSIP.v7-induced serum Ab between the three groups. This has been shown to provide an indirect readout for Ag-specific antibody-dependent cellular cytotoxicity

(ADCC).¹⁷ Similarly to nAb titers, a sharp increase of recombinant soluble (rs) Fc γ RIIIa binding activity was observed in both IM groups after each boost followed by a decrease. We observed that the SQ formulation generated higher rsFc γ RIIIa binding levels than MPLA by the IM route with both groups inducing significantly higher rsFc γ RIIIa binding activity than the MPLA-SC induced (Figure 2G). Although the SQ-IM group displayed a more homogeneous response, levels of binding became significantly higher than the MPLA-IM group after the third injection (W26, $p = 0.0411$; W28, $p = 0.026$) (Figure 2H). These results highlight that not only the route but also the adjuvant impact rsFc γ RIIIa binding activity. Overall, we demonstrated that ConM SOSIP.v7-specific humoral responses were more efficiently induced by the IM than the SC route.

Both the adjuvant and route of immunization affect myeloid cell dynamics

The route- and adjuvant-dependent differences we observed in the anti-Env antibody response argue for a role of early innate immunity in shaping the nAb response. Here, we focused on the myeloid cell compartment because of its role in capturing and presenting vaccine antigens to B and T lymphocytes, in addition to its contribution to inflammation. Mass cytometry was used to extensively characterize the differentiation and functional markers in the heterogeneous blood cell population. Importantly, many of the cell markers we studied in cynomolgus macaques have human counterparts, emphasizing the relevance of this species as a model for evaluating human candidate vaccines. In addition, the antibody panel used in our study consisted of anti-human antibodies cross-reacting with macaque cell markers, thus facilitating the translatability of preclinical study protocols to human clinical trials samples.

A spanning-tree progression analysis of density-normalized events (SPADE) was performed on mass cytometry-generated data to identify leukocyte clusters displaying similar phenotypes (Figure S4A). Major cell populations were defined based on CD3, CD4, CD8, CD20, and HLA-DR expression, which allowed for the identification of 225 myeloid cell clusters (Lin $^-$ HLA-DR $^+$). Based on cell population dynamics following vaccine injection, MPLA-IM induced stronger mobilization of total myeloid cells than the other adjuvants and routes within the first 24 h (Figures S4B-S4D). Granulocytes were not evaluated in this study due to the technical limitation of using frozen and thawed whole blood samples. To better visualize the cluster phenotypes, we then performed hierarchical clustering based on their relative marker levels (Figure 3). Clusters displaying similar phenotypes were gathered into 28 phenotypic families (PFs), described in Table 1. The cluster dendrogram divides the PFs into three superfamilies: (1) HLA-DR $^+$ CD14 $^+$ CD11b hi , which we identified as monocytes, (2) HLA-DR $^{mid/hi}$ -CD14 $^-$ -CD11c $^-$, which we identified as a subset of dendritic cells (DCs), and (3) HLA-DR $^{lo/mid}$ -CD14 $^-$ -CD11c $^{+}$ -CD16 $^+$, which we identified as another subset of DCs. We determined the impact of ConM SOSIP.v7 immunization on these populations by investigating the differences in cell abundance at different time points after vaccination (Figure 4A and S5 and Table S1). The MPLA-IM group showed significant changes in the myeloid compartment with the frequency of nine PFs significantly increased as early as 24 h following the first

injection (Figure 4A and Table S1). These changes affected monocyte populations with profiles of classical monocytes (PF10, $p = 0.03$), non-classical monocytes (PF19, $p = 0.03$), intermediate monocytes (PF22, $p = 0.03$), and moDCs (PF2, PF15, PF25, $p = 0.03$). These last PFs displayed the most significant changes through time for all vaccines, especially for MPLA-IM (Figure 4B). The first injection also induced an increase in the frequency of cDC1-like cells (PF28, $p = 0.03$; PF16, $p = 0.03$) and HLA-DR lo -CD11c hi -CD16 hi DCs (PF14, $p = 0.03$). The first boost injection only mobilized monocyte populations (PF10, PF15, PF2, and PF25, $p = 0.03$). Finally, the second boost mobilized a much wider range of myeloid cells. In addition to the monocyte families, there was an increase in the frequency of cells with a macrophage phenotype (PF27, $p = 0.03$), cDC1-like cells (PF28, PF26, and PF16, $p = 0.03$), and HLA-DR lo -CD11c hi -CD16 hi DCs (PF17, PF4, PF5, PF14, PF6, PF18, and PF7, $p = 0.03$). Overall, the use of MPLA by the IM route appeared to mainly recruit and elicit monocyte/macrophage populations, with an important extension to DC populations after the third vaccine injection, compared with previous time points, indicating that there are host changes over time that affect the quality of the innate response.

The MPLA-SC group mostly displayed changes within the monocyte compartment. MoDCs (PF2, PF15, and PF25, $p = 0.03$) were the only subsets significantly induced 24 h after the first injection, along with a cDC2 subpopulation (PF24, $p = 0.03$). Similar to MPLA-IM, the second immunization mobilized classical monocytes (PF10, $p = 0.03$) and moDCs (PF2, PF15, and PF25, $p = 0.03$) as well as intermediate monocytes. Finally, seven PFs showed significant changes after the last immunization, with increasing frequencies of monocyte populations (PF2, PF15, PF22, PF25, $p = 0.03$), as well as cDC2 (PF24, $p = 0.03$) and HLA-DR lo -CD11c hi -CD16 hi DCs (PF4, $p = 0.03$). Conversely, the PF23 pDC subset showed a significant decrease relative to the baseline level. Thus, SC injection of MPLA shows similar monocyte mobilization as MPLA-IM but of lower amplitude. We found no significant amplification of DCs in the MPLA-SC group, highlighting the influence of the administration route on the quality of the innate response, despite the use of the same adjuvant.

Few significant differences were observed for this group when compared with the SQ-IM group. Most changes after the first injection occurred within the monocyte compartment (PF1, PF2, PF3, and PF19) except for the PF11 HLA-DR $^{mid/hi}$ -CD14 $^-$ -CD11c $^-$ DC subpopulation. The frequency of classical PF1 and PF3 monocytes, non-classical PF19 monocytes, and PF11 cDC1 decreased after ConM SOSIP.v7 injection, whereas that of PF2 moDCs showed a marked increase relative to baseline levels. The second injection only mobilized PF2 moDCs, and we observed a loss of PF11 cDC1 and PF16/PF17 HLA-DR lo -CD11c hi -CD16 hi DCs. Finally, similar to groups 1 and 2, the final injection induced strong mobilization of PF2, PF15, and PF25 moDCs.

Vaccine-induced blood cell signatures

We identified vaccine signatures by performing linear discriminant analysis (LDA) (Figures 5A and 5B). We grouped PFs sharing close profiles of changes over time into eight kinetic families

Cell Reports Medicine

Article

CellPress
OPEN ACCESS

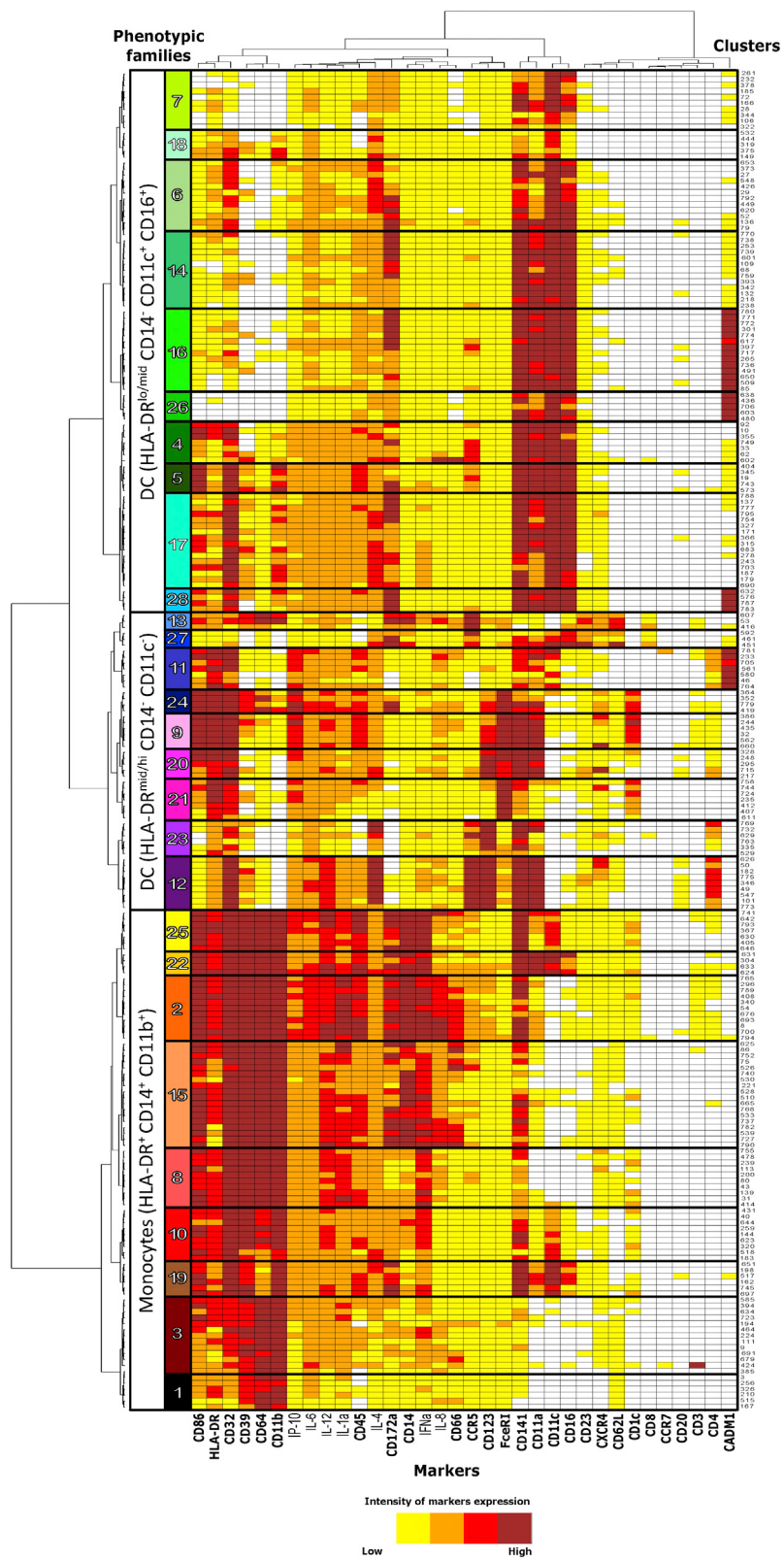


Figure 3. Phenotypic diversity of the blood myeloid cell compartment

The heatmap shows the hierarchical clustering and gathering of all myeloid cell SPADE clusters. Marker expression is shown in columns and cell clusters in rows. Twenty-eight phenotypic families were defined by proximity in the cluster dendrogram and manually annotated. The marker dendrogram represents markers with similar expression patterns. Markers used by SPADE unsupervised analysis for the clustering are written in bold.

Table 1. Characterization of the main myeloid cell populations

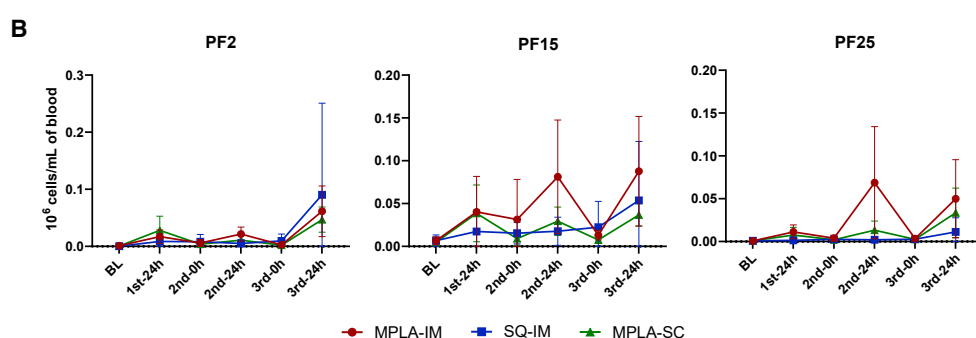
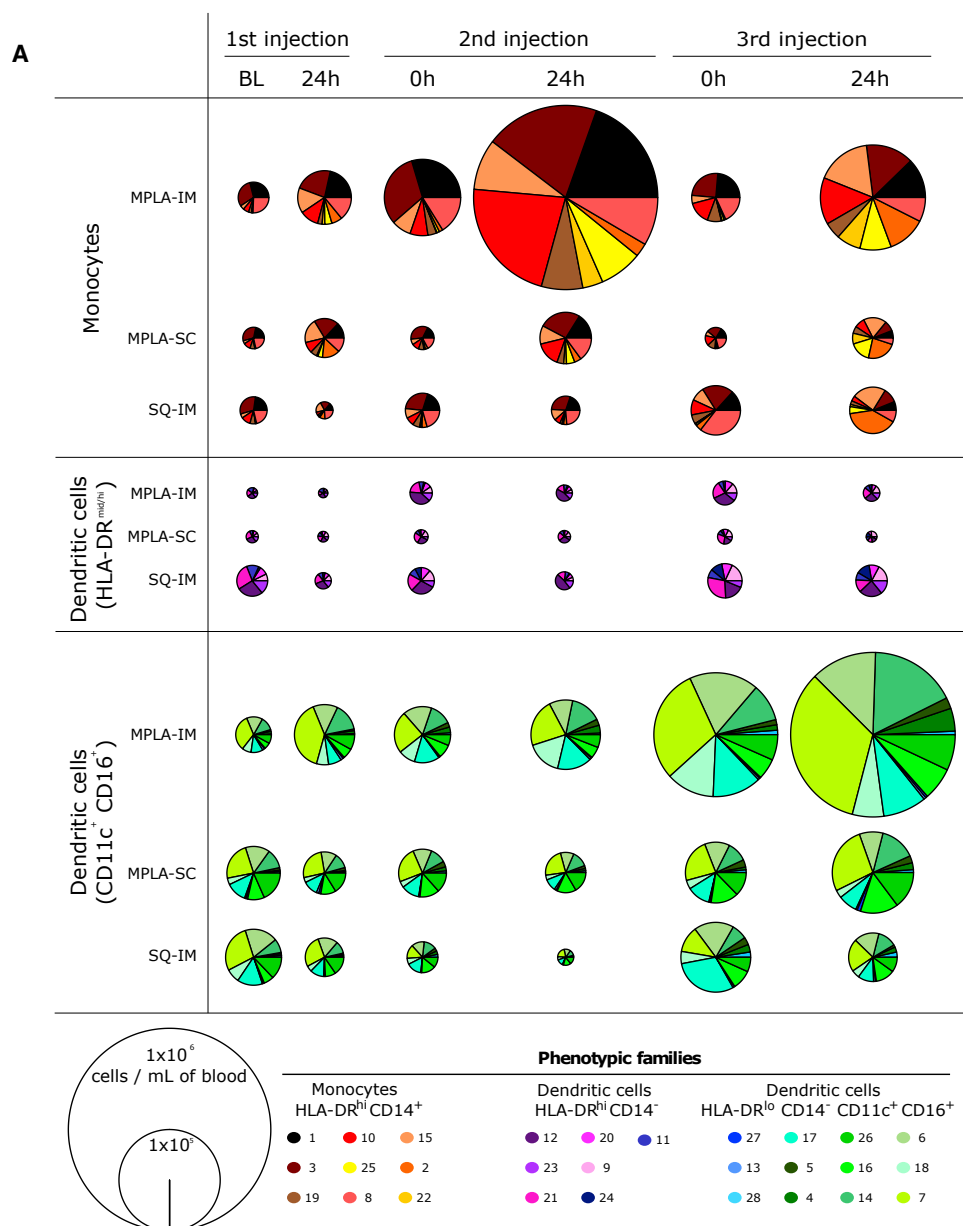
Kinetic families	Population characteristics	Phenotypic families	Subsets characteristics	Cell population*	References
KF-I	HLA-DR ⁺ , CD64 ^{hi} , CD86 ^{hi} , CD11b ^{hi}	1	CD14 ^{lo} , CD32 ^{mid}	classical monocytes	Nakaya et al. ⁷ ; Tsang et al. ⁸ ; Trautmann and Sekaly ⁹ ; Mooney et al. ¹⁰ ; Reimann et al. ¹¹ ; Estes et al. ¹² ; Sanders and Moore ¹³ ; De Taeye et al. ¹⁴ ; Sliopen et al. ¹⁵ ; Brouwer et al. ¹⁶
		3	CD14 ^{lo} , CD32 ⁺		
		10	CD14 ^{lo} , CD32 ^{hi}		
		15	CD14 ⁺ , CD1c ^{lo}	MoDC	
		25	CD14 ⁺ , CD1c ^{lo}		
		19	CD14 ^{lo} , CD16 ⁺ , CD11c ⁺	non-classical monocytes	
		22	CD14 ⁺ , CD16 ⁺ , CD11c ⁺	intermediate monocytes	
KF-II	HLA-DR ^{hi} , CD32 ^{hi} , CD64 ^{hi} , CD86 ^{hi} , CD11b ^{hi}	2	CD14 ⁺ , CD1c ^{lo}	MoDC	Reimann et al. ¹¹ ; Zhang et al. ¹⁸
		20	FcεR ^{hi} , CD32 ^{hi} , CD86 ^{hi} , CD4 ^{lo}	putative cDC2	Reimann et al. ¹¹ ; De Taeye et al. ¹⁴ ; Wines et al. ¹⁷ ; Calabro et al. ¹⁹
		9	CD1c ⁺ , FcεR ^{hi} , CD32 ^{hi} , CD86 ^{hi} , CD4 ^{lo}	cDC2	
		24			
KF-III	HLA-DR ^{mid} , CD11c ⁺ , CD16 ⁺ , CD32 ⁺	28	CADM1 ⁺	cDC1 like DC	De Taeye et al. ¹⁴ ; Wines et al. ¹⁷
		4	/	DC	/
		5			
		6	/	DC	/
KF-IV	HLA-DR ^{lo} , CD11c ^{hi} , CD16 ^{hi}	7			
		14			
		18	CD11a ^{lo}		
		8	CD14 ^{lo}	classical monocytes	Nakaya et al. ⁷ ; Tsang et al. ⁸ ; Trautmann and Sekaly ⁹ ; Mooney et al. ¹⁰ ; Reimann et al. ¹¹ ; Estes et al. ¹² ; Sanders and Moore ¹³ ; De Taeye et al. ¹⁴ ; Sliopen et al. ¹⁵ ; Brouwer et al. ¹⁶
KF-V	HLA-DR ⁺	17	/	DC	/
		11	CADM1 ⁺ , CD1c ⁻ , CD172a ^{lo} , CD16 ^{lo}	cDC1	De Taeye et al. ¹⁴ ; Wines et al. ¹⁷

(Continued on next page)

Table 1. Continued

Kinetic families	Population characteristics	Phenotypic families	Subsets characteristics	Cell population*	References
KF-VI	HLA-DR ^{lo} , CD123 ⁺	21	CD1c ⁺ , FcεRI ^{hi} , CD86 ^{mid} CD123 ⁻ , CD4 ⁻	immature cDC2	Pauthner et al. ²⁰
		12	CD11a ^{hi} , CD4 ⁺ , CCR5 ⁺	pDC	Reimann et al. ¹¹ ; Estes et al. ¹² ; Wines et al. ¹⁷ ; Pauthner et al. ²⁰ ; Calabro et al. ¹⁹ ; O'Hagan et al. ²¹ ; Rosenbaum et al. ²² ; Anderson et al. ²³ ; Sanders et al. ²⁴
		23	CD11a ^{var} , CD4 ^{lo} , CCR5 ^{var}	pDC/blood DC precursor	
KF-VII	HLA-DR ^{lo} , CD14 ⁺ , CD11b ⁺ , CD64 ⁺ , CD11c ⁻ , CD16 ⁻	13	CCR5 ⁺ , CXCR4 ⁺ , CD62L ⁺	putative macrophages	/
	HLA-DR ^{mid} , CD14 ⁺ , CD11b ⁻ , CD64 ⁻ , CD11c ⁺ , CD16 ⁺	27	CCR5 ⁺ , CXCR4 ⁺ , CD62L ⁺	putative macrophages	/
KF-VIII	HLA-DR ^{lo} , CD11c ^{hi} , CD16 ^{hi}	16	CADM1 ⁺	cDC1 like DC	De Taeye et al. ¹⁴ ; Wines et al. ¹⁷
		26			

The phenotypic composition of each kinetic family is detailed. The main phenotypic characteristics used to identify cell populations according to the expression profile shown in the heatmap (Figure 3) are indicated. *proposal of cell annotation. Absence of data were indicated with /.



(legend on next page)

(KFs, **Table 1**), taking into account the correlation between variations in abundance among PFs (**Figures S6** and **S7** and **Table S2**). LDA differentiated the vaccine regimens for every time point (**Figure 5A**). Then, a second LDA was performed to identify KF associated to the vaccine regimens (**Figure 5B**). In this model, KF-III (CD11c⁺-CD16⁺ DCs) was associated with MPLA-IM. Similarly, KF-VIII was associated with MPLA-SC, composed of two PFs (16 and 26) belonging to CD11c⁺-CD16⁺ DCs and showing high expression of CADM1, suggesting a cDC1-like signature. By contrast, SQ-IM was characterized by highly activated moDCs (PF2) and cDC2 (PF9, 20, 21, and 24) from KF-II but also immature cDC2 from KF-V and pDCs from KF-VI. Additionally, the LDA score of KF-I monocytes (PF1, 3, 10, 15, 19, 22, and 25), KF-VII (PF13 and 27), and KF-IV (PF8 and 17) did discriminate SQ-IM from MPLA vaccines but could not be associated either with MPLA-IM or MPLA-SC, suggesting an MPLA adjuvant signature for those KFs.

Next, we identified the main phenotypic differences between cell populations using the Kolmogorov-Smirnov distance (**Figure 5C**). The expression of HLA-DR, CD11b, CD45, CD64, CD39, CD14, CD86, and CD32, indicative of a highly activated state, was significantly stronger for monocytes belonging to the SQ-IM signature than to the MPLA signature. MPLA injected via the IM route induced DCs expressing lower levels of HLA-DR, CD39, CD123, and CD86, but higher levels of CD11c and CD16 than SQ injected via the same route (SQ-IM group). Finally, the SC route (MPLA-SC group) appears to differ from the IM route through high CADM1 expression.

In conclusion, each vaccine strategy induced a unique innate cell signature (**Figure 5D**), allowing to discriminate between vaccine routes and adjuvants and defined by a combination of a small set of markers: HLA-DR, CD39, CD86, CD11b, CD45, CD64, CD14, CD32, CD11c, CD4, CD16, CD123, and CADM1.

Association of innate and adaptive immunity

We then investigated whether this set of markers could be used to predict the magnitude of the nAb response, IgG binding response, and Fc-mediated effector functions of IgGs (**Figure 2**). A generalized linear model constructed with KF abundances and antibody titers, neutralizing or Fc_γRIIIA functions, measured 2 weeks after the second and third injection, was employed as predictive model (**Figure 6**).

Interestingly, three KFs for MPLA-IM (KF-II, III, and VII) and four for SQ-IM (KF-III, V, VII, and VIII) significantly correlated with nAb production ($p < 0.05$). KF-II, characterized by high expression of moDC and cDC2 markers (**Figure 5D**), was the family that most positively associated with high nAb titers for the MPLA-IM (**Figure 6A**). These cells are reported to display strong CD4⁺ T cell priming activity, notably for T helper 2 (Th2) cells, known to be involved in Ab responses. Consistently, this family was also positively associated with IgG binding titers for MPLA-SC and was not

associated with IgG binding titers for MPLA-IM (**Figure 6C**). KF-III composed of HLA-DR^{lo}-CD11c⁺-CD16⁺ DC was negatively associated to nAb production ($p = 0.004$) but was positively associated with rsFc_γRIIIa binding activity along with KF-V (**Figure 6E**).

For the SQ-IM group, and in marked contrast to MPLA-IM, the model positively associated KF-III with the nAb titer (**Figure 6A**) and monocytes from KF-I with rsFc_γRIIIa binding activity (**Figure 6E**). KF-VII, presumably composed of macrophage populations based on secondary markers expression, was also positively associated with nAb production, IgG, and rsFc_γRIIIa binding activities (**Figures 6A, 6C, and 6E**, respectively) for the SQ-IM group. Two KFs were negatively associated with SQ-IM nAb titers, both sharing similar features. Indeed, KF-V and KF-VIII both showed high CADM1 expression, mostly attributed to the cDC1 phenotype and cytotoxic response (**Figure 6A**). The CADM1⁺ cells of KF-V were HLA-DR^{hi}-CD11c⁻-CD16⁻, implying a cDC1 phenotype, whereas cells belonging to KF-VIII showed the opposite pattern of HLA-DR^{lo}-CD11c⁺-CD16⁺ expression, characteristic of cDC1-like cells (**Figure 5D**). CADM1⁺ cells from KF-VIII were also negatively associated with IgG binding for both MPLA-SC and SQ-IM group and with rsFc_γRIIIa for all three groups (**Figures 6C and 6E**).

The robustness and accuracy of the model were confirmed by correlating predicted and observed values for every immune parameter studied (**Figures 6B, 6D, and 6F**). The observed nAb titers strongly correlated with those predicted by the model for both the MPLA-IM and SQ-IM vaccine strategies ($r = 0.97$ and $r = 0.9$, respectively). A strong correlation of IgG binding titers was also found for SQ-IM and MPLA-SC ($r = 0.89$ and $r = 0.92$, respectively) (**Figure 6D**) as well as MPLA-IM and SQ-IM with rsFc_γRIIIa binding activity ($r = 0.9$ and $r = 0.75$, respectively) (**Figure 6F**). However, no reliable prediction could be made regarding MPLA-SC nAb titers and rsFc_γRIIIa binding activity because they were only observed at low level after the third injection and not in all individuals.

These results demonstrate the ability of our model to predict humoral response, including IgG binding titers, nAb activity, and Fc_γRIIIa engagement, through the characterization of innate cell populations as early as 1 day after vaccine injections.

DISCUSSION

Vaccine parameters, such as adjuvant and administration route, strongly influence the quality of the innate immune response and, ultimately, the adaptive immune response.^{18–22} NHPs are particularly relevant for such translational immunology studies because of the high similarity between the organization of the macaque and human immune systems. Here, we demonstrate in NHPs that it is possible to anticipate the quality of specific antibody responses based solely on the early innate response. We show that autologous ConM SOSIP.v7-specific IgG binding titers, nAb

Figure 4. Follow-up of monocytes and dendritic cells population enrichment

The pie charts show the average phenotypic family cell abundance between immunization groups within the monocyte and dendritic cell compartments (A). Phenotypic families are represented using the same colors and numbers as in **Figure 3**. The cell numbers correlate with the size of the segments in the pie charts and are given as 10^6 cells per mL of blood.

(B) Mean cell abundances dynamic and SD from the top three phenotypic families that display the most significant variations over the different time points. p values for the changes are presented in **Table S1** and the fold change in **Figure S5**.

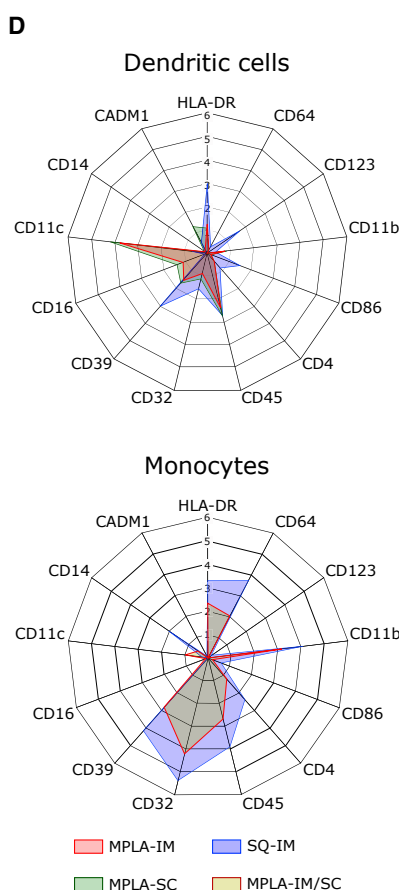
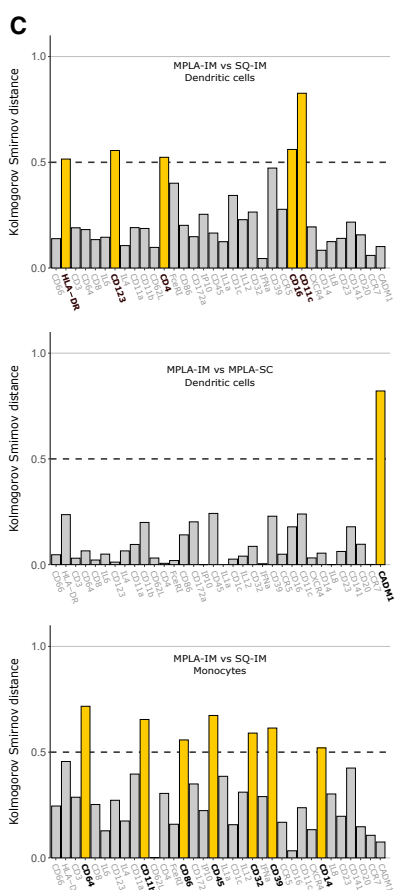
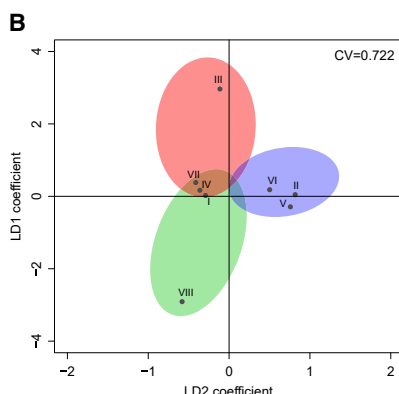
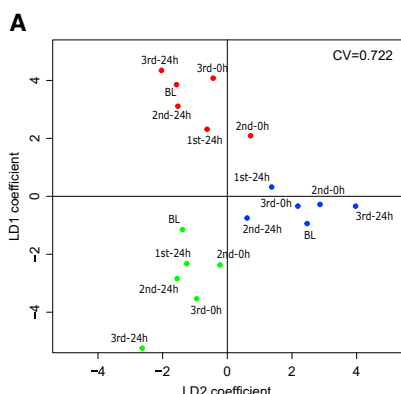


Figure 5. Identification of vaccine cell signatures

(A) Linear discriminant analysis in two dimensions (LD 1 and LD 2) performed using mean kinetic family abundances of all individuals to discriminate vaccine regimens at each time point.

(B) LDA analysis conducted with the mean abundances of KF abundances for all individuals and all time point to identify the contribution of each KF to discriminate vaccine regimens. The colored areas show the association of kinetic families with the MPLA-IM (red), MPLA-SC (green), and SQ-IM (blue) injections. The areas are positioned according to the LDA results in (A) separating the different vaccine regimens. Kinetic families for which the Euclidian distance to the origin did not reach the threshold of 0.5 (black circle) were not considered as discriminant between vaccines.

(C) Identification of the vaccine-associated KF (defined in B) markers that contribute the most to discriminate vaccine regimens. The differential expression for each marker between vaccines is quantified by the Kolmogorov-Smirnov distance indicating the maximal distance between cumulative distribution function (CDF). DCs and monocytes from each signature were separated to establish distances and the threshold used to identify discriminant markers were represented with dot lines.

(D) Median signal intensity (MSI) distributions of markers previously revealed in (C) for each population belonging to vaccine signatures, with MPLA-IM in red, MPLA-SC in green, and SQ-IM in blue. Monocyte signatures for both MPLA injections overlap, as they are characterized by the same kinetic families.

Discrepancies between adjuvants occurred especially after the third injection, where SQ-IM vaccinated animals displayed a higher and more homogeneous rsFc γ RIIla binding activity than MPLA-IM, suggesting that SQ-IM ConM SOSIP.v7 vaccines have better abilities to induce FcR-mediated effector functions. Though, a SQ-SC group would be of interest to verify if IM induced more efficient humoral responses than SC independently of the adjuvants and to confirm our hypothesis.

There are reported evidences that early events following vaccine injections affecting APC targeting, activation, and antigen processing and presentation impact the quality of adaptive response. Indeed, Schifanella et al. reported in the NHP model that “The relationship between vaccine efficacy and the neutralization profile of the challenge virus appear to be linked to the different immunological spaces created by MF59 and Alum via CXCL10 and IL-1 β , respectively,”²⁶ suggesting a role for innate cells in the quality of induced nAb. This study confirms observations of the same group of authors who demonstrated that “Vaccine efficacy was associated with alum-induced, but not with MF59-induced, envelope (Env)-dependent mucosal innate

production, and rsFc γ RIIla binding activity are induced more efficiently by the IM than the SC route when considering MPLA. However, the nAb responses induced by ConM SOSIP.v7 decayed quickly, which is consistent with many previous observations using HIV-1 Env-based vaccines, including gp120s and SOSIP trimers.^{23,24} These observations imply that HIV-1 Env-based vaccines are poorly able at generating long-lived plasma cells and should guide strategies to improve the durability of anti-Env immunity. We have previously studied the Ab specificities induced by the ConM SOSIP.v7 immunogen in rabbits and determined that the dominant nAb response is directed against a region involving V1, V2, and V3.^{15,25}

Cell Reports Medicine

Article

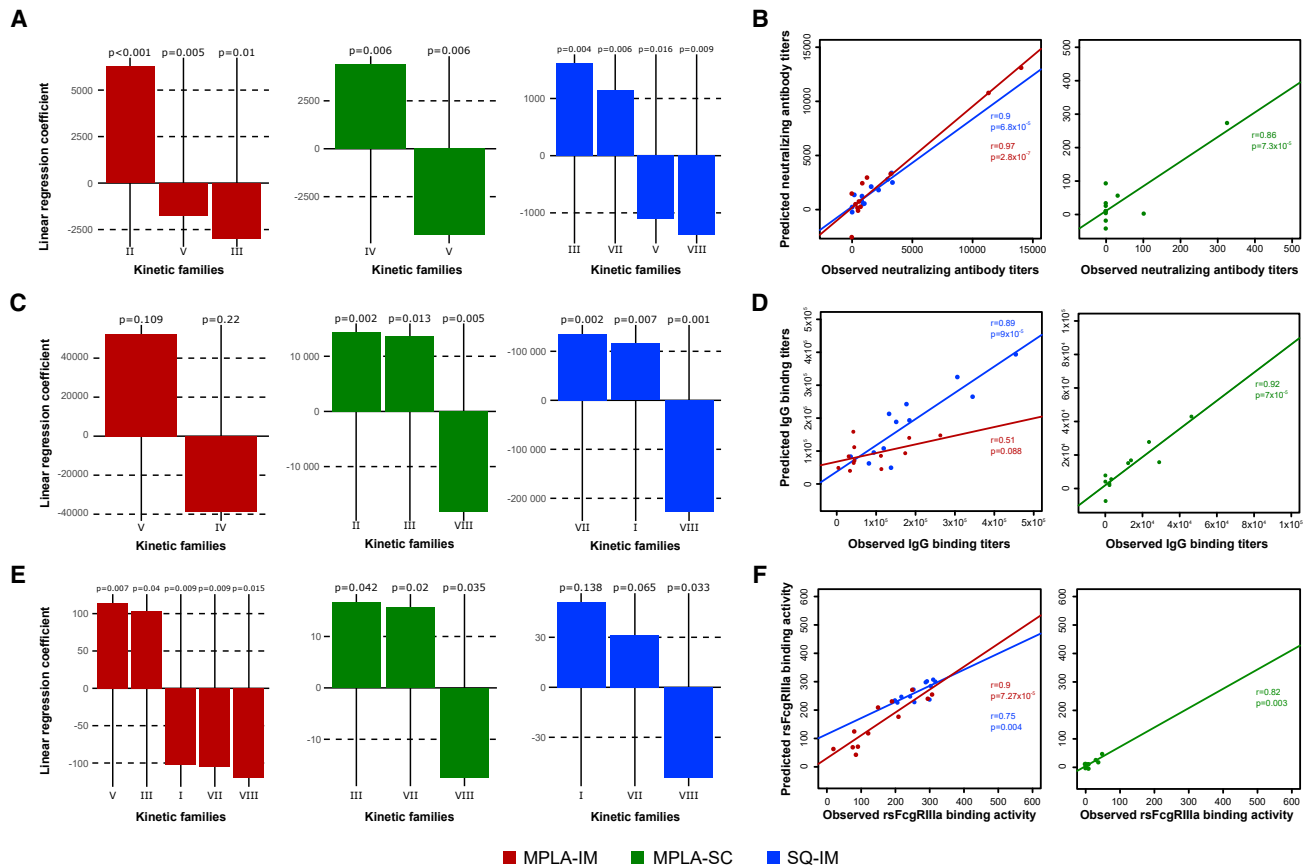


Figure 6. The abundance of innate immune cell populations predicts ConM SOSIP.v7 humoral responses

A linear regression was employed to assess the relationship of the kinetic family cell abundance 24 h after the second and third injections with three biological outcomes: the nAb titer (A), the IgG binding titer (C), and the rsFc γ RIIIa binding activity (E). MPLA-IM, MPLA-SC, and SQ-IM are displayed in red, green, and blue respectively. Linear regression coefficients with a p value ≤ 0.05 are considered necessary and sufficient to predict those humoral parameters. Iterative linear regressions were generated until all coefficients had a p value ≤ 0.05 . (B, D, and F) represent the correlation of the observed and predicted values by the linear regression for nAb titer, IgG binding titer and the rsFc γ RIIIa binding activity, respectively. The Pearson correlation coefficient and p values are shown.

lymphoid cells (ILCs) that produce interleukin (IL)-17, as well as with mucosal IgG to the gp120 variable region 2 (V2) and the expression of 12 genes, ten of which are part of the RAS pathway.²⁷ Similarly, the route of administration, and therefore the type of locally targeted APC, has been described as an important factor driving the quality of the neutralizing response against an SOSIP protein. Pauthner et al. demonstrated that subcutaneous immunizations induce stronger nAb responses against tier-2 HIV than intramuscular immunizations. Contrary to this study, we demonstrated that intramuscular immunizations elicit higher nAb responses against the SOSIP protein. The use of ISCOMATRIX as adjuvant by Pauthner et al. may lead to a different APC targeting, activation, and antigen processing and presentation then generating different nAb responses from what we observed.

Our results suggest that MPLA mainly affects the expansion of monocyte, moDC, and HLA-DR lo -CD11c $^{+}$ -CD16 $^{+}$ DC populations, especially when combined with the IM route. This may reflect adjuvants' properties to mobilize immune cells into tissues as shown in mice with MF59, an oil in water emulsion similar

to SQ.²⁸ Nevertheless, adjuvants alone could not explain the differences we observed. Indeed, the quality of innate immune responses is also dependent on immune cells tissues colonization, as previously reported.²² Ols et al.²⁹ showed that an IM injection induced a greater antigen uptake by antigen-presenting cells than an SC injection of Env proteins in MPLA liposomes. They hypothesized that this may be due to a better formation of immune complexes when subjects are re-exposed because of the high vascularization of muscles. Such an effect, combined with the increasing number of circulating moDCs and HLA-DR lo -CD11c $^{+}$ -CD16 $^{+}$ DCs following ConM SOSIP.v7 immunization, could explain the higher nAb titers we observed following IM injections. Strikingly, the later monocyte activation and higher proportion of CADM1 $^{+}$ cells observed for the MPLA-SC compared with the other vaccine strategies may also be involved in the delayed nAb production observed in this group.

The dynamic changes observed for HLA-DR lo -CD11c $^{+}$ -CD16 $^{+}$ DCs following the MPLA-IM injections may also be associated with the properties of the tissue, as we previously showed a higher proportion of CD11c $^{+}$ DC infiltration in the muscle than

in the skin following an SC modified vaccinia Ankara (MVA) vaccine injection.²²

The panel we used lacked antigen targeting receptors to address the antigen presentation capacities of DC, but the vaccine-induced signatures on all other markers and prediction analysis we performed may indeed help to speculate on DCs functionalities. In our study, cDC2 was identified as the SQ-IM vaccine group signature and was also positively associated with nAb production for MPLA-IM vaccine. However, the low abundance of variations detected suggests that cDC2 alone may not be the only APC implicated in the functional outcomes. The PF15 and PF25, identified as moDCs—known to have potent antigen presentation capacities—were also strongly mobilized by MPLA-IM and SQ-IM vaccines. Highly activated moDCs from PF2 were also recruited by the two groups and the SQ-IM group in particular. In addition to its similarity of phenotypic profile with cDC2, moDC expresses DC-SIGN and the macrophage mannose receptor, two receptors implicated with antigen sensing and induction of Th2 responses and then able to drive immune response toward antibodies production.³⁰

Noteworthy, studies on antigen delivery in mice demonstrated that targeting CD11c led to the induction of strong CD4⁺ and CD8⁺ T cells response in addition to strong antibody responses.^{31,32} The CD11c⁺ DC subsets abundance we observed suggest its key role in vaccine response orientation. This may be particularly true for MPLA-IM group where some of CD11c⁺ DC kinetics families (KF-III) constitute the vaccine signature.

On the other hand, the MPLA-SC group can be discriminated from the two other route/adjuvant combinations based on CADM1 expression by cDC1, which is classically associated with CD8⁺ T cells and Th1 priming. In addition, cDC1 subsets we identified also express Clec9A, a C-type lectin receptor known for its implication in the generation of cytotoxic CD8 T cell responses. We may thus speculate that if not optimal for antibody production, this adjuvant/route combination would be of interest for promoting cellular immunity. The key role of CADM1 in vaccine response orientation is conferment by the negative association we observed for this marker with MPLA-IM and SQ-IM in induced antibody responses.

Fc γ RIIIA and Fc γ RIIIB, two isoforms of CD16, have been associated with innate cell cytotoxicity.³³ Monocytes are known to express CD16, and although CD16⁺ DCs remain a controversial subset, Fromm et al.³⁴ demonstrated that CD16⁺ monocytes and CD16⁺ DCs were two phenotypically and functionally distinguishable populations that have been identified to be able to perform ADCC.^{35,36} Our data show an important mobilization of monocytes and CD16⁺ DCs in the blood of all animals, and especially for the MPLA-IM group. However, a greater rsFc γ RIIIA binding activity was observed in the SQ-IM vaccinated animals, where those populations were less represented. This suggests that rsFc γ RIIIA binding activity may not be exclusively explained by monocytes and CD16⁺ DCs recruitment. Indeed, other CD16⁺ innate populations, such as neutrophils and NK cells, known to exert cytotoxic activity, might have been underestimated in our study.³⁷ We recently reported that polymorphonuclear (PMN) cells, in particular, are key players in vaccine responses.^{38,39} Unfortunately, granulocytes were unexplored in our study because of technical limitations. Future studies should assess the value of

integrating PMN and NK markers in such kind of analysis, in order to correlate these populations to rsFc γ RIIIA binding activity and thus more finely predict vaccine responses.

In addition to PMN and NK cells, using similar approaches for the study of B and T lymphocytes, including antigen-specific cells, would be of interest to characterize the installation of vaccine response, as it has been shown that increased antibody responses depend on enhanced interactions between APCs and CD4⁺ T cells and B cells.

In the field of HIV vaccines, an important role of myeloid cell-expressing markers was also identified in our NHP study. Indeed, in a human systems vaccinology approach of the ALVAC-HIV vaccine, Andersen-Nissen and colleague observed an enrichment of monocytes and CD16⁺ monocytes-associated transcripts.⁴⁰ Also, NHP studies based on the ALVAC-SIV have associated monocytes signatures with a decreased risk of SIV-mac251 acquisition.^{27,41} In our manuscript, we also highlighted an important role of monocytes following the different vaccines including CD16⁺ non-classical and intermediate monocytes, especially for animals immunized with the HIV glycoprotein in MPLA adjuvant and by IM route. Furthermore, we also evidenced a role for CD11c⁺-CD16⁺ DCs that was not mentioned in these previous studies.

It is possible that the changes in cell populations we observed in the cynomolgus macaque model may be of interest in the design and monitoring of vaccine responses in humans, although species specificities in immune cell compartments need to be considered when transferring knowledge from animal studies to clinical trials.⁴²⁻⁴⁴

In conclusion, we show that autologous Ab binding titers and neutralizing activity are induced more efficiently by the IM than SC route when MPLA is used as adjuvant and that the efficacy of MPLA and SQ is in the same range when the IM route is used, even though immune pathways involved seem to differ. We also reveal an association between early-occurring myeloid cell signatures following immunization and adaptive immune parameters. These findings provide new insights on immune mechanisms of interest for vaccine innovation and demonstrate that monitoring of innate signatures during early vaccine development could help minimizing the risk of failure during clinical development phases.

Limitations of the study

The results from this study may inform future strategies for evaluating the effectiveness of HIV-1 vaccines in preclinical animal models and humans. However, it is important to note that we lack data on autologous and heterologous tier-2 viruses' neutralization, which represent a limitation in our study as the induction of bnAbs is expected to be required for an effective HIV vaccine.

While rhesus macaques have been used for many HIV vaccine studies, we and others have extensively used cynomolgus macaques for assessing host immune response to SIV/SIV infection and to HIV vaccines.⁴⁵⁻⁴⁹ A direct comparison of both species should reveal if any of these models is more representative for human responses. However, most antibodies used to phenotype cluster determinants and to characterize cytokine production are anti-human determinant antibodies selected to cross-react with macaque determinants. As a consequence,

Cell Reports Medicine

Article



reagents availability represents a technical limitation that drives panel design, and some markers classically used to characterize cell populations in humans may not be available for NHPs. Furthermore, anti-human antibodies may result in slightly altered signal detection in flow and mass cytometry due to differences in binding affinity on macaque epitopes. Finally, markers expression may differ between species as some of them might be specific to a given species. Furthermore, a given marker expressed in both human and macaque may not be identified in the same cell population, thus limiting the full translation of the preclinical studies to the human situation.⁵⁰

STAR★METHODS

Detailed methods are provided in the online version of this paper and include the following:

- KEY RESOURCES TABLE

- RESOURCE AVAILABILITY

- Lead contact
- Materials availability
- Data and code availability

- EXPERIMENTAL MODEL AND SUBJECT DETAILS

- Ethics and biosafety statement
- Animals and study design
- Adjuvants

- METHOD DETAILS

- ELISA reagents and procedures
- Neutralization assay
- ELISA-based rsFc γ RIIla dimer-binding assay
- Antibody coupling with lanthanide isotopes
- Staining and CyTOF acquisition
- Data processing
- Cell population identification
- Heatmap representation
- Phenotypic and kinetic families
- Negative-stain electron microscopy

- QUANTIFICATION AND STATISTICAL ANALYSIS

- Statistics
- Linear discriminant analysis
- Cytocompare
- Generalized linear model

SUPPLEMENTAL INFORMATION

Supplemental information can be found online at <https://doi.org/10.1016/j.xcrm.2022.100751>.

ACKNOWLEDGMENTS

We thank the staff of the animal facility of IDMIT, particularly B. Delache, M. Pottier, S. Langlois, J.M. Robert, N. Dhooge, and R. Ho Tsong Fang. We also thank S. Kent, M. Hogarth, and B. Wines for providing the dimeric Fc γ RIIla protein. Dietmar Katinger provided the adjuvants. This study was supported by the European Union's Horizon 2020 (EAVI2020, grant N°681137), the European Infrastructure TRANSVAC2 (grant N° 730964), the Agence Nationale de Recherche sur le SIDA et les hépatites virales (ANRS) and the Bill and Melinda Gates Foundation (OPP1115782). R.W.S. is a recipient of a Vici fellowship from the Netherlands Organisation for Scientific Research (NWO). The Infectious Disease Models and Innovative Therapies Research Infrastructure (IDMIT) is

supported by the "Programmes Investissements d'Avenir" (PIA), managed by the ANR under references ANR-11-INBS-0008 and ANR-10-EQPX-02-01. J.L.P. received a PhD scholarship from the University of Paris-Saclay. We thank the Fondation Dormeur Vaduz for the donation of instruments relevant to this project.

AUTHOR CONTRIBUTIONS

A.B.W. and O.G. and performed electron microscopy experiments. A.S.B. contributed to the mass cytometry experiments design. A.S.G. coordinated the cytometry platform and experiments. E.G. contributed to the data analysis. E.M.L. managed the mass cytometer and contributed to the results analysis. G.S. contributed to the design of the study and the analysis of the data and coordinated the neutralization assays. I.B. designed and produced the immunogens. J.L.P. designed and supervised the mass cytometry experiments and contributed to the data analysis. M.C. coordinated the FcgR-binding assays and contributed to analysis of the data. M.T. performed the neutralization assays and analysis. M.V.T. performed the mass cytometry experiments, analyzed the data, and wrote the article. N.D.B. managed the ethical authorizations, prepared the vaccines, and contributed to the study design, to coordination, and to the data analyses. P.M. contributed to the design of the study, coordinated the study and experiments, prepared the vaccines, and contributed to the data analysis. P.M.K. supervised the ELISA experiments. R.L.G. contributed to the study design and the results analysis. R.J.S. coordinated the EAVI2020 project and contributed to the study design and to the results analysis. R.S. contributed to the study design and coordinated the immunogens production. Y.A. performed and analyzed the ELISA. All authors reviewed and edited the manuscript.

DECLARATION OF INTERESTS

The authors declare no competing interests.

Received: September 24, 2021

Revised: June 9, 2022

Accepted: September 2, 2022

Published: September 26, 2022

REFERENCES

1. United Nations Joint Programme on HIV/AIDS (UNAIDS) (2019). UNAIDS Data 2019, p. 476.
2. Gaucher, D., Therrien, R., Kettaf, N., Angermann, B.R., Boucher, G., Filali-Mouhim, A., Moser, J.M., Mehta, R.S., Drake, D.R., 3rd, Castro, E., et al. (2008). Yellow fever vaccine induces integrated multilineage and polyfunctional immune responses. *J. Exp. Med.* 205, 3119–3131.
3. Querec, T.D., Akondy, R.S., Lee, E.K., Cao, W., Nakaya, H.I., Teuwen, D., Pirani, A., Gernert, K., Deng, J., Marzolf, B., et al. (2009). Systems biology approach predicts immunogenicity of the yellow fever vaccine in humans. *Nat. Immunol.* 10, 116–125.
4. Hou, J., Wang, S., Jia, M., Li, D., Liu, Y., Li, Z., Zhu, H., Xu, H., Sun, M., Lu, L., et al. (2017). A systems vaccinology approach reveals temporal transcriptomic changes of immune responses to the yellow fever 17D vaccine. *J. Immunol.* 199, 1476–1489.
5. Rechtien, A., Richert, L., Lorenzo, H., Martrus, G., Hejblum, B., Dahlke, C., Kasonta, R., Zinser, M., Stubbe, H., Matschl, U., et al. (2017). Systems vaccinology identifies an early innate immune signature as a correlate of antibody responses to the ebola vaccine rVSV-ZEBOV. *Cell Rep.* 20, 2251–2261.
6. Li, S., Roushail, N., Duraisingham, S., Romero-Steiner, S., Presnell, S., Davis, C., Schmidt, D.S., Johnson, S.E., Milton, A., Rajam, G., et al. (2014). Molecular signatures of antibody responses derived from a systems biology study of five human vaccines. *Nat. Immunol.* 15, 195–204.
7. Nakaya, H.I., Clutterbuck, E., Kazmin, D., Wang, L., Cortese, M., Bosinger, S.E., Patel, N.B., Zak, D.E., Aderem, A., Dong, T., et al. (2016). Systems

- biology of immunity to MF59-adjuvanted versus nonadjuvanted trivalent seasonal influenza vaccines in early childhood. *Proc. Natl. Acad. Sci. USA* **113**, 1853–1858.
- 8. Tsang, J.S., Schwartzberg, P.L., Kotliarov, Y., Biancotto, A., Xie, Z., Germain, R.N., Wang, E., Olnes, M.J., Narayanan, M., Golding, H., et al. (2014). Global analyses of human immune variation reveal baseline predictors of postvaccination responses. *Cell* **157**, 499–513.
 - 9. Trautmann, L., and Sekaly, R.P. (2011). Solving vaccine mysteries: a systems biology perspective. *Nat. Immunol.* **12**, 729–731.
 - 10. Mooney, M., McWeeney, S., Canderan, G., and Sékaly, R.P. (2013). A systems framework for vaccine design. *Curr. Opin. Immunol.* **25**, 551–555.
 - 11. Reimann, K.A., Parker, R.A., Seaman, M.S., Beaudry, K., Beddall, M., Peterson, L., Williams, K.C., Veazey, R.S., Montefiori, D.C., Mascola, J.R., et al. (2005). Pathogenicity of simian-human immunodeficiency virus SHIV-89.6P and SIVmac is attenuated in cynomolgus macaques and associated with early T-lymphocyte responses. *J. Virol.* **79**, 8878–8885.
 - 12. Estes, J.D., Wong, S.W., and Brenchley, J.M. (2018). Nonhuman primate models of human viral infections. *Nat. Rev. Immunol.* **18**, 390–404.
 - 13. Sanders, R.W., and Moore, J.P. (2017). Native-like Env trimers as a platform for HIV-1 vaccine design. *Immunol. Rev.* **275**, 161–182. <https://doi.org/10.1111/imr.12481>.
 - 14. De Taeye, S.W., Ozorowski, G., de la Peña, A.T., Guttman, M., Julien, J.-P., van den Kerkhof, T.L.G.M., Burger, J.A., Pritchard, L.K., Pugach, P., Yasmeen, A., et al. (2015). Immunogenicity of stabilized HIV-1 envelope trimers with reduced exposure of non-neutralizing epitopes. *Cell*. <https://doi.org/10.1016/j.cell.2015.11.056>.
 - 15. Sliepen, K., Han, B.W., Bontjer, I., Mooij, P., Garces, F., Behrens, A.J., Rantalainen, K., Kumar, S., Sarkar, A., Brouwer, P.J.M., et al. (2019). Structure and immunogenicity of a stabilized HIV-1 envelope trimer based on a group-M consensus sequence. *Nat. Commun.* **10**, 2355.
 - 16. Brouwer, P.J.M., Antanasijevic, A., Berndsen, Z., Yasmeen, A., Fiala, B., Bijl, T.P.L., Bontjer, I., Bale, J.B., Sheffler, W., Allen, J.D., et al. (2019). Enhancing and shaping the immunogenicity of native-like HIV-1 envelope trimers with a two-component protein nanoparticle. *Nat. Commun.* **10**, 4272.
 - 17. Wines, B.D., Vanderven, H.A., Esparon, S.E., Kristensen, A.B., Kent, S.J., and Hogarth, P.M. (2016). Dimeric Fc γ R ectodomains as probes of the Fc receptor function of anti-influenza virus IgG. *J. Immunol.* **197**, 1507–1516.
 - 18. Zhang, L., Wang, W., and Wang, S. (2015). Effect of vaccine administration modality on immunogenicity and efficacy. Preprint at Expert Rev. Vaccines **14**, 1509–1523. <https://doi.org/10.1586/14760584.2015.1081067>.
 - 19. Calabro, S., Tritto, E., Pezzotti, A., Taccone, M., Muzzi, A., Bertholet, S., De Gregorio, E., O'Hagan, D.T., Baudner, B., and Seubert, A. (2013). The adjuvant effect of MF59 is due to the oil-in-water emulsion formulation, none of the individual components induce a comparable adjuvant effect. *Vaccine* **31**, 3363–3369.
 - 20. Pauthner, M., Havenar-Daughton, C., Sok, D., Nkolola, J.P., Bastidas, R., Boopathy, A.V., Carnathan, D.G., Chandrashekhar, A., Cirelli, K.M., Cottrell, C.A., et al. (2017). Elicitation of robust tier 2 neutralizing antibody responses in nonhuman primates by HIV envelope trimer immunization using optimized approaches. *Immunity* **46**, 1073–1088.e6.
 - 21. O'Hagan, D.T., Ott, G.S., De Gregorio, E., and Seubert, A. (2012). The mechanism of action of MF59 – an innately attractive adjuvant formulation. *Vaccine* **30**, 4341–4348.
 - 22. Rosenbaum, P., Tchitchek, N., Joly, C., Rodriguez Pozo, A., Stimmer, L., Langlois, S., Hocini, H., Gosse, L., Pejoski, D., Cosma, A., et al. (2020). Vaccine inoculation route modulates early immunity and consequently antigen-specific immune response. *SSRN J.* <https://doi.org/10.2139/ssrn.3535877>.
 - 23. Anderson, K.P., Lucas, C., Hanson, C.V., Londe, H.F., Izu, A., Gregory, T., Ammann, A., Berman, P.W., and Eichberg, J.W. (1989). Effect of dose and immunization schedule on immune response of baboons to recombinant glycoprotein 120 of HIV-1. *J. Infect. Dis.* **160**, 960–969.
 - 24. Sanders, R.W., van Gils, M.J., Derking, R., Sok, D., Ketis, T.J., Burger, J.A., Ozorowski, G., Cupo, A., Simonich, C., Goo, L., et al. (2015). HIV-1 VACCINES. HIV-1 neutralizing antibodies induced by native-like envelope trimers. *Science* **349**, aac4223.
 - 25. Brouwer, P.J.M., Antanasijevic, A., de Gast, M., Allen, J.D., Bijl, T.P.L., Yasmeen, A., Ravichandran, R., Burger, J.A., Ozorowski, G., Torres, J.L., et al. (2021). Immunofocusing and enhancing autologous Tier-2 HIV-1 neutralization by displaying Env trimers on two-component protein nanoparticles. *NPJ Vaccines* **6**, 24.
 - 26. Schifanella, L., Barnett, S.W., Bissa, M., Galli, V., Doster, M.N., Vaccari, M., Tomaras, G.D., Shen, X., Phogat, S., Pal, R., et al. (2019). ALVAC-HIV B/C candidate HIV vaccine efficacy dependent on neutralization profile of challenge virus and adjuvant dose and type. *PLoS Pathog.* **15**, e1008121.
 - 27. Vaccari, M., Fourati, S., Gordon, S.N., Brown, D.R., Bissa, M., Schifanella, L., Silva de Castro, I., Doster, M.N., Galli, V., Omsland, M., et al. (2018). HIV vaccine candidate activation of hypoxia and the inflammasome in CD14+ monocytes is associated with a decreased risk of SIVmac251 acquisition. *Nat. Med.* **24**, 847–856.
 - 28. Mosca, F., Tritto, E., Muzzi, A., Monaci, E., Bagnoli, F., Iavarone, C., O'Hagan, D., Rappuoli, R., and De Gregorio, E. (2008). Molecular and cellular signatures of human vaccine adjuvants. *Proc. Natl. Acad. Sci. USA* **105**, 10501–10506.
 - 29. Ols, S., Yang, L., Thompson, E.A., Pushparaj, P., Tran, K., Liang, F., Lin, A., Eriksson, B., Karlsson Hedestam, G.B., Wyatt, R.T., and Loré, K. (2020). Route of vaccine administration alters antigen trafficking but not innate or adaptive immunity. *Cell Rep.* **30**, 3964–3971.e7.
 - 30. Lehmann, C.H.K., Heger, L., Heidkamp, G.F., Baranska, A., Lühr, J.J., Hoffmann, A., and Dudziak, D. (2016). Direct delivery of antigens to dendritic cells via antibodies specific for endocytic receptors as a promising strategy for future therapies. *Vaccines* **4**, 8.
 - 31. Castro, F.V.V., Tutt, A.L., White, A.L., Teeling, J.L., James, S., French, R.R., and Glennie, M.J. (2008). CD11c provides an effective immunotarget for the generation of both CD4 and CD8 T cell responses. *Eur. J. Immunol.* **38**, 2263–2273.
 - 32. White, A.L., Tutt, A.L., James, S., Wilkinson, K.A., Castro, F.V.V., Dixon, S.V., et al. (2010). Ligation of CD11c during vaccination promotes germinal centre induction and robust humoral responses without adjuvant. *Immunology* **131**, 141–151.
 - 33. Zhang, Y., Boesen, C.C., Radaev, S., Brooks, A.G., Fridman, W.H., Sautes-Fridman, C., and Sun, P.D. (2000). Crystal structure of the extracellular domain of a human Fc γ RIII. *Immunity* **13**, 387–395.
 - 34. Fromm, P., Papadimitriou, M., Hsu, J., Larsen, S.R., Gibson, J., Bradstock, K., Kupresanin, F., Clark, G., and Hart, D.N. (2016). CD16+ dendritic cells are a unique myeloid antigen presenting cell population. *Blood* **128**, 4897.
 - 35. Schmitz, M., Zhao, S., Schäkel, K., Bornhäuser, M., Ockert, D., and Rieber, E.P. (2002). Native human blood dendritic cells as potent effectors in antibody-dependent cellular cytotoxicity. *Blood* **100**, 1502–1504.
 - 36. Yeap, W.H., Wong, K.L., Shimasaki, N., Teo, E.C.Y., Quek, J.K.S., Yong, H.X., Diong, C.P., Bertoletti, A., Linn, Y.C., and Wong, S.C. (2016). CD16 is indispensable for antibody-dependent cellular cytotoxicity by human monocytes. *Sci. Rep.* **6**, 34310–34322.
 - 37. Palgen, J.L., Tchitchek, N., Huot, N., Elhmouzi-Younes, J., Lefebvre, C., Rosenbaum, P., Dereuddre-Bosquet, N., Martinon, F., Hocini, H., Cosma, A., et al. (2019). NK cell immune responses differ after prime and boost vaccination. *J. Leukoc. Biol.* **105**, 1055–1073.
 - 38. Palgen, J.L., Tchitchek, N., Elhmouzi-Younes, J., Delandre, S., Namet, I., Rosenbaum, P., Dereuddre-Bosquet, N., Martinon, F., Cosma, A., Lévy, Y., et al. (2018). Prime and boost vaccination elicit a distinct innate myeloid cell immune response. *Sci. Rep.* **8**, 3087.
 - 39. Palgen, J.L., Tchitchek, N., Rodriguez-Pozo, A., Jouhault, Q., Abdelghahhab, H., Dereuddre-Bosquet, N., Contreras, V., Martinon, F., Cosma, A.,

Cell Reports Medicine

Article



- Lévy, Y., et al. (2020). Innate and secondary humoral responses are improved by increasing the time between MVA vaccine immunizations. *NPJ Vaccines* 5, 24.
40. Andersen-Nissen, E., Fiore-Gartland, A., Ballweber Fleming, L., Carpp, L.N., Naidoo, A.F., Harper, M.S., Voillet, V., Grunenberg, N., Laher, F., Innes, C., et al. (2021). Innate immune signatures to a partially-efficacious HIV vaccine predict correlates of HIV-1 infection risk. *PLoS Pathog.* 17, e1009363.
41. Gorini, G., Fourati, S., Vaccari, M., Rahman, M.A., Gordon, S.N., Brown, D.R., Law, L., Chang, J., Green, R., Barrenäs, F., et al. (2020). Engagement of monocytes, NK cells, and CD4+ Th1 cells by ALVAC-SIV vaccination results in a decreased risk of SIVmac251 vaginal acquisition. *PLoS Pathog.* 16, e1008377.
42. Autissier, P., Soulard, C., Burdo, T.H., and Williams, K.C. (2010). Immuno-phenotyping of lymphocyte, monocyte and dendritic cell subsets in normal rhesus macaques by 12-color flow cytometry: clarification on DC heterogeneity. *J. Immunol. Methods* 360, 119–128.
43. Sugimoto, C., Hasegawa, A., Saito, Y., Fukuyo, Y., Chiu, K.B., Cai, Y., Breed, M.W., Mori, K., Roy, C.J., Lackner, A.A., et al. (2015). Differentiation kinetics of blood monocytes and dendritic cells in macaques: insights to understanding human myeloid cell development. *J. Immunol.* 195, 1774–1781.
44. Elhoumzi-Younes, J., Palgen, J.L., Tchitchev, N., Delandre, S., Namet, I., Bodinham, C.L., Pizzoferro, K., Lewis, D.J., Le Grand, R., Cosma, A., and Beignon, A.S. (2017). In depth comparative phenotyping of blood innate myeloid leukocytes from healthy humans and macaques using mass cytometry. *Cytometry* 91, 969–982.
45. Moriarty, R.V., Rodgers, M.A., Ellis, A.L., Balgeman, A.J., Larson, E.C., Hopkins, F., Chase, M.R., Maiello, P., Fortune, S.M., Scanga, C.A., and O'Connor, S.L. (2022). Spontaneous control of SIV replication does not prevent T cell dysregulation and bacterial dissemination in animals Co-infected with M. tuberculosis. *Microbiol. Spectr.* 10, e0172421.
46. Nzounza, P., Martin, G., Dereuddre-Bosquet, N., Najburg, V., Gosse, L., Ruffié, C., Combrebet, C., Petitdemange, C., Souquère, S., Schlecht-Louf, G., et al. (2021). A recombinant measles virus vaccine strongly reduces SHIV viremia and virus reservoir establishment in macaques. *NPJ Vaccines* 6, 123.
47. Cavarelli, M., Hua, S., Hantour, N., Tricot, S., Tchitchev, N., Gommet, C., Hocini, H., Chapon, C., Dereuddre-Bosquet, N., and Le Grand, R. (2021). Leukocytospermia induces intraepithelial recruitment of dendritic cells and increases SIV replication in colorectal tissue explants. *Commun. Biol.* 4, 861.
48. le Grand, R., Dereuddre-Bosquet, N., Dispineri, S., Gosse, L., Desjardins, D., Shen, X., Tolazzi, M., Ochsenbauer, C., Saidi, H., Tomaras, G., et al. (2016). Superior efficacy of a human immunodeficiency virus vaccine combined with antiretroviral prevention in simian-human immunodeficiency virus-challenged nonhuman primates. *J. Virol.* 90, 5315–5328.
49. Lemaitre, J., Desjardins, D., Gallouët, A.S., Gomez-Pacheco, M., Bourgeois, C., Favier, B., Sáez-Cirión, A., Le Grand, R., and Lambotte, O. (2022). Expansion of immature neutrophils during SIV infection is associated with their capacity to modulate T-cell function. *Front. Immunol.* 13, 781356.
50. Jacquelin, B., Mayau, V., Targat, B., Liovat, A.S., Kunkel, D., Petitjean, G., Dillies, M.A., Roques, P., Butor, C., Silvestri, G., et al. (2009). Nonpathogenic SIV infection of African green monkeys induces a strong but rapidly controlled type I IFN response. *J. Clin. Invest.* 119, 3544–3555.
51. Vishwanathan, S.A., Burgener, A., Bosinger, S.E., Tharp, G.K., Guenthner, P.C., Patel, N.B., Birse, K., Hanson, D.L., Westmacott, G.R., Henning, T.R., et al. (2015). Cataloguing of potential HIV susceptibility factors during the menstrual cycle of pig-tailed macaques by using a systems biology approach. *J. Virol.* 89, 9167–9177.
52. Han, Q., Bradley, T., Williams, W.B., Cain, D.W., Montefiori, D.C., Saunders, K.O., Parks, R.J., Edwards, R.W., Ferrari, G., Mueller, O., et al. (2020). Neonatal rhesus macaques have distinct immune cell transcriptional profiles following HIV envelope immunization. *Cell Rep.* 30, 1553–1569.e6.
53. Heyndrickx, L., Heath, A., Sheik-Khalil, E., Alcamí, J., Bongertz, V., Jansson, M., Malnati, M., Montefiori, D., Moog, C., Morris, L., et al. (2012). International network for comparison of HIV neutralization assays: the NeutNet report II. *PLoS One* 7, e36438.
54. Supaphiphat, K., Bernard-Stoecklin, S., Gommet, C., Delache, B., Dereuddre-Bosquet, N., Kent, S.J., Wines, B.D., Hogarth, P.M., Le Grand, R., and Cavarelli, M. (2020). Innate and adaptive anti-SIV responses in macaque semen: implications for infectivity and risk of transmission. *Front. Immunol.* 11, 850.
55. Han, G., Spitzer, M.H., Bendall, S.C., Fanti, W.J., and Nolan, G.P. (2018). Metal-isotope-tagged monoclonal antibodies for high-dimensional mass cytometry. *Nat. Protoc.* 13, 2121–2148.
56. Finck, R., Simonds, E.F., Jager, A., Krishnaswamy, S., Sachs, K., Fanti, W., Pe'er, D., Nolan, G.P., and Bendall, S.C. (2013). Normalization of mass cytometry data with bead standards. *Cytometry A* 83, 483–494.
57. Kleinsteuber, K., Corleis, B., Rashidi, N., Nchinda, N., Lisanti, A., Cho, J.L., Medoff, B.D., Kwon, D., and Walker, B.D. (2016). Standardization and quality control for high-dimensional mass cytometry studies of human samples. *Cytometry A* 89, 903–913.
58. Qiu, P., Simonds, E.F., Bendall, S.C., Gibbs, K.D., Jr., Bruggner, R.V., Linderman, M.D., Sachs, K., Nolan, G.P., and Plevritis, S.K. (2011). Extracting a cellular hierarchy from high-dimensional cytometry data with SPADE. *Nat. Biotechnol.* 29, 886–891.
59. Gautreau, G., Pejoski, D., Le Grand, R., Cosma, A., Beignon, A.S., and Tchitchev, N. (2017). SPADEVizR: an R package for visualization, analysis and integration of SPADE results. *Bioinformatics* 33, 779–781. <https://doi.org/10.1093/bioinformatics/btw708>.
60. Suloway, C., Pulokas, J., Fellmann, D., Cheng, A., Guerra, F., Quispe, J., Stagg, S., Potter, C.S., and Carragher, B. (2005). Automated molecular microscopy: the new Legion system. *J. Struct. Biol.* 151, 41–60.
61. Lander, G.C., Stagg, S.M., Voss, N.R., Cheng, A., Fellmann, D., Pulokas, J., Yoshioka, C., Irving, C., Mulder, A., Lau, P.W., et al. (2009). Appion: an integrated, database-driven pipeline to facilitate EM image processing. *J. Struct. Biol.* 166, 95–102.
62. Pugach, P., Ozorowski, G., Cupo, A., Ringe, R., Yasmeen, A., de Val, N., Derking, R., Kim, H.J., Korzun, J., Golabek, M., et al. (2015). A native-like SOSIP.664 trimer based on an HIV-1 subtype B env gene. *J. Virol.* 89, 3380–3395.
63. Sanders, R.W., Derking, R., Cupo, A., Julien, J.P., Yasmeen, A., de Val, N., Kim, H.J., Blattner, C., de la Peña, A.T., Korzun, J., et al. (2013). A next-generation cleaved, soluble HIV-1 env trimer, BG505 SOSIP.664 gp140, expresses multiple epitopes for broadly neutralizing but not non-neutralizing antibodies. *PLoS Pathog.* 9, e1003618.
64. Platon, L., Pejoski, D., Gautreau, G., Targat, B., Le Grand, R., Beignon, A.S., and Tchitchev, N. (2018). A computational approach for phenotypic comparisons of cell populations in high-dimensional cytometry data. *Methods* 132, 66–75.

STAR★METHODS

KEY RESOURCES TABLE

REAGENT or RESOURCE	SOURCE	IDENTIFIER
Antibodies		
CD66abce Antibody, anti-human	Miltenyi Biotec	Custom reagent (TET2)
Purified anti-human HLA-DR Antibody	Biolegend	Cat#307612; RRID:AB_314690
BD Pharmingen™ Purified mouse anti-human CD3	BD Biosciences	Cat#551916; RRID:AB_394293
CD64 Antibody, anti-human	Miltenyi Biotec	Cat# 130-108-046; RRID:AB_2658939
BD Pharmingen™ Purified mouse anti-human CD8	BD Biosciences	Cat# 555364; RRID:AB_395767
IL-6 Antibody, anti-human	Miltenyi Biotec	Cat#130-096-093; RRID:AB_2652449
BD Pharmingen™ Purified Mouse Anti-Human CD123	BD Biosciences	Cat# 554527; RRID:AB_395455
BD Pharmingen™ Purified Mouse Anti-Human IL-4	BD Biosciences	Cat# 554515; RRID:AB_398567
CD11a Antibody, anti-human	Miltenyi Biotec	Custom reagent (HI111)
BD Pharmingen™ Purified Mouse Anti-Human CD11b	BD Biosciences	Cat# 555386; RRID:AB_395787
CD62L Antibody, anti-human	Miltenyi Biotec	Custom reagent (SK11)
BD Pharmingen™ Purified Mouse Anti-Human CD4	BD Biosciences	Cat# 550625; RRID:AB_393787
Anti-human FcεRI Prufied	eBioscience	14-5899-82
BD Pharmingen™ Purified Mouse Anti-Human CD86	BD Biosciences	Cat# 555663; RRID:AB_396017
CD172a Antibody, anti-human	Miltenyi Biotec	Custom reagent (15-414/REA144 ; RRID:AB_2801909)
IP-10 Antibody, anti-human	Miltenyi Biotec	Cat#130-108-047 ; RRID:AB_2651479
BD Pharmingen™ Purified Mouse Anti-Human CD45	BD Biosciences	Cat# 552566; RRID:AB_394433
IL-1a Antibody, anti-human	Miltenyi Biotec	Custom reagent (364-3B3-14)
Anti-hCD1c Affinity Purified Goat IgG	R&D systems	Cat# AF5910; RRID:AB_1964521
IL-12 Antibody, anti-human	Miltenyi Biotec	Custom reagent (C8.6 ; RRID:AB_10829623)
BD Pharmingen™ Purified Mouse Anti-Human CD32	BD Biosciences	Cat# 555447; RRID:AB_395840
IFNa Antibody, anti-human	Miltenyi Biotec	130-108-050; RRID:AB_2659989
Purified anti-human CD39 (MaxPar® Ready)	Biolegend	Cat#328221; RRID:AB_2563747
BD Pharmingen™ Purified Mouse Anti-Human CD195 (CCR5)	BD Biosciences	Cat# 556041; RRID:AB_396312
CD16 Antibody, anti-human	Miltenyi Biotec	130-108-027 ; RRID:AB_2655423
Purified anti-human CD11c (MaxPar® Ready)	Biolegend	Cat#301639; RRID:AB_2562812
BD Pharmingen™ Purified Mouse Anti-Human CD184 (CXCR4)	BD Biosciences	Cat# 555972; RRID:AB_396265
BD Pharmingen™ Purified Mouse Anti-Human CD14	BD Biosciences	Cat# 555396; RRID:AB_395797
BD Pharmingen™ Purified Mouse Anti-Human IL-8	BD Biosciences	Cat# 554717; RRID:AB_398583
Mouse anti-human CD23	Beckman Coulter	IMBULK1
BD Pharmingen™ Purified Mouse Anti-Human CD141	BD Biosciences	Cat# 559780; RRID:AB_397321
BD Pharmingen™ Purified Mouse Anti-Human CD20	BD Biosciences	Cat# 556631; RRID:AB_396500
CCR7 Antibody, anti-human	Miltenyi Biotec	Custom reagent (G043H7)
Anti-SynCAM (TSLC1/CADM1)	MBL	Cat# CM004-3; RRID:AB_592783
Goat anti-Monkey IgG horseradish peroxidase labelled	AbSerotec	AAI42P
Biological samples		
Cynomolgus macaques PBMCs	IDMIT facility, CEA de Fontenay-aux-roses, France	N/A
Cynomolgus macaques serum	IDMIT facility, CEA de Fontenay-aux-roses, France	N/A

(Continued on next page)

Cell Reports Medicine

Article



Continued

REAGENT or RESOURCE	SOURCE	IDENTIFIER
Chemicals, peptides, and recombinant proteins		
Maxpar® X8 Antibody Labelling Kit, Tag-141Pr to 176Yb	Fluidigm	201141A to 201176A
Cell-ID™ Intercalator-Ir—500 μM	Fluidigm	201192B
Cell-ID™ Intercalator-Rh—2000 μM	Fluidigm	201103B
ConM SOSIP.v7 protein	Rogier Sanders (Sleipen et al., 2019)	https://doi.org/10.1038/s41467-019-1026-5
Mono Phosphoryl Lipid A (MPLA adjuvant)	Polymun Scientific (Klosterneuburg, Austria)	N/A
Squalen Emulsion (SQ adjuvant)	Polymun Scientific (Klosterneuburg, Austria)	N/A
BSA cat#A7906-1kg	Sigma Aldrich	SLBS4333
Purified dimeric macaque rsFcγRIIa Ile158 ectodomain biotin	Hogarth laboratory	N/A
Ultra streptavidin HRP	Thermo Scientific	cat# N504
TMB	Thermo Scientific	cat# 34028-250mL
HCL 1N	VWR	MC3006470500
EDTA	Sigma Aldrich	cat# E5391-250g
Tween 20	Sigma Aldrich	cat# P7949-100mL
SOSIP antigens	Rogier Sanders Amsterdam University Medical Centers, Amsterdam Netherlands	N/A
Bright-Glo	Promega	Cat# E2620
Experimental models: Cell lines		
HEK293F cells	Invitrogen	R79009
HEK-293T/17	CFAR-NIBSC, UK	Cat# 5016
TZM-bl	CFAR-NIBSC, UK	Cat#ARP5011
Experimental models: Organisms/strains		
Cynomolgus macaques: <i>Macaca fascicularis</i>	AAALAC certified breeding centers	N/A
Recombinant DNA		
HIV-1 backbone pSG3 ΔEnv	David C. Montefiori Duke Human Vaccine Institute and Center for HIV-AIDS Vaccine Immunology, Duke University Medical Center, Durham, NC, USA	N/A
pSVIII-93MW 965.26	CFAR-NIBSC, UK	Cat# 2073
pConM SOSIP.v7 HIV-1	Rogier Sanders Amsterdam University Medical Centers, Amsterdam Netherlands	N/A
Software and algorithms		
MatLab compiler software	Beckman Coulter	N/A
CyTOF software	Fluidigm	N/A
Cytobank Premium	Beckman Coulter	N/A
R software		N/A
SPADEVizR R package	https://github.com/tchitchev-lab/ SPADEVizR	N/A
“MASS” R package	https://CRAN.R-project.org/ package=MASS	N/A
Leginon	(Suloway et al., 2005)	https://nramm.nysbc.org/software/ ; RRID:SCR_016731
Appion	(Lander et al., 2009)	https://nramm.nysbc.org/software/ ; RRID:SCR_016734

(Continued on next page)

Continued

REAGENT or RESOURCE	SOURCE	IDENTIFIER
Other		
F96 Nunc maxisorp plate	Scientific laboratory supplies	# 442404
Infectious molecular clone (IMC) ConM	Rogier Sanders (Sliepen et al., 2019)	https://doi.org/10.1038/s41467-019-10262-5
Mithras luminometer	Berthold Italia S.r.l	N/A

RESOURCE AVAILABILITY

Lead contact

Correspondence and requests for materials should be addressed to Roger Le Grand (roger.le-grand@cea.fr).

Materials availability

This study did not generate new unique reagents. Requests for materials will require specific agreements and should be addressed to the [lead contact](#), Roger Le Grand.

Data and code availability

The data that support the findings of this study are available from the corresponding author upon reasonable request. This paper does not report original code. Any additional information required to reanalyze the data reported in this work paper is available from the [lead contact](#) upon request.

EXPERIMENTAL MODEL AND SUBJECT DETAILS

Ethics and biosafety statement

Cynomolgus macaques (*Macaca fascicularis*) originating from Mauritius and imported from AAALAC certified breeding centers were used in this study. All animals were housed in groups at the IDMIT infrastructure facilities (CEA, Fontenay-aux-roses, Animal facility authorization #D92-032-02, Prefecture des Hauts de Seine, France) and in compliance with European Directive 2010/63/EU, the French regulations, and the Standards for Humane Care and Use of Laboratory Animals, of the Office for Laboratory Animal Welfare (OLAW, assurance number #A5826-01, US). The protocols were approved by the institutional ethical committee “Comité d’Ethique en Expérimentation Animale du Commissariat à l’Energie Atomique et aux Energies Alternatives » (CEtEA #44) under statement number A15-073. The study was authorized by the “Research, Innovation and Education Ministry” under registration number APA-FIS#3132-2015121014521340.

Animals and study design

Eighteen adult, female cynomolgus macaques, aged 33 to 42 months, were randomly assigned to three experimental groups of six animals each. All animals were immunized at W0, W8, and W24 with 20 µg ConM SOSIP formulated either with 500 µg MPLA liposomes (MPLA) or 0.5 mL squalene emulsion (SQ). The vaccine was divided between each thigh. One group was immunized by the subcutaneous (SC) route with the MPLA regimen (MPLA-SC), one received the MPLA regimen by the intramuscular (IM) route (MPLA-IM), and the third group received the SQ by the IM route (SQ-IM).

Group size of animals has been defined accordingly to the primary end-point of the study aiming at identifying the best combination of route and adjuvant for generating neutralizing antibodies when comparing the means of the experimental groups. A level of significance of 5% ($\alpha = 0.05$) and a target power of 80% ($1 - \beta = 0.8$) was established. As a consequence, the system biology approach we proposed for identification of early cellular markers predicting Nab response, was exploratory and the N was not defined accordingly to this secondary objective. However, the size of our experimental groups is in the range of similar previously published studies using NHP.⁵⁰⁻⁵²

Animals were observed daily, and clinical exams were performed at baseline and at each bleeding, as described in [Figure 1](#), on anesthetized animals using ketamine (5 mg.kg⁻¹) and metedomidine (0.042 mg.kg⁻¹). Body weight and rectal temperature were recorded, and blood was collected. Blood cell counts, hemoglobin levels, and the hematocrit were determined from EDTA blood using a HMX A/L analyzer (Beckman Coulter). *ConM SOSIP.v7*.

ConM SOSIP.v7 protein was expressed and purified as published previously.^{15,16} In brief, *ConM SOSIP.v7* was expressed in transiently transfected HEK293F cells (Invitrogen, catalog number R79009) and purified from vacuum-filtered (0.2 µm filters) transfection supernatants by PGT145 bNAb-affinity chromatography. The protein was verified by SDS-PAGE analysis and Blue native PAGE analysis as described.^{15,16}

Adjuvants

The MPLA liposomes and squalene emulsion were manufactured at Polymun Scientific (Klosterneuburg, Austria). MPLA batch number MPLA/L02/0.2 μm -filtered was mixed extemporaneously at 500 $\mu\text{g}/\text{mL}$ with 20 μg SOSIP in PBS to 1 mL. Squalene emulsion batch IMP/300916/10.22- μm filtered was composed of an oil phase (5% v/v squalene and 0.5% w/v Span 85) in an aqueous phase (0.5% w/v Tween 80) and 0.5 mL was mixed with 20 μg SOSIP extemporaneously in PBS to 1 mL.

METHOD DETAILS

ELISA reagents and procedures

Antigen-specific IgG levels were assessed by capture ELISA using Myc-c tagged ConM SOSIP.664 v7 for capture by monoclonal Ab 9E10 (ATCC hybridoma). Nunc MaxiSorp high binding 96-well plates (Thermo Fisher Scientific) were coated with 2.5 $\mu\text{g}/\text{mL}$ of 9E10 Ab in 100 $\mu\text{L}/\text{well}$ 1x PBS. The last 3 columns of each plate were coated with goat anti-human Kappa and goat anti-human Lambda (Southern Biotech) for the captured standard IgG, 1:2,000 for each antibody in 100 $\mu\text{L}/\text{well}$ 1x PBS. The plates were incubated overnight at +4°C, washed 4 times with 350 $\mu\text{L}/\text{well}$ 1x PBS-0.05% Tween 20, tapped dry and blocked 1 h at +37°C with 200 $\mu\text{L}/\text{well}$ casein buffer (Thermo Fisher Scientific). Following 4 washes, 1 $\mu\text{g}/\text{mL}$ ConM SOSIP.664 v7 Myc-HIS trimers in 100 $\mu\text{L}/\text{well}$ casein buffer were loaded onto the plates and standard wells with 100 $\mu\text{L}/\text{well}$ CB without tagged protein. After a 1 h incubation at +37°C, plates were washed again and diluted samples added in triplicate wells in 50 $\mu\text{L}/\text{well}$ casein buffer (1:100, 1:1,000, 1:10,000 dilutions). The cynomolgus macaque IgG standard (Molecular Innovations) was serially diluted in casein buffer starting at 200 ng/mL (1:5 serial dilution) and then loaded onto the standard wells (50 $\mu\text{L}/\text{well}$). The plates were incubated at +37°C for 1 h, washed and mouse anti-rhesus monkey IgG Fc biotinylated Ab (Southern Biotech) loaded using a 1:50,000 dilution in 100 $\mu\text{L}/\text{well}$ casein buffer. Following another hour incubation at +37°C and washing step, poly-HRP40 was loaded onto the wells at 1:10,000 dilution in casein buffer (100 $\mu\text{L}/\text{well}$). Finally, after 1 h at +37°C, the plates were washed, tapped dry and developed for 5 min with 50 $\mu\text{L}/\text{well}$ Sureblue TMB substrate and stopped with 50 $\mu\text{L}/\text{well}$ Stop solution (KPL). A KC4 Spectrophotometer (BioTek) was used to read the absorbance at 450 nm and a 4-PL fit curve was used to determine the standard curves and the linear range where the appropriate sample dilution would fall into. Standard curves and raw data were interpolated in the SoftMax Pro software (Molecular Devices), exported as text files, analysed in Excel (Microsoft) and plotted in Prism v7.0 (GraphPad Software).

Neutralization assay

Env-pseudotyped virus (PSV) 93MW965.26 and infectious molecular clone (IMC) ConM¹⁵ were produced in HEK293T cells, tittered and used in TZM-bl assay to determine nAb responses as previously described.⁵³ Briefly, duplicates of six steps of 3-fold dilution, starting with 1:20 of each serum, were incubated with viral supernatant (at relative luminescence units (RLU) between 150,000 and 200,000) for 1 h. Thereafter, 10⁴ TZM-bl cells were added, and plates incubated for 48 h at 37°C, when Bright-Glo Luciferase assay system (Promega, Madison, Wisconsin, USA) was added to measure luciferase activity with a Mithras luminometer (Berthold, Germany). Positive controls were sera of HIV-1-infected individuals and monoclonal antibodies with known neutralizing titers. Testing against VSV was used to exclude unspecific reactions. Neutralization titers were defined as the sample dilution at which RLU were reduced by 50% compared to virus control wells after subtraction of background RLU in control wells with only cells. Inhibitory concentrations 50 (IC50) were calculated with a linear interpolation method using the mean of the duplicate responses.⁵³

ELISA-based rsFc γ RIIIa dimer-binding assay

The protocol of the ELISA-based IgG assay using recombinant soluble Fc γ RIIIa dimer has been previously described.^{17,54} Briefly, ELISA plates (MaxiSorp plates; Nalgene Nunc, Rochester, NY) were coated overnight at 4°C with ConM SOSIP.v7 protein diluted to 50 ng per well in PBS, as well as no Ag as a negative control. HIVIG (#3957; National Institutes of Health AIDS Reagent) was used at 5 $\mu\text{g}/\text{mL}$ to normalize the results across all plates. Coated plates were subsequently washed with PBS containing 0.05% Tween 20 (Sigma-Aldrich) (PBST) and blocked with blocking buffer, consisting of PBS containing 1 mM EDTA and 1% BSA (both from Sigma-Aldrich), for 1 h at 37°C. Macaque sera were diluted 1/50 in blocking buffer and incubated for 1 h at 37°C. After washing 5 times the plates with PBST, purified dimeric macaque rsFc γ RIIIa-biotin (I158 allele) was added to the plate at a concentration of 0.1 $\mu\text{g}/\text{mL}$ and the plates incubated for 1 h at 37°C. Plates were washed again 5 times with PBST, before horseradish peroxidase (HRP)-conjugated streptavidin (Thermo Fisher Scientific) was added and the plates incubated for another 1 h at 37°C. After washing, the color was developed using 3,3',5,5-tetramethylbenzidine (TMB) (Life Technologies), followed by the addition of 1 M HCl stop solution. The absorbance at a wavelength of 450 nm was recorded. The no-Ag values were subtracted from each Ag sample. The resulting absorbance values were multiplied by the serum dilution factor. A positive signal was defined as an absorbance higher than the mean +3 x SD of the one obtained using sera from macaques before immunization.

Antibody coupling with lanthanide isotopes

Four hundred micrograms of each antibody was conjugated to metals using MaxPar X8 conjugation kits (DVS Science) following the manufacturer's instructions. Briefly, lanthanides were loaded onto the polymer and then purified by centrifugation through an AMICON 3-kDa filter (Merck Millipore). Antibodies were also purified using an AMICON 50-kDa filter and partially reduced by TCEP-R-Buffer before conjugation to the metal-loaded polymers.⁵⁵ Following conjugation, antibodies were resuspended at

1 µg/µL in Candor PBS Antibody Stabilization solution (Candor Bioscience) with 0.05% sodium azide and stored at 4°C. All conjugated monoclonal Ab used for labeling are shown in [Table S3](#). The same batch of Ab were used for the different timepoints.

Staining and CyTOF acquisition

Whole blood was collected in heparin/lithium tubes and cryopreserved in 10% FCS/DMSO. Samples were rapidly thawed, washed with RPMI medium, and then incubated in RPMI supplemented with 10 mg/mL DNase for 30 min at 37°C. Cells were then resuspended in 1× PBS and incubated for 15 min at 37°C with 1 µL Intercalator-Rh (DVS Sciences). After washing in PBS-0.5% BSA, cells were stained for 30 min at 4°C, washed with 1× PBS, fixed with PBS-1.6% PFA, and washed with 1× Perm/Wash Buffer (eBiosciences). After permeabilization with 1× Perm/Wash (eBiosciences), intracellular staining was performed for 30 min at 4°C. Cells were washed, fixed in 1.6% PFA, and washed with Barcode Perm Buffer (DVS) before barcoding with a unique combination of three palladium isotopes (DVS, Fluidigm) according to the manufacturer's recommendations. Cells were then washed with PBS and resuspended in PBS-1.6% PFA containing 0.5 µL Intercalator-Ir (DVS Sciences). Barcoded samples were pooled and stored overnight at 4°C. Before acquisition, cells were washed with milli-Q water and filtered through a cap filter with 35-µm pores (BD Biosciences). Normalization beads (Eq Beads, Fluidigm) were added to the tube and the acquisition was performed using a Helios mass cytometer (Fluidigm). Data were acquired for six consecutive days (3 animals per day).

Data processing

MatLab compiler software⁵⁶ was used on FCS files to compensate for signal loss by the detector during acquisition based on the signal given by the Eq Beads. Normalized data from each acquisition were concatenated (Cytobank concatenation tool) and all conditions separated according to their barcode signal using CyTOF software (Fluidigm). In addition, as we previously describe, we used the same sample for each experiment to control the quality of each staining/acquisition and thus its reproducibility.⁵⁷ Eq beads, dead cells, and cell doublets were excluded from the resulting FCS files, as well as nonspecifically stained CD66⁺CD3⁺ eosinophils, as previously described.⁴⁴

Cell population identification

The spanning-tree progression analyses of density-normalized events algorithm (SPADE)⁵⁸ was used on the entire data set of macaque samples to cluster cell populations displaying similar phenotypes. The following markers were used for clustering: CD66, HLA-DR, CD3, CD64, CD8, CD123, CD11a, CD11b, CD62L, CD4, FcεRI, CD86, CD172a, CD45, CD1c, CD32, CD39, CCR5, CD16, CD11c, CXCR4, CD14, CD23, CD141, CD20, CCR7, and CADM1. A random pre-downsampling of 11,478 cells (corresponding to the number of cells contained in the smallest sample) was performed on all samples to allow an equal contribution of each sample to create the tree of cell clusters. All cells from every sample were then assigned to a cluster according to their phenotype.

The SPADEVizR R package⁵⁹ was used to perform quality control on the SPADE clusters. Clusters of good quality were defined based on a narrow (IQR ≤ 2) and unimodal distribution (Hartigan's dip test, p ≤ 0.05) for each marker. After benchmarking of SPADE parameters, the optimal SPADE used 800 clusters and a downsampling limit of 30%, resulting in 64.62% of clusters of good quality.

Heatmap representation

A heatmap representation of the clusters was generated using SPADEVizR according to the mean median MSI of each sample, in which they were divided into five categories between the 5th and 95th percentile. For each cluster, samples contributing <10 cells were excluded. Hierarchical clustering of cell clusters and markers was performed using the Euclidean metric based on the ward.D linkage.

Phenotypic and kinetic families

We created phenotypic families, which grouped cell clusters that displayed similar phenotypes. This strategy avoids "over-clustering", as clusters may account for diverse activation or maturation stages, and favors the identification of actual subpopulations by their phenotypic characteristics. The phenotypic families (PF) were grouped accordingly to their evolution at the different time points of the study. We thus grouped the PF with similar evolution trends in "kinetics families" (KF). The grouping of PF to form KF was performed using a hierarchical method based on the Pearson correlation and complete linkage.

Negative-stain electron microscopy

Trimer and adjuvants were co-formulated as described above (see "[Adjuvants](#)") using the same ratios, scaled down 10-fold (i.e. total volume 0.1 mL). The formulations were incubated for 1 h at 37°C and diluted 1:10 in Tris-buffered saline before applying 3 µL onto glow-discharged carbon-coated Cu400 mesh grids (Electron Microscopy Services). The samples were blotted using filter paper and the grids were then negatively stained with 2% (w/v) uranyl formate for 60 s. Data were collected on a Tecnai Spirit transmission electron microscope, operating at 120 keV. Nominal magnification was 52,000× with a resulting pixel size of 2.05 Å at the specimen plane, and an average defocus of -1.50 µm was used. Micrographs were recorded using a Tietz 4k x 4k TemCam-F416 CMOS camera. Data collection was performed using Leginon automated imaging interface,⁶⁰ and data processing (particle picking, extraction and 2D classifications) was performed using the Appion data processing suite.⁶¹ Data processing procedures to determine amount of native-like trimers is described in detail elsewhere.⁶² Briefly, 2D class averages were visually inspected. Trimers visually similar to

those previously described for BG505 SOSIP.664⁶³ or B41 SOSIP.664⁶² were considered to have an overall native structure. Any particles that did not clearly show a central, triangular mass were classified as non-native.

QUANTIFICATION AND STATISTICAL ANALYSIS

Statistics

R software was employed to perform SPADE algorithm and statistical analysis related to mass cytometry was performed using SPADEVizR (available at <https://github.com/tchitchek-lab/SPADEVizR>) and “MASS” R package (available at <https://CRAN.R-project.org/package=MASS>). Comparisons of cell abundances were performed using the Mann-Whitney-Wilcoxon test, with p-values < 0.05 considered significant. No correction was applied because limited number of animals (n = 6) per groups. Because of this limitation, our intention was to use this approach to generate hypothesis rather than generalized observations. Thus, we tolerate a part of false-discovery rate in order to not exclude false negative data. Furthermore, as we performed a longitudinal follow up on the same macaque over time, comparisons are not independent to each other, so this would likely over-correct p-values.

Linear discriminant analysis

Linear discriminant analysis was performed using mean of non-standardized cell abundances of all individuals, to preserve the contribution of each variable and to differentiate vaccine regimens for each timepoint and identify KF associated to the different vaccines. In Figure 5A, the mean KF abundances of all individual was used as entry parameters to differentiate vaccine regimens at the different timepoint. In Figure 5B, mean KF abundances for all individuals and all timepoint were employed to identify the contribution of each KF to the different vaccine regimens discrimination.

Cytocompare

Distributions of marker expression were compared using the CytoCompare R package⁶⁴ to identify the contribution of each marker in the discrimination of vaccine signature. This R package use the Kolmogorov Smirnov distance to assess the maximum distance between cumulative distribution function (CDF) of the different markers based on their median signal intensity (MSI) for dendritic cells and monocytes. Then, as we aimed to prioritize the identification of a top discriminant markers (although, all markers could be statistically discriminant), we determined the threshold of 0.5, rather than Selecting a top set of markers in each comparison with the highest KS distance as we previously reported.³⁷

Generalized linear model

A generalized linear model was used to assess the link between innate and adaptive responses after the two boosts. SPADEVizR R package is able to generate generalized linear models (GLM) to predict biological outcome associated to each sample based on cluster abundances. This method aims to identify a linear combination of clusters abundances that correlate with a biological outcomes from a training dataset. Based on these linear combinations, we can then predict biological outcomes for a test dataset. The abundance profiles of kinetic families for each individual 24h after the second and third injection (n = 12 for each vaccine regimen) were used as the entry parameter. The values to predict were the nAb titers, IgG binding titers and rsFcgrIIIa binding activities. Abundances 24h after the baseline were not included as no nAb were detected for this timepoint. Then, iterative linear regressions were generated until all coefficients had a p -value ≤ 0.05 . At each iteration, the coefficient having the highest p-value higher than 0.05 was removed. One value was excluded from both the IgG binding and nAb model because titers at W26 for one animal were not included in the confidence interval.

Supplemental information

**Innate cell markers that predict anti-HIV
neutralizing antibody titers
in vaccinated macaques**

Matthieu Van Tilburgh, Pauline Maisonnasse, Jean-Louis Palgen, Monica Tolazzi, Yoann Aldon, Nathalie Dereuddre-Bosquet, Mariangela Cavarelli, Anne-Sophie Beignon, Ernesto Marcos-Lopez, Anne-Sophie Gallouet, Emmanuel Gilson, Gabriel Ozorowski, Andrew B. Ward, Ilja Bontjer, Paul F. McKay, Robin J. Shattock, Gabriella Scarlatti, Rogier W. Sanders, and Roger Le Grand

Innate cell markers that predict anti-HIV neutralizing antibody titers in vaccinated macaques

Supplementary materials

Authors: Matthieu Van Tilbeurgh¹, Pauline Maisonnasse¹, Jean-Louis Palgen¹, Monica Tolazzi², Yoann Aldon³, Nathalie Dereuddre-Bosquet¹, Mariangela Cavarelli¹, Anne-Sophie Beignon¹, Ernesto Marcos-Lopez¹, Anne-Sophie Gallouet¹, Emmanuel Gilson⁴, Gabriel Ozorowski⁵, Andrew B. Ward⁵, Ilja Bontjer⁶, Paul F. McKay³, Robin J. Shattock³, Gabriella Scarlatti², Rogier W. Sanders^{6,7}, and Roger Le Grand^{1*}.

Affiliations:

¹ Université Paris-Saclay, Inserm, CEA, Center for Immunology of Viral, Auto-immune, Hematological and Bacterial diseases » (IMVA-HB/IDMIT), 92265 Fontenay-aux-Roses & 94270 Le Kremlin-Bicêtre, France

² Viral Evolution and Transmission Unit, Division of Immunology, Transplantation and Infectious Diseases, IRCCS Ospedale San Raffaele, 20132 Milan, Italy

³ Imperial College London, Faculty of Medicine, Department of Infectious Disease, London, United Kingdom.

⁴ Life & Soft, 28 rue de la Redoute, 92260 Fontenay-aux-Roses, France

⁵ Department of Integrative Structural and Computational Biology, The Scripps Research Institute, La Jolla, CA 92037, USA.

⁶ Department of Medical Microbiology and Infection Prevention, Amsterdam University Medical Centers, Location AMC, University of Amsterdam, 1105 AZ Amsterdam, the Netherlands

⁷ Department of Microbiology and Immunology, Weill Medical College of Cornell University, New York, NY 10021, USA

* Corresponding author: roger.le-grand@cea.fr

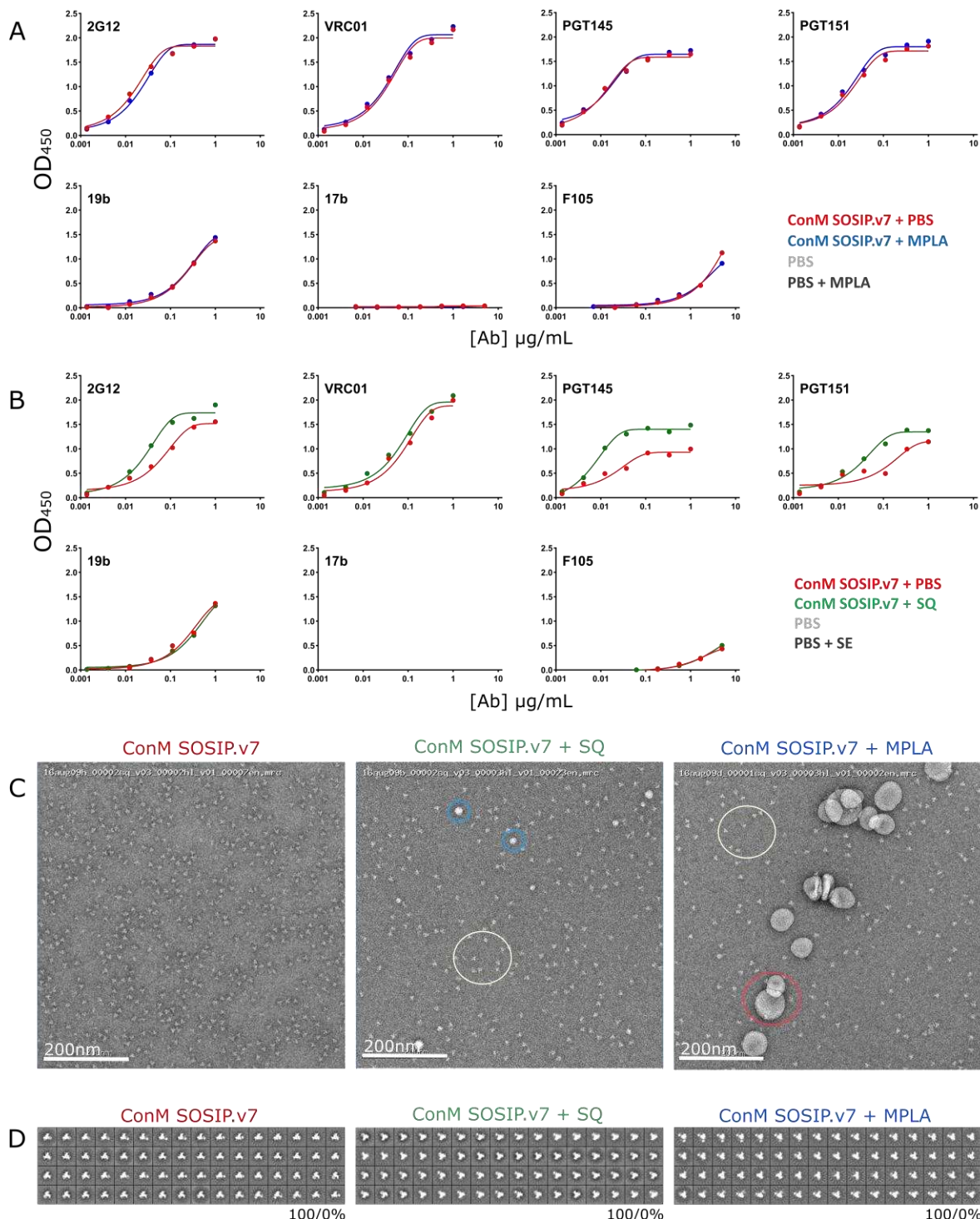


Figure S1. Formulation of ConM SOSIP.v7 with MPLA and SQ adjuvants (related to figure 2). D7324-tagged ConM SOSIP.v7 was incubated with the corresponding adjuvant for 1 h at 37°C and the antigenicity (**A**, **B**) and morphology (**C**, **D**) were subsequently assessed by D7324-capture ELISA and negative-stain electron microscopy, respectively. (**C**) Electron micrographs of ConM SOSIP.v7 plus adjuvants; White, blue and red circles identified respectively trimers, Squalene and MPLA. (**D**) 2D-class averages of ConM SOSIP.v7 proteins in formulations. Percentage of native-like/non-native trimers (see *Materials and Methods*) are listed below each set of class averages.

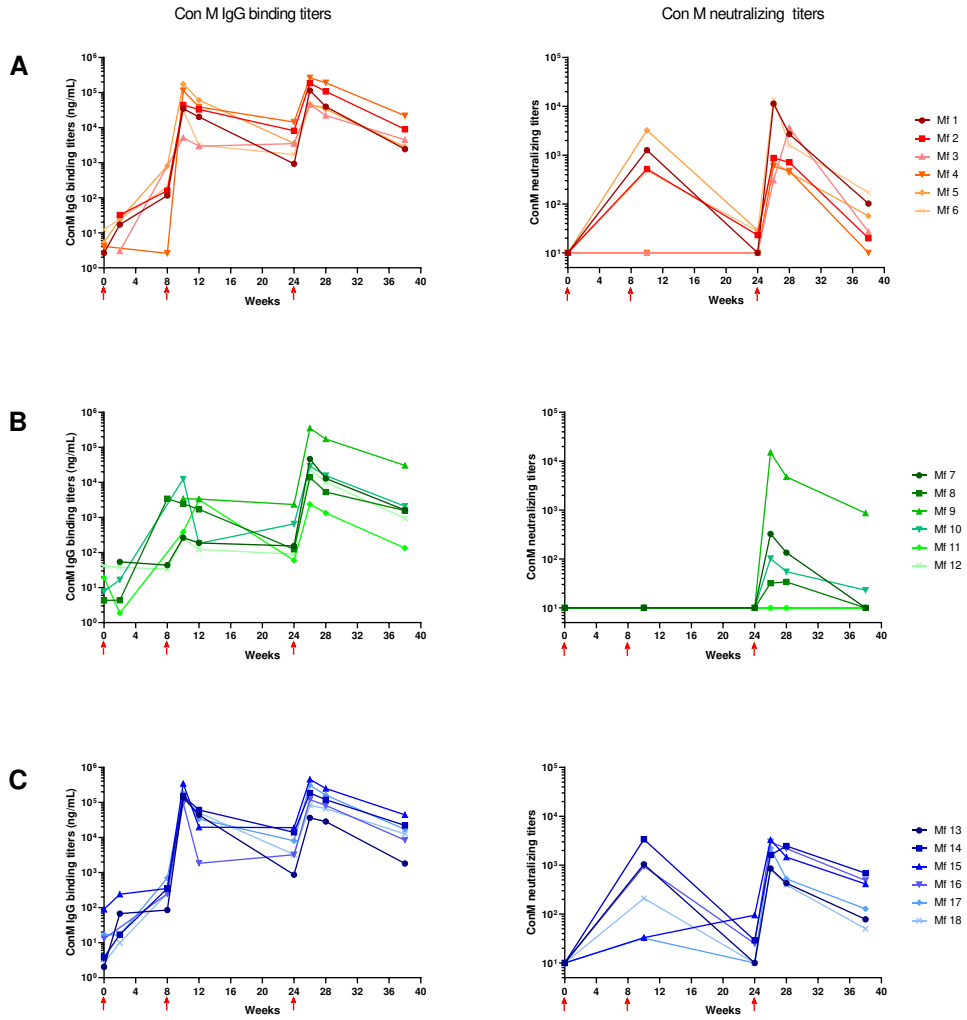


Figure S2. Individual ConM SOSIP v7 humoral responses (related to figure 2). ConM IgG binding and neutralizing titers of cynomolgus macaques from the MPLA-IM (A), MPLA-SC (B), and SQ-IM (C) groups, with red, green, and blue shading, respectively. Immunizations (week 0, 8, and 24) are indicated by the red arrows.

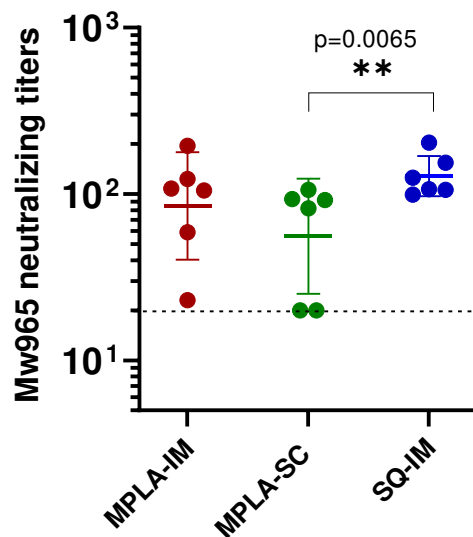


Figure S3: Heterologous neutralization against MW965 virus (related to figure 2). MW965 neutralizing titers were measured at week (W)28. Animals from the MPLA-IM group are displayed in red, the MPLA-SC group in green, and the SQ-IM group in blue. The geometric mean and geometric SD are represented. Comparison realized with a Mann-Whitney-Wilcoxon test with p .values < 0.05 are displayed.

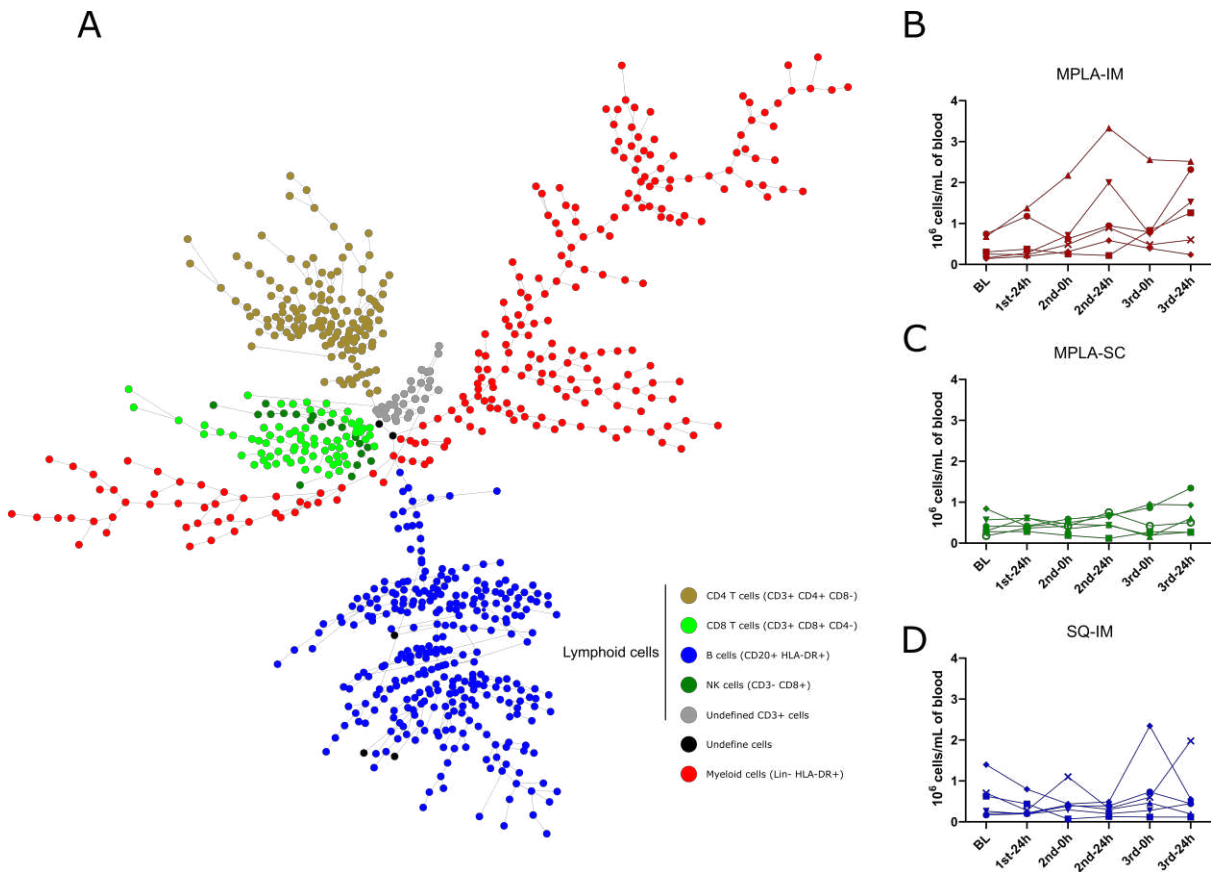


Figure S4. Identification of major cell populations using the SPADE clustering method following immunizations with SOSIP v7 ConM (related to figure 3). (A) SPADE tree created using the entire mass cytometry data set. Each dot represents a cell cluster. Major cell populations are annotated according to their phenotype: B cells ($CD20^+$ $HLA-DR^+$ $CD1c^+$), T cells ($CD3^+$ $CD4^+$ or $CD8^+$), NK cells ($CD3^-$ $CD8^+$), undefined lymphocytes ($CD3^+$ $CD4^-$ $CD8^{low/-}$), and undefined cells. All remaining cell clusters are considered to be myeloid cells. Phenotypically similar clusters were linked using a minimal spanning-tree approach of the SPADE algorithm. Kinetics of the myeloid cells compartment depending on the vaccine: (B) MPLA-IM, (C) MPLA-SC and (D) SQ-IM.

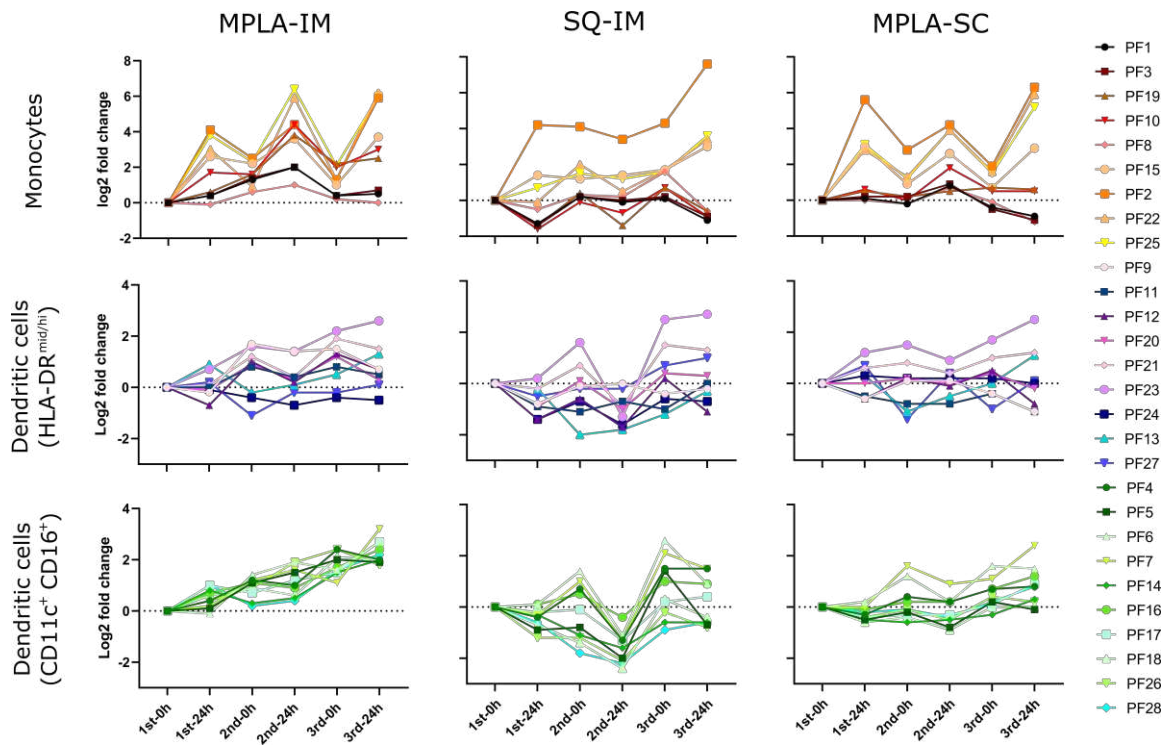


Figure S5. Variation of phenotypic families following immunization (related to figure 4).
Mean log₂ fold changes relative to the baseline values are displayed for each superfamily. Each color is assigned to a phenotypic family according to the colors defined in the heatmap (Fig.3).

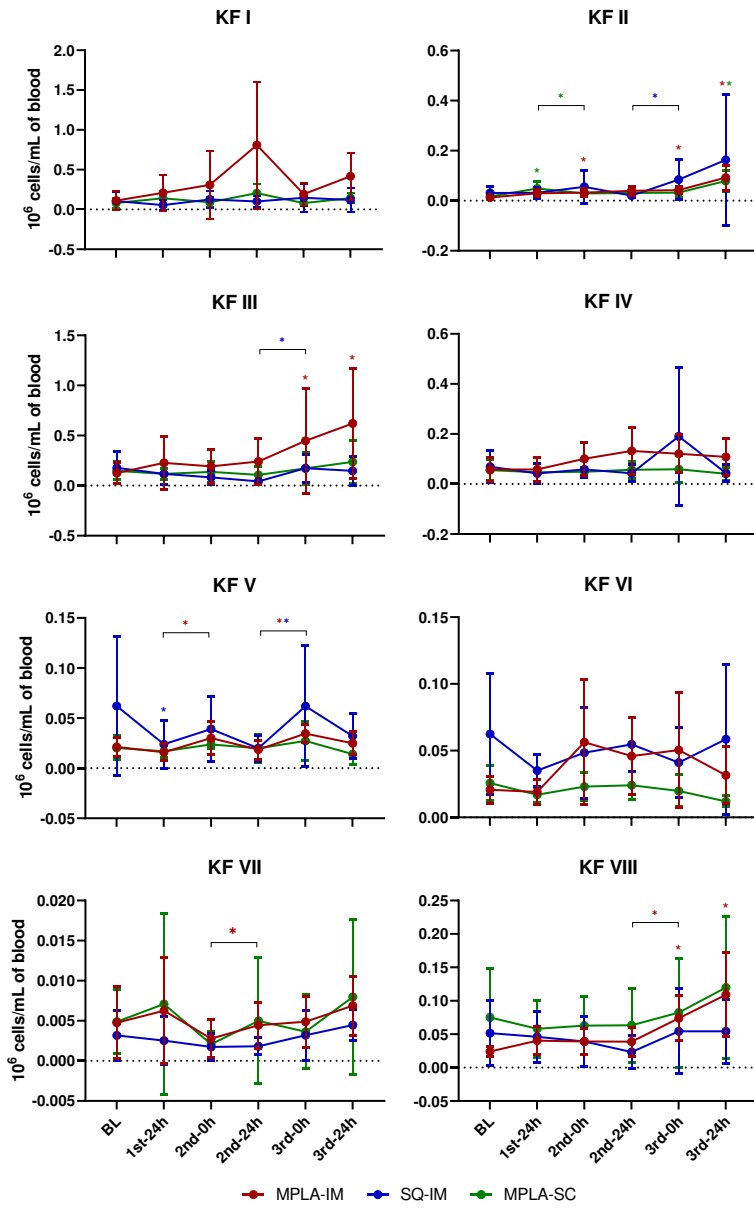


Figure S6. Dynamics of kinetic families following vaccine injections (related to figure 5). Phenotypic families were regrouped by similar dynamics to form eight kinetic families. The graphs show the mean cell number per mL of blood for all individuals ($n=6$) for each injection (MPLA-IM in red, MPLA-SC in green, and SQ-IM in blue). Significant differences relative to baseline values are indicated by a star and black lines are used to show significant differences compared to the previous time-point. P-values are shown in Table S2.

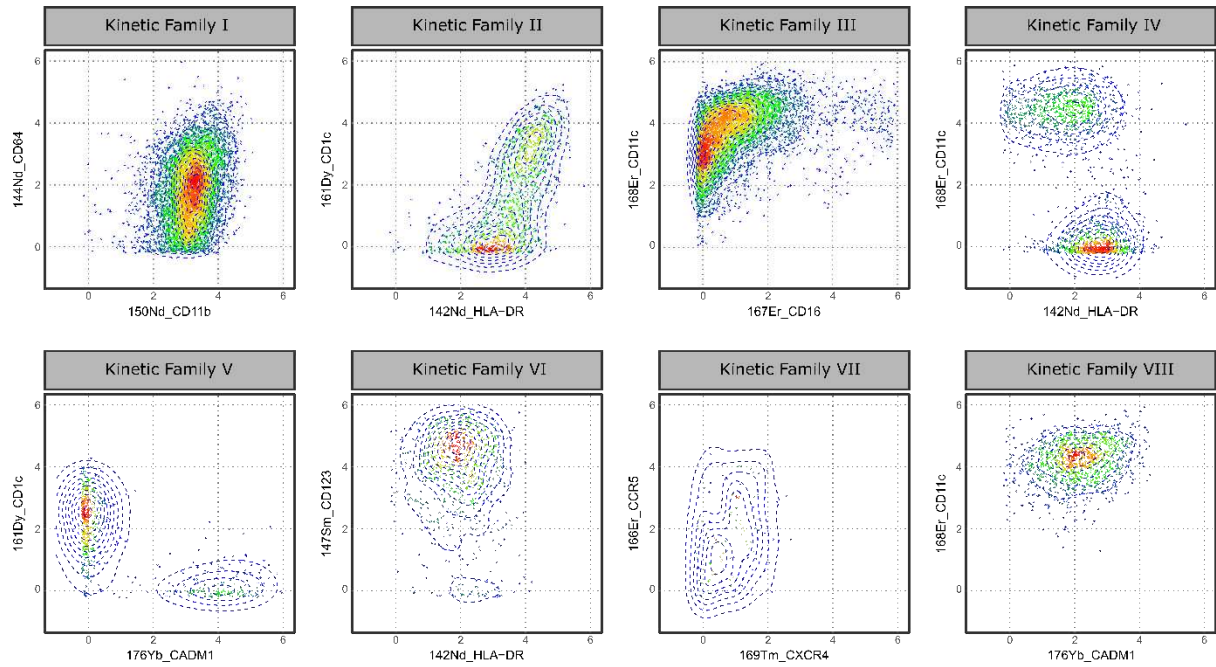


Figure S7: Main characteristics of kinetic families expression profiles (related to figure 5). Each dotplot represents the mean signal intensity (MSI) of all cells contained by a kinetic family (KF) without vaccines segregation. Markers are chosen according to the main population characteristics as defined in Table 1.

Table S1. p-values of differences in cell numbers within phenotypic families (related to figure 4). Comparisons were made using the Mann-Whitney Wilcoxon test. P-values ≤ 0.05 are shown in red.

Conditions	Timepoints	PF1	PF3	PF19	PF10	PF8	PF15	PF2	PF22	PF25	PF12	PF23	PF21	PF20	PF9	PF24	PF11	PF27	PF13	PF28	PF17	PF5	PF4	PF26	PF16	PF14	PF6	PF18	PF7
Comparison between conditions	Baseline	0.94	0.70	0.59	0.82	0.82	0.82	0.70	0.94	0.82	0.09	0.18	0.09	0.48	0.39	0.04	0.31	0.18	0.94	0.82	1.00	0.70	0.48	0.39	1.00	0.94	0.70	0.82	
	1st-24h	0.18	0.13	0.24	0.04	0.18	0.13	0.09	0.06	0.03	0.03	0.06	1.00	0.94	0.70	0.94	0.48	0.24	0.70	0.82	0.48	0.82	0.59	0.48	0.59	0.94	1.00	0.59	
	2nd-0h	0.94	0.94	1.00	0.82	0.18	0.39	0.82	0.70	0.70	0.18	0.39	0.94	0.48	0.31	0.94	0.48	0.75	1.00	0.82	0.48	0.39	0.48	0.31	0.59	0.70	0.18	0.94	0.31
	2nd-24h	0.48	0.18	0.24	0.02	0.70	0.18	0.13	0.06	0.02	0.03	0.09	0.94	0.44	0.39	0.31	0.94	0.24	0.70	0.82	0.31	0.18	0.31	0.24	0.18	0.13	0.39	0.94	0.06
	3rd-0h	0.94	0.59	0.39	0.70	0.94	0.48	0.48	0.94	1.00	0.09	0.31	0.48	0.31	0.31	0.13	0.13	0.70	0.18	0.59	0.31	0.70	1.00	0.39	0.82	0.48	0.39	0.24	1.00
	3rd-24h	0.82	1.00	0.18	0.13	0.48	0.82	0.59	0.03	0.09	0.00	0.02	0.03	0.31	0.48	0.70	0.31	0.39	0.94	1.00	0.82	0.24	0.24	0.39	0.39	0.48	0.94	0.82	0.39
	Baseline	1.00	0.59	0.13	0.94	0.59	0.94	1.00	0.48	0.94	0.03	0.06	0.06	0.03	0.31	0.13	0.48	0.82	0.39	0.24	0.31	0.94	0.82	0.59	0.18	0.94	0.59	0.48	0.94
	1st-24h	0.18	0.06	0.24	0.02	0.18	0.06	0.24	0.009	0.009	0.03	0.31	0.39	0.24	0.13	0.09	0.48	0.18	0.13	0.94	0.48	1.00	0.94	0.94	0.94	0.48	0.94	1.00	0.82
	2nd-0h	0.48	0.39	0.82	0.39	0.39	1.00	0.82	0.94	0.70	0.94	1.00	1.00	0.94	0.31	0.31	0.59	0.13	0.70	0.59	0.31	0.31	0.70	0.82	0.24	0.24	0.48	0.24	
	2nd-24h	0.09	0.03	0.04	0.06	0.06	0.04	0.03	0.06	0.04	0.59	0.48	1.00	0.70	0.82	0.59	1.00	0.06	0.09	0.04	0.39	0.24	0.18	0.09	0.31	0.31	0.13		
	3rd-0h	0.06	0.06	0.06	0.03	0.09	0.18	0.59	0.06	0.09	0.39	0.59	0.48	0.48	0.94	0.82	0.09	0.59	0.59	0.13	0.04	0.09	0.13	0.24	0.06	0.31	0.24	0.09	
	3rd-24h	0.39	0.31	1.00	0.13	0.31	0.94	0.59	0.59	0.94	0.48	0.94	0.70	0.48	0.03	0.39	0.18	1.00	0.70	1.00	1.00	0.94	0.18	0.59	0.09	0.70	0.94	0.09	
	Baseline	0.70	0.94	0.39	0.24	0.59	0.59	0.82	0.94	0.94	0.48	0.94	0.70	0.70	0.48	0.70	0.24	0.48	0.94	0.24	0.39	0.94	0.82	0.09	0.13	1.00	0.39	0.59	
	1st-24h	0.82	0.94	0.94	0.48	1.00	1.00	0.59	0.48	0.82	0.94	0.94	0.13	0.31	0.03	0.09	0.70	0.48	1.00	0.70	0.70	0.48	0.94	0.39	0.48	0.70	0.59	0.94	1.00
	2nd-0h	0.31	0.13	0.94	0.39	0.02	0.24	0.59	0.48	0.39	0.18	0.18	0.94	0.59	0.82	0.24	0.39	0.59	0.59	0.82	0.94	0.70	0.70	0.24	0.82	0.48	0.94	0.39	0.94
	2nd-24h	0.18	0.31	0.31	0.09	0.09	0.06	0.18	0.09	0.09	0.13	0.59	0.82	0.94	0.39	0.82	0.70	0.48	0.31	0.59	0.59	0.39	0.82	0.59	0.39	0.70	0.59	0.48	
	3rd-0h	0.24	0.00	0.09	0.09	0.04	0.13	1.00	0.24	0.13	0.59	0.70	0.31	0.59	0.94	0.06	0.48	0.18	0.48	0.13	0.18	0.48	0.82	0.18	0.24	0.31	0.24	0.31	
	3rd-24h	0.04	0.06	0.39	0.09	0.04	0.06	0.59	0.94	0.82	0.31	0.13	0.06	0.48	0.82	0.70	0.70	0.39	0.31	0.18	0.70	0.31	0.82	0.94	0.18	0.31	0.24	0.24	
Comparison with the previous timepoint	2nd-0h vs 1st-24h	0.22	0.09	0.31	0.84	0.09	0.22	0.06	0.09	0.06	0.03	0.31	0.03	0.03	0.03	0.09	0.31	0.31	0.06	0.09	0.16	0.03	0.03	0.84	0.22	1.00	0.44	0.22	0.56
	2nd-24h vs 2nd-0h	0.03	0.03	0.06	0.06	0.09	0.03	0.03	0.06	0.03	0.31	0.31	0.03	0.16	0.09	0.69	0.69	0.06	0.03	0.69	0.84	0.84	1.00	0.22	0.44	0.44	0.03	0.31	0.16
	3rd-0h vs 2nd-24h	0.03	0.03	0.22	0.06	0.22	0.06	0.06	0.06	0.06	0.69	0.69	0.03	0.09	0.06	0.31	1.00	0.69	1.00	0.03	0.22	1.00	0.69	0.06	0.16	0.44	0.03	0.31	0.03
	3rd-24h vs 3rd-0h	1.00	0.44	1.00	1.00	0.69	0.03	0.03	0.03	0.03	0.31	0.84	0.06	0.06	0.56	0.44	0.69	0.06	0.31	0.56	0.31	0.84	0.06	0.16	0.31	0.06	0.44	0.16	
	2nd-0h vs 1st-24h	1.00	0.84	0.84	0.31	0.69	0.84	0.56	0.24	0.44	0.03	0.44	0.84	0.31	0.69	0.44	0.09	0.09	0.16	0.16	0.09	0.03	0.84	0.22	0.56	0.84	0.09	0.44	0.84
	MPLA-SC	0.16	0.16	0.84	0.03	0.16	0.03	0.03	0.03	0.03	0.69	1.00	0.56	0.56	0.31	0.22	0.84	0.09	0.44	0.22	0.22	0.22	1.00	0.84	0.09	0.16	0.44	0.31	0.31
	3rd-0h vs 2nd-24h	0.09	0.06	0.84	0.16	0.09	0.03	0.06	0.06	0.03	0.56	0.84	0.44	0.44	0.31	1.00	0.44	0.31	0.09	0.09	0.16	0.22	0.44	0.44	0.09	0.31	0.31	0.31	
	3rd-24h vs 3rd-0h	0.22	0.44	0.84	1.00	0.09	0.03	0.03	0.03	0.03	1.00	0.09	0.84	1.00	0.31	0.09	0.16	1.00	0.09	0.69	1.00	0.03	0.16	0.16	0.06	0.84	0.56	0.06	
	2nd-0h vs 1st-24h	0.09	0.06	0.06	0.06	0.06	0.06	0.03	0.03	0.03	0.03	0.03	0.03	0.03	0.03	0.03	0.03	0.03	0.03	0.03	0.03	0.03	0.03	0.03	0.03	0.03	0.03	0.03	0.03
	SQ-IM	0.84	0.84	0.16	0.44	0.84	0.09	0.03	0.03	0.03	0.06	0.31	0.06	0.03	0.16	0.56	1.00	0.03	0.03	0.03	0.09	0.09	0.06	0.06	0.06	0.03	0.03	0.03	0.06
Comparison with baseline	1st-24h	0.44	0.44	0.03	0.03	0.84	0.03	0.03	0.03	0.03	0.31	1.00	0.06	0.56	1.00	0.06	1.00	0.44	0.69	0.03	0.69	0.84	0.56	0.44	0.03	0.03	0.84	0.44	0.44
	2nd-0h	0.16	0.09	0.16	0.16	0.22	0.16	0.03	0.31	0.09	0.06	0.44	0.09	0.09	0.03	0.03	0.16	0.22	0.06	0.06	0.69	0.03	0.22	0.09	0.44	1.00	0.03	0.03	0.03
	2nd-24h	0.06	0.06	0.06	0.03	0.09	0.03	0.06	0.03	0.06	0.84	1.00	0.69	0.56	0.06	0.22	0.84	0.09	0.44	0.06	0.22	0.56	0.16	0.16	0.69	0.31	0.69	0.31	
	3rd-0h	0.09	0.22	0.09	0.03	0.84	0.03	0.03	0.22	0.03	0.16	1.00	0.03	0.03	0.03	0.31	0.44	0.56	0.03	0.06	0.16	0.03	0.16	0.03	0.03	0.03	0.03	0.03	
	3rd-24h	0.22	0.22	0.06	0.03	0.84	0.03	0.03	0.03	0.03	0.56	0.22	0.44	0.56	0.16	0.06	0.44	0.03	0.84	0.03	0.03	0.03	0.03	0.03	0.03	0.03	0.03	0.03	
	1st-24h	1.00	1.00	0.31	0.31	1.00	0.03	0.03	0.06	0.03	0.31	0.56	0.56	1.00	0.22	0.03	0.84	1.00	0.84	0.44	0.44	0.16	1.00	0.56	1.00	0.31	0.31	0.84	
	2nd-0h	0.56	0.84	0.84	0.56	0.16	0.06	0.09	0.16	0.84	0.31	0.44	0.69	0.09	0.16	0.84	0.31	0.03	0.44	0.84	0.09	0.03	0.56	0.69	1.00	0.56	0.56	0.44	
	2nd-24h	0.44	0.16	0.69	0.03	0.16	0.03	0.03	0.03	1.00	0.56	1.00	1.00	0.44	0.06	0.44	0.44	0.31	0.44	0.44	0.22	0.16	1.00	0.84	0.22	0.44	0.56	0.56	0.56
	3rd-0h	0.84	0.84	0.31	0.44	0.84	0.09	0.03	0.03	0.06	0.69	0.44	0.16	0.84	0.44	0.06	1.00	0.84	0.06	0.44	0.44	0.22	0.16	1.00	0.69	0.84	0.84	0.84	
	3rd-24h	0.22	0.31	0.44	0.31	0.16	0.03	0.03	0.03	0.03	0.16	0.56	0.22	0.44	0.03	1.00	0.31	0.44	0.69	1.00	0.09	0.03	0.84	0.09	0.16	0.03	0.03	0.03	
SQ-IM	1st-24h	0.03	0.03	0.03	0.06																								

Table S2. p-values of differences in cell number between kinetic families (related to figure 5). Comparisons were made using the Mann-Whitney Wilcoxon test. P-values ≤ 0.05 are shown in red.

Conditions		Timepoint	KF I	KF II	KF III	KF IV	KF V	KF VI	KF VII	KF VIII
Comparison between conditions	MPLA-SC vs SQ-IM	Baseline	0.937	0.240	0.937	0.937	0.132	0.132	0.180	0.589
		1st-24h	0.041	0.394	0.485	0.132	0.937	0.009	0.485	0.394
		2nd-0h	0.699	0.589	0.240	0.589	0.485	0.065	0.589	0.394
		2nd-24h	0.065	0.132	0.240	0.699	0.937	0.026	0.699	0.240
		3rd-0h	0.937	0.180	0.485	0.485	0.394	0.132	0.589	0.485
		3rd-24h	0.310	0.818	0.394	0.937	0.132	0.004	0.589	0.240
Comparison with the previous timepoint	MPLA-IM vs SQ-IM	Baseline	0.937	0.240	0.699	0.937	0.132	0.015	0.699	0.394
		1st-24h	0.041	1.000	0.937	0.485	1.000	0.041	0.093	0.699
		2nd-0h	0.589	0.699	0.485	0.310	0.818	0.937	0.394	0.699
		2nd-24h	0.026	0.065	0.132	0.041	1.000	0.485	0.065	0.180
		3rd-0h	0.485	0.310	0.394	0.699	0.818	1.000	0.394	0.310
		3rd-24h	0.065	0.699	0.065	0.093	0.818	0.589	0.180	0.180
Comparison with baseline	MPLA-IM vs MPLA-SC	Baseline	0.818	0.485	0.699	1.000	0.589	0.485	0.818	0.132
		1st-24h	0.937	0.240	1.000	0.589	0.699	0.699	0.589	0.589
		2nd-0h	0.132	0.937	0.818	0.093	0.937	0.093	0.937	0.394
		2nd-24h	0.093	0.240	0.485	0.132	0.818	0.132	0.310	0.699
		3rd-0h	0.041	0.394	0.310	0.093	0.818	0.132	0.240	0.937
		3rd-24h	0.132	0.699	0.310	0.093	0.132	0.240	0.589	1.000
	MPLA-IM	2nd-0h vs 1st-24h	0.313	0.688	1.000	0.156	0.031	0.063	0.156	1.000
		2nd-24h vs 2nd-0h	0.031	0.438	0.219	0.156	0.063	0.313	0.031	1.000
		3rd-0h vs 2nd-24h	0.063	0.563	0.156	0.688	0.031	1.000	0.844	0.031
		3rd-24h vs 3rd-0h	0.063	0.063	0.563	0.219	0.063	0.563	0.063	0.219
		2nd-0h vs 1st-24h	0.219	0.031	0.844	0.844	0.094	0.094	0.219	0.313
		2nd-24h vs 2nd-0h	0.031	0.844	0.219	0.438	0.688	1.000	0.313	1.000
	MPLA-SC	3rd-0h vs 2nd-24h	0.063	0.688	0.313	1.000	0.313	0.563	0.688	0.313
		3rd-24h vs 3rd-0h	0.063	0.063	0.094	0.313	0.094	0.063	0.156	0.094
		2nd-0h vs 1st-24h	0.156	0.438	1.000	0.563	0.438	0.563	0.688	0.563
		2nd-24h vs 2nd-0h	1.000	0.063	0.156	0.438	0.063	0.438	0.688	0.094
		3rd-0h vs 2nd-24h	0.844	0.031	0.031	0.063	0.031	0.438	0.563	0.063
		3rd-24h vs 3rd-0h	0.563	0.844	0.688	0.156	0.563	1.000	0.313	0.844
	SQ-IM	1st-24h	0.031	0.063	0.313	0.844	0.219	0.219	0.438	0.156
		2nd-0h	0.156	0.031	0.219	0.219	0.688	0.094	0.063	0.156
		2nd-24h	0.031	0.063	0.219	0.156	0.438	0.156	0.844	0.313
		3rd-0h	0.063	0.031	0.031	0.156	0.063	0.156	0.844	0.031
		3rd-24h	0.031	0.031	0.031	0.438	0.688	0.438	0.219	0.031
		1st-24h	0.219	0.031	0.688	0.844	0.844	0.313	1.000	1.000
	MPLA-SC	2nd-0h	1.000	0.156	0.688	0.844	0.563	1.000	0.094	1.000
		2nd-24h	0.094	0.156	0.438	0.844	0.844	1.000	0.563	0.563
		3rd-0h	0.688	0.438	0.844	0.844	0.313	0.688	0.313	0.844
		3rd-24h	0.219	0.031	0.313	0.563	0.219	0.063	0.438	0.156
		1st-24h	0.063	0.563	0.063	0.063	0.031	0.219	0.313	0.438
		2nd-0h	0.688	0.438	0.563	1.000	0.844	0.313	0.438	0.563
	SQ-IM	2nd-24h	1.000	0.563	0.063	0.313	0.063	0.844	0.313	0.219
		3rd-0h	0.313	0.063	0.688	0.219	0.844	0.156	1.000	0.844
		3rd-24h	1.000	0.063	1.000	0.688	0.438	1.000	0.438	0.844

Table S3. Myeloid panel used for the mass-cytometry experiment (related to STAR Methods section). The metal and antibody clone associations are shown. Intracellular markers are shown in bold.

Metal	Antibody	Clone
Pr(141)	CD66abce	TET2
Nd(142)	HLA-DR	L243
Nd(143)	CD3	SP34.2
Nd(144)	CD64	10.1
Nd(145)	CD8	RPAT8
Nd(146)	IL6	MQ2.13A5
Sm(147)	CD123	7G3
Nd(148)	IL4	8D48
Sm(149)	CD11a	HI111
Nd(150)	CD11b	ICRF144
Eu(151)	CD62L	SK11
Sm(152)	CD4	L200
Eu(153)	FcεRI	AER37
Sm(154)	CD86	IT2.2
Gd(156)	CD172a	15-414 / REA144
Gd(158)	IP10	6D4
Tb(159)	CD45	D058-1283
Gd(160)	IL1a	364/3B3
Dy(161)	CD1c	AF-5910
Dy(162)	IL-12	C8.6
Dy(163)	CD32abc	FLI8.26
Dy(164)	IFNa	LT27/295
Ho(165)	CD39	eBioA1
Er(166)	CD195 (CCR5)	3A9
Er(167)	CD16	3G8
Er(168)	CD11c	3.9
Tm(169)	CD184 (CXCR4)	12G5
Er(170)	CD14	M5E2
Yb(171)	IL8	6265.8
Yb(172)	CD23	9P25
Yb(173)	CD141	1A4
Yb(174)	CD20	2H7
Lu(175)	CCR7	G043H7
Yb(176)	CADM1	3E 1

Pr: Praseodymium Gd: Gadolinium

Nd: Neodymium Tb: Terbium

Sm: Samarium

Dy: Dysprosium

Eu: Europium

Ho: Holmium

Er: Erbium

Tm: Thulium

Yb: Ytterbium

Lu: Lutecium

II. Identification de biomarqueurs précoces associés à la réponse neutralisante à long terme du vaccin contre le virus de la fièvre jaune

1) Caractérisation de la réponse LT CD4+ précoce

Dans cette étude longitudinale d'un an, nous nous sommes concentrés sur l'étude de la réponse vaccinale contre le virus de la Fièvre Jaune dans le sang à l'aide du vaccin vivant commercial Stamaril® et d'un vaccin inactivé.

Comme attendu, nous avons pu observer des différences notables de la réponse neutralisante entre les vaccins. Le vaccin Stamaril apparaît comme plus efficace pour induire ces anticorps mais également pour induire une réponse anticorps persistante. A l'inverse, le vaccin inactivé nécessite une injection de rappel pour induire une réponse équivalente et le titre en anticorps n'est pas stable mais diminue au cours du temps.

Les objectifs principaux ont consisté en la caractérisation de la réponses T CD4+ induite par les vaccins et l'identification des mécanismes précoces de la réponse T CD4+ associés avec la persistance de la réponse anticorps neutralisante. Pour cela nous avons eu recours à diverses techniques pour étudier l'environnement, la mobilisation et la prolifération des sous-populations du compartiment T CD4+ et leurs fonctions:

- Les fonctionnalités des cellules spécifiques ont été explorées grâce une stimulation *in vitro* par le virus vaccinal vivant purifié.
- Un traitement avec l'anlogue de thymidine 5-Iodo-2'-deoxyuridine (IdU) a également été effectué chez 3 animaux de chaque groupe. Ce composé a la capacité de s'intégrer à l'ADN des cellules en prolifération au cours du traitement, permettant ainsi un suivi de la mobilisation et de la prolifération des cellules en réponse à l'injection du vaccin, mais également de suivre leur persistance au cours du temps (Figure 18). La dose (60mg/kg/jour), la durée du traitement (une injection par jour pendant 4 jours) ainsi que la fenêtre de réponse ciblée, de J3 à J6 après la primo-injection, ont été déterminés sur la base de précédentes études ([Erez et al., 2019; Tuttle et al., 2010](#)), en tenant compte des risques de toxicité pour l'animal et des contraintes liées à l'expérimentation.

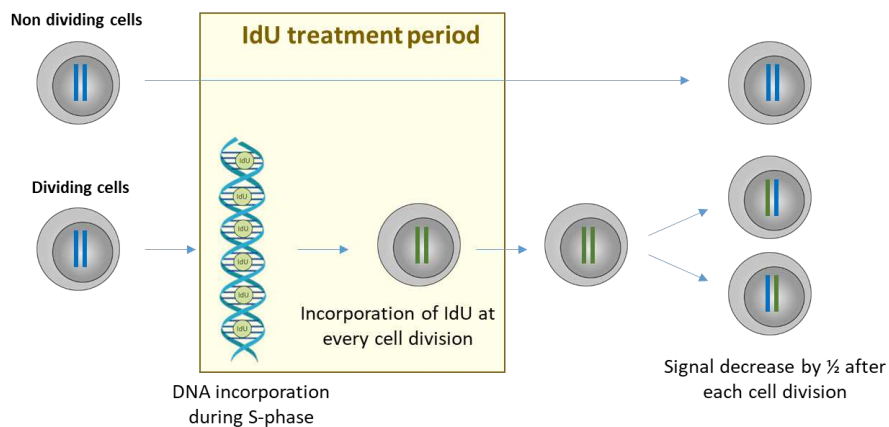


Figure 18: Schéma descriptif du mécanismes d'incorporation de la 5-Iodo-2'-deoxyuridine (IdU). Les thymidines endogènes vont entrer en compétition avec l'IdU lors de la phase de synthèse de l'ADN. Après l'arrêt du traitement, le niveau d'IdU libre chute rapidement. Le signal IdU va ensuite diminuer par deux à chaque division cellulaire et peut être directement mesuré par le cytomètre de masse avec la masse de l'iode.

A l'aide de la cytométrie de masse et d'une analyse non supervisée nous avons capturé la diversité phénotypique et fonctionnelle du compartiment T CD4+. Ainsi nous avons pu identifier des différences significatives d'abondance de populations LT CD4+ entre les vaccins dès J7 après injection, de même que des différences phénotypiques liées à l'induction et à la maintenance des cellules mémoires. Nous avons également observé une mobilisation et une diversité de fonctions plus importante pour le vaccin inactivé suite à la re-stimulation spécifique.

Les résultats présentés ci-après ont été généré dans une étude en collaboration avec Sanofi Pasteur. Ils constituent une ébauche d'article mais requiert une analyse bio-statistiques des données plus approfondie afin d'identifier d'éventuels facteurs prédictifs de la persistance de la réponse vaccinale.

Unraveling early CD4⁺ T-cell events to identify predictive biomarkers of a persistent neutralizing response to yellow fever vaccine

Authors: Matthieu Van Tilbeurgh¹, Pauline Maisonnasse¹, Emmanuel Gilson², Caroline Manet¹, Ernesto Marcos-Lopez¹, Marco Leonec¹, Nathalie Dereuddre-Bosquet¹, Julie Bigay¹, Anne-Sophie Gallouet¹, Frédéric Martinon¹, Catherine Caillet³, Eric Ginoux², Nathalie Mantel³, Pascal Blanc³, and Roger Le Grand¹.

Affiliations:

¹ Université Paris-Saclay, Inserm, CEA, Center for Immunology of Viral, Auto-immune, Hematological and Bacterial diseases » (IMVA-HB/IDMIT), Fontenay-aux-Roses & Le Kremlin-Bicêtre, France

² Life & Soft, 28 rue de la Redoute, 92260 Fontenay-aux-Roses, France

³ Vaccine Research and Development, Sanofi, Marcy l'Etoile, France

Abstract

Vaccines represent one of the most effective strategies to fight infectious diseases. However, there is a need to increase our knowledge on the immune mechanisms that drive the protective response to improve currently available vaccines and their coverage and develop vaccines for diseases, such as AIDS, tuberculosis, and malaria. Here, we characterized the early CD4⁺ T-cell response to yellow fever (YF) vaccines as a model to assess markers predictive of the durability of neutralizing antibody responses. By comparing the commercial Stamaril® vaccine to a β -propiolactone-inactivated YF vaccine, we identified differences in regulatory T cells and three types of circulating follicular helper cells (CD127⁺ PD-1⁻, CD127^{mid} PD-1⁻ CD25⁺, and CD127^{lo} PD-1⁺) that could affect antibody persistence.

Introduction

The use of vaccines has dramatically expanded to become one of the most effective preventive strategies in the fight against infectious diseases. Vaccines were directly involved in the eradication of smallpox and have been involved in the decrease in the incidence of numerous diseases, such as measles, diphtheria, and poliomyelitis [1], [2]. The development of vaccines with a durable response that require limited or no boosts is among the key parameters in the control of infectious diseases. In addition to improving coverage, limited intervention also enhances vaccine acceptance. Despite the existence of vaccines that confer long-term protection, including for life, the immune mechanisms that provide long-term memory are not fully understood. Increasing our knowledge of the associated molecular and cellular

mechanisms is of primary importance for the development of a new generation of vaccines with improved efficacy.

In addition to the many known functions of CD4⁺ T cells, several studies have highlighted the importance of CD4⁺ T cells in the quality of immune responses following vaccination. For example, CD4⁺ Th1 cells have been shown to be associated with a decreased risk of SIV acquisition after ALVAC-SIV vaccination [3] and the early CD4 T-cell response following vaccination for influenza predicts the persistence of long-term neutralizing antibodies (nAbs)[4]. In addition, recent studies have unraveled the contribution of pre-existing memory CD4⁺ T cells in shaping vaccine immune responses and antibody production [5], [6].

Immunity conferred by vaccines is based on memory cells, of which the characteristics include extended survival, strong self-renewal and proliferative capacities, and the ability to quickly acquire effector functions upon re-exposure to infectious agents. For several vaccines, such as those against smallpox and yellow fever (YF), long-term vaccine-specific CD4⁺ memory T cells are still detectable in humans up to 83 years post-immunization [7], [8]. Repeated exposure to the same pathogen is a known mechanism for the renewal and maintenance of memory-cell pools through the re-stimulation and proliferation of antigen-specific cells. However, life-long memory has been demonstrated for the YF vaccine, even for individuals who do not live in endemic areas [9].

Systems vaccinology approaches, using advanced OMIC technologies that allow deep analyses combining multiple molecular and cellular dimensions, have helped to decipher the immune mechanisms of vaccine responses. Such strategies have been used in numerous vaccine studies, some of which have shown a role for CD4 T cells in vaccine outcomes [3], [10].

Here, we aimed to investigate the central role of CD4⁺ T cells in vaccine-induced long-term memory using the YF vaccine (YF-17D-204 strain, Stamaril®) as a model. In addition, we aimed to identify early CD4⁺ T-cell signatures predictive of long-term efficacy. Cynomolgus macaques were chosen as the non-human primate (NHP) model, as they reproduce the dynamics and symptoms of human YF infections. Furthermore, the YF-17D vaccine strain is able to replicate in NHPs as in humans and recapitulates the profile of cellular and humoral responses induced in vaccinated humans.

We also studied a β-propiolactone-inactivated YF-17D-204 vaccine, which shows a lower ability to induce nAbs following immunization [11], to detect early markers associated with the durability of nAb responses and formulate hypotheses on new mechanisms that contribute to long-term memory We used several approaches, including mass cytometry, to

compare the CD4⁺ T-cell changes induced by Stamaril® to those induced by the inactivated YF-17D-204 vaccine.

Results

The attenuated YF vaccine is superior to inactivated vaccine in inducing neutralizing antibodies distant from injection

We vaccinated two groups of cynomolgus macaques either with a human dose of Stamaril® by the subcutaneous route (ST group) or with an equivalent dose of β-propiolactone-inactivated YF-17D-204 (IN group) vaccine using a prime-boost strategy with an interval of 28 days (Fig. 1). Both vaccines induced a nAb response with titers superior to protective levels, but with different kinetic profiles. In addition, one of nine animals in the ST group (CU279) and one of nine in the IN group (CU072) showed different nAb kinetic profiles from those of the other animals of the same group (Fig. S1A). Indeed, CU279 showed a rapid decay of nAb levels, whereas nAb levels of CU072 progressively increased. In addition, these animals showed particular plasma cytokine signatures that were distinct from those of the group, including before immunization (Fig. S1B). Aside from the atypical nAb response profiles, these animals also behaved as highly atypical outliers in terms of the cytokine secretion profile (ref section and/or sup data). For all remaining animals, Stamaril® induced rapid and strong neutralization activity in the serum (Fig. 2). On the contrary, one injection was not sufficient to achieve similar initial nAb levels with the IN vaccine. Both groups showed comparable nAb titers at month 3 post-immunization (mean ± SD of 3.59 ± 0.49 and 3.38 ± 0.49, respectively). After month 3, nAb titers remained stable for the ST group, whereas they started to decrease in the IN group, falling to significantly lower titers after one year post-immunization (3.64 ± 0.47 over 2.76 ± 0.49, p = 0.004). We excluded the two macaques with atypical profiles from the further group analyses to improve the comparison of the distinct nAb kinetic profiles of the two groups of animals and treated them as outliers.

In vivo incorporation of 5-Iodo-2'-deoxyuridine (IdU) detected by mass-cytometry highlights early changes and long-term persistence of vaccine-induced CD4⁺ T cells

5'-Iododeoxyuridine (IdU) incorporation into the DNA of proliferating cells allows the assessment of cell subset mobilization and in vivo proliferation following vaccine injection (Fig. 3 and S2). We treated three animals in each group daily by intravenous injection of IdU between D3 and D6 after the first vaccine injection.

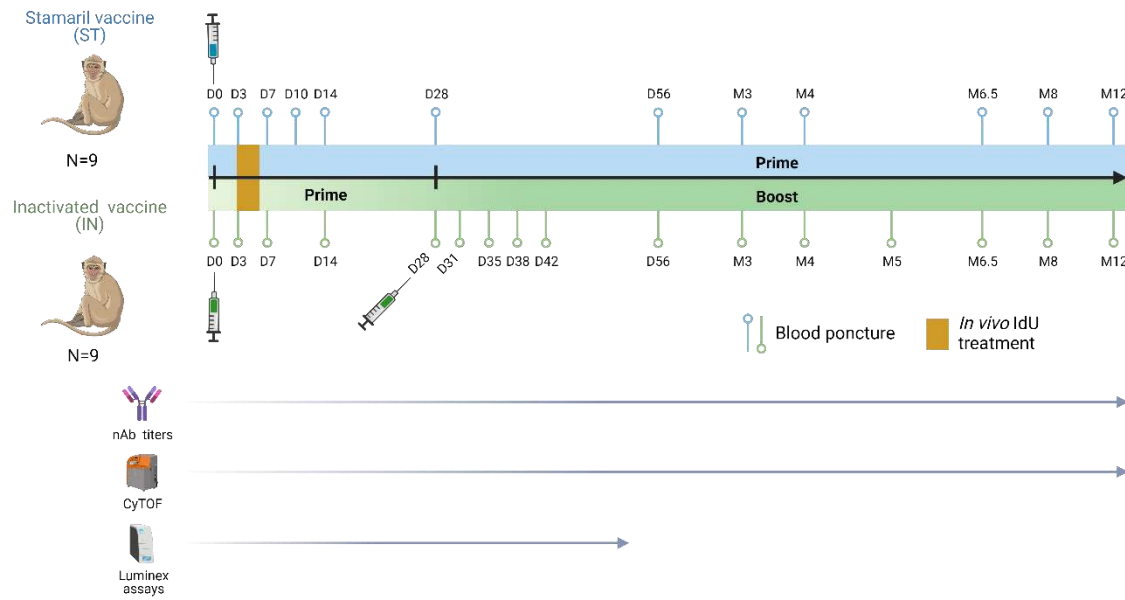


Figure 1: Experimental design. Two groups of cynomolgus macaques ($n = 9$) were immunized (indicated with syringe icon) with a single injection of Stamaril (blue), or with two injections of inactivated Stamaril (green) twenty-eight days apart. Blood sampling was performed at indicated time points to assess nAb titers, PBMCs by mass-cytometry, or cytokines. Daily i.v. injections of 5'-Iododeoxyuridine (IdU) were administered to $n = 3$ animal per group from D3 to D6 after primary immunization. For technical reasons mass cytometry was not performed at D3 and D31.

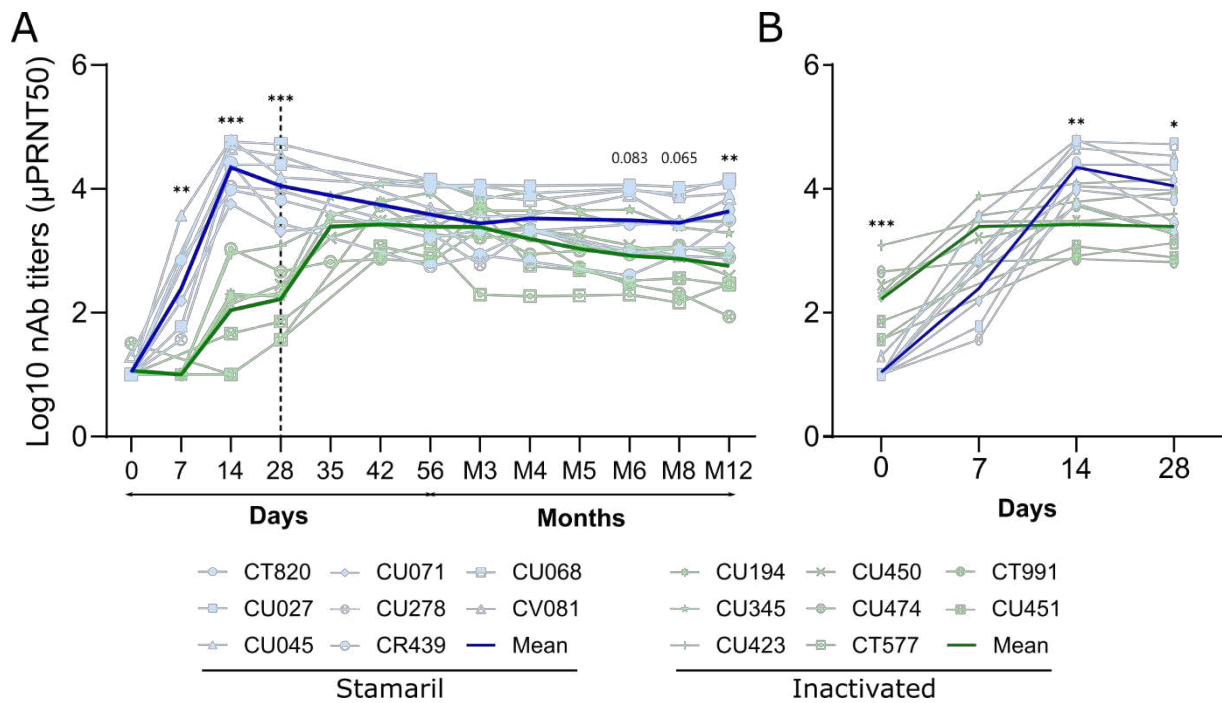


Figure 2: Neutralizing antibody titers from immunized macaques. Neutralizing antibody (nAB) titers were measured from the serum of individual animals after immunization with Stamaril (blue; $n = 8$) or inactivated Stamaril (green; $n = 8$) up to 12 month post-immunization (A). Line in bold represents the geometric mean titer for each group. Black dotted line indicates time of boost immunization for the inactivated Stamaril group. Side-by-side comparison of nAB titers elicited by primary Stamaril injection (day 0-28) vs inactivated Stamaril boost (day 28-56) (days after the specific injection are shown) (B). Significant differences in nAB titers between groups are indicated (Mann-Whitney test).

We observed similar frequencies and absolute numbers of blood CD4⁺ IdU⁺ T cells over time between the IN- and ST-vaccinated animals, peaking at D7 in both groups (Fig. 3A and C). Then, the proportion of IdU⁺ CD4⁺ T cells slowly decreased for both vaccine groups, although there was a slight increase in IdU⁺ cell numbers three days after the IN boost (D35), suggesting the recruitment of a number of these cells in the recall response. Interestingly, IdU⁺ vaccine-responsive cells could be detected in peripheral blood one year after the end of treatment, suggesting that they contribute to immune memory.

There was a higher proportion of Ki-67⁺ IdU⁺ CD4⁺ T cells in the ST group, indicating a greater proliferative phase than for the IN group ($80.50\% \pm 6.25$ vs $60.30\% \pm 5.78$). This trend was confirmed following analysis of the absolute numbers (Fig. 3B and C). After the peak, the fraction of proliferating IdU⁺ CD4⁺ T cells dropped rapidly, indicating a slowdown of the CD4⁺ T-cell expansion phase by D14. However, we again observed a slight increase in Ki-67⁺ cell numbers after the IN boost, showing a recall response. Interestingly, a low level of proliferation was maintained by a small fraction of IdU⁺ cells in both groups (Fig. 3C and D).

We then characterized the memory phenotype of the persisting cells. IdU incorporation was different within the memory CD4⁺ T cell subsets between the two vaccine groups (Fig. 3E and F). Naïve cells (CD45RA⁺ CD45RO⁻ CD27⁺) represented a small proportion of total IdU⁺ cells on D7 for the ST group and, in particular, for the IN group ($20.20\% \pm 1.34$ and $2.68\% \pm 1.84$, respectively). The frequency of IdU⁺ central memory T cells (Tcm, CD45RA⁻ CD45RO⁺ CD27⁺) increased until D28 for both vaccines. The low proportion of naïve and Tcm IdU⁺ CD4⁺ T cells on D7 was contrasted by the large mobilization of effector memory T cells (Tem, CD45RA⁻ CD45RO⁺ CD27⁻), as Tem represented $69.13\% \pm 4.12$ and $35.2\% \pm 2.64$ of all IdU⁺ cells for the IN and ST groups, respectively. Thereafter, Tem showed a decrease in frequency and absolute numbers by D14 for the IN group and, to a lower extent, for the ST group. This downward trend persisted over time for both vaccines.

The ST vaccine was also more prone to mobilize effector T cells (Teff, CD45RA⁺ CD27⁻ CD38⁺) by D7 than the IN vaccine, but similarly to Tem, this cell population rapidly decreased.

In addition, the number of terminal effector memory cells (Temra, CD45RA⁺ CD27⁻ CD38⁻) and stem cell memory T cells (Tscm, CD45RA⁺ CD27⁺ CD95⁺ CD38⁻) remained stable over time, but with a lower proportion within the ST group (Fig. 3E). Interestingly, IdU⁺ Tscm where poorly represented on D7 in the IN group, but where enriched by D14 ($0.50\% \pm 0.86$ and $7.30\% \pm 1.37$, respectively). In the absence of free IdU, these results suggest that naïve IdU⁺ CD4⁺ T cells may have differentiated into Tscm, undergone activation-induced cell death, or

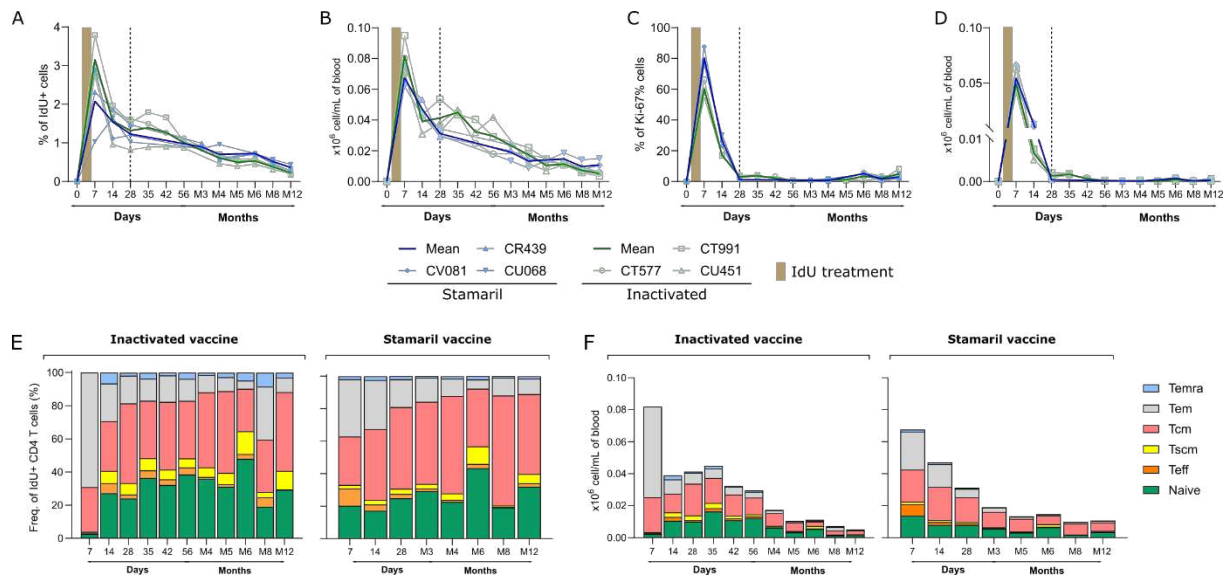


Figure 3: Follow-up of CD4⁺ T cell mobilization *in vivo* after YF-vaccine by IdU treatment. Frequencies of IdU⁺ cells (**A**) and absolute number of IdU⁺ cells in whole blood (**B**). Frequency of double-positive Ki-67⁺ IdU⁺ (**C**), and absolute number of double-positive Ki-67⁺ IdU⁺ CD4⁺ T cells in whole blood (**D**). IdU treatment period is highlighted in yellow and the time of boost in the inactivated Stamaril group is indicated by dotted lines. Distribution of effector/memory subsets as a frequency of total IdU⁺ CD4⁺ T cells were compared between vaccine groups (**E**), and absolute number of effector/memory subsets in whole blood were compared between vaccine groups (**F**). Gating strategy for defining effector/memory subsets is displayed in **Fig S2**.

migrated to other tissues. These results also suggest that the Tscm compartment is established very early during the immunization process and persists for at least one year.

Although our panels were not designed to extensively characterize CD8⁺ T cells, our analysis also confirmed that the ST vaccine more strongly induced the mobilization of NK and CD8⁺ T cells (Fig. S3) than the IN vaccine.

In conclusion, these results show that responding IdU⁺ cells to both vaccines persist over time and can be detected more than one year after injection of the vaccine. We also observed that effector and effector memory cells were rapidly induced by both vaccines, with an evolution in favor of Tcm over time for both. Nevertheless, more IdU⁺ memory cells persisted over time, at least for the ST vaccine. Interestingly, the small fraction of these cells still in an active proliferating state months after vaccine injection and IdU treatment argues for the maintenance of vaccine-specific cells through proliferation.

Early occurring cTfh and Treg as potential biomarkers of nAb persistence

We first explored the CD4⁺-T cell compartment following YF immunization by focusing on the characterization of non-stimulated bulk blood cells *ex vivo* using mass cytometry and the spanning-tree progression analyses of the density-normalized events (SPADE) algorithm. IdU was excluded from the SPADE analysis, as this treatment was performed only on three animals of each group. Hierarchical clustering of the 750 SPADE clusters allowed the definition of cell populations, which we named “phenotypic families” (PFs). This second step divided CD4⁺ T-cell clusters into 40 PFs, including canonical populations corresponding to naïve (PF6, 7, 8, 9, 13, 21, 22, 25, and 37), Tcm (PF2, 5, 12, 17, 23, 24, 27, 29, and 33), Tem (PF3, 4, 18, 19, 20, 30, and 39), Temra (PF11), Teff (PF10, 14, 15, 28, and 32), and CD4⁺ CD8⁺ T cells (PF1, 13, 26, 34, and 40). The large number of markers that can be simultaneously analyzed by mass cytometry also makes possible the detection of a wide range of undefined cell populations (PF31, 35, 36, and 38) and those with intermediate phenotypes, thus favoring the exploration of new maturation/transition states induced by vaccines and highlighting the tremendous plasticity of CD4⁺ T-cell subsets. Accordingly, a proposed annotation is presented in Table 1 (detailed phenotypes in Fig. S4), in which intermediate phenotypes are called “transitory” cell populations, as previously reported in other studies.

We first observed that the expression of certain markers was strongly linked to the differentiation state of the CD4⁺ T cells. Indeed, CD3 and CD45 showed opposite co-expression dynamics relative to CD4 expression between naïve and memory cells (fully differentiated or

Table 1: Deep characterization and annotation of CD4+ T cell phenotype families by mass cytometry.
Proposal of annotation for Phenotypic Families.

Phenotypic Family	Cell population (memory status)	Characteristic markers	Comments
PF1	Double positive Temra	CD4+ CD8+ CD45RA+ CD45RO- CD27 ^{lo/mid} CCR7-	<ul style="list-style-type: none"> CD95+ PD-1+ ICOS^{lo} CD62L- CD127- Proliferating family (Ki-67⁺) Dowregulation of CD45, CD3 and CD38 Expression of TGFb
PF2	Transitory Tcm	CD45RA ^{lo} CD45RO ^{mid} CD27 ⁺	Activated cells (CD40L+ CD69+ CD62L-)
PF3	Transitory Tem	CD45RO+ CD27 ^{mid} CCR7-	<ul style="list-style-type: none"> Proliferating family (Ki-67⁺) Highly activated (CD95+ PD-1^{hi})
PF4	Th1 Tem	CD45RO+ CD27- CD62L-	Proliferating cells (Ki-67 ⁺)
PF5	Transitory cell to Tcm	CD45RA ^{lo} CD45RO+ CD27 ^{mid/+}	CXCR3 ^{lo} and downregulation of CXCR4 suggesting Th2
PF6	Naive cells	CD45RA ^{lo/+} CD45RO- CD27 ⁺	<ul style="list-style-type: none"> CD95+ ICOS^{lo} CD62L⁺ Heterogeneous for CXCR3 Downregulation of CD4
PF7	Naive cells	CD45RA ^{mid/+} CD45RO- CD27 ⁺ CCR7+	<ul style="list-style-type: none"> CD95+ ICOS^{lo} CD62L⁺ Downregulation of CD4
PF8	Naive cells	CD45RA ^{mid/+} CD45RO- CD27 ⁺ CCR7+	<ul style="list-style-type: none"> CD95+ ICOS^{lo} CD62L^{lo} Downregulation of CD4
PF9	Naive cells	CD45RA+ CD45RO- CD27 ⁺ CCR7+	<ul style="list-style-type: none"> CD95+ ICOS^{lo} CD62L⁺ Upregulation of CD4
PF10	Transitory cell	CD45RA ^{lo} CD45RO- CD27 ^{mid/+} CCR7 ^{lo}	CD95+ ICOS ⁺ CD62L-
PF11	Temra	CD45RA+ CD45RO- CD27 ^{lo/mid} CCR7-	<ul style="list-style-type: none"> CD95+ ICOS^{lo} CD62L- CD127- Dowregulation of CD45, CD3 and CD38 Expression of TGFb
PF12	cTfh Transitory cell to Tcm phenotype	CXCR5+ Bcl6 ^{mid} CD45RA ^{lo/mid} CD45RO ^{lo} CD27 ⁺	CD127 ⁺ CD95+ ICOS ⁺ CD62L ^{-/+}
PF13	Naive cells	CD45RA ^{lo/mid} CD45RO- CD27 ⁺ CCR7 ^{mid}	<ul style="list-style-type: none"> CD95+ ICOS^{lo} CD62L⁺ CXCR3^{lo} Downregulation of CD4
PF14	Transitory cells	CD45RA ^{lo} CD45RO- CD27 ^{mid} CCR7-	<ul style="list-style-type: none"> CD95+ ICOS⁺ CD62L⁻ Downregulation of CXCR4
PF15	Transitory cells	CD45RA ^{lo} CD45RO ^{lo} CD27 ⁻	<ul style="list-style-type: none"> CD95+ ICOS⁺ CD62L⁻ Low production of IL-4 and IL-13 suggesting Th2 Proliferative family (Ki-67^{hi})
PF16	Double positive Temra	CD4+ CD8+ CD45RA+ CD45RO- CD27 ^{mid} CCR7-	<ul style="list-style-type: none"> CD95+ PD-1+ ICOS^{lo} CD62L- CD127- Dowregulation of CD45, CD3 and CD38 Expression of TGFb
PF17	Tcm	CD45RA ^{lo} CD45RO ^{lo/mid} CD27 ⁺	CD95+ ICOS ⁺ CD62L ⁺
PF18	Tem activated	CD45RO+ CD27 ^{mid} CCR7-	<ul style="list-style-type: none"> CD95^{hi} ICOS⁺ CD62L- CD25^{lo/+} Low production of IL-13 suggesting Th2
PF19	Tem highly activated	CD45RO+ CD27 ^{mid} CCR7-	<ul style="list-style-type: none"> CD95^{hi} PD1⁺ ICOS⁺ CD62L⁻ CD25⁺ OX40⁺
PF20	Tem	CD45RO+ CD27 ^{lo} CCR7-	CD95 ^{lo/+} ICOS ⁺ CD62L-
PF21	Naive transitory cell	CD45RA ^{lo/mid} CD45RO- CD27 ^{lo} CCR7 ^{lo/mid}	CD95 ^{lo/mid} ICOS ^{mid/+} CD62L ⁻
PF22	Naive cells	CD45RA+ CD45RO- CD27 ⁺ CCR7 ^{mid}	<ul style="list-style-type: none"> CD95+ ICOS^{lo} CD62L^{lo} Downregulation of CD4
PF23	Naive Treg	CD25 ^{hi} FoxP3 ^{+/hi} CD127 ⁻	CD45RA+ CD45RO- CD27 ⁺
PF24	Treg Tem	CD45RO ^{mid/+} CD27 ⁺ CD25 ⁺ FoxP3 ⁺	CD95 ^{hi} ICOS ⁺ CD62L ⁺
PF25	Naive cells	CD45RA ^{lo} CD45RO- CD27 ⁺ CCR7 ^{lo}	<ul style="list-style-type: none"> CD95^{lo} ICOS^{mid} CD62L⁺ Downregulation of CD4
PF26	Double positive naive cells	CD4+ CD8+ CD45RA+ CD45RO- CD27 ^{mid} CCR7 ^{lo}	
PF27	cTfh Transitory cell to Tcm phenotype	CXCR5+ PD1 ^{hi} CD40L ^{lo/mid} CD45RA ^{lo/mid} CD45RO ^{lo} CD27 ⁺	CD127 ^{lo} CD95+ ICOS ⁺ CD62L ⁻
PF28	Effector transitory cells	CD45RA ^{lo} CD45RO- CD27- CCR7+	CD95 ^{lo} ICOS ^{lo} CD62L ⁻
PF29	Tcm	CD45RO+ CD45RA ^{lo} CD27 ⁺	<ul style="list-style-type: none"> CD95+ ICOS^{hi} CD62L⁻ Proliferative family (Ki-67^{hi})
PF30	Tem	CD45RO+ CD45RA ^{lo} CD27 ⁻	<ul style="list-style-type: none"> CD95^{hi} ICOS^{hi} Proliferative family (Ki-67^{hi}) Downregulation of CD3
PF31 and PF35	Undetermined cells	CD45RA ^{mid} CD45RO+ CD27 ^{hi} CCR7-	<ul style="list-style-type: none"> CD95^{lo} ICOS^{mid} CD62L⁻ Expression of various cytokines Potential unspecific binding
PF32	Effector transitory cell	CD45RA ^{lo/mid} CD45RO- CD27 ^{mid} CCR7 ^{lo}	CD95 ^{lo/+} ICOS ⁺ CD62L ⁻ CD38-
PF33	cTfh Transitory cell to Tcm	CXCR5+ Bcl6 ^{mid} CD45RA ^{lo/mid} CD45RO ^{lo} CD27 ⁺ CCR7 ^{lo}	<ul style="list-style-type: none"> CD95+ ICOS⁺ CD62L^{-/+} CD25⁺
PF34	Double positive Tem cells	CD4+ CD8+ CD45RO ^{mid} CD27 ^{mid} CCR7-	CD95 ^{hi} ICOS ^{mid} CD62L ⁻
PF36	Transitory cell	CD45RA+ CD45RO+ CD27 ^{hi} CCR7-	<ul style="list-style-type: none"> CD95+ ICOS^{lo} CD62L⁻ Proliferative family (Ki-67⁺)
PF37	Transitory naive cell to Tcm	CD45RA ^{lo} CD45RO- CD27 ⁺ CCR7 ^{lo}	<ul style="list-style-type: none"> CD95+ ICOS⁺ CD62L⁻ Downregulation of CD4
PF38	Transitory cells	CD45RA ^{lo} CD45RO ^{mid/+} CD27 ^{mid/+} CCR7-	CD95 ^{lo/+} ICOS ^{hi} CD62L ⁻
PF39	Activated Tem	CD45RA ^{lo} CD45RO ^{mid/+} CD27- CCR7-	<ul style="list-style-type: none"> CD95^{hi} ICOS⁺ CD62L⁻ CD40L⁺ CD69⁺ TNFα⁺ IL-2⁺ Proliferative family (Ki-67⁺)
PF40	Double positive effector T cells	CD4+ CD8+ CD45RA+ CD45RO ^{lo} CD27 ⁻	<ul style="list-style-type: none"> CD95^{mid} ICOS^{mid} CD62L⁻ CD69⁺ Expression of IL-17a

transitory). A loss of CD3 and CD45 and an increase in CD4 expression was observed as cells became engaged in activated or memory phenotypes. The co-stimulatory molecule ICOS also showed an expression profile similar to that of CD4, but tended to revert to a naïve expression profile in highly differentiated Temra cells.

Following YF immunization, 23 PFs showed significant changes from baseline for the IN vaccinees and 14 for the ST vaccinees. Interestingly, 15 PFs were differently enriched between the two vaccines (PF2, 8, 11, 12, 14, 18, 22, 23, 25, 27, 30, 33, 35, 38, and 40) and seven were shared between groups, mostly at early time points (Fig 4).

Three circulating follicular helper T-cell (cTfh) PFs and a regulatory T-cell (Treg) PF appeared to be involved with early differences between the vaccines. PF12, 27, and 33 cTfh were characterized as CXCR5⁺ ICOS⁺ Bcl6^{lo/mid} CCR7^{lo} Tcm or the transitory Tcm phenotype. The proportion of PF12 and 33 decreased by D7 for the IN group ($p = 0.0028$ and $p = 0.0048$, respectively) (Fig. 4A and B). This change significantly differed between vaccines ($p = 0.0075$ and $p = 0.018$, respectively) (Fig. 4C). We observed a higher proportion of PF33 for the ST group on D14 ($p = 0.019$). This change was then followed by a trend towards an increasing proportion over time. The proportion of PF33 was also slightly increased on D31 for the IN-vaccinated animals after the boost (Fig 4D).

Conversely, PF27 cTfh were enriched in the IN group on D3 and D7 relative to the ST group ($p = 0.04$ and $p = 0.026$, respectively), with three animals showing a larger increase than the rest of the group. Interestingly, these three animals showed the highest PF27 abundance and lowest Nab titers on D14 and M12. The proportion of PF27 cTfh then decreased rapidly and the cells were not amplified by the boost, whereas an increase was noted three months after immunization in the ST group ($p = 0.021$).

This cTfh cell populations showed differences in CD127 (IL-7R), CD25, and PD-1 expression. CD127 expression differentiated CD127^{lo} PF27 cTfh from CD127⁺ PF12 and PF33. Conversely, PF33 was the only cTfh population that expressed CD25, suggesting a regulatory Tfh phenotype. Surprisingly, PF27 expressed high levels of PD-1, which is usually observed in B-cell follicles, but it was not expressed by PF12 or PF33.

The Treg (PF23) population (CD25^{hi} FoxP3^{+/hi} CD127⁻) was significantly more abundant on D3 and D14 in the IN than ST group ($p = 0.0094$ and $p = 0.002$, respectively). By D28, Treg levels in the IN group decreased to a similar abundance as that observed in ST-vaccinated animals.

In conclusion, we found evidence of kinetic differences in the abundance of cTfh and Treg between vaccines possibly associated with differences in the persistence of the nAb

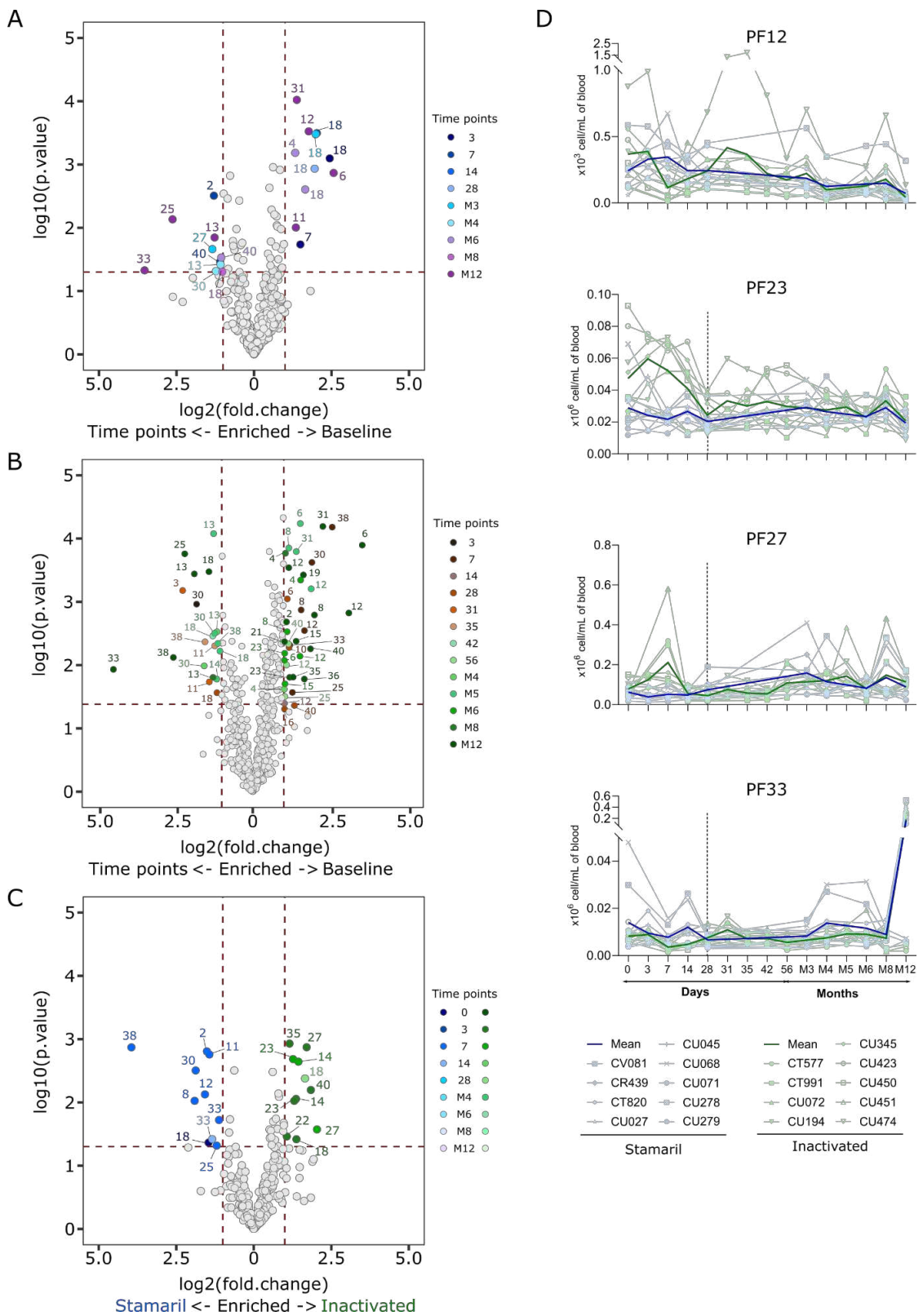


Figure 4: Enrichment of CD4⁺ T cell phenotypic families (PF) following YF immunization. Volcano plots of PF (defined in Table 1) enrichment at different time points compared to D0 after immunization with Stamaril (A) or inactivated Stamaril (B). Volcano plots of differentially-enriched PF between vaccines depending on time points (C). (D): Kinetic of representative PF, Stamaril and Inactivated vaccine are displayed in blue and green, respectively.

response observed between the two vaccines. We also found differences in PD-1 expression that could be possibly associated with reduced B-cell activity. Finally, the differential expression of CD25 and CD127 in cTfh suggests different functions for these cells, as it may result in different IL-2 and IL-7 signaling.

Greater ability of the IN vaccine to induce YF antigen-specific cytokine-producing cells

We then characterized the induction of the long-term memory induced by the YF vaccine by focusing on YF-specific cell functions through the assessment of intracellular cytokine staining following overnight *ex-vivo* stimulation with purified YF-17D virus. A t-distributed stochastic neighbor embedding analysis (tSNE) was carried out using all CD40L⁺ CD4⁺ T cells and cytokines as entry parameters (Fig 5A), identifying 40 cell subpopulations (Fig 5B and 5C, Table 2).

We observed an increase in YF antigen stimulation-responding CD40L⁺ CD4⁺ T cells after both IN injections, with peaks on D14 and D42 (Fig. S5A). Only a slight increase of CD40L⁺ CD4⁺ T cells could be observed seven days after the IN boost in the non-stimulated condition (NS), suggesting the presence of cells that had already been stimulated *in vivo* by the YF antigen or by a bystander effect. However, from M4 to M12, activated CD4⁺ T cells showed similar levels between the NS and YF conditions. Interestingly, we observed a similar proportion of CD40L⁺ CD4⁺ T cells following ST injection for both the NS and YF conditions throughout the study.

Independently of vaccine or cell stimulation, most activated CD4⁺ T cells did not produce cytokines, or only at low levels, and most activated cytokine-producing (ACP) cells did not show significant differences between the vaccine or stimulation conditions. However, the ST vaccine showed a lower ability than the IN vaccine to trigger cytokine-producing cells upon YF stimulation. Nonetheless, eight ACP cell populations were significantly enriched following YF stimulation of cells obtained from ST-vaccinated animals (Fig 6A and S5B). Most were composed of Tcm. Cells from ACP9 were identified as being of the Th2 type due to their production of IL-4 and proliferation following *ex-vivo* stimulation. IL-2 producing cells from ACP19 were also significantly enriched upon YF stimulation. On the contrary, ACP38, composed of non-memory cells, showed a slight decrease in abundance following YF stimulation, suggesting that most YF specific-responding CD40L⁺ CD4⁺ T cells were contained in this cell population before *ex-vivo* stimulation. In addition, ACP20, defined as cTfh, based on its IL-21 expression, was slightly enriched on D14 and D28 and then the proportion remained

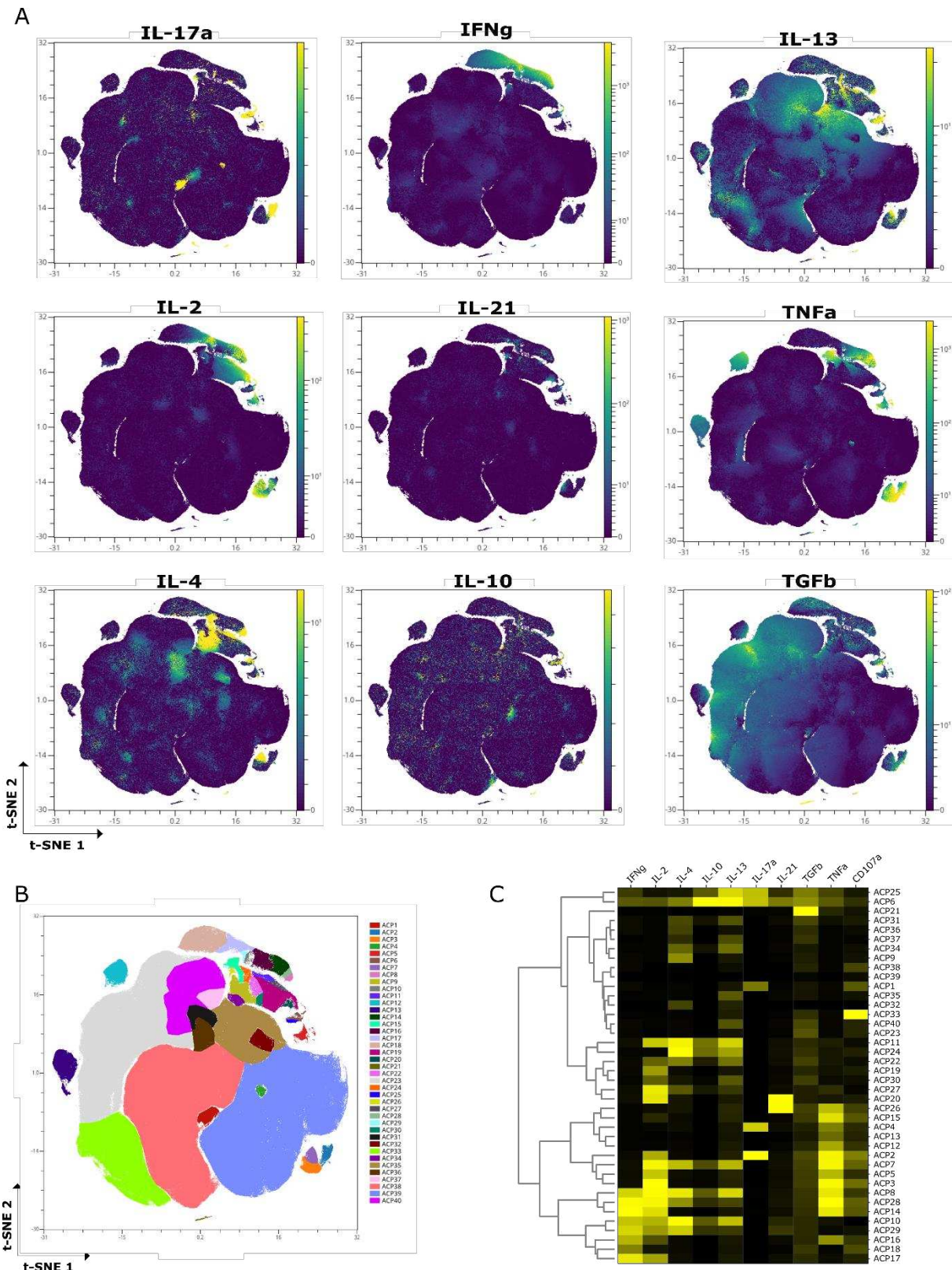


Figure 5: Vaccine-induced CD4 T cell responses display diverse cytokine-producing abilities upon stimulation with purified YF virus. Distribution of *in vitro* blood-derived activated CD40L+ CD4 T cell populations by tSNE, using cytokine expression (A). Activated cytokine producing cell (ACP) populations were manually gated according cytokine expression and are displayed in (B). (C): Heatmap displaying the median intensity of cytokine expression within each ACP in blood identified by tSNE analysis.

Table 2: Yellow fever fever-specific CD4+ T cells ACP annotation and phenotype diversity upon in vitro stimulation. Proposal of annotation for ACP cell subsets based on their functional profile and memory status.

Activated CD4 T cell population	Main cytokine	Supplementary functions	Cell type	Memory status
ACP10	IL-2 IL-4 IL-13	IL-21 (some cells) IFNg		
ACP8	IL-2 IL-4 IL-13	IFNg TNFa		Tem
ACP28	IL-2 IL-4	IFNg TNFa		
ACP29	IFNg IL-2	IL-4	Polyfunctional cells	
ACP6	IFNg IL-2 IL-4 IL-10 (some cells) IL-13	IL-17a IL-21 (some cells) TGFb TNFa		
ACP25	IFNg ^{lo} IL-13 IL-17a	TGFb TNFa		
ACP20	IL-21	IL-2	Tfh	Tcm
ACP26		TNFa		
ACP14	IFNg	IL-2 TNFa cytotoxic activity	Th1	Tcm
ACP16		IL-2 TNFa		
ACP17		IL-2		
ACP18		cytotoxic activity		Transitory memory cells
ACP27	IL-2	IL-4 IL-13	Th2	Tcm
ACP32	IL-4 ^{lo}			Transitory memory cells
ACP36		TGFb ^{lo}		
ACP9	IL-4			Tcm
ACP35	IL-13 ^{lo}			non memory cells
ACP30		IL-2 ^{lo}		Transitory memory cells
ACP40		TGFb ^{lo}		non memory cells
ACP37	IL-4 ^{lo} IL-13 ^{lo}			non memory cells
ACP31				Tcm
ACP34				
ACP24			Tem	
ACP11	IL-4 IL-13	IL-2		
ACP22		IL-2 TNFa		
ACP7				
ACP1	IL-17a	cytotoxic activity	Th17	non memory cells
ACP4	IL-17a	TNFa		Tcm
ACP2		IL-2 TNFa cytotoxic activity		Tem
ACP21	TGFb ^{hi}		Treg	Tcm + Tscm
ACP12	TNFa		non identified cells	Tcm or non memory cells
ACP13				Tcm
ACP15		IL-2 (some cells)		Transitory memory cells
ACP19	IL-2			non memory cells
ACP23	TGFb ^{lo}			Tcm
ACP5	TNFa			Tem
ACP3	IL-2			
ACP33		cytotoxic activity		non memory cells
ACP38				
ACP39				

stable until D90, before decreasing. Four ACP cell populations with profiles potentially associated with a Th1 cellular response included ACP14 and ACP16, which produced IFN γ , IL-2, and TNF α , with a peak on D14, and ACP5, which produced TNF α . Interestingly, ACP17, which expressed both IFN γ and IL-2, was the only ACP population that showed a greater increase in cytokine staining upon stimulation on D14 for the ST than IN vaccine. However, despite similar extracellular marker and cytokine expression profiles, we observed differences in CD27 expression between the vaccine groups for ACP17 (Fig 6B). Indeed, ST-vaccinated animals showed a high intensity of CD27 staining, whereas most cells were CD27-negative or had downregulated CD27 in the IN group. This indicates that ACP17 is composed of two different cell subsets depending on the immunization group: Tcm for ST and Tem for IN. Furthermore, ACP17 cells tended to display higher intensity IFN γ and IL-2 staining, suggesting functional differences.

Conversely, activated cells from IN-vaccinated animals showed a greater diversity of functions in response to YF stimulation, as well as a higher proportion of polyfunctional cells. The abundance of most ACP populations was much higher by D14, with increases after the boost for ACP 7, 8, 9, 10, 11, 20, 22, 24, 28, and 29, and it was significantly higher than that in ST-vaccinated animals (Fig 6A). Contrary to ST-vaccinated animals, the ACP populations of IN-vaccinated animals were mainly composed of Tem, with high polyfunctional ability (APC8, 10, and 28) and a Th2 phenotype (ACP7, 11, 22 and 24). ACP9 and 20 were identified as Tcm. On the contrary, the proportion of ACP5 producing TNF α , Th1 type cells from ACP14 and 16, ACP19, producing IL-2, and the Th2 type ACP27 decreased over time, despite a slight effect of the boost. We also identified cell populations, ACP26 and 34 (central memory Tfh and Th2, respectively), that were only triggered after the IN boost. The proportion of all these ACP populations rapidly decreased by M3 to levels similar to those of the ST group. Only ACP3, 7, and 15, commonly producing TNF α , persisted for up to one year, with a higher level than in the ST group.

Finally, ACP23, 38, and 40 showed particular dynamics, as specific stimulation induced a decrease in the abundance of these populations relative to that of the NS condition, especially for the IN vaccine. These ACP populations represented the largest proportion of activated CD4 $^{+}$ T cells, but no cytokine production was detected for ACP38 and only very low levels of TGF β and IL-13 were observed for ACP23 and 40, respectively. The CD45RA $^{+}$ CD45RO $^{-}$ phenotype and the weak expression of CD95 suggest that these were not memory cells, with a poor activation profile. However, the decrease observed during the acute phase of the vaccine

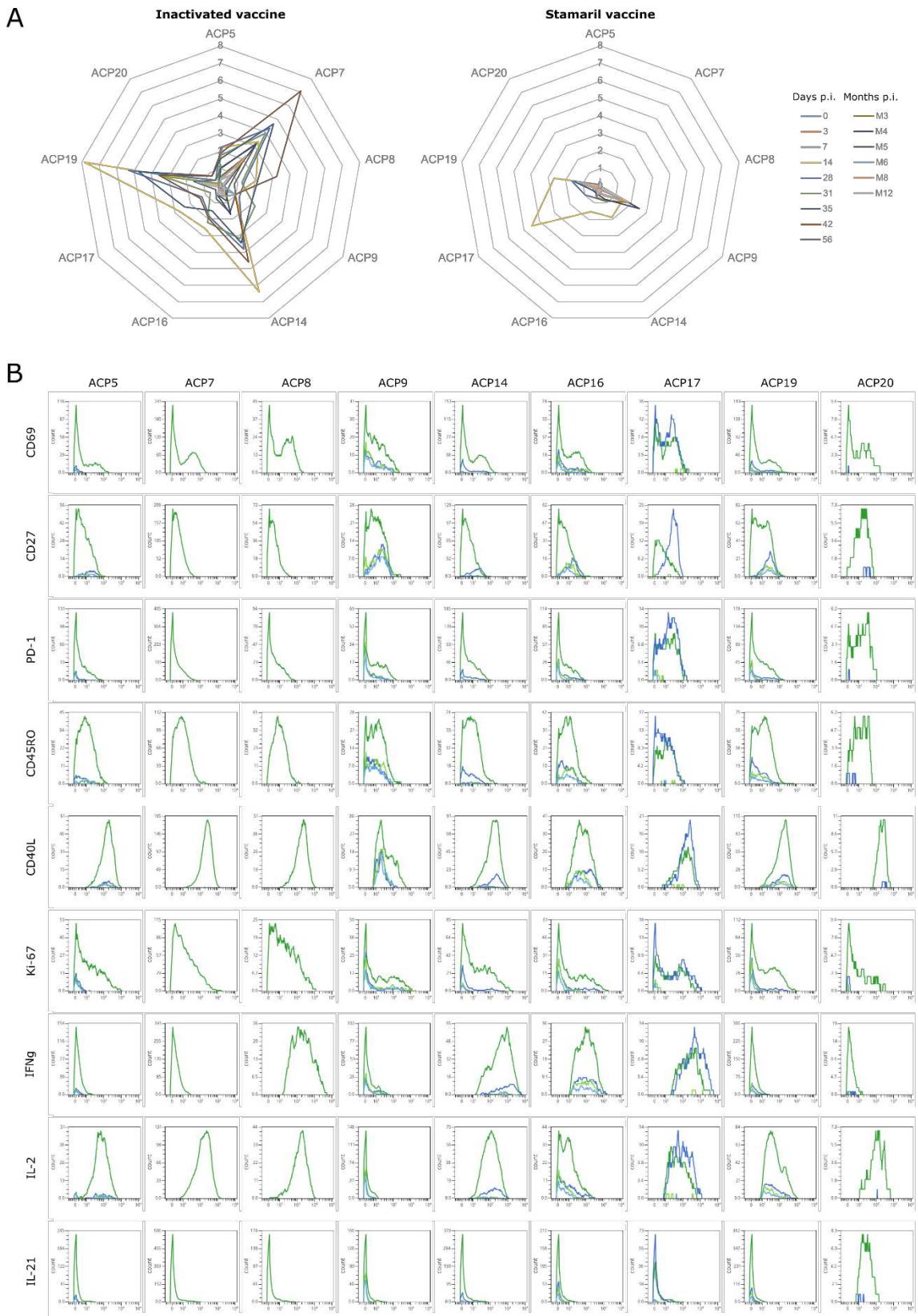


Figure 6: Kinetics of activated cytokine CD4+ T cells population elicited by *in vitro* YF immunization. (A): Mean relative abundances of ACP cell population significantly enriched by ST vaccine and two ACP cell population (7 and 8) specifically enriched in IN vaccine (as a percentage of CD40L+ CD4 T cells) after stimulation *in vitro* with purified YF-17D virus compare to NS condition (Fig S5). Timepoints are indicated by line color. (B): Histograms displaying a reduce set of markers intensity for ACP presented in (A).

response after specific stimulation may reflect a shift from poorly activated YF-specific cells in the NS condition to an active cytokine-production profile. Furthermore, as most cells from ACP 23, 38, and 40 did not respond to YF stimulation, it is possible that these cell populations also contained activated bystander and non-specific cells.

These results emphasize differences in YF-specific memory subsets in the blood, with a trend towards the persistence of effector memory cells following IN vaccination and central memory cells following ST vaccination. Furthermore, in contrast to the greater cell mobilization and larger number of functional activities observed in the IN group upon specific stimulation, the cells of the ST group poorly respond to stimulation and those cells that were activated were mainly focused on cellular responses.

Cytokine responses highlight a stronger antiviral response following Stamaril vaccination

We assessed the immune environment of CD4⁺ T cells early following vaccine injection by measuring changes in the level of several cytokines in the plasma.

The mean cytokine concentrations over the first two to three months following immunization (Fig. 7A) were highly similar between the two vaccines. However, as early as day 3, the ST vaccine induced the synthesis of significant levels of cytokines involved in anti-viral responses, including IFN2 α ($39.24 \text{ pg.mL}^{-1} \pm 21.75$, $p = 0.00015$) and I-TAC ($39.65 \text{ pg.mL}^{-1} \pm 40.757$, $p = 0.007$), and markers of cytotoxic responses, including elevated levels of perforin in the plasma ($7152.19 \text{ pg.mL}^{-1} \pm 4477.40$; $p = 0.028$), relative to the response to the prime vaccination with the IN vaccine (Fig 7B and 7C). IP-10 showed a similar trend, but it was not statistically significant.

Stamaril® also induced a stronger inflammatory response, illustrated by an increase in IL-6 production from D0 to D7 ($12.79 \text{ pg.mL}^{-1} \pm 5.34$, $p = 0.003$), than after the IN prime injection. The low level of IL-6 after the IN prime injection contrasts with a significant boost effect for this cytokine at D35 (Fig 7C), reaching a similar level to that induced by D7 by the ST vaccine ($12.30 \text{ pg.mL}^{-1} \pm 7.22$). We also observed a similar trend for IL-8 for three animals in each vaccine group (Fig. S6A).

Furthermore, we detected cytokines involved in the control of the inflammatory response at higher concentrations for the ST than IN group, especially on D3, after both the prime ($30.19 \text{ pg.mL}^{-1} \pm 21.88$ and $8.31 \text{ pg.mL}^{-1} \pm 8.54$, $p = 0.028$) and boost ($30.19 \text{ pg.mL}^{-1} \pm$

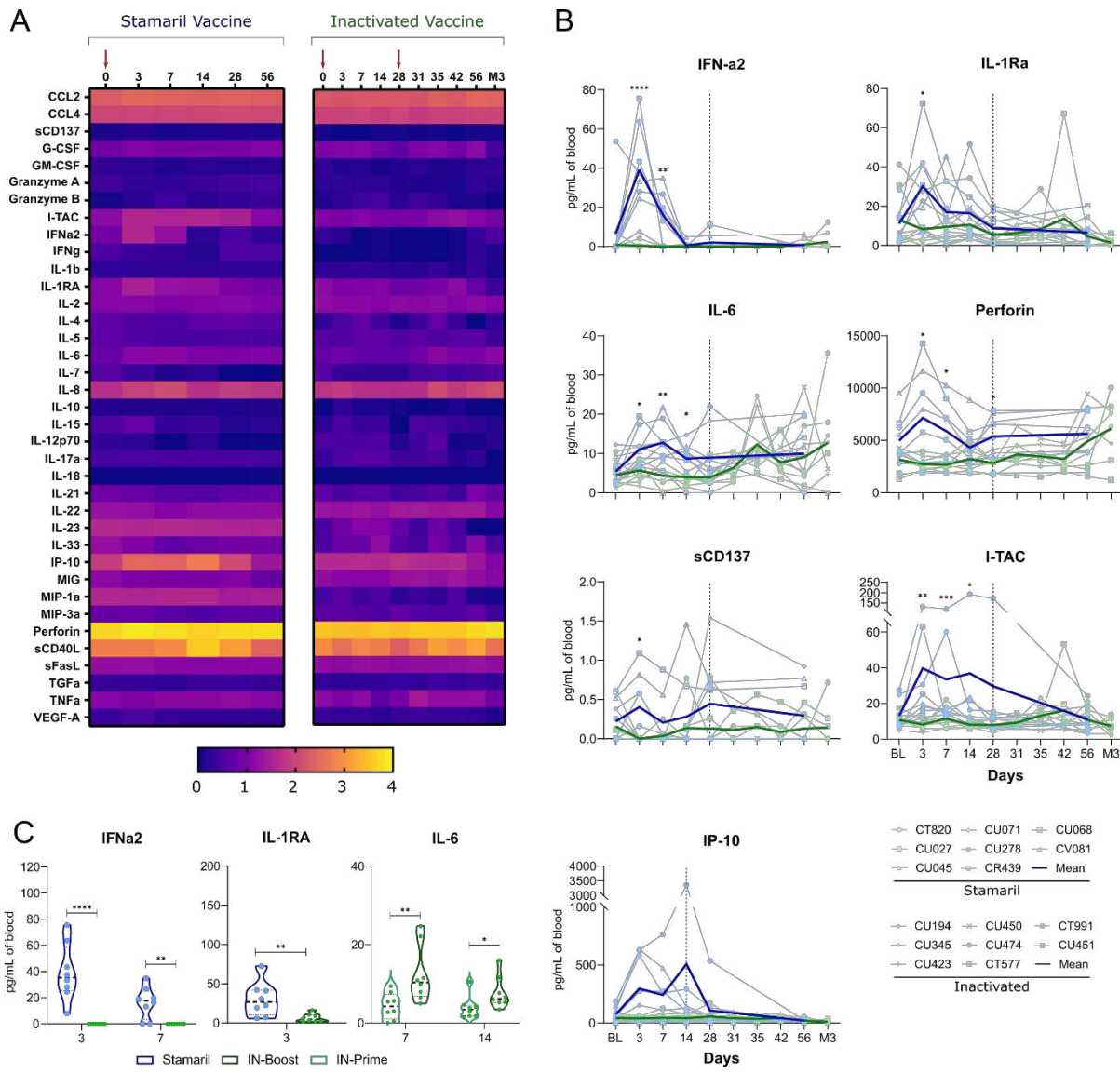


Figure 7: Soluble factor response in plasma after Yellow fever immunization. Heatmap of mean analyte concentration from plasma ($\log_{10}[CK+1]$ transformation) at the different timepoints after immunization with Stamaril (blue) or inactivated Stamaril (green) vaccine ($n = 8$ per group). Immunization and boost time points are indicated with red arrows (A). Kinetics of perforin, IFN α 2, IL-1Ra, IL-6, I-TAC, sCD137 and IP-10 from the plasma of individual Stamaril (blue) or inactivated Stamaril (green)-immunized animals (B). Black dotted line indicates time of inactivated Stamaril boost. Arithmetic mean concentration for each analyte is displayed by a bold line. Comparison of the IFN α 2, IL-1Ra and IL-6 response to Stamaril immunization, or inactivated Stamaril prime (IN-Prime) or boost (IN-Boost). Significant variation between immunization groups or between time points are shown (Mann-Whitney test).

21.88 and $6.43 \text{ pg.mL}^{-1} \pm 5.19$, $p = 0.005$) for IL-1RA and on D3 post-prime for sCD137 ($0.40 \text{ pg.mL}^{-1} \pm 0.42$ and $0.001 \text{ pg.mL}^{-1} \pm 0.004$, $p = 0.025$).

Interestingly, outlier animal CU279 from the ST group showed a high background level at baseline for IFN γ , IL-1RA, IL-12p70, sFasL, and TNF α (Fig S1B). Following vaccine injection, this animal showed a strong and persistent Granzyme B response, in addition to high levels of numerous cytokines involved in cytotoxic activity, including sFasL and IL-12p70, (Fig S6B). The particular immunological status at baseline for this animal, suggested by its unique cytokine-expression profile, may have been associated with its lower nAb response, contrasting with that of the other animals of this group (Fig S1A).

The second outlier animal, CU072, belonging to the IN vaccine group, also showed a high background level of IFN γ at baseline, as well as for perforin and cytokines, such as IL-6 and sCD40L (Fig S1B). IL-6, IL-8, and sCD40L were also strongly induced after the prime, with a peak on D14 before a decrease by D28 (Fig S6B). A boost effect was also observed for these cytokines, with a higher level of IL-6 than that following the prime injection, and, to a lesser extent, for IL-8 and sCD40L. As for CU279 in the ST group, such an atypic environment before vaccine injection may have favored a stronger nAb response at the peak (D14) (Fig S1A) and, conversely to the other animals of the same group, a progressive increase after the boost. The high production of IL-4 after the prime is of interest, as it may have favored this antibody production profile (Fig S6B). These two animals highlight the importance of the current immune status at the time of vaccination in shaping the immune response.

Discussion

This study confirms the greater ability of the live attenuated YF vaccine to induce a strong and persistent nAb response relative to two injections of the inactivated vaccine required to induce equivalent titers at M3 post-vaccination. The differences between the profiles of these antibodies offer a unique opportunity to explore the early associated immune mechanisms.

Interestingly, we observed marked NK and IdU $^+$ CD8 T cell mobilization triggered by the Stamaril® vaccine relative to the inactivated vaccine, with a greater recall of IFN γ - and TNF α -producing Th1 cells than Th2 cells upon YF-specific stimulation. On the contrary, the IN vaccine induced a strong and multifunctional YF-specific response upon stimulation. In our study, we used a purified YF-17D strain to recall specific CD4 $^+$ T cells. The use of such a stimulating condition could bias the activation of envelope-specific clones, as the time of stimulation is likely too short to induce non-structural proteins that may be recognized by cells generated by the ST vaccine. Thus, our observations might reflect a restricted repertoire of

specific cells, especially because cells specific for NS1 and NS3 have been identified as the most abundant CD4 T-cell clones in vaccinated humans [12]. This might explain the lower recall ability of the ST vaccine relative to the IN vaccine, for which the entire CD4 T-cell repertoire was directed against the envelope protein. Future analysis using specific peptides would be of great interest to further characterize the YF CD4⁺ T-cell immune response.

Consistent with previous results, the cellular response observed for Stamaril® is supported by a pronounced plasma antiviral response [13]. However, the most significant cytokine changes were observed on D3, implying that if any cytokines are involved in the nAb response, they should be investigated very early after vaccination.

Such a response and the involvement of Th1 cells in cellular responses are intriguing for the ST vaccine, as a stronger nAb response was detected than for the IN vaccine. Studies have shown Th cell plasticity in response to the cytokine composition in the cell environment. Thus, under the influence of IL-4 and IL-2 signaling, Th cells could differentiate towards a Th1 phenotype and thus favor humoral responses. Furthermore, in Peyer's patches, Tregs and Th17 cells have demonstrated the ability to differentiate into Tfh cells and provide B cell help and support IgA production [14], [15]. An equivalent mechanism within lymph nodes might be involved in the stronger nAb response of the ST vaccine relative to the IN vaccine.

In our study, we only focused on T-dependent B-cell activation, but it is known that viruses can induce T-independent antibody responses. Using virus-like particles, Liao et al. showed that pre-germinal center B-cell activation and affinity maturation can occur without T-cell help [16]. Interestingly, they also showed that the induction of long-lived memory B cells can also be triggered in a T cell-independent manner, as virus like particle-specific cells were detected one year after immunization. It would be informative to investigate whether such mechanisms can explain the nAb response observed for the ST vaccine, despite a pronounced Th1-specific response.

Nevertheless, we were able to observe differences in cTfh and Treg cell dynamics between the two vaccines, arguing for their potential role in the induction and persistence of the nAb response.

Interestingly, cTfh differed in CD127 (IL-7R) expression, with a CD127^{lo} phenotype for PF27 and a CD127⁺ phenotype for PF12 and 33. It has been previously shown that IL-7 is involved in CD4⁺ T memory cell homeostasis and survival by upregulating the anti-apoptotic factor Bcl-2 and downregulating pro-apoptotic factors [17], [18]. In addition, Kaech *et al.* showed that cells with a memory fate express CD127 [19]. Furthermore, McKinstry *et al.* showed that late IL-2 signaling favors CD127 expression by effector cells, hence supporting a

memory-cell fate [20]. Thus, our observations of differences in CD127 expression may suggest variable sensitivity of cTfh to maintenance signaling induced by IL-7, with PF12 and 33 displaying the highest potential for long-term persistence.

PD-1⁺ CCR7^{lo} cTfh have been previously described in the blood and shown to be a potent inducer of the humoral response [21]. The higher abundance of such a cell population in the blood following ST vaccination suggests their having a role in the nAb response. It may be surprising that these cells were more abundant following IN vaccination, especially in animals displaying the lowest nAb response. However, Ab functionalities other than neutralizing ability may have been promoted in these vaccinated animals. It could thus be informative to assess the total IgG response to identify whether the IN vaccine shows a reduced ability to induce a humoral response or only that of nAbs.

Concerning CD25⁺ cTfh cells, Li and Pauza showed that these cells are associated with increased B-cell survival and memory differentiation in secondary lymphoid organs [22]. Whether such cells can display similar functions in blood needs to be addressed to determine how the ST vaccine induces a persistent nAb response.

The memory phenotype of specific cells may also be linked to the persistence of nAbs. Indeed, the IN vaccine showed a dominant effector and effector-memory phenotype. Such cells are known to show a lower capacity for proliferation and differentiation than Tcm. Furthermore, these cells are able to migrate to tissues to fight pathogens and would thus be essentially unavailable to recirculate in the peripheral blood. On the contrary, Tcm are able to circulate in the blood and secondary lymphoid organs, such as the bone marrow. It has been shown that certain pathogen-specific memory T cells preferentially persist for extended periods of time in the bone marrow and are able to recirculate [23], [24]. Interestingly, bone marrow is also a niche for long-lived plasma cells [25], [26]. This might favor the persistence of nAbs following ST vaccination, whereas the Tem phenotype of IN-specific cells would suggest the persistence of memory within tissues. Such studies emphasize the lack of data on T-cell migration to tissues, especially secondary lymphoid organs. Identifying the mechanisms of long-term nAb responses might indeed require the study of Tfh-B cell interactions within germinal centers, as well as the interplay between CD4⁺ T cells and long-lived plasma cells within the bone marrow.

Our results are contrary to those of a preclinical study of Monath *et al.*, in which a single injection of the IN vaccine was sufficient to induce nAb titers in a range similar to that of the ST vaccine [27]. This, however, may be related to differences in experimental design, because in our study, the IN vaccine doses were injected via the subcutaneous route to correspond to ST immunization, whereas Monath *et al.* used the intramuscular route. This could be related to the

colonization of targeted tissues by innate cells, especially antigen-presenting cells, as we demonstrated in previous studies that the route of injection influences the quality of humoral responses [28], [29]. Thus, it is possible that certain properties of live attenuated vaccines could favor nAb induction via the subcutaneous route relative to other routes and, thus, explain the differences between our study and that of Monath *et al.* Innate immunity could also support humoral responses or contribute to Th cell plasticity through cytokine production. The characteristics of innate immunity need to be further studied to decipher the immune mechanisms that lead to the induction of nAbs and their persistence.

In conclusion, system vaccinology approaches to study the YF vaccine mostly identified gene signatures that correlate with and predict the magnitude of nAb and CD8⁺ T-cell responses. Thus, our analysis could take advantage of computational analysis to strengthen our observations and identify YF CD4⁺ T-cell signatures and biomarkers that could be correlated with and predict long-term neutralizing responses in the blood.

Materials and Methods

Ethics and biosafety statement

Cynomolgus macaques (*Macaca fascicularis*) originating from Mauritius and imported from AAALAC certified breeding centers were used in this study. All animals were housed in groups at the IDMIT infrastructure facilities (CEA, Fontenay-aux-Roses, animal facility authorization #D92-032-02, Prefecture des Hauts de Seine, France) and in compliance with European Directive 2010/63/EU, French regulations, and the Standards for Humane Care and Use of Laboratory Animals, of the Office for Laboratory Animal Welfare (OLAW, assurance number #A5826-01, US). The protocols were approved by the institutional ethics committee “Comité d’Ethique en Expérimentation Animale du Commissariat à l’Energie Atomique et aux Energies Alternatives » (CEtEA #44) and authorized by the “Research, Innovation and Education Ministry” under registration number APAFIS#24620-2020031115133688 v1.

Animals and study design

Eighteen adult female cynomolgus macaques, aged 54 to 57 months, were randomly assigned to two experimental groups of nine animals each. One group of animals was immunized one time with the Stamaril® vaccine and animals from the second group were immunized with the inactivated YF vaccine using a prime-boost strategy, with the injections 28 days apart. As the Stamaril® vaccine requires only a single injection, immunization and

sampling were synchronized with the boost of the inactivated vaccine. The blood responses for all animals were studied. To investigate the mechanisms that drive long-term persistence of YF immune memory, three animals from each group were also used to characterize the YF-specific immune responses in secondary lymphoid organs involved with the induction and persistence of memory: lymph nodes and bone marrow. Only three animals were used from each group due to the potential impact of such sampling procedures on the immune response. To increase the number of draining lymph nodes, the vaccine doses were split in half between the right and left inguinal area. The other animals were immunized with the full dose of each vaccine in the inguinal area.

Animals were observed daily and clinical exams were performed at baseline and at each bleeding, as described in Fig. 1, on anesthetized animals using ketamine (5 mg.kg⁻¹) and medetomidine (0.042 mg.kg⁻¹). Body weight and rectal temperature were recorded and blood was collected. Blood cell counts, hemoglobin levels, and the hematocrit were determined from EDTA blood using a HMX A/L analyzer (Beckman Coulter).

Immunization

The live, attenuated YF-17D-204 reference vaccine (Stamaril® batch #R3P101V Sanofi) was provided as a powder and diluent (0.4% sodium chloride) for reconstitution immediately before use in 0.5 mL dose volumes containing at least 1000 IU.

The inactivated vaccine was produced by one amplification of the Stamaril® batch on Vero cells at a multiplicity of infection of 0.01. The virus-containing supernatant was purified and concentrated using a Capto™core 700 (Cytiva) column. The virus was then inactivated for 16 h at 4°C following a 1:1000 dilution in beta-propiolactone (BPL) (Sigma) before heat-inactivation of the BPL by incubation for 2 h at 37°C. The inactivated whole virions were extemporaneously formulated in 0.2% alum hydroxide (Sanofi).

In vivo 5-Iodo-2'-deoxyuridine treatment

IdU (MP Biomedicals™, catalog N°11473040) was prepared at 7 mg/ml in PBS with 0.007 M NaOH and filter sterilized prior to intravenous inoculation at 60 mg/kg. Cynomolgus macaques received daily IdU injections between day 3 and day 6 post-immunization for the Stamaril® group or post-prime for the inactivated group. IdU is a thymidine analogue that is incorporated into the replicating DNA of dividing cells and can thus be detected in these cells or their progeny by mass cytometry[30] or immunohistochemistry[31].

Neutralization assay

YF-17D nAbs in the serum were titrated on VERO cells using the µPRNT50 method as previously described.[32] Briefly, the heat-inactivated sera were serially diluted two-fold in IMDM (4% FCS) starting from a 1:10 dilution. YF-17D Stamaril® virus grown on Vero cells was diluted to obtain 4000 µPFU/mL in IMDM and incubated for 90 min with two-fold diluted serum samples (v/v). The virus/serum mixture was then added to confluent Vero cells in 96-well plates (35,000 cells/well) and incubated for 45 ± 2 h at 37 ± 3°C. After incubation, the cells were fixed with 85% acetone before immunostaining. Plates were blocked with PBS (containing 0.05% Tween 20 and 2.5% skim milk) and incubated first with the anti-flavivirus monoclonal antibody 4G2 and then with a goat anti-mouse IgG HRP conjugate. Plates were stained using Trueblue™ chromogen. Plaques were counted using a Viruscope reader (Microvision™) or Cytation 7 device (Biotek™).

The final titer was calculated using the least squares method and corresponded to the reciprocal of the dilution demonstrating neutralization of 50% of the plaques. The LOD of the µPRNT50 assay was approximately 20 when the first dilution of serum tested was 1:10. For calculation of the mean value per group, an arbitrary value of half of the LOD was assigned to all samples below the LOD, i.e., 10.

Plasma cytokine analysis

Cytokines were quantified in EDTA-treated plasma using the NHP ProcartaPlex immunoassay for CCL-2 (also known as MCP-1), CCL4 (MIP-1b), sCD137, G-CSF, GM-CSF, Granzyme A, Granzyme B, ITAC, IFN α 2, IFN γ , IL-1 β , IL-1RA, IL-2, IL-4, IL-5, IL-6, IL-7, IL-8, IL-10, IL-12p70, IL-15, IL-17A, IL-18, IL-21, IL-22, IL-23, IL-33, IP-10, MIG, MIP-1 α , MIP-3 α , Perforin, sCD40L, sFasL, TGF α , TNF α , and VEGF- α and a Bioplex 200 analyzer (Bio-Rad) according to the manufacturer's instructions.

Antibody coupling with lanthanide isotopes

Four hundred micrograms of each antibody was conjugated to the metals using MaxPar X8 conjugation kits (Fluidigm) following the manufacturer's instructions. Briefly, lanthanides were loaded onto the polymer and then purified by centrifugation through an AMICON 3-kDa filter (Merck Millipore). A Maxpar MCP9 Antibody labeling kit was used for antibodies coupled with cadmium isotopes. Antibodies were also purified using an AMICON 50-kDa filter and partially reduced by TCEP-R-Buffer before conjugation to the metal-loaded polymers[33]. Cd-conjugated antibodies were purified using an AMICON 100-kDa filter. Following conjugation, antibodies were resuspended at 1 µg/µL in Candor PBS Antibody Stabilization

solution (Candor Bioscience) with 0.05% sodium azide and stored at 4°C. All conjugated monoclonal Abs used for labeling are shown in [Table S1](#).

Staining and CyTOF acquisition

PBMCs were isolated from NHP whole blood collected in heparin/lithium tubes by density gradient purification before being specifically stimulated overnight. Cells were then washed in cell-staining media (CSM, Fluidigm) and resuspended in CSM and incubated for 15 min at 37°C with 1 µL Intercalator-Rh (DVS Sciences). After washing in CSM, cells were extracellularly stained for 30 min at 4°C, washed with CSM and fixed with PBS-1.6% PFA. Cells were washed with Barcode Perm Buffer (DVS) before barcoding with a unique combination of three palladium isotopes (Fluidigm) according to the manufacturer's recommendations. Cells were then fixed with PBS-1.6% PFA and barcoded samples were pooled in one tube. After washes in 1X Permeabilization Buffer (eBiosciences), intracellular staining was performed for 30 min at 4°C. Cells were then washed with PBS and resuspended in PBS-1.6% PFA containing DNA Intercalator-Ir (DVS Sciences) and stored overnight at 4°C. Before acquisition, cells were washed with milli-Q water and filtered through a cap filter with 35-µm pores (BD Biosciences). Normalization beads (Eq Beads, Fluidigm) were added to the tube and the acquisition was performed using a Helios mass cytometer (Fluidigm).

Cell stimulation

For specific in-vitro cell stimulation, freshly isolated PBMCs from each animal were divided into non-stimulated and YFV-stimulated groups. Cytostim (Miltenyi), at a final concentration of 20 µL/mL, was used as a stimulation control. For each condition, 3×10^6 cells were used per well in a 96-well plate. Specific cell stimulation was performed with an overnight co-culture of highly purified YF virus (Sanofi Pasteur) at 5×10^8 PFU/mL. Brefeldin A at 10 µg/mL final concentration was added after 4 h to block cytokine secretion.

Data processing

CyTOF software (Fluidigm) was used on FCS files to compensate for signal loss by the detector during acquisition based on the signal given by the Eq Beads. Normalized data from each acquisition were concatenated (Cytobank concatenation tool) when required and all conditions were separated according to their barcode signal using CyTOF software. In addition, we used the same sample for each experiment to control for the quality of each staining/acquisition, and thus its reproducibility, as previously described[34]. Data cleaning was performed using OMIQ software to exclude ion cloud doublets, acquisition artefacts, Eq

beads, cell doublets, and dead cells from the resulting FCS files, as well as lineage-positive cells (CD20, CD14, CD66, CD34, and CD163).

Identification of cell populations

The spanning-tree progression analyses of the density-normalized events algorithm (SPADE)[35] was used on the non-stimulated data set of macaque samples to cluster cell populations displaying similar phenotypes. The following markers were used for clustering: HLA-DR, CD8, CD69, CD3, CD4, CD27, CD45, ICOS, CD127, PD1, CD45RA, CD45RO, CD62L, CD25, CXCR4, CD40L, FoxP3, Bcl-6, CD38, CD95, Ki-67, CCR7, CD107a, CXCR5, OX40, and CXCR3. Random pre-downsampling of 15,574 cells (corresponding to the number of cells contained in the smallest sample) was performed on all samples to allow for an equal contribution of each sample to create the cell-cluster tree. All cells from every sample were then assigned to a cluster according to their phenotype. The SPADEVizR R package[36] was used to perform the extended data analysis.

A heatmap representation of the clusters was generated using SPADEVizR according to the mean median MSI of each sample, in which they were divided into five categories between the 5th and 95th percentile. For each cluster, samples contributing < 10 cells were excluded. Hierarchical clustering of cell clusters and markers was performed using the Euclidean metric based on the ward.D linkage.

We created phenotypic families, which grouped cell clusters that displayed similar phenotypes. This strategy avoids “over-clustering”, as clusters may account for diverse activation or maturation stages, and favors the identification of actual subpopulations by their phenotypic characteristics.

Differentially abundant clusters, relative to baseline or between vaccines, based on absolute abundances were generated using a Student paired t-test. For time points for which data were not available, a Student unpaired t-test was performed.

A t-distributed stochastic neighbor embedding analysis (tSNE) was used to identify YF-specific CD4⁺ T-cell functions upon stimulation. Only YF-activated CD40L⁺ CD4⁺ T cells were included in this analysis. The following markers were used for the analysis: CD107a, IFN γ , IL-2, IL-4, IL-10, IL-13, IL-17a, IL-21, TGF β , and TNF α . Activated cytokine producing (ACP) cells were manually gated according to cytokine expression. Comparisons of activated cell populations between stimulation condition and between vaccines were performed using Mann-Whitney tests.

Bibliography

- [1] C. M. C. Rodrigues and S. A. Plotkin, ‘Impact of Vaccines; Health, Economic and Social Perspectives’, *Front Microbiol*, vol. 11, p. 1526, Jul. 2020, doi: 10.3389/FMICB.2020.01526/XML/NLM.
- [2] R. Rappuoli, M. Pizza, G. del Giudice, and E. de Gregorio, ‘Vaccines, new opportunities for a new society’, *Proceedings of the National Academy of Sciences*, vol. 111, no. 34, pp. 12288–12293, Aug. 2014, doi: 10.1073/PNAS.1402981111.
- [3] G. Gorini *et al.*, ‘Engagement of monocytes, NK cells, and CD4+ Th1 cells by ALVAC-SIV vaccination results in a decreased risk of SIVmac251 vaginal acquisition’, *PLoS Pathog*, vol. 16, no. 3, 2020, doi: 10.1371/JOURNAL.PPAT.1008377.
- [4] G. Galli *et al.*, ‘Adjuvanted H5N1 vaccine induces early CD4+ T cell response that predicts long-term persistence of protective antibody levels’, *Proc Natl Acad Sci U S A*, vol. 106, no. 10, pp. 3877–3882, Mar. 2009, doi: 10.1073/PNAS.0813390106.
- [5] G. Elias *et al.*, ‘Preexisting memory CD4 T cells in naïve individuals confer robust immunity upon hepatitis B vaccination’, *Elife*, vol. 11, Jan. 2022, doi: 10.7554/ELIFE.68388.
- [6] S. L. Campion *et al.*, ‘Preexisting memory CD4+ T cells contribute to the primary response in an HIV-1 vaccine trial’, *J Clin Invest*, vol. 131, no. 23, Dec. 2021, doi: 10.1172/JCI150823.
- [7] E. Hammarlund, M. W. Lewis, J. M. Hanifin, M. Mori, C. W. Koudelka, and M. K. Slifka, ‘Antiviral Immunity following Smallpox Virus Infection: a Case-Control Study’, *J Virol*, vol. 84, no. 24, pp. 12754–12760, Dec. 2010, doi: 10.1128/JVI.01763-10/ASSET/D0463550-9784-4717-8FE1-1E1602DEAC93/ASSETS/GRAFIC/ZJV9990939810003.JPG.
- [8] B. Combadiere *et al.*, ‘Distinct Time Effects of Vaccination on Long-Term Proliferative and IFN- γ -producing T Cell Memory to Smallpox in Humans’, *J Exp Med*, vol. 199, no. 11, p. 1585, Jun. 2004, doi: 10.1084/JEM.20032083.
- [9] N. P. Lindsey *et al.*, ‘Persistence of yellow fever virus-specific neutralizing antibodies after vaccination among US travellers’, *J Travel Med*, vol. 25, no. 1, pp. 1–6, Jan. 2018, doi: 10.1093/JTM/TAY108.
- [10] J. Hou *et al.*, ‘A Systems Vaccinology Approach Reveals Temporal Transcriptomic Changes of Immune Responses to the Yellow Fever 17D Vaccine’, *The Journal of Immunology*, vol. 199, no. 4, pp. 1476–1489, Aug. 2017, doi: 10.4049/jimmunol.1700083.
- [11] T. P. Monath *et al.*, ‘An inactivated cell-culture vaccine against yellow fever’, *New England Journal of Medicine*, vol. 364, no. 14, pp. 1326–1333, Apr. 2011, doi: 10.1056/NEJMoa1009303.
- [12] E. A. James, R. E. LaFond, T. J. Gates, D. T. Mai, U. Malhotra, and W. W. Kwok, ‘Yellow Fever Vaccination Elicits Broad Functional CD4 + T Cell Responses That Recognize Structural and Nonstructural Proteins’, *J Virol*, vol. 87, no. 23, pp. 12794–12804, Dec. 2013, doi: 10.1128/jvi.01160-13.
- [13] T. Querec *et al.*, ‘Yellow fever vaccine YF-17D activates multiple dendritic cell subsets via TLR2, 7, 8, and 9 to stimulate polyvalent immunity’, *J Exp Med*, vol. 203, no. 2, pp. 413–424, Feb. 2006, doi: 10.1084/JEM.20051720.
- [14] M. Tsuji *et al.*, ‘Preferential generation of follicular B helper T cells from Foxp3+ T cells in gut Peyer’s patches’, *Science*, vol. 323, no. 5920, pp. 1488–1492, Mar. 2009, doi: 10.1126/SCIENCE.1169152.
- [15] K. Hirota *et al.*, ‘TH17 cell plasticity in Peyer’s patches is responsible for induction of T cell-dependent IgA responses’, *Nat Immunol*, vol. 14, no. 4, p. 372, Apr. 2013, doi: 10.1038/NI.2552.
- [16] W. Liao, Z. Hua, C. Liu, L. Lin, R. Chen, and B. Hou, ‘Characterization of T-Dependent and T-Independent B Cell Responses to a Virus-like Particle’, *The Journal of Immunology*, vol. 198, no. 10, pp. 3846–3856, May 2017, doi: 10.4049/JIMMUNOL.1601852/-/DCSUPPLEMENTAL.
- [17] A. R. Khaled *et al.*, ‘Bax deficiency partially corrects interleukin-7 receptor alpha deficiency’, *Immunity*, vol. 17, no. 5, pp. 561–573, Nov. 2002, doi: 10.1016/S1074-7613(02)00450-8.
- [18] R. M. Kondrack, J. Harbertson, J. T. Tan, M. E. McBreen, C. D. Surh, and L. M. Bradley, ‘Interleukin 7 Regulates the Survival and Generation of Memory CD4 Cells’, *Journal of Experimental Medicine*, vol. 198, no. 12, pp. 1797–1806, Dec. 2003, doi: 10.1084/JEM.20030735.
- [19] S. M. Kaech, J. T. Tan, E. J. Wherry, B. T. Konieczny, C. D. Surh, and R. Ahmed, ‘Selective expression of the interleukin 7 receptor identifies effector CD8 T cells that give rise to long-lived memory cells’, *Nat Immunol*, vol. 4, no. 12, pp. 1191–1198, Dec. 2003, doi: 10.1038/NI1009.
- [20] K. K. McKinstry *et al.*, ‘Effector CD4 T-cell transition to memory requires late cognate interactions that induce autocrine IL-2’, *Nature Communications 2014 5:1*, vol. 5, no. 1, pp. 1–12, Nov. 2014, doi: 10.1038/ncomms6377.
- [21] J. He *et al.*, ‘Circulating precursor CCR7(lo)PD-1(hi) CXCR5⁺ CD4⁺ T cells indicate Tfh cell activity and promote antibody responses upon antigen reexposure’, *Immunity*, vol. 39, no. 4, pp. 770–781, Oct. 2013, doi: 10.1016/J.IMMUNI.2013.09.007.

- [22] H. Li and C. D. Pauza, ‘CD25(+) Bcl6(low) T follicular helper cells provide help to maturing B cells in germinal centers of human tonsil’, *Eur J Immunol*, vol. 45, no. 1, pp. 298–308, Jan. 2015, doi: 10.1002/EJI.201444911.
- [23] K. Tokoyoda *et al.*, ‘Professional memory CD4+ T lymphocytes preferentially reside and rest in the bone marrow’, *Immunity*, vol. 30, no. 5, pp. 721–730, May 2009, doi: 10.1016/j.immuni.2009.03.015.
- [24] A. Okhrimenko *et al.*, ‘Human memory T cells from the bone marrow are resting and maintain long-lasting systemic memory’, *Proc Natl Acad Sci U S A*, vol. 111, no. 25, pp. 9229–9234, Jun. 2014, doi: 10.1073/PNAS.1318731111/-/DCSUPPLEMENTAL.
- [25] M. K. Slifka, M. Matloubian, and R. Ahmed, ‘Bone marrow is a major site of long-term antibody production after acute viral infection.’, *J Virol*, vol. 69, no. 3, p. 1895, Mar. 1995, doi: 10.1128/JVI.69.3.1895-1902.1995.
- [26] S. M. Lightman, A. Utley, and K. P. Lee, ‘Survival of Long-Lived Plasma Cells (LLPC): Piecing Together the Puzzle’, *Front Immunol*, vol. 10, no. MAY, 2019, doi: 10.3389/FIMMU.2019.00965.
- [27] T. P. Monath *et al.*, ‘Inactivated yellow fever 17D vaccine: Development and nonclinical safety, immunogenicity and protective activity’, *Vaccine*, vol. 28, no. 22, pp. 3827–3840, May 2010, doi: 10.1016/j.vaccine.2010.03.023.
- [28] P. Rosenbaum *et al.*, ‘Vaccine Inoculation Route Modulates Early Immunity and Consequently Antigen-Specific Immune Response’, *SSRN Electronic Journal*, Feb. 2020, doi: 10.2139/ssrn.3535877.
- [29] M. van Tilbeurgh *et al.*, ‘Innate cell markers that predict anti-HIV neutralizing antibody titers in vaccinated macaques’, *Cell Rep Med*, vol. 0, no. 0, p. 100751, Sep. 2022, doi: 10.1016/J.XCRM.2022.100751.
- [30] A. Erez, R. Mukherjee, and G. Altan-Bonnet, ‘Quantifying the Dynamics of Hematopoiesis by In Vivo IdU Pulse-Chase, Mass Cytometry, and Mathematical Modeling’, *Cytometry A*, vol. 95, no. 10, pp. 1075–1084, Oct. 2019, doi: 10.1002/CYTO.A.23799.
- [31] A. H. Tuttle *et al.*, ‘Immunofluorescent Detection of Two Thymidine Analogs (Cl^dU and IdU) in Primary Tissue’, *JoVE (Journal of Visualized Experiments)*, vol. 46, no. 46, p. e2166, Dec. 2010, doi: 10.3791/2166.
- [32] F. Piras-Douce *et al.*, ‘Next generation live-attenuated yellow fever vaccine candidate: Safety and immuno-efficacy in small animal models’, *Vaccine*, vol. 39, no. 13, pp. 1846–1856, Mar. 2021, doi: 10.1016/J.VACCINE.2021.02.033.
- [33] G. Han, M. H. Spitzer, S. C. Bendall, W. J. Fantl, and G. P. Nolan, ‘Metal-isotope-tagged monoclonal antibodies for high-dimensional mass cytometry’, *Nat Protoc*, vol. 13, no. 10, pp. 2121–2148, Oct. 2018, doi: 10.1038/s41596-018-0016-7.
- [34] K. Kleinstreuer *et al.*, ‘Standardization and quality control for high-dimensional mass cytometry studies of human samples’, *Cytometry A*, vol. 89, no. 10, pp. 903–913, Oct. 2016, doi: 10.1002/CYTO.A.22935.
- [35] P. Qiu *et al.*, ‘Extracting a cellular hierarchy from high-dimensional cytometry data with SPADE’, *Nat Biotechnol*, vol. 29, no. 10, pp. 886–891, Oct. 2011, doi: 10.1038/nbt.1991.
- [36] G. Gautreau, D. Pejoski, R. le Grand, A. Cosma, A. S. Beignon, and N. Tchitchek, ‘SPADEVizR: An R package for visualization, analysis and integration of SPADE results’, *Bioinformatics*, 2017, doi: 10.1093/bioinformatics/btw708.

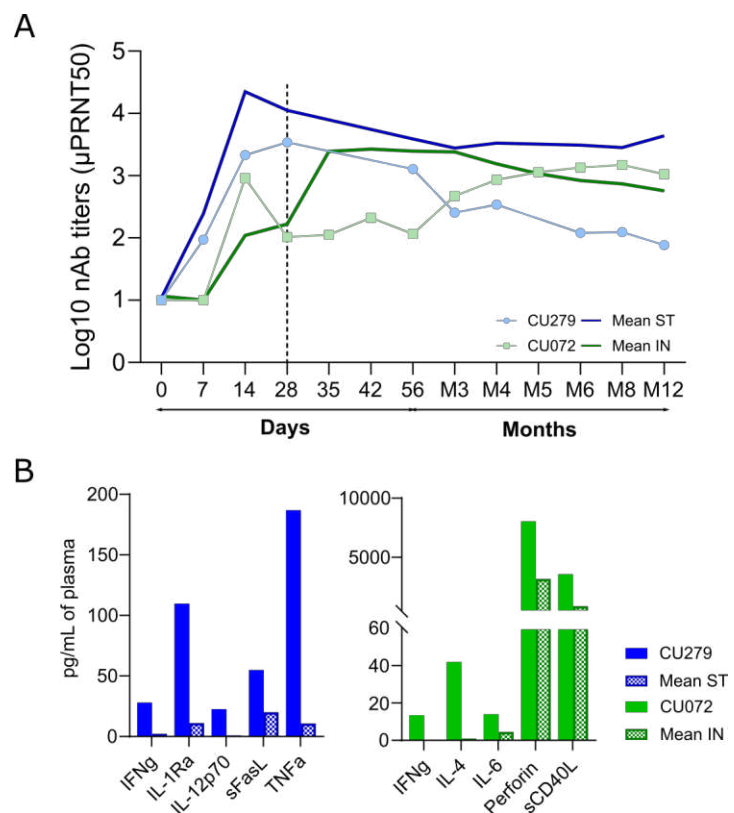


Figure S3: Distinct neutralizing antibody kinetics for outlier animals. (A): Neutralizing antibody response in serum of macaques after vaccine injection. Log10 of neutralizing titers for animals identified as outliers within Stamaril and Inactivated vaccines. Log of geometric mean titers without outliers for both vaccine group are shown. (B): Pre-existent cytokines level of outlier animals at baseline. In both panel, ST vaccine is in blue and IN vaccine is in green.

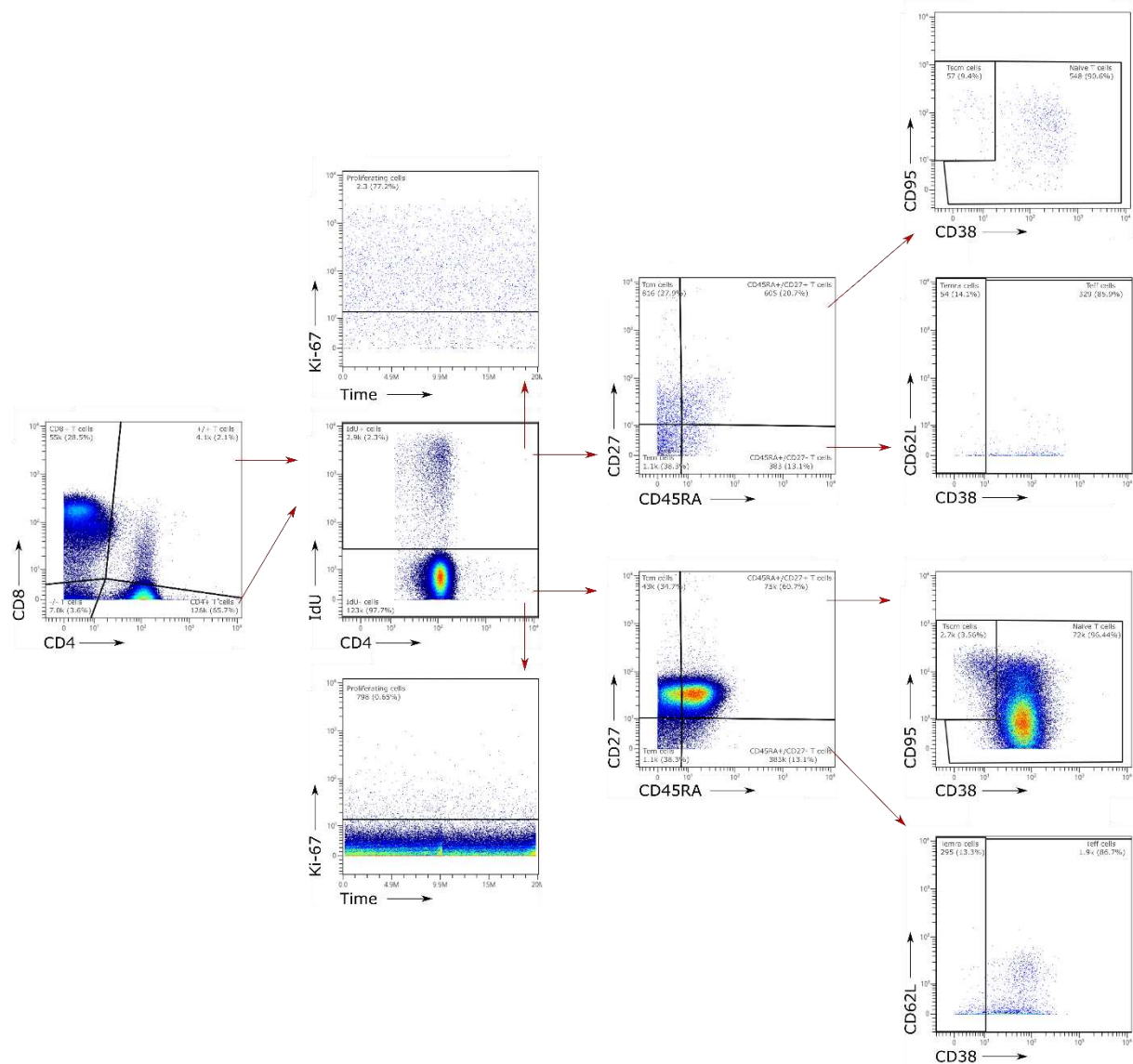


Figure S2: Mass-cytometry gating strategy for defining effector/memory IdU+ CD4+ T cells. IdU+ effector/memory CD4+ T cells were defined from day 7 post-immunization PBMC, as this time point had the strongest signal for IdU. Ion cloud doublets, EQ-Beads, cell doublets, dead cells, CD45⁻ cells and lineage⁺ cells (CD20⁺ CD14⁺ CD66⁺ CD34⁺ and CD163⁺) were dumped, before naïve (CD45RA⁺ CD27⁺ CD38⁺ CD95⁻), central memory (Tcm: CD45RA⁻ CD27⁺), stem cell memory (Tscm: CD45RA⁺ CD27⁺ CD38⁻ CD95⁺), effector cell (Teff: CD45RA⁺ CD27⁻ CD38⁺), effector memory (Tem: CD45RA⁻ CD27⁻) and terminally effector cells (Temra: CD45RA⁺ CD27⁻ CD38⁻) were defined.

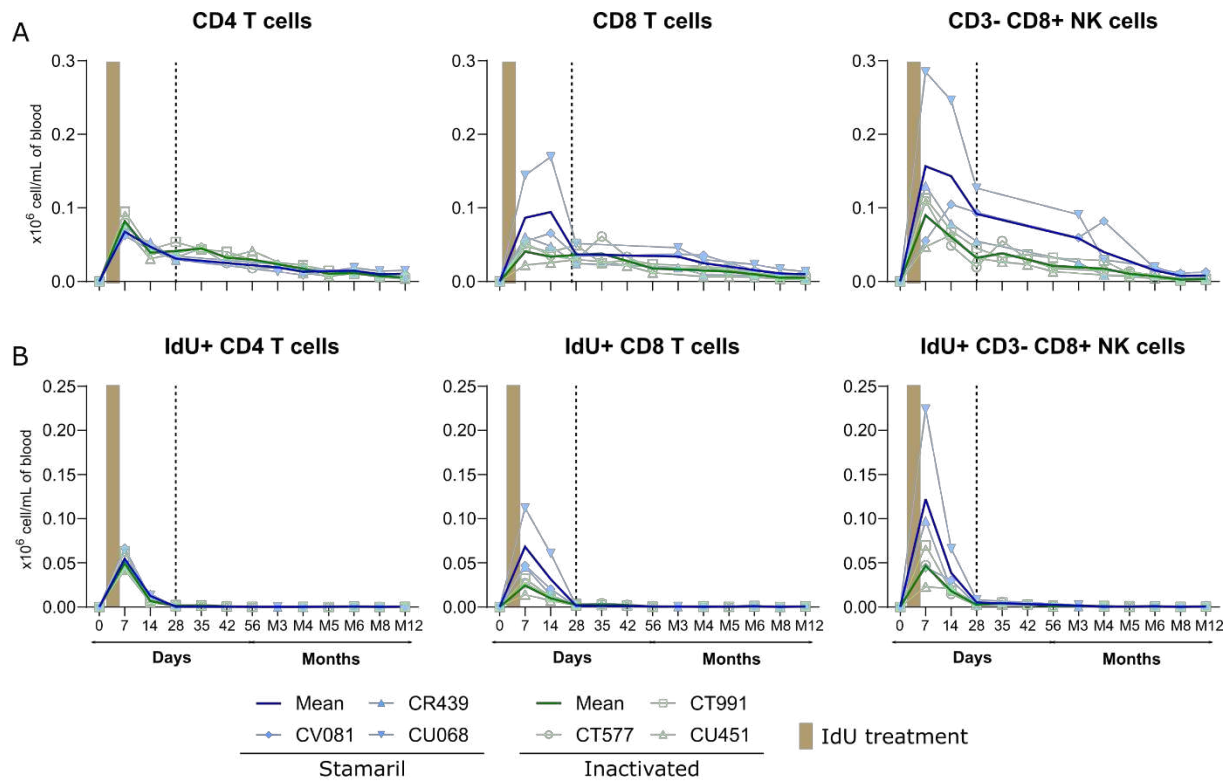


Figure S3: Follow up of YF-vaccine induced cell mobilization by in vivo IdU treatment (n=3). (A): Absolute number of IdU+ cells among main lymphoid cell population. (B): Absolute number of proliferating IdU+ cells among main lymphoid cell population identified with the expression of Ki-67. IdU treatment period has been shown in yellow on graphs and the IN-boost is indicated by dot lines. Gating strategy to identify memory cell subsets are displayed in Fig S2.

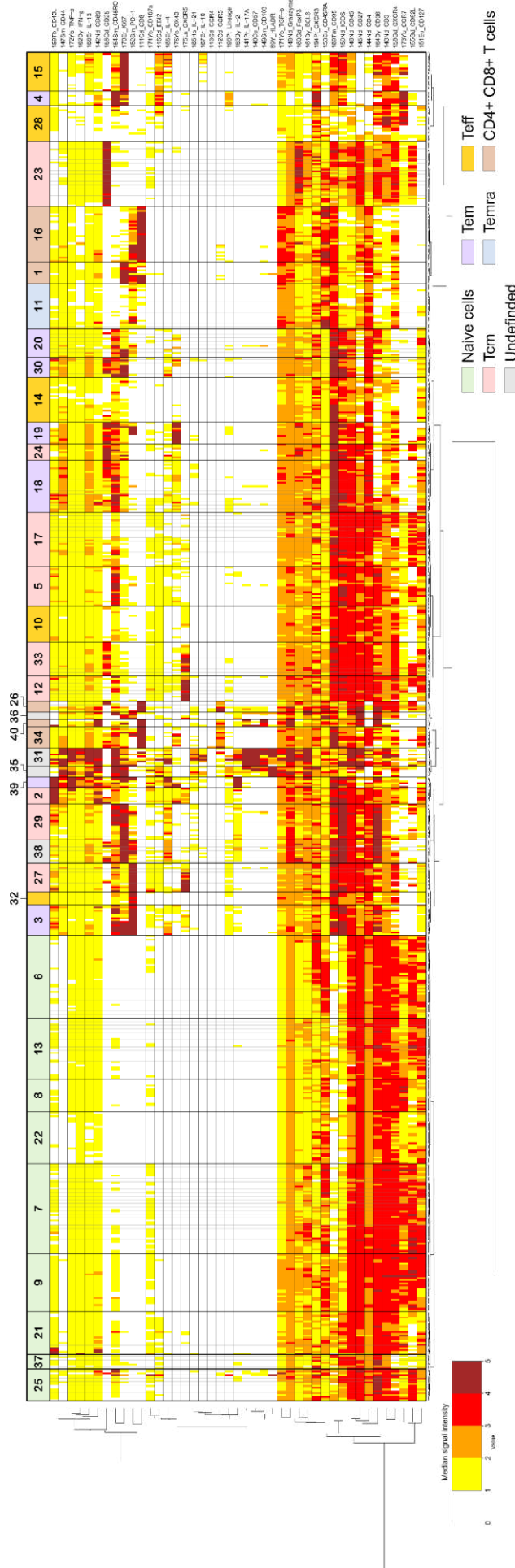
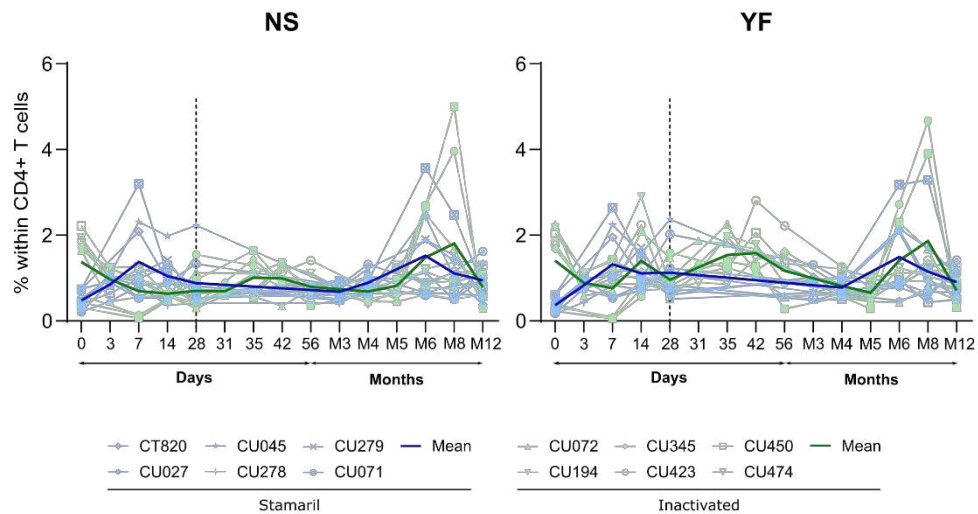


Figure S4: SPADE hierarchical clustering showing the phenotypic diversity of the CD4+ T cell compartment. The forty phenotypic families were manually annotated and defined by the gathering of cell clusters displaying similar phenotype. Expression pattern proximity are shown by the cluster dendrogram. Marker expression is shown in columns and cell clusters in rows. Markers used by SPADE unsupervised analysis for the clustering are written in bold. Effector/memory phenotypic families were identified in color.

A



B

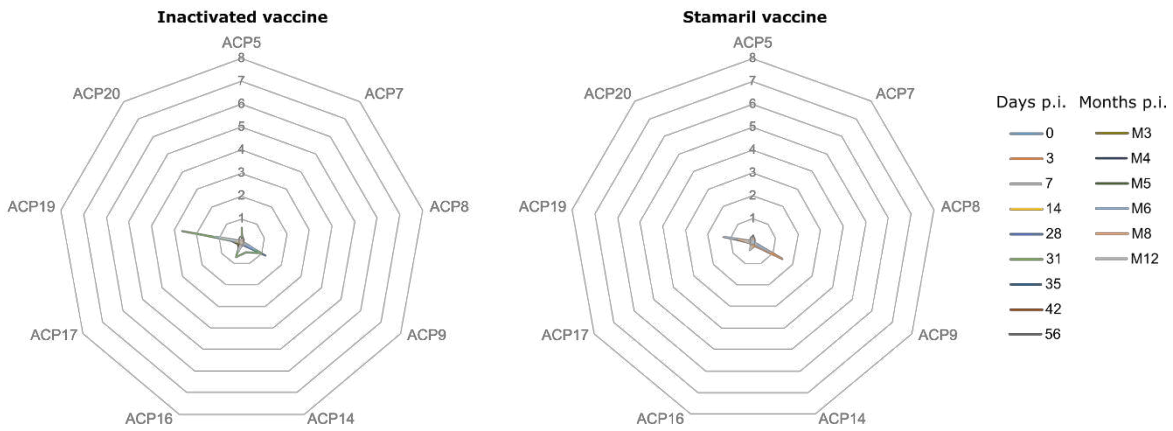


Figure S5: YF vaccines induce specific cell activation and functionality. (A): Abundances of activated CD40L+ cells among CD4 T cell depending on purified YF virus (YF) *in vitro* stimulation and non-stimulated condition (NS). (B): Mean relative abundances of the top nine ACP (% of CD40L+ CD4 T cells) displayed in Fig.6 without *in vitro* stimulation. Timepoint are indicated in colored lines.

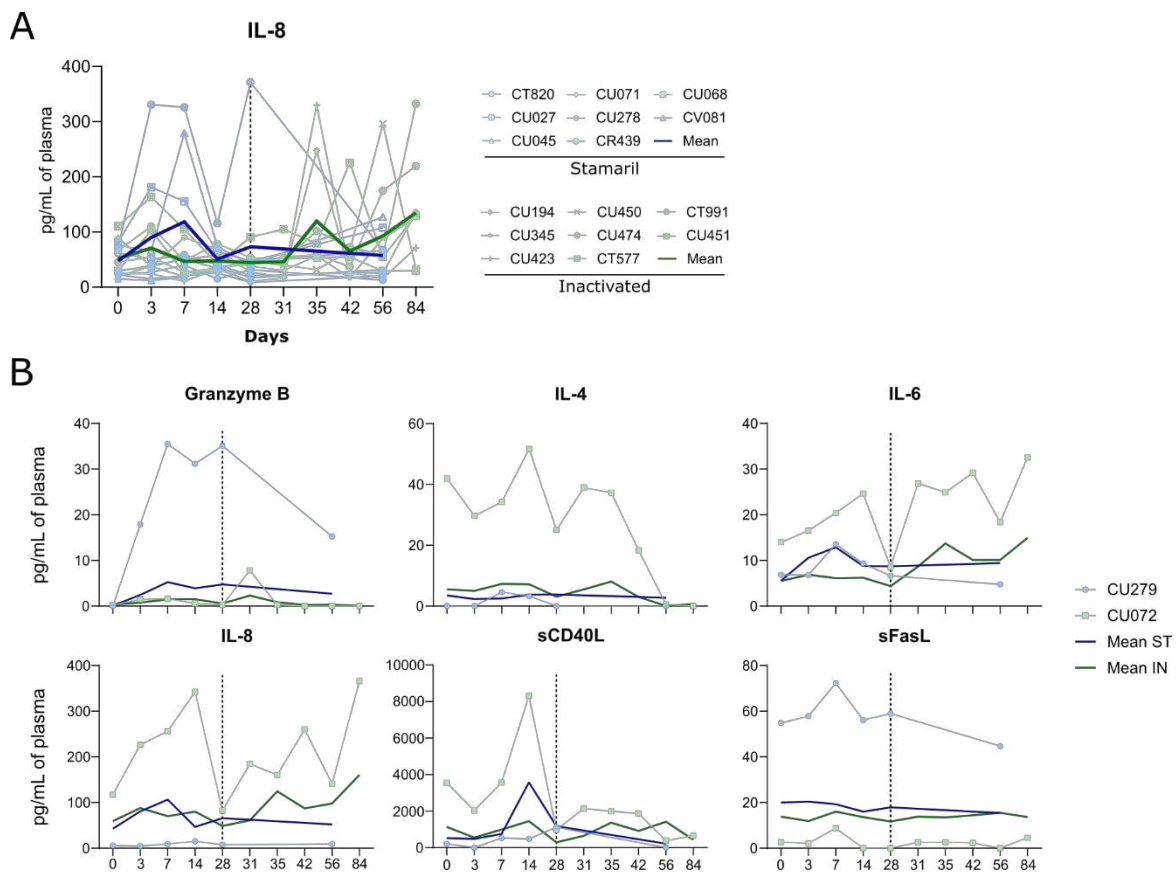


Figure S6: Soluble factors response in plasma after Yellow fever vaccine injection. Individual kinetics of IL-18 ($n = 8$) from animals immunized with Stamaril or inactivated Stamaril are displayed in blue and green, respectively. IL-18 mean concentration is displayed by a bold line, colored for each group (A). (B): Comparison of the IFNa2, IL-1Ra and IL-6 response induce by Stamaril, or inactivated Stamaril prime or boost over time for outlier animals, compared to the geometric mean titers for each group without outliers. Dotted line indicates the time of boost for the inactivated Stamaril group.

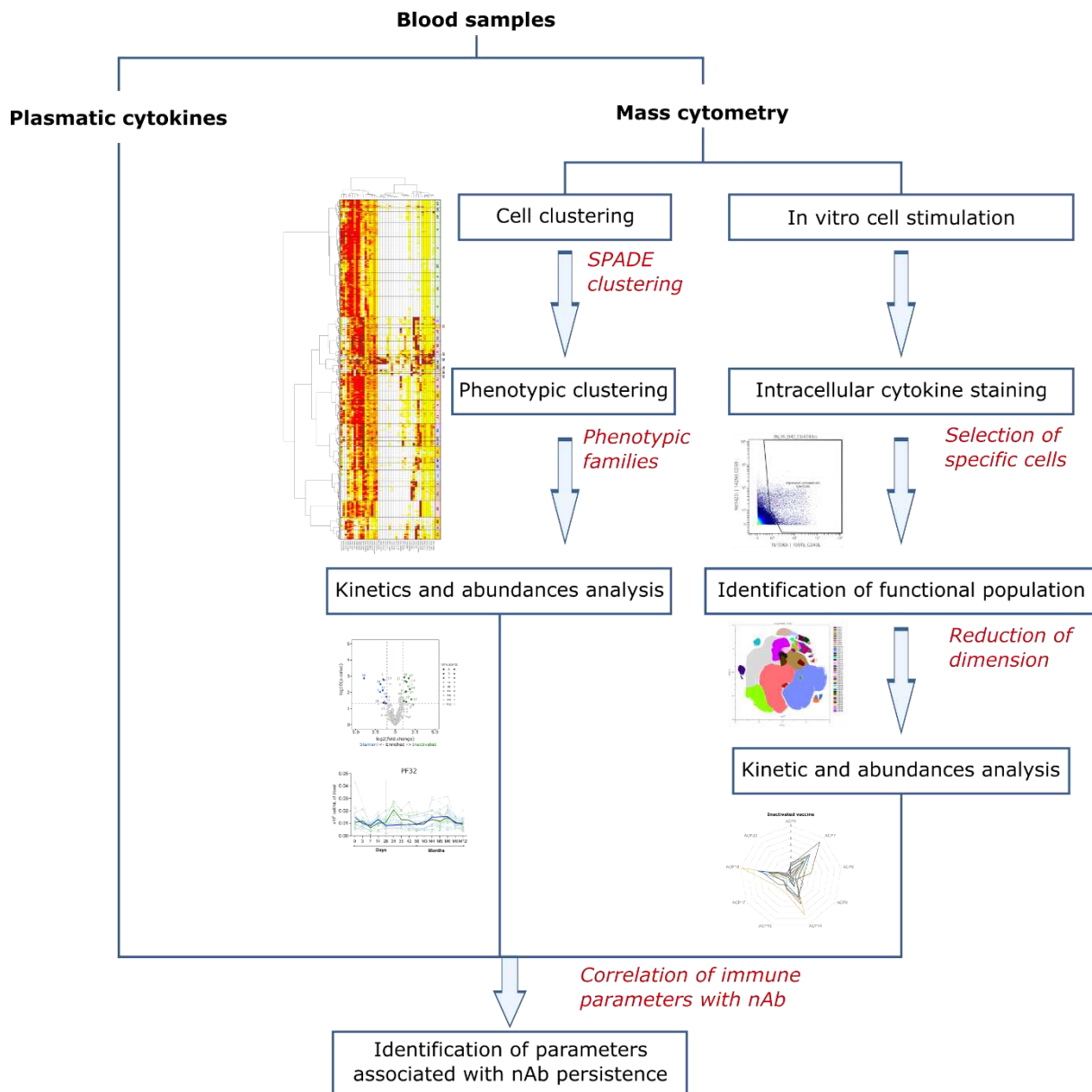


Figure S7: Blood sample analysis pipeline. Plasma cytokines and mass cytometry were used to characterize immune responses elicited to YF immunization. Non-supervised analysis of mass cytometry data was performed ex vivo using SPADE to assess phenotypic diversity and kinetics, or were stimulated *in vitro* to assess the functionality of YF-specific CD4+ T cell responses. All immune parameters were included in computational analysis, to correlate nAb production with biomarkers of nAb persistence.

Table S1: Antibody marker panel used for mass-cytometry deep phenotyping. Metal tags and antibody clone associations are shown. Intracellular markers are in bold.

Metal	Antibody	Clone
89Y	HLA-DR	L243
111Cd	CD8	RPAT8
112Cd	CCR5 (CD195)	3A9
113Cd	CCR4	1G1
116Cd	EBI2	SA313E4
140Ce	CD57	HNKI
141Pr	IL-17A	eBio64DEC17
142Nd	CD69	FN50
143Nd	CD3	SP34.2
144Nd	CD4	L200
145Nd	CD27	M-T271
146Nd	CD45	D058-1283
147Sm	CD44	IM7
148Nd	Granzyme B	GB11/REA226
149Sm	CD103	Ber-ACT8
150Nd	ICOS (CD278)	C398.4A
151Eu	CD127 (IL-7Ra)	MB1518C9
152Sm	PD1 (CD279)	EH12.2H7
153Eu	CD45RA	5H9
154Sm	CD45RO	UCHL1
155Gd	CD62L	SK11
156Gd	CD25	4 e3
158Gd	CXCR4 (CD184)	12G5
159Tb	CD40L (CD154)	TRAP1
160Gd	FoxP3	206D
161Dy	Bcl-6	K112-91
162Dy	IFNg	B27
163Dy	IL-2	MQ1-17H12
164Dy	CD38	AT1
165Ho	IL-21	3A3-N2
166Er	IL-4	7A3-3
167Er	IL-10	JES3-9D7
168Er	IL-13	JES10-5A2.2
169Tm	CD95	DX2
170Er	Ki-67	B56/REA183
171Yb	TGFb	TW4-6H10
172Yb	TNFa	MAb11
173Yb	CCR7 (CD197)	G043H7/REA546
174Yb	CD107a	H4A3
175Lu	CXCR5 (CD185)	MU5UBEE
176Yb	OX40 (CD134)	L106
194Pt	CXCR3 (CD183)	G025H7
198Pt	Lineage	

2) Analyses complémentaires

Dans cette première partie d'étude, nous avons décrit les différences observées suite à l'immunisation des macaques cynomolgus avec les vaccins contre la fièvre jaune Stamaril et inactivé. Nous avons commencé à utiliser le package R « SPADEVizR » pour exploiter les données générées par l'analyse SPADE. Similairement à la méthode que nous avons employé dans l'étude des voies d'injections et des adjuvants, l'objectif de cette étude vise à identifier des signatures et des biomarqueurs précoce de la réponse anticorps, plus particulièrement sa persistance.

La prochaine étape consiste maintenant à intégrer les données de cinétiques des populations LT CD4+ et LT CD4+ spécifiques ainsi que le dosage des cytokines plasmatiques au sein d'analyses complémentaires (PCA/LDA/LASSO). Ce type d'analyses pourrait nous permettre d'identifier des signatures vaccinales pour les deux vaccins fièvre jaune utilisé que nous pourrions par la suite corrélérer avec la réponse neutralisante afin d'en prédire la persistance de manière précoce.

Nous avons également pour objectif d'enquêter de manière plus approfondie sur le profil des animaux « outlier » afin de comprendre, préciser et/ou confirmer les différences précédemment observées entre les groupes vaccinaux.

Cette stratégie se base sur de précédentes analyses réalisées au sein du CEA mais nécessitera probablement de l'ajuster en fonction des différences dans le « design » expérimental.

D. DISCUSSION ET PERSPECTIVES

I. Limites expérimentales

1) Le modèle PNH

Le modèle des PNH a été largement exploité pour étudier et comprendre les réponses vaccinales contre le VIH ou la fièvre jaune dans le but de transposer les résultats chez l'Homme. Bien que les systèmes immunitaires humain et simien soient évolutivement, phénotypiquement et fonctionnellement très proche, y compris dans l'abondance et la distribution des différentes populations cellulaire, certaines limites existent et doivent être prises en compte dans la transposition des résultats.

Premièrement, la majorité des anticorps utilisés pour la caractérisation des cellules en cytométrie ont pour cible des épitopes humains. Malgré la proximité avec les PNH, certaines différences évolutives peuvent être la source d'une absence de réaction croisée entre les espèces. Deuxièmement, ces différences peuvent être la conséquence d'une affinité réduite des anticorps de détection pouvant altérer la sensibilité de détection. Troisièmement, l'expression d'un marqueur peut varier entre les espèces. En effet, il est possible qu'un marqueur ne soit pas exprimé par l'une des espèces ou qu'il n'identifie pas les mêmes populations cellulaires ([Elhmouzi-Younes et al., 2017](#)).

2) La cytométrie de masse

Le choix de la cytométrie de masse et du grand nombre de marqueurs observables qu'elle procure nous a permis, pour les deux études, d'effectuer une caractérisation poussée des différents phénotypes de cellules innées myéloïdes et des lymphocytes T CD4+. Nous avons notamment pu mettre en évidence la diversité de ces deux compartiments mais également d'appréhender leur grande plasticité en identifiant de nombreux phénotypes intermédiaires par rapport aux descriptions présentes dans la littérature.

Cependant, comme mentionné dans la section « Limites du modèle PNH », nous nous sommes confrontés à la difficulté de trouver des anticorps de détection cross-réactifs avec le macaque cynomolgus. Cette limite a restreint l'identification des différentes sous

populations au cours de ces études. En particulier, nous n'avons pas pu inclure de marqueurs phénotypiques nous permettant de caractériser les Th9 ou les Th22.

3) Marquage *in vivo* de la prolifération cellulaire induite par les vaccins

Au cours de l'étude de l'impact de la réponse T CD4+ sur la persistance de la réponse mémoire, nous avons démontré l'intérêt d'employer un analogue de la thymidine pour suivre la mobilisation et la prolifération cellulaire induite par la vaccination ainsi que la persistance à long terme de ces cellules. Cependant nous avons également observé une diminution rapide du nombre et de la proportion de cellules IdU+ dès l'arrêt du traitement. Nous savons que la majorité des cellules impliquées dans l'expansion clonale sera éliminée lors de la phase de contraction et que seule une faible proportion de cellules mémoires sera détectable dans la circulation périphérique. Cependant, nombre de cellules en prolifération lors de la réponse vaccinale (et du traitement) vont également migrer dans les tissus et y exercer leurs fonctions effectrices. Il serait donc intéressant d'enquêter plus en détails sur le devenir de ces cellules dans les tissus ainsi que leur persistance.

De plus, il est important de noter que l'IdU s'incorpore de manière non-spécifique au sein de toutes les cellules en prolifération. Nous sommes donc dans l'impossibilité d'identifier de manière précise la proportion des cellules spécifiques de la réponse vaccinale (que nous supposons être la plus abondante), de la prolifération dite « bystander » et de la prolifération homéostatique. Afin de réduire l'impact de la prolifération non spécifique, nous avons intégré le marqueur CD34 dans le panel pour permettre d'éliminer les progéniteurs précoces hautement prolifératifs des prélèvements de moelle osseuse.

Toutefois, nous manquons d'un groupe témoin d'incorporation pour lequel aucune immunisation ne serait effectuée qui pourrais nous permettre d'identifier la proportion de cellule impliquées dans la prolifération homéostatique dans les différents tissus. Pour compenser le manque d'informations sur la spécificité des cellules IdU+, il serait intéressant de combiner cette approche avec un tri cellulaire et le séquençage des TCR. De cette manière, en comparant les résultats avec les banques de données disponibles sur la fièvre jaune, nous pourrions établir un suivi précis des clones spécifiques et de leur

spécificité antigénique au cours du temps, particulièrement pour les points de temps tardifs.

Enfin, le faible nombre d'animaux ayant reçu le traitement IdU, bien que suffisant pour nous indiquer une tendance plus importante du Stamaril à mobiliser les T CD8 et les NK, ne nous a pas permis de réaliser des analyses statistiques.

4) Stimulation ex vivo avec le virus vaccinal vivant purifié

L'utilisation du virus purifié pour la stimulation spécifique des LT CD4+ pourrait être à l'origine des différences observées en induisant un biais de sélection. En effet, le temps de stimulation relativement court pourrait activer uniquement les clones spécifiques de l'enveloppe virale. Or le Stamaril est un vaccin vivant réplicatif permettant l'exposition d'antigènes dirigés contre les protéines non structurales. De plus, il a été rapporté que la protéine NS3 est un des antigènes majoritaires des réponses spécifiques ([James et al., 2013](#)). A la différence du vaccin inactivé où l'ensemble du répertoire des LT spécifiques est dirigé contre l'enveloppe virale, la stimulation des animaux du groupe Stamaril ne nous permettrait donc pas d'observer l'intégralité du compartiment spécifique. Il apparaît donc indispensable de caractériser la spécificité des cellules mobilisées par la stimulation afin de pouvoir identifier des signatures vaccinales précises impliquées dans la persistance de la réponse neutralisante.

II. Discussion des données observées

L'objectif de ces études a été d'identifier des biomarqueurs précoce de la qualité des réponses humorales induite par des vaccins VIH et YF. Pour cela nous avons développé une stratégie d'analyse non supervisée exploitant l'algorithme SPADE et le package R SPADEVizR ([Gautreau et al., 2017; Platon et al., 2018](#)) afin de:

- déterminer l'impact de différents adjuvants et voies d'injection sur la qualité de la réponse humorale en caractérisant les réponses innées suite à la vaccination VIH par des protéines SOSIP.

- Identifier des biomarqueurs de la persistance de la réponse neutralisantes en caractérisant la réponse T CD4+ dans le cas de la vaccination contre la fièvre jaune.

Dans l'étude des vaccins SOSIP, nous avons montré que la voie intramusculaire est plus efficace que la voie sous-cutanée pour induire des réponses anticorps. Ces résultats s'opposent à ceux précédemment obtenus par Pauthner *et al.* dans le cas d'un vaccin similaire ([Pauthner et al., 2017](#)). En effet, ils ont montré que contrairement à nous, la production d'anticorps neutralisants est plus importante lors d'une injection sous-cutanée comparée à une injection intramusculaire. Outre la différence de modèle PNH (Rhésus vs Cynomolgus) et les différences de version des protéines SOSIP, nos études diffèrent dans les adjuvants utilisés : ISCOMATRIX™ contre MPLA et SQ. Ces résultats soulignent probablement l'importance des adjuvants dans l'induction et la qualité des réponses immunitaires car ces derniers ne sont pas détectés par les même PRR. Dans notre cas, le MPLA, un agoniste de TLR4 induit l'activation des divers IRF via l'activation de la voie de signalisation TRIF alors que le SQ mobilise la signalisation ([Alving et al., 2012; Calabro et al., 2013; O'Hagan et al., 2012](#)). En conséquence, bien que nous ayons observé une réponse anticorps similaire entre les deux adjuvants, les mobilisations de cellules innées précoces suite aux injections diffèrent. Ainsi nous avons observés une plus grande proportion de monocytes et de DC CD11c+ CD16+ suite aux immunisations avec le MPLA comparé au SQ. Cette mobilisation de monocytes a par ailleurs déjà été observée dans le cas de l'utilisation du vaccin recombinant ALVAC-HIV dérivé du canari pox qui a permis une diminution du risque d'acquisition du SIV chez des PNH ([Andersen-Nissen et al., 2021; Gorini et al., 2020; Vaccari et al., 2018](#)).

De manière similaire aux adjuvants, la détection des Flavivirus implique une diversité de PRR conduisant à l'induction de nombreuses voies d'activation cellulaires ([S. Chen et al., 2017](#)). Il a notamment été observé par Querec et al. que la souche vaccinale YF-17D est capable d'activer de nombreuses sous populations de cellules dendritiques via la stimulation de TLR (TLR2, 7, 8 et 9) mais également des RLR cytoplasmique RIG-I et MDA5 aboutissant a de fortes réponses antivirales Th1 et T CD8+, tout comme dans nos observations ([T. Querec et al., 2006; T. D. Querec et al., 2009](#)). Les auteurs ont rapporté

qu'une déficience en Myd88 chez la souris, conduit à des réponses Th1 altérées, or Myd88 est associé à la signalisation des TLR7, 8 et 9. Nous pourrions donc supposer que le Stamaril engage préférentiellement ces TLR, ainsi que la détection des antigènes par RIG-I/MDA5 suite à la prolifération virale dans le cytoplasme, conduisant aux réponses observées dans leur étude et la nôtre. Querec *et al.* ont également observé qu'une déficience en TLR2 chez les souris altère la balance Th1/Th2 en faveur des Th1. La déficience en myd88, aussi impliquée dans la signalisation TLR2, altère seulement la réponse Th1. Cela suggère que d'autres mécanismes de détection que le TLR2 sont impliqués dans l'induction des réponses Th2. Nous pouvons donc supposer que l'absence de capacité de prolifération et/ou que l'inactivation au β -propiolactone altèrent la capacité de la souche vaccinale à activer les TLR7, 8 et 9 ainsi que les RLR intracellulaires, favorisant l'induction de réponses Th2.

Nous pourrions nous demander : est-ce qu'un ou plusieurs mécanismes de détection de la souche YF-17D sont associés avec la persistance de la protection à long terme ?

Au cours de ce projet, nous avons montré que l'injection des ConM SOSIP.v7 par voie sous-cutanée favorisait l'induction de cDC1 CADM1+ réputée promouvoir les réponses Th1 et les réponses cellulaires cytotoxiques. Nous pouvons donc supposer que la mobilisation de cellules NK et de LT CD8+ plus importante pour le Stamaril ainsi qu'un enrichissement préférentiel de Th1 (indépendamment du potentiel biais de stimulation) découle des propriétés de la voie sous-cutanée à induire l'activation des cDC1. Nous n'avons pas analysé la réponse innée dans le cas de la vaccination Stamaril mais le dosage des cytokines plasmatiques a mis en évidence une forte réponse antivirale incluant la production d'IFN- λ , produit en quantité par les cDC1, supportant ainsi cette hypothèse.

Nous avions émis l'hypothèse que le vaccin inactivé serait moins compétent que le Stamaril pour induire une réponse neutralisante persistante. Suite à la vaccination, une production plus rapide et de plus forte amplitude pour le Stamaril a été détectée. Cette amplitude de réponse n'a pas été compensée par le rappel du vaccin inactivé, de même que le titre en anticorps neutralisants ne s'est pas maintenu au cours du temps. Toutefois, nous avons observé que la réponse neutralisante induite par le Stamaril s'établit malgré des conditions de réponses Th1. Ces résultats viennent s'ajouter à de nombreux travaux mettant en évidence les limites de la dichotomie Th1/Th2 pour justifier l'induction des

réponses humorales. En effet, nous avons évoqué dans l'introduction l'importante plasticité du compartiment T CD4+ en fonction de la signalisation par les cytokines (Hegazy et al., 2022; Martinez-Sanchez et al., 2018). Dans notre cas, l'étude de Lu et al. est particulièrement intéressante car les auteurs ont mis en évidence une reprogrammation des populations Th1 en Tfh1 pouvant ainsi favoriser et orienter la réponse anticorps (Lu et al., 2011). Dans une autre étude, Nakayamada et al. ont démontré que le signal de différenciation des Th1 par l'IL-12 induit également l'activation des gènes *Il21* et *Bcl6* donnant lieu à la formation d'un phénotype intermédiaire Th1-Tfh1 (Nakayamada et al., 2011) qui en va s'orienter en effecteur Th1 ou Tfh1 respectivement en cas de stimulation TCR forte ou insuffisante (Padhan et al., 2021). Ainsi nous pouvons supposer que la mobilisation des Th1 dans le cas de la vaccination Stamaril permet non seulement l'induction d'une forte réponse cellulaire, mais peut également être la source de la réponse neutralisante grâce à la plasticité cellulaire du compartiment Th1. Cette hypothèse est d'autant plus probable que Baiyegunhi et al. ont associé positivement la fréquence des Tfh1 avec la réponse IgG anti-VIH à en prédire leur titre après un an d'infection (Baiyegunhi et al., 2018).

Une étude réalisé au CEA a mis en évidence dans le cas d'une vaccination contre le MVA l'importance de la composition en cellules immunitaire et particulièrement en APC des tissus ciblé par les voies d'injections (Rosenbaum et al., 2020). De plus, il a été montré que la vascularisation des tissus facilitent la diffusion de l'antigène et la prise en charge de l'antigène en favorisant la migration des effecteurs cellulaires contribuant ainsi à l'orientation de la réponse immunitaire (Ols et al., 2020). Ainsi la voie d'injection pourrait également influencer la qualité de la réponse induite par la vaccination YF. Nous n'avons pas fait de comparaison des voies d'injection dans cette étude, mais notre design expérimental s'appuie sur l'étude préclinique de Monath et al. où la voie intramusculaire a été employée pour immuniser des PNH avec le vaccin inactivé (Monath et al., 2010). Contrairement à nos résultats, ils ont observé qu'une seule injection était suffisante pour induire un titre en anticorps neutralisants similaire à celui du Stamaril. Cependant, l'étude conduite au CEA sur les voies d'injections, a mis en évidence que la vaccination sous-cutanée avec le MVA induit des titres en anticorps plus élevés que les voies intramusculaire et intradermique (Rosenbaum et al., 2020). Ces résultats combinés aux observations faites sur les réponses neutralisantes induites par les vaccins YF mettent en

évidence un rôle potentiel des propriétés de l'immunogène sur la qualité de la réponse humorale en fonction de la voie d'injection.

La caractérisation des populations de LT CD4+ suite à la vaccination contre la fièvre jaune nous ont permis de mettre en évidence de potentiels signatures et biomarqueurs pouvant être associé à la persistance du titre en anticorps neutralisant. Cependant, la qualité de la réponse neutralisante du Stamaril malgré l'induction d'une réponse cellulaire soulève l'hypothèse de l'existence d'autres mécanismes que les LT CD4 dans l'induction et la persistance de la réponse humorale. Les propriétés de l'immunogène lui-même pourraient apporter un élément de réponse. En effet, dans notre étude nous avons tenu compte uniquement de la réponse T CD4+ dans la maturation des réponses B suite à la vaccination, or nous avons évoqué dans l'introduction la capacité de certains antigènes à déclencher des réponses B T-indépendantes. Il a été démontré que ces réponses sont capables d'aboutir à la formation de cellules B mémoires et de plasmocytes à longue durée de vie de haute affinité envers l'antigène ([Liao et al., 2017a](#); [Liu et al., 2022](#)). Il serait intéressant d'enquêter plus en détails sur la capacité de la souche vivante YF-17D à induire ce type de réponse.

Nous avons observé une persistance de la réponse neutralisante dans le cas du vaccin Stamaril un an après l'immunisation. Toutefois, cette persistance a été décrite sur plusieurs décennies en l'absence de rappel ou d'exposition au virus sauvage, supposant une persistance de l'antigène au sein de l'organisme permettant la maintien de la protection à long terme ([Lindsey et al., 2018](#)). De plus, avec le traitement IdU *in vivo* nous avons observé une persistance à long terme des cellules mobilisées lors de la réponse vaccinale (identifiées comme spécifiques aux vaccins), ainsi qu'une prolifération à bas niveau d'une partie de ces cellules plusieurs mois après l'immunisation suggérant une réactivation ponctuelle des cellules spécifiques. Il a été précédemment rapporté dans différents modèle infectieux que des antigènes sont capables de persister dans différents tissus, et particulièrement dans les ganglions plusieurs semaines après la clairance virale ([Jolley-Gibbs et al., 2005](#); [D. L. Turner et al., 2007](#); [Zammit et al., 2006](#)). Les études de Jolley-Gibbs *et al.* et Turner *et al.* ont démontré l'impact de cette persistance dans les ganglions sur la différenciation des LT CD4+ en cellules mémoires ([Jolley-Gibbs et al., 2005](#); [Turner et al., 2007](#)). Ces résultats suggèrent donc que la persistance de l'antigène

influence la qualité de la réponse mémoire et potentiellement leur maintien à long terme. Cependant les mécanismes de cette persistance restent encore à déterminer. Nous avons déjà détaillé dans l'introduction que les FDC au sein des GC sont capables de stocker les antigènes sous forme de complexes immuns pour induire une maturation des LB prolongée (Heesters et al., 2013). Cependant, nous ne disposons pas de données sur la durée de cette persistance au sein des FDC et sur leur rôle potentiel dans des réexpositions ponctuelles à l'antigène. De plus, nous disposons de peu d'informations sur les réservoirs cellulaires potentiels de la souche vaccinale YF-17D, susceptibles d'induire une réactivation à bas bruits des cellules mémoires.

III. Perspectives

Dans un premier temps, afin d'étudier les différences de spécificité de réponses mentionnées précédemment suite au potentiel biais de stimulation par le virus entier, nous allons prochainement réaliser des expériences de stimulation *in vitro* avec des peptides spécifiques des protéines NS3 ou de l'enveloppe virale. Pour cela, un panel de cytométrie en flux a été créé, reprenant un certain nombre de marqueurs d'activation, de fonctionnalité et d'identification des différents phénotypes mémoires dans le but de pouvoir transposer les résultats à ceux obtenus en cytométrie de masse. Cette analyse nous permettrait de mieux identifier les mécanismes précoce de la réponse T CD4+ et une identification plus fine des cellules spécifiques persistantes.

Parallèlement, nous sommes actuellement en collaboration avec l'entreprise Life&Soft pour travailler sur l'analyse des données. Nous avons pour objectif de définir des stratégies d'analyse bio-statistiques permettant d'identifier des biomarqueurs précoce de la réponse T CD4+ associés à la persistance de la réponse neutralisante.

Les OLII tels que les ganglions jouent un rôle capital dans l'induction de la mémoire, ainsi que la moelle osseuse dans le renouvellement et la persistance à long terme des cellules mémoires. Pour compléter notre étude des prélèvements ont été réalisé et acquis en cytométrie de masse sur trois animaux de chaque groupe mais n'ont pas encore été analysés. Ces résultats pourront par la suite être mis en regard de ceux obtenus dans le sang, notamment avec les cTfh. Nous pourrions ainsi envisager de corrélér les cTfh

observés dans le sang avec l'activité des Tfh dans les ganglions et la maturation des cellules B.

Comme nous l'avons décrit dans l'introduction, la réponse immunitaire se caractérise par un ensemble d'interactions qui ne peuvent être résumées par l'étude d'une seule partie de la réponse immunitaire. Ces constatations ont motivé la mise en place au CEA d'un projet plus large, visant à étudier de manière approfondie les différents aspects de la réponse immunitaire contre la Fièvre Jaune afin d'identifier et comprendre les mécanismes de la persistance de la mémoire à long terme. En conséquence, nous avons en parallèle de l'étude des T CD4 lancé une étude centrée sur la qualité de la réponse B et de son implication dans la persistance de la protection. Enfin, une étude visant à suivre la persistance d'antigènes du virus de la fièvre jaune dans le modèle du macaque cynomolgus va également être lancée prochainement afin de répondre aux interrogations mentionnées dans la section précédente.

Au sein de différentes études menées au CEA, nous avons mis en évidence l'impact des modalités vaccinales sur la qualité de la réponse de différents compartiments de l'immunité innée en lien avec la qualité des réponses humorale ([J. Palgen et al., 2019](#); [J. L. Palgen et al., 2018, 2020](#)) s. Cependant, nous manquons encore d'informations sur les interactions de cette immunité innée avec les compartiments adaptatifs déterminant la qualité de la réponse vaccinale. Une étude approfondie de ces interactions permettrait d'améliorer grandement nos connaissances des mécanismes associés.

Le développement d'un modèle vaccinal *in silico* construit à l'aide de données multiples prenant en compte les différents. Un tel modèle permettrait de faciliter l'étude de la réponse aux adjuvants, voies d'immunisation, l'âge de l'individus, par exemple. Très récemment, Voutouri *et al.* ont développé un modèle mathématique de la réponse immune contre le SARS-CoV-2 dans le but de simuler l'impact de différents traitements en fonction d'une large gamme de paramètres immunitaires d'un individu ([Voutouri et al., 2021](#)). Dans le cas du SARS-CoV-2, des modélisations mathématiques ont également été développer chez les PNH afin de modéliser la dynamique virale ou pour identifier des corrélats de protection ([Alexandre et al., 2022](#); [Gonçalves et al., 2021](#)). Appliquer de tels modèles à un candidat vaccin permettrait d'accélérer l'identification dès les étapes

précoce de développement quels seraient les immunogènes les plus susceptibles d'induire une réponse immunitaire efficace.

BIBLIOGRAPHIE

- Acosta-Rodriguez, E. v., Rivino, L., Geginat, J., Jarrossay, D., Gattorno, M., Lanzavecchia, A., Sallusto, F., & Napolitani, G. (2007). Surface phenotype and antigenic specificity of human interleukin 17-producing T helper memory cells. *Nature Immunology*, 8(6), 639–646. <https://doi.org/10.1038/NI1467>
- Ahmed, R., Bevan, M. J., Reiner, S. L., & Fearon, D. T. (2009). The precursors of memory: models and controversies. *Nature Reviews. Immunology*, 9(9), 662–668. <https://doi.org/10.1038/NRI2619>
- Akiyama, M., Yasuoka, H., Yamaoka, K., Suzuki, K., Kaneko, Y., Kondo, H., Kassai, Y., Koga, K., Miyazaki, T., Morita, R., Yoshimura, A., & Takeuchi, T. (2016). Enhanced IgG4 production by follicular helper 2 T cells and the involvement of follicular helper 1 T cells in the pathogenesis of IgG4-related disease. *Arthritis Research & Therapy*, 18(1). <https://doi.org/10.1186/S13075-016-1064-4>
- Akondy, R. S., Fitch, M., Edupuganti, S., Yang, S., Kissick, H. T., Li, K. W., Youngblood, B. A., Abdelsamed, H. A., McGuire, D. J., Cohen, K. W., Alexe, G., Nagar, S., McCausland, M. M., Gupta, S., Tata, P., Haining, W. N., McElrath, M. J., Zhang, D., Hu, B., ... Ahmed, R. (2017). Origin and differentiation of human memory CD8 T cells after vaccination. *Nature*, 552(7685), 362–367. <https://doi.org/10.1038/nature24633>
- Alexandre, M., Marlin, R., Prague, M., Coleon, S., Kahlaoui, N., Cardinaud, S., Naninck, T., Delache, B., Surenaud, M., Galhaut, M., Dereuddre-Bosquet, N., Cavarelli, M., Maisonnasse, P., Centlivre, M., Lacabaratz, C., Wiedemann, A., Zurawski, S., Zurawski, G., Schwartz, O., ... Thiébaut, R. (2022). Modelling the response to vaccine in non-human primates to define SARS-CoV-2 mechanistic correlates of protection. *ELife*, 11. <https://doi.org/10.7554/ELIFE.75427>
- Allen, C. D. C., & Cyster, J. G. (2008). Follicular dendritic cell networks of primary follicles and germinal centers: phenotype and function. *Seminars in Immunology*, 20(1), 14. <https://doi.org/10.1016/J.SMIM.2007.12.001>
- Aloisi, F., & Pujol-Borrell, R. (2006). Lymphoid neogenesis in chronic inflammatory diseases. *Nature Reviews. Immunology*, 6(3), 205–217. <https://doi.org/10.1038/NRI1786>
- Alving, C. R., Rao, M., Steers, N. J., Matyas, G. R., & Mayorov, A. v. (2012). Liposomes containing lipid A: An effective, safe, generic adjuvant system for synthetic vaccines. *Expert Review of Vaccines*, 11(6), 733–744. <https://doi.org/10.1586/erv.12.35>
- Andersen-Nissen, E., Fiore-Gartland, A., Fleming, L. B., Carppi, L. N., Naidoo, A. F., Harper, M. S., Voillet, V., Grunenberg, N., Laher, F., Innes, C., Bekker, L. G., Kublin, J. G., Huang, Y., Ferrari, G., Tomaras, G. D., Gray, G., Gilbert, P. B., & McElrath, M. J.

(2021). Innate immune signatures to a partially-efficacious HIV vaccine predict correlates of HIV-1 infection risk. *PLoS Pathogens*, 17(3).
<https://doi.org/10.1371/JOURNAL.PPAT.1009363>

Ansel, K. M., Ngo, V. N., Hyman, P. L., Luther, S. A., Förster, R., Sedgwick, J. D., Browning, J. L., Upp, M., & Cyster, J. G. (2000). A chemokine-driven positive feedback loop organizes lymphoid follicles. *Nature*, 406(6793), 309–314.
<https://doi.org/10.1038/35018581>

Araya, N., Sato, T., Ando, H., Tomaru, U., Yoshida, M., Coler-Reilly, A., Yagishita, N., Yamauchi, J., Hasegawa, A., Kannagi, M., Hasegawa, Y., Takahashi, K., Kunitomo, Y., Tanaka, Y., Nakajima, T., Nishioka, K., Utsunomiya, A., Jacobson, S., & Yamano, Y. (2014). HTLV-1 induces a Th1-like state in CD4+CCR4+ T cells. *Journal of Clinical Investigation*, 124(8), 3431–3442. <https://doi.org/10.1172/JCI75250>

Arts, R. J. W., Moorlag, S. J. C. F. M., Novakovic, B., Stunnenberg, H. G., van Crevel, R., & Netea Correspondence, M. G. (2018). BCG Vaccination Protects against Experimental Viral Infection in Humans through the Induction of Cytokines Associated with Trained Immunity In Brief. *Cell Host & Microbe*, 23, 89–100.
<https://doi.org/10.1016/j.chom.2017.12.010>

Aydar, Y., Sukumar, S., Szakal, A. K., & Tew, J. G. (2005). The influence of immune complex-bearing follicular dendritic cells on the IgM response, Ig class switching, and production of high affinity IgG. *Journal of Immunology (Baltimore, Md.: 1950)*, 174(9), 5358–5366. <https://doi.org/10.4049/JIMMUNOL.174.9.5358>

Bachem, A., Güttler, S., Hartung, E., Ebstein, F., Schaefer, M., Tannert, A., Salama, A., Movassaghi, K., Opitz, C., Mages, H. W., Henn, V., Kloetzel, P. M., Gurka, S., & Kroczeck, R. A. (2010). Superior antigen cross-presentation and XCR1 expression define human CD11c+CD141+ cells as homologues of mouse CD8+ dendritic cells. *Journal of Experimental Medicine*, 207(6), 1273–1281.
<https://doi.org/10.1084/JEM.20100348>

Baiyegunhi, O., Ndlovu, B., Ogunshola, F., Ismail, N., Walker, B. D., Ndung'u, T., & Ndhlovu, Z. M. (2018). Frequencies of Circulating Th1-Biased T Follicular Helper Cells in Acute HIV-1 Infection Correlate with the Development of HIV-Specific Antibody Responses and Lower Set Point Viral Load. *Journal of Virology*, 92(15), 659–677. <https://doi.org/10.1128/JVI.00659-18>

Bajaña, S., Turner, S., Paul, J., Ainsua-Enrich, E., & Kovats, S. (2016). IRF4 and IRF8 Act in CD11c+ Cells To Regulate Terminal Differentiation of Lung Tissue Dendritic Cells. *Journal of Immunology (Baltimore, Md.: 1950)*, 196(4), 1666–1677.
<https://doi.org/10.4049/JIMMUNOL.1501870>

Baliu-Piqué, M., Verheij, M. W., Drylewicz, J., Ravesloot, L., de Boer, R. J., Koets, A., Tesselaar, K., & Borghans, J. A. M. (2018). Short lifespans of memory T-cells in bone marrow, blood, and lymph nodes suggest that T-cell memory is maintained by

continuous self-renewal of recirculating cells. *Frontiers in Immunology*, 9(SEP), 2054. <https://doi.org/10.3389/FIMMU.2018.02054/FULL>

Ballesteros-Tato, A., León, B., Graf, B. A., Moquin, A., Adams, P. S., Lund, F. E., & Randall, T. D. (2012). Interleukin-2 inhibits germinal center formation by limiting T follicular helper cell differentiation. *Immunity*, 36(5), 847–856. <https://doi.org/10.1016/J.IMMUNI.2012.02.012>

Banchereau, J., & Steinman, R. M. (1998). Dendritic cells and the control of immunity. *Nature*, 392(6673), 245–252. <https://doi.org/10.1038/32588>

Banchereau, J., Thompson-Snipes, L. A., Zurawski, S., Blanck, J. P., Cao, Y., Clayton, S., Gorvel, J. P., Zurawski, G., & Klechevsky, E. (2012). The differential production of cytokines by human Langerhans cells and dermal CD14(+) DCs controls CTL priming. *Blood*, 119(24), 5742–5749. <https://doi.org/10.1182/BLOOD-2011-08-371245>

Bao, M., & Liu, Y. J. (2013). Regulation of TLR7/9 signaling in plasmacytoid dendritic cells. *Protein & Cell*, 4(1), 40–52. <https://doi.org/10.1007/S13238-012-2104-8>

Barnes, J. L., Plank, M. W., Asquith, K., Maltby, S., Sabino, L. R., Kaiko, G. E., Lochrin, A., Horvat, J. C., Mayall, J. R., Kim, R. Y., Hansbro, P. M., Keely, S., Belz, G. T., Tay, H. L., & Foster, P. S. (2021). T-helper 22 cells develop as a distinct lineage from Th17 cells during bacterial infection and phenotypic stability is regulated by T-bet. *Mucosal Immunology*, 14(5), 1077–1087. <https://doi.org/10.1038/S41385-021-00414-6>

Barreiro, O., de La Fuente, H., Mittelbrunn, M., & Sánchez-Madrid, F. (2007). Functional insights on the polarized redistribution of leukocyte integrins and their ligands during leukocyte migration and immune interactions. *Immunological Reviews*, 218(1), 147–164. <https://doi.org/10.1111/J.1600-065X.2007.00529.X>

Barrett, A. D., & Teuwen, D. E. (2009). Yellow fever vaccine - how does it work and why do rare cases of serious adverse events take place? *Current Opinion in Immunology*, 21(3), 308–313. <https://doi.org/10.1016/J.COI.2009.05.018>

Bauquet, A. T., Jin, H., Paterson, A. M., Mitsdoerffer, M., Ho, I. C., Sharpe, A. H., & Kuchroo, V. K. (2009). The costimulatory molecule ICOS regulates the expression of c-Maf and IL-21 in the development of follicular T helper cells and TH-17 cells. *Nature Immunology*, 10(2), 167–175. <https://doi.org/10.1038/NI.1690>

Bekeredjian-Ding, I. B., Wagner, M., Hornung, V., Giese, T., Schnurr, M., Endres, S., & Hartmann, G. (2005). Plasmacytoid Dendritic Cells Control TLR7 Sensitivity of Naive B Cells via Type I IFN. *The Journal of Immunology*, 174(7), 4043–4050. <https://doi.org/10.4049/JIMMUNOL.174.7.4043>

Bendall, S. C., Nolan, G. P., Roederer, M., & Chattopadhyay, P. K. (2012). A deep profiler's guide to cytometry. In *Trends in Immunology*. <https://doi.org/10.1016/j.it.2012.02.010>

- Bentebibel, S. E., Lopez, S., Obermoser, G., Schmitt, N., Mueller, C., Harrod, C., Flano, E., Mejias, A., Albrecht, R. A., Blankenship, D., Xu, H., Pascual, V., Banchereau, J., Garcia-Sastre, A., Palucka, A. K., Ramilo, O., & Ueno, H. (2013). Induction of ICOS⁺CXCR3⁺CXCR5⁺ T H cells correlates with antibody responses to influenza vaccination. *Science Translational Medicine*, 5(176).
<https://doi.org/10.1126/SCITRANSLMED.3005191>
- Binley, J. M., Sanders, R. W., Clas, B., Schuelke, N., Master, A., Guo, Y., Kajumo, F., Anselma, D. J., Maddon, P. J., Olson, W. C., & Moore, J. P. (2000). A Recombinant Human Immunodeficiency Virus Type 1 Envelope Glycoprotein Complex Stabilized by an Intermolecular Disulfide Bond between the gp120 and gp41 Subunits Is an Antigenic Mimic of the Trimeric Virion-Associated Structure. *Journal of Virology*.
<https://doi.org/10.1128/JVI.74.2.627-643.2000>
- Biswas, M., Sarkar, D., Kumar, S. R. P., Nayak, S., Rogers, G. L., Markusic, D. M., Liao, G., Terhorst, C., & Herzog, R. W. (2015). Synergy between rapamycin and FLT3 ligand enhances plasmacytoid dendritic cell-dependent induction of CD4⁺CD25⁺FoxP3⁺Treg. *Blood*, 125(19), 2937. <https://doi.org/10.1182/BLOOD-2014-09-599266>
- Bjornson-Hooper, Z. B., Fragiadakis, G. K., Spitzer, M. H., Chen, H., Madhireddy, D., Hu, K., Lundsten, K., McIlwain, D. R., & Nolan, G. P. (2022). A Comprehensive Atlas of Immunological Differences Between Humans, Mice, and Non-Human Primates. *Frontiers in Immunology*, 13. <https://doi.org/10.3389/FIMMU.2022.867015>
- Blasius, A. L., & Beutler, B. (2010). Intracellular Toll-like Receptors. *Immunity*, 32(3), 305–315. <https://doi.org/10.1016/J.IMMUNI.2010.03.012>
- Blink, E. J., Light, A., Kallies, A., Nutt, S. L., Hodgkin, P. D., & Tarlinton, D. M. (2005). Early appearance of germinal center-derived memory B cells and plasma cells in blood after primary immunization. *The Journal of Experimental Medicine*, 201(4), 545–554. <https://doi.org/10.1084/jem.20042060>
- Bonecchi, R., Bianchi, G., Bordignon, P. P., D'Ambrosio, D., Lang, R., Borsatti, A., Sozzani, S., Allavena, P., Gray, P. A., Mantovani, A., & Sinigaglia, F. (1998). Differential expression of chemokine receptors and chemotactic responsiveness of type 1 T helper cells (Th1s) and Th2s. *The Journal of Experimental Medicine*, 187(1), 129–134. <https://doi.org/10.1084/JEM.187.1.129>
- Boniface, K., Bernard, F.-X., Garcia, M., Gurney, A. L., Lecron, J.-C., & Morel, F. (2005). IL-22 inhibits epidermal differentiation and induces proinflammatory gene expression and migration of human keratinocytes. *Journal of Immunology (Baltimore, Md.: 1950)*, 174(6), 3695–3702. <https://doi.org/10.4049/JIMMUNOL.174.6.3695>
- Booth, N. J., McQuaid, A. J., Sobande, T., Kissane, S., Agius, E., Jackson, S. E., Salmon, M., Falciani, F., Yong, K., Rustin, M. H., Akbar, A. N., & Vukmanovic-Stejic, M. (2010). Different Proliferative Potential and Migratory Characteristics of Human CD4⁺ Regulatory T Cells That Express either CD45RA or CD45RO. *The Journal of Immunology*, 184(8), 4317–4326. <https://doi.org/10.4049/JIMMUNOL.0903781>

Broker, T., Riedinger, M., & Karjalainen, K. (1997). Targeted expression of major histocompatibility complex (MHC) class II molecules demonstrates that dendritic cells can induce negative but not positive selection of thymocytes in vivo. *The Journal of Experimental Medicine*, 185(3), 541–550.
<https://doi.org/10.1084/JEM.185.3.541>

Bryant, J. E., Holmes, E. C., & Barrett, A. D. T. (2007). Out of Africa: A Molecular Perspective on the Introduction of Yellow Fever Virus into the Americas. *PLOS Pathogens*, 3(5), e75. <https://doi.org/10.1371/JOURNAL.PPAT.0030075>

Burchill, M. A., Yang, J., Vogtenhuber, C., Blazar, B. R., & Farrar, M. A. (2007). IL-2 Receptor β-Dependent STAT5 Activation Is Required for the Development of Foxp3+ Regulatory T Cells. *The Journal of Immunology*, 178(1), 280–290.
<https://doi.org/10.4049/JIMMUNOL.178.1.280>

Burel, J. G., Qian, Y., Lindestam Arlehamn, C., Weiskopf, D., Zapardiel-Gonzalo, J., Taplitz, R., Gilman, R. H., Saito, M., de Silva, A. D., Vijayanand, P., Scheuermann, R. H., Sette, A., & Peters, B. (2017). An Integrated Workflow To Assess Technical and Biological Variability of Cell Population Frequencies in Human Peripheral Blood by Flow Cytometry. *Journal of Immunology (Baltimore, Md.: 1950)*, 198(4), 1748–1758.
<https://doi.org/10.4049/JIMMUNOL.1601750>

Calabro, S., Tritto, E., Pezzotti, A., Taccone, M., Muzzi, A., Bertholet, S., de Gregorio, E., O'Hagan, D. T., Baudner, B., & Seubert, A. (2013). The adjuvant effect of MF59 is due to the oil-in-water emulsion formulation, none of the individual components induce a comparable adjuvant effect. *Vaccine*, 31(33), 3363–3369.
<https://doi.org/10.1016/j.vaccine.2013.05.007>

Campion, S. L., Brenna, E., Thomson, E., Fischer, W., Ladell, K., McLaren, J. E., Price, D. A., Frahm, N., McElrath, J. M., Cohen, K. W., Maenza, J. R., Walsh, S. R., Baden, L. R., Haynes, B. F., Korber, B., Borrow, P., & McMichael, A. J. (2021). Preexisting memory CD4+ T cells contribute to the primary response in an HIV-1 vaccine trial. *The Journal of Clinical Investigation*, 131(23). <https://doi.org/10.1172/JCI150823>

Campion, S. L., Brodie, T. M., Fischer, W., Korber, B. T., Rossetti, A., Goonetilleke, N., McMichael, A. J., & Sallusto, F. (2014). Proteome-wide analysis of HIV-specific naive and memory CD4+ T cells in unexposed blood donors. *Journal of Experimental Medicine*, 211(7), 1273–1280. <https://doi.org/10.1084/JEM.20130555>

Cannons, J. L., Qi, H., Lu, K. T., Dutta, M., Gomez-Rodriguez, J., Cheng, J., Wakeland, E. K., Germain, R. N., & Schwartzberg, P. L. (2010). Optimal germinal center responses require a multistage T cell:B cell adhesion process involving integrins, SLAM-associated protein, and CD84. *Immunity*, 32(2), 253–265.
<https://doi.org/10.1016/J.IMMUNI.2010.01.010>

Cannons, J. L., Yu, L. J., Jankovic, D., Crotty, S., Horai, R., Kirby, M., Anderson, S., Cheever, A. W., Sher, A., & Schwartzberg, P. L. (2006). SAP regulates T cell-mediated help for

humoral immunity by a mechanism distinct from cytokine regulation. *The Journal of Experimental Medicine*, 203(6), 1551. <https://doi.org/10.1084/JEM.20052097>

Carotta, S., Dakic, A., D'Amico, A., Pang, S. H. M., Greig, K. T., Nutt, S. L., & Wu, L. (2010). The transcription factor PU.1 controls dendritic cell development and Flt3 cytokine receptor expression in a dose-dependent manner. *Immunity*, 32(5), 628–641. <https://doi.org/10.1016/J.IMMUNI.2010.05.005>

Carrasco, Y. R., & Batista, F. D. (2006). B-cell activation by membrane-bound antigens is facilitated by the interaction of VLA-4 with VCAM-1. *The EMBO Journal*, 25(4), 889. <https://doi.org/10.1038/SJ.EMBOJ.7600944>

Casamayor-Palleja, M., Khan, M., & MacLennan, I. C. M. (1995). A subset of CD4+ memory T cells contains preformed CD40 ligand that is rapidly but transiently expressed on their surface after activation through the T cell receptor complex. *Journal of Experimental Medicine*, 181(4), 1293–1301. <https://doi.org/10.1084/JEM.181.4.1293>

Cavarelli, M., Hua, S., Hantour, N., Tricot, S., Tchitchev, N., Gommet, C., Hocini, H., Chapon, C., Dereuddre-Bosquet, N., & le Grand, R. (2021). Leukocytospermia induces intraepithelial recruitment of dendritic cells and increases SIV replication in colorectal tissue explants. *Communications Biology*, 4(1). <https://doi.org/10.1038/S42003-021-02383-9>

Chamaillard, M., Hashimoto, M., Horie, Y., Masumoto, J., Qiu, S., Saab, L., Ogura, Y., Kawasaki, A., Fukase, K., Kusumoto, S., Valvano, M. A., Foster, S. J., Mak, T. W., Nuñez, G., & Inohara, N. (2003). An essential role for NOD1 in host recognition of bacterial peptidoglycan containing diaminopimelic acid. *Nature Immunology*, 4(7), 702–707. <https://doi.org/10.1038/NI945>

Chang, J. T., Palanivel, V. R., Kinjyo, I., Schambach, F., Intlekofer, A. M., Banerjee, A., Longworth, S. A., Vinup, K. E., Mrass, P., Oliaro, J., Killeen, N., Orange, J. S., Russell, S. M., Weninger, W., & Reiner, S. L. (2007). Asymmetric T lymphocyte division in the initiation of adaptive immune responses. *Science (New York, N.Y.)*, 315(5819), 1687–1691. <https://doi.org/10.1126/SCIENCE.1139393>

Chan, T. D., Gatto, D., Wood, K., Camidge, T., Basten, A., & Brink, R. (2009). Antigen affinity controls rapid T-dependent antibody production by driving the expansion rather than the differentiation or extrafollicular migration of early plasmablasts. *Journal of Immunology (Baltimore, Md.: 1950)*, 183(5), 3139–3149. <https://doi.org/10.4049/JIMMUNOL.0901690>

Chaudhury, S., Duncan, E. H., Atre, T., Storme, C. K., Beck, K., Kaba, S. A., Lanar, D. E., & Bergmann-Leitner, E. S. (2018). Identification of Immune Signatures of Novel Adjuvant Formulations Using Machine Learning. *Scientific Reports*, 8(1). <https://doi.org/10.1038/s41598-018-35452-x>

- Chen, L. L., Frank, A. M., Adams, J. C., & Steinman, R. M. (1978). Distribution of horseradish peroxidase (HRP)-anti-HRP immune complexes in mouse spleen with special reference to follicular dendritic cells. *The Journal of Cell Biology*, 79(1), 184–199. <https://doi.org/10.1083/JCB.79.1.184>
- Chen, S., Wu, Z., Wang, M., & Cheng, A. (2017). Innate Immune Evasion Mediated by Flaviviridae Non-Structural Proteins. *Viruses*, 9(10). <https://doi.org/10.3390/V9100291>
- Choi, Y. S., Kageyama, R., Eto, D., Escobar, T. C., Johnston, R. J., Monticelli, L., Lao, C., & Crotty, S. (2011). ICOS receptor instructs T follicular helper cell versus effector cell differentiation via induction of the transcriptional repressor Bcl6. *Immunity*, 34(6), 932–946. <https://doi.org/10.1016/J.IMMUNI.2011.03.023>
- Chow, K. v., Lew, A. M., Sutherland, R. M., & Zhan, Y. (2016). Monocyte-Derived Dendritic Cells Promote Th Polarization, whereas Conventional Dendritic Cells Promote Th Proliferation. *The Journal of Immunology*, 196(2), 624–636. <https://doi.org/10.4049/JIMMUNOL.1501202>
- Cisse, B., Caton, M. L., Lehner, M., Maeda, T., Scheu, S., Locksley, R., Holmberg, D., Zweier, C., den Hollander, N. S., Kant, S. G., Holter, W., Rauch, A., Zhuang, Y., & Reizis, B. (2008). Transcription factor E2-2 is an essential and specific regulator of plasmacytoid dendritic cell development. *Cell*, 135(1), 37–48. <https://doi.org/10.1016/J.CELL.2008.09.016>
- Cohn, L., Chatterjee, B., Esselborn, F., Smed-Sörensen, A., Nakamura, N., Chalouni, C., Lee, B. C., Vandlen, R., Keler, T., Lauer, P., Brockstedt, D., Mellman, I., & Delamarre, L. (2013). Antigen delivery to early endosomes eliminates the superiority of human blood BDCA3+ dendritic cells at cross presentation. *The Journal of Experimental Medicine*, 210(5), 1049–1063. <https://doi.org/10.1084/JEM.20121251>
- Colletti, N. J., Liu, H., Gower, A. C., Alekseyev, Y. O., Arendt, C. W., & Shaw, M. H. (2016). TLR3 signaling promotes the induction of unique human BDCA-3 dendritic cell populations. *Frontiers in Immunology*, 7(MAR), 88. <https://doi.org/10.3389/FIMMU.2016.00088/BIBTEX>
- Collison, L. W., Chaturvedi, V., Henderson, A. L., Giacomin, P. R., Guy, C., Bankoti, J., Finkelstein, D., Forbes, K., Workman, C. J., Brown, S. A., Rehg, J. E., Jones, M. L., Ni, H. T., Artis, D., Turk, M. J., & Vignali, D. A. A. (2010). IL-35-mediated induction of a potent regulatory T cell population. *Nature Immunology*, 11(12), 1093–1101. <https://doi.org/10.1038/NI.1952>
- Coquery, C. M., Loo, W. M., Wade, N. S., Bederman, A. G., Tung, K. S., Lewis, J. E., Hess, H., & Erickson, L. D. (2015). BAFF regulates follicular helper t cells and affects their accumulation and interferon- γ production in autoimmunity. *Arthritis & Rheumatology (Hoboken, N.J.)*, 67(3), 773–784. <https://doi.org/10.1002/ART.38950>

- Cote-Sierra, J., Foucras, G., Guo, L., Chiodetti, L., Young, H. A., Hu-Li, J., Zhu, J., & Paul, W. E. (2004). Interleukin 2 plays a central role in Th2 differentiation. *Proceedings of the National Academy of Sciences of the United States of America*, 101(11), 3880–3885. <https://doi.org/10.1073/PNAS.0400339101>
- Crotty, S. (2014). T Follicular Helper Cell Differentiation, Function, and Roles in Disease. In *Immunity*. <https://doi.org/10.1016/j.immuni.2014.10.004>
- Crotty, S. (2015). A brief history of T cell help to B cells. *Nature Reviews Immunology*. <https://doi.org/10.1038/nri3803>
- Cyster, J. G., & Schwab, S. R. (2012). Sphingosine-1-phosphate and lymphocyte egress from lymphoid organs. *Annual Review of Immunology*, 30, 69–94. <https://doi.org/10.1146/ANNUREV-IMMUNOL-020711-075011>
- Dalai, S. K., Khoruzhenko, S., Drake, C. G., Jie, C. C., & Sadegh-Nasseri, S. (2011). Resolution of infection promotes a state of dormancy and long survival of CD4 memory T cells. *Immunology and Cell Biology*, 89(8), 870–881. <https://doi.org/10.1038/ICB.2011.2>
- Darrasse-Jèze, G., Deroubaix, S., Mouquet, H., Victora, G. D., Eisenreich, T., Yao, K. H., Masilamani, R. F., Dustin, M. L., Rudensky, A., Liu, K., & Nussenzweig, M. C. (2009). Feedback control of regulatory T cell homeostasis by dendritic cells in vivo. *Journal of Experimental Medicine*, 206(9), 1853–1862. <https://doi.org/10.1084/JEM.20090746>
- de Quaglia e Silva, J. C., della Coletta, A. M., Gardizani, T. P., Romagnoli, G. G., Kaneno, R., & Dias-Melicio, L. A. (2019). Involvement of the Dectin-1 Receptor upon the Effector Mechanisms of Human Phagocytic Cells against Paracoccidioides brasiliensis. *Journal of Immunology Research*, 2019. <https://doi.org/10.1155/2019/1529189>
- de Taeye, S. W., Ozorowski, G., Torrents De La Peña, A., Guttman, M., Julien, J. P., van den Kerkhof, T. L. G. M., Burger, J. A., Pritchard, L. K., Pugach, P., Yasmeen, A., Crampton, J., Hu, J., Bontjer, I., Torres, J. L., Arendt, H., Destefano, J., Koff, W. C., Schuitemaker, H., Eggink, D., ... Sanders, R. W. (2015). Immunogenicity of Stabilized HIV-1 Envelope Trimers with Reduced Exposure of Non-neutralizing Epitopes. *Cell*. <https://doi.org/10.1016/j.cell.2015.11.056>
- Diehl, S., Anguita, J., Hoffmeyer, A., Zapton, T., Ihle, J. N., Fikrig, E., & Rincón, M. (2000a). Inhibition of Th1 differentiation by IL-6 is mediated by SOCS1. *Immunity*, 13(6), 805–815. [https://doi.org/10.1016/S1074-7613\(00\)00078-9](https://doi.org/10.1016/S1074-7613(00)00078-9)
- Diehl, S., Anguita, J., Hoffmeyer, A., Zapton, T., Ihle, J. N., Fikrig, E., & Rincón, M. (2000b). Inhibition of Th1 Differentiation by IL-6 Is Mediated by SOCS1. *Immunity*, 13(6), 805–815. [https://doi.org/10.1016/S1074-7613\(00\)00078-9](https://doi.org/10.1016/S1074-7613(00)00078-9)
- di Pucchio, T., Chatterjee, B., Smed-Sörensen, A., Clayton, S., Palazzo, A., Montes, M., Xue, Y., Mellman, I., Banchereau, J., & Connolly, J. E. (2008). Direct proteasome-

independent cross-presentation of viral antigen by plasmacytoid dendritic cells on major histocompatibility complex class I. *Nature Immunology*, 9(5), 551–557.
<https://doi.org/10.1038/NI.1602>

Djuretic, I. M., Levanon, D., Negreanu, V., Groner, Y., Rao, A., & Ansel, K. M. (2007). Transcription factors T-bet and Runx3 cooperate to activate Ifng and silence Il4 in T helper type 1 cells. *Nature Immunology*, 8(2), 145–153.
<https://doi.org/10.1038/NI1424>

Duhen, T., Geiger, R., Jarrossay, D., Lanzavecchia, A., & Sallusto, F. (2009). Production of interleukin 22 but not interleukin 17 by a subset of human skin-homing memory T cells. *Nature Immunology*, 10(8), 857–863. <https://doi.org/10.1038/NI.1767>

Dzionaek, A., Fuchs, A., Schmidt, P., Cremer, S., Zysk, M., Miltenyi, S., Buck, D. W., & Schmitz, J. (2000). BDCA-2, BDCA-3, and BDCA-4: three markers for distinct subsets of dendritic cells in human peripheral blood. *Journal of Immunology (Baltimore, Md.: 1950)*, 165(11), 6037–6046.
<https://doi.org/10.4049/JIMMUNOL.165.11.6037>

Eguílez-Gracia, I., Bosco, A., Dollner, R., Melum, G. R., Lexberg, M. H., Jones, A. C., Dheyaaldeen, S. A., Holt, P. G., Bækkevold, E. S., & Jahnsen, F. L. (2016). Rapid recruitment of CD14(+) monocytes in experimentally induced allergic rhinitis in human subjects. *The Journal of Allergy and Clinical Immunology*, 137(6), 1872–1881.e12. <https://doi.org/10.1016/J.JACI.2015.11.025>

Elhmouzi-Younes, J., Palgen, J.-L., Tchitchev, N., Delandre, S., Namet, I., Bodinham, C. L., Pizzoferro, K., Lewis, D. J. M., le Grand, R., Cosma, A., & Beignon, A.-S. (2017). In depth comparative phenotyping of blood innate myeloid leukocytes from healthy humans and macaques using mass cytometry. *Cytometry Part A*, 91(10), 969–982.
<https://doi.org/10.1002/cyto.a.23107>

Elias, G., Meysman, P., Bartholomeus, E., de Neuter, N., Keersmaekers, N., Suls, A., Jansens, H., Souquette, A., de Reu, H., Emonds, M. P., Smits, E., Lion, E., Thomas, P. G., Mortier, G., van Damme, P., Beutels, P., Laukens, K., van Tendeloo, V., & Ogunjimi, B. (2022). Preexisting memory CD4 T cells in naïve individuals confer robust immunity upon hepatitis B vaccination. *ELife*, 11.
<https://doi.org/10.7554/ELIFE.68388>

Erez, A., Mukherjee, R., & Altan-Bonnet, G. (2019). Quantifying the Dynamics of Hematopoiesis by In Vivo IdU Pulse-Chase, Mass Cytometry, and Mathematical Modeling. *Cytometry. Part A: The Journal of the International Society for Analytical Cytology*, 95(10), 1075–1084. <https://doi.org/10.1002/CYTO.A.23799>

Eyerich, S., Eyerich, K., Pennino, D., Carbone, T., Nasorri, F., Pallotta, S., Cianfarani, F., Odorisio, T., Traidl-Hoffmann, C., Behrendt, H., Durham, S. R., Schmidt-Weber, C. B., & Cavani, A. (2009). Th22 cells represent a distinct human T cell subset involved in epidermal immunity and remodeling. *Journal of Clinical Investigation*, 119(12), 3573–3585. <https://doi.org/10.1172/JCI40202>

- Fazilleau, N., McHeyzer-Williams, L. J., Rosen, H., & McHeyzer-Williams, M. G. (2009). The function of follicular helper T cells is regulated by the strength of T cell antigen receptor binding. *Nature Immunology*, 10(4), 375. <https://doi.org/10.1038/NI.1704>
- Feinberg, H., Jégouzo, S. A. F., Rex, M. J., Drickamer, K., Weis, W. I., & Taylor, M. E. (2017). Mechanism of pathogen recognition by human dectin-2. *The Journal of Biological Chemistry*, 292(32), 13402–13414. <https://doi.org/10.1074/JBC.M117.799080>
- Feng, S., Chen, T., Lei, G., Hou, F., Jiang, J., Huang, Q., Peng, Y., Ye, C., Hu, D. L., & Fang, R. (2019). Absent in melanoma 2 inflammasome is required for host defence against Streptococcus pneumoniae infection. *Innate Immunity*, 25(7), 412–419. <https://doi.org/10.1177/1753425919860252>
- Fiege, J. K., Stone, I. A., Fay, E. J., Markman, M. W., Wijeyesinghe, S., Macchietto, M. G., Shen, S., Masopust, D., & Langlois, R. A. (2019). The Impact of TCR Signal Strength on Resident Memory T Cell Formation during Influenza Virus Infection. *The Journal of Immunology*, 203(4), 936–945. <https://doi.org/10.4049/JIMMUNOL.1900093/-/DCSUPPLEMENTAL>
- Fiorentino, D. F., Zlotnik, A., Vieira, P., Mosmann, T. R., Howard, M., Moore, K. W., & O'Garra, A. (1991). IL-10 acts on the antigen-presenting cell to inhibit cytokine production by Th1 cells. *The Journal of Immunology*, 146(10).
- Flacher, V., Bouschbacher, M., Verronèse, E., Massacrier, C., Sisirak, V., Berthier-Vergnes, O., de Saint-Vis, B., Caux, C., Dezutter-Dambuyant, C., Lebecque, S., & Valladeau, J. (2006). Human Langerhans cells express a specific TLR profile and differentially respond to viruses and Gram-positive bacteria. *Journal of Immunology (Baltimore, Md.: 1950)*, 177(11), 7959–7967. <https://doi.org/10.4049/JIMMUNOL.177.11.7959>
- Förster, R., Schubel, A., Breitfeld, D., Kremmer, E., Renner-Müller, I., Wolf, E., & Lipp, M. (1999). CCR7 Coordinates the Primary Immune Response by Establishing Functional Microenvironments in Secondary Lymphoid Organs. *Cell*, 99(1), 23–33. [https://doi.org/10.1016/S0092-8674\(00\)80059-8](https://doi.org/10.1016/S0092-8674(00)80059-8)
- Fujio, K., Okamura, T., & Yamamoto, K. (2010). The Family of IL-10-secreting CD4+ T cells. *Advances in Immunology*, 105(C), 99–130. [https://doi.org/10.1016/S0065-2776\(10\)05004-2](https://doi.org/10.1016/S0065-2776(10)05004-2)
- Fujita, H., Nogales, K. E., Kikuchi, T., Gonzalez, J., Carucci, J. A., & Krueger, J. G. (2009). Human Langerhans cells induce distinct IL-22-producing CD4+ T cells lacking IL-17 production. *Proceedings of the National Academy of Sciences of the United States of America*, 106(51), 21795–21800. <https://doi.org/10.1073/PNAS.0911472106>
- Furio, L., Billard, H., Valladeau, J., Péguet-Navarro, J., & Berthier-Vergnes, O. (2009). Poly(I:C)-Treated human langerhans cells promote the differentiation of CD4+ T

cells producing IFN-gamma and IL-10. *The Journal of Investigative Dermatology*, 129(8), 1963–1971. <https://doi.org/10.1038/JID.2009.21>

Galli, G., Medini, D., Borgogni, E., Zedda, L., Bardelli, M., Malzone, C., Nuti, S., Tavarini, S., Sammicheli, C., Hilbert, A. K., Brauer, V., Banzhoff, A., Rappuoli, R., del Giudice, G., & Castellino, F. (2009). Adjuvanted H5N1 vaccine induces early CD4+ T cell response that predicts long-term persistence of protective antibody levels. *Proceedings of the National Academy of Sciences of the United States of America*, 106(10), 3877–3882. <https://doi.org/10.1073/PNAS.0813390106>

Gao, Y., Nish, S. A., Jiang, R., Hou, L., Licona-Limón, P., Weinstein, J. S., Zhao, H., & Medzhitov, R. (2013). Control of T Helper 2 Responses by Transcription Factor IRF4-Dependent Dendritic Cells. *Immunity*, 39(4), 722–732. <https://doi.org/10.1016/J.IMMUNI.2013.08.028>

Gautreau, G., Pejoski, D., le Grand, R., Cosma, A., Beignon, A. S., & Tchitchev, N. (2017). SPADEVizR: An R package for visualization, analysis and integration of SPADE results. *Bioinformatics*. <https://doi.org/10.1093/bioinformatics/btw708>

Gebhardt, T., Whitney, P. G., Zaid, A., MacKay, L. K., Brooks, A. G., Heath, W. R., Carbone, F. R., & Mueller, S. N. (2011). Different patterns of peripheral migration by memory CD4+ and CD8+ T cells. *Nature*, 477(7363), 216–219. <https://doi.org/10.1038/NATURE10339>

Ghoreschi, K., Laurence, A., Yang, X. P., Tato, C. M., McGeachy, M. J., Konkel, J. E., Ramos, H. L., Wei, L., Davidson, T. S., Bouladoux, N., Grainger, J. R., Chen, Q., Kanno, Y., Watford, W. T., Sun, H. W., Eberl, G., Shevach, E. M., Belkaid, Y., Cua, D. J., ... O'Shea, J. J. (2010). Generation of pathogenic TH17 cells in the absence of TGF-β signalling. *Nature* 2010 467:7318, 467(7318), 967–971. <https://doi.org/10.1038/nature09447>

Girardin, S. E., Boneca, I. G., Viala, J., Chamaillard, M., Labigne, A., Thomas, G., Philpott, D. J., & Sansonetti, P. J. (2003). Nod2 is a general sensor of peptidoglycan through muramyl dipeptide (MDP) detection. *The Journal of Biological Chemistry*, 278(11), 8869–8872. <https://doi.org/10.1074/JBC.C200651200>

Girard, J. P., Moussion, C., & Förster, R. (2012). HEVs, lymphatics and homeostatic immune cell trafficking in lymph nodes. *Nature Reviews Immunology*, 12(11), 762–773. <https://doi.org/10.1038/NRI3298>

Gonçalves, A., Maisonnasse, P., Donati, F., Albert, M., Behillil, S., Contreras, V., Naninck, T., Marlin, R., Solas, C., Pizzorno, A., Lemaitre, J., Kahlaoui, N., Terrier, O., Fang, R. H. T., Enouf, V., Dereuddre-Bosquet, N., Brisebarre, A., Touret, F., Chapon, C., ... Guedj, J. (2021). SARS-CoV-2 viral dynamics in non-human primates. *PLoS Computational Biology*, 17(3). <https://doi.org/10.1371/JOURNAL.PCBI.1008785>

Goodridge, H. S., Ahmed, S. S., Curtis, N., Kollmann, T. R., Levy, O., Netea, M. G., Pollard, A. J., van Crevel, R., & Wilson, C. B. (2016). Harnessing the beneficial heterologous

effects of vaccination. *Nature Reviews Immunology* 2016 16(6), 392–400.
<https://doi.org/10.1038/nri.2016.43>

Gorini, G., Fourati, S., Vaccari, M., Rahman, M. A., Gordon, S. N., Brown, D. R., Law, L., Chang, J., Green, R., Barrenäs, F., Liyanage, N. P. M., Doster, M. N., Schifanella, L., Bissa, M., de Castro, I. S., Washington-Parks, R., Galli, V., Fuller, D. H., Santra, S., ... Franchini, G. (2020). Engagement of monocytes, NK cells, and CD4+ Th1 cells by ALVAC-SIV vaccination results in a decreased risk of SIVmac251 vaginal acquisition. *PLoS Pathogens*, 16(3).
<https://doi.org/10.1371/JOURNAL.PPAT.1008377>

Gottschalk, R. A., Corse, E., & Allison, J. P. (2010). TCR ligand density and affinity determine peripheral induction of Foxp3 in vivo. *The Journal of Experimental Medicine*, 207(8), 1701–1711. <https://doi.org/10.1084/JEM.20091999>

Grajales-Reyes, G. E., Iwata, A., Albring, J., Wu, X., Tussiwand, R., Kc, W., Kretzer, N. M., Briseño, C. G., Durai, V., Bagadia, P., Haldar, M., Schönheit, J., Rosenbauer, F., Murphy, T. L., & Murphy, K. M. (2015). Batf3 maintains autoactivation of Irf8 for commitment of a CD8α(+) conventional DC clonogenic progenitor. *Nature Immunology*, 16(7), 708–717. <https://doi.org/10.1038/NI.3197>

Grakoui, A., Bromley, S. K., Sumen, C., Davis, M. M., Shaw, A. S., Allen, P. M., & Dustin, M. L. (1999). The immunological synapse: a molecular machine controlling T cell activation. *Science (New York, N.Y.)*, 285(5425), 221–227.
<https://doi.org/10.1126/SCIENCE.285.5425.221>

Green, J. A., Suzuki, K., Cho, B., Willison, L. D., Palmer, D., Allen, C. D. C., Schmidt, T. H., Xu, Y., Proia, R. L., Coughlin, S. R., & Cyster, J. G. (2011). The sphingosine 1-phosphate receptor S1P2 maintains the homeostasis of germinal center B cells and promotes niche confinement. *Nature Immunology* 2011 12:7, 12(7), 672–680.
<https://doi.org/10.1038/ni.2047>

Grossman, W. J., Verbsky, J. W., Barchet, W., Colonna, M., Atkinson, J. P., & Ley, T. J. (2004). Human T regulatory cells can use the perforin pathway to cause autologous target cell death. *Immunity*, 21(4), 589–601.
<https://doi.org/10.1016/J.IMMUNI.2004.09.002>

Groux, H., O'Garra, A., Bigler, M., Rouleau, M., Antonenko, S., de Vries, J. E., & Roncarolo, M. G. (1997). A CD4+T-cell subset inhibits antigen-specific T-cell responses and prevents colitis. *Nature* 1997 389:6652, 389(6652), 737–742.
<https://doi.org/10.1038/39614>

Gujer, C., Sandgren, K. J., Douagi, I., Adams, W. C., Sundling, C., Smed-Sörensen, A., Seder, R. A., Hedestam, G. B. K., & Loré, K. (2011). IFN-α produced by human plasmacytoid dendritic cells enhances T cell-dependent naïve B cell differentiation. *Journal of Leukocyte Biology*, 89(6), 811–821. <https://doi.org/10.1189/JLB.0810460>

- Gunn, M. D., Ngo, V. N., Ansel, K. M., Ekland, E. H., Cyster, J. G., & Williams, L. T. (1998). A B-cell-homing chemokine made in lymphoid follicles activates Burkitt's lymphoma receptor-1. *Nature*, 391(6669), 799–803. <https://doi.org/10.1038/35876>
- Hagan, T., Cortese, M., Roushphal, N., Boudreau, C., Linde, C., Maddur, M. S., Das, J., Wang, H., Guthmiller, J., Zheng, N. Y., Huang, M., Uphadhyay, A. A., Gardinassi, L., Petitdemange, C., McCullough, M. P., Johnson, S. J., Gill, K., Cervasi, B., Zou, J., ... Pulendran, B. (2019). Antibiotics-Driven Gut Microbiome Perturbation Alters Immunity to Vaccines in Humans. *Cell*, 178(6), 1313-1328.e13. <https://doi.org/10.1016/J.CELL.2019.08.010>
- Hale, J. S., & Ahmed, R. (2015). Memory T follicular helper CD4 T cells. *Frontiers in Immunology*, 6(FEB). <https://doi.org/10.3389/FIMMU.2015.00016>
- Haller, S., Duval, A., Migliorini, R., Stevanin, M., Mack, V., & Acha-Orbea, H. (2017). Interleukin-35-Producing CD8 α + Dendritic Cells Acquire a Tolerogenic State and Regulate T Cell Function. *Frontiers in Immunology*, 8(FEB). <https://doi.org/10.3389/FIMMU.2017.00098>
- Hammarlund, E., Lewis, M. W., Hanifin, J. M., Mori, M., Koudelka, C. W., & Slifka, M. K. (2010). Antiviral Immunity following Smallpox Virus Infection: a Case-Control Study. *Journal of Virology*, 84(24), 12754–12760. <https://doi.org/10.1128/JVI.01763-10/ASSET/D0463550-9784-4717-8FE1-1E1602DEAC93/ASSETS/GRAPHIC/ZJV9990939810003.JPG>
- Hanayama, R., Tanaka, M., Miyasaka, K., Aozasa, K., Koike, M., Uchiyama, Y., & Nagata, S. (2004). Autoimmune disease and impaired uptake of apoptotic cells in MFG-E8-deficient mice. *Science (New York, N.Y.)*, 304(5674), 1147–1150. <https://doi.org/10.1126/SCIENCE.1094359>
- Haniffa, M., Shin, A., Bigley, V., McGovern, N., Teo, P., See, P., Wasan, P. S., Wang, X. N., Malinarich, F., Malleret, B., Larbi, A., Tan, P., Zhao, H., Poidinger, M., Pagan, S., Cookson, S., Dickinson, R., Dimmick, I., Jarrett, R. F., ... Ginhoux, F. (2012). Human Tissues Contain CD141hi Cross-Presenting Dendritic Cells with Functional Homology to Mouse CD103+ Nonlymphoid Dendritic Cells. *Immunity*, 37(1), 60. <https://doi.org/10.1016/J.IMMUNI.2012.04.012>
- Heesters, B. A., Chatterjee, P., Kim, Y. A., Gonzalez, S. F., Kuligowski, M. P., Kirchhausen, T., & Carroll, M. C. (2013). Endocytosis and recycling of immune complexes by follicular dendritic cells enhances B cell antigen binding and activation. *Immunity*, 38(6), 1164–1175. <https://doi.org/10.1016/J.IMMUNI.2013.02.023>
- Hegazy, A. N., Peine, C., Niesen, D., Panse, I., Vainshtein, Y., Kommer, C., Zhang, Q., Brunner, T. M., Peine, M., Fröhlich, A., Ishaque, N., Marek, R. M., Zhu, J., Höfer, T., & Löhnig, M. (2022). Plasticity and lineage commitment of individual Th1 cells are determined by stable T-bet expression quantities. *BioRxiv*, 2022.08.14.503916. <https://doi.org/10.1101/2022.08.14.503916>

- Hémont, C., Neel, A., Heslan, M., Braudeau, C., & Josien, R. (2013a). Human blood mDC subsets exhibit distinct TLR repertoire and responsiveness. *Journal of Leukocyte Biology*, 93(4), 599–609. <https://doi.org/10.1189/JLB.0912452>
- Hémont, C., Neel, A., Heslan, M., Braudeau, C., & Josien, R. (2013b). Human blood mDC subsets exhibit distinct TLR repertoire and responsiveness. *Journal of Leukocyte Biology*, 93(4), 599–609. <https://doi.org/10.1189/JLB.0912452>
- Hendriks, J., Gravestein, L. A., Tesselaar, K., van Lier, R. A. W., Schumacher, T. N. M., & Borst, J. (2000). CD27 is required for generation and long-term maintenance of T cell immunity. *Nature Immunology*, 1(5), 433–440. <https://doi.org/10.1038/80877>
- Herndler-Brandstetter, D., Landgraf, K., Jenewein, B., Tzankov, A., Brunauer, R., Brunner, S., Parson, W., Kloss, F., Gassner, R., Lepperdinger, G., & Grubeck-Loebenstein, B. (2011). Human Bone Marrow Hosts Polyfunctional Memory CD4 + and CD8 + T Cells with Close Contact to IL-15-Producing Cells . *The Journal of Immunology*, 186(12), 6965–6971. <https://doi.org/10.4049/jimmunol.1100243>
- Hirota, K., Turner, J. E., Villa, M., Duarte, J. H., Demengeot, J., Steinmetz, O. M., & Stockinger, B. (2013). TH17 cell plasticity in Peyer's patches is responsible for induction of T cell-dependent IgA responses. *Nature Immunology*, 14(4), 372. <https://doi.org/10.1038/NI.2552>
- Hou, C., Wu, Q., Ouyang, C., & Huang, T. (2016). Effects of an intravitreal injection of interleukin-35-expressing plasmid on pro-inflammatory and anti-inflammatory cytokines. *International Journal of Molecular Medicine*, 38(3), 713–720. <https://doi.org/10.3892/IJMM.2016.2688>
- Hou, J., Wang, S., Jia, M., Li, D., Liu, Y., Li, Z., Zhu, H., Xu, H., Sun, M., Lu, L., Zhou, Z., Peng, H., Zhang, Q., Fu, S., Liang, G., Yao, L., Yu, X., Carpp, L. N., Huang, Y., ... Shao, Y. (2017). A Systems Vaccinology Approach Reveals Temporal Transcriptomic Changes of Immune Responses to the Yellow Fever 17D Vaccine. *The Journal of Immunology*, 199(4), 1476–1489. <https://doi.org/10.4049/jimmunol.1700083>
- Hwang, E. S., Szabo, S. J., Schwartzberg, P. L., & Glimcher, L. H. (2005). T helper cell fate specified by kinase-mediated interaction of T-bet with GATA-3. *Science (New York, N.Y.)*, 307(5708), 430–433. <https://doi.org/10.1126/SCIENCE.1103336>
- Ivanov, I. I., McKenzie, B. S., Zhou, L., Tadokoro, C. E., Lepelley, A., Lafaille, J. J., Cua, D. J., & Littman, D. R. (2006). The orphan nuclear receptor ROR γ T directs the differentiation program of proinflammatory IL-17+ T helper cells. *Cell*, 126(6), 1121–1133. <https://doi.org/10.1016/J.CELL.2006.07.035>
- James, E. A., LaFond, R. E., Gates, T. J., Mai, D. T., Malhotra, U., & Kwok, W. W. (2013). Yellow Fever Vaccination Elicits Broad Functional CD4 + T Cell Responses That Recognize Structural and Nonstructural Proteins . *Journal of Virology*, 87(23), 12794–12804. <https://doi.org/10.1128/jvi.01160-13>

- Jardine, L., Barge, D., Ames-Draycott, A., Pagan, S., Cookson, S., Spickett, G., Haniffa, M., Collin, M., & Bigley, V. (2013). Rapid detection of dendritic cell and monocyte disorders using CD4 as a lineage marker of the human peripheral blood antigen-presenting cell compartment. *Frontiers in Immunology*, 4(DEC).
- [https://doi.org/10.3389/FIMMU.2013.00495/ABSTRACT](https://doi.org/10.3389/FIMMU.2013.00495)
- Jarjour, M., Jorquera, A., Mondor, I., Wienert, S., Narang, P., Coles, M. C., Klauschen, F., & Bajénoff, M. (2014). Fate mapping reveals origin and dynamics of lymph node follicular dendritic cells. *The Journal of Experimental Medicine*, 211(6), 1109–1122.
- <https://doi.org/10.1084/JEM.20132409>
- Jay, D. C., Mitchell, D. M., & Williams, M. A. (2013). Bim Mediates the Elimination of Functionally Unfit Th1 Responders from the Memory Pool. *PLOS ONE*, 8(6), e67363. <https://doi.org/10.1371/JOURNAL.PONE.0067363>
- Jego, G., Palucka, A. K., Blanck, J. P., Chalouni, C., Pascual, V., & Banchereau, J. (2003). Plasmacytoid dendritic cells induce plasma cell differentiation through type I interferon and interleukin 6. *Immunity*, 19(2), 225–234.
- [https://doi.org/10.1016/S1074-7613\(03\)00208-5](https://doi.org/10.1016/S1074-7613(03)00208-5)
- Jolley-Gibbs, D. M., Brown, D. M., Dibble, J. P., Haynes, L., Eaton, S. M., & Swain, S. L. (2005). Unexpected prolonged presentation of influenza antigens promotes CD4 T cell memory generation. *The Journal of Experimental Medicine*, 202(5), 697.
- <https://doi.org/10.1084/JEM.20050227>
- Joffre, O. P., Sancho, D., Zelenay, S., Keller, A. M., & Reis E Sousa, C. (2010). Efficient and versatile manipulation of the peripheral CD4+ T-cell compartment by antigen targeting to DNGR-1/CLEC9A. *European Journal of Immunology*, 40(5), 1255–1265.
- <https://doi.org/10.1002/EJI.201040419>
- Johnston, R. J., Poholek, A. C., DiToro, D., Yusuf, I., Eto, D., Barnett, B., Dent, A. L., Craft, J., & Crotty, S. (2009). Bcl6 and Blimp-1 are reciprocal and antagonistic regulators of T follicular helper cell differentiation. *Science (New York, N.Y.)*, 325(5943), 1006–1010. <https://doi.org/10.1126/SCIENCE.1175870>
- Jones, C. P., Gregory, L. G., Causton, B., Campbell, G. A., & Lloyd, C. M. (2012). Activin A and TGF- β promote TH9 cell-mediated pulmonary allergic pathology. *The Journal of Allergy and Clinical Immunology*, 129(4), 1000.
- <https://doi.org/10.1016/J.JACI.2011.12.965>
- Jongbloed, S. L., Kassianos, A. J., McDonald, K. J., Clark, G. J., Ju, X., Angel, C. E., Chen, C. J. J., Dunbar, P. R., Wadley, R. B., Jeet, V., Vulink, A. J. E., Hart, D. N. J., & Radford, K. J. (2010). Human CD141+ (BDCA-3)+ dendritic cells (DCs) represent a unique myeloid DC subset that cross-presents necrotic cell antigens. *The Journal of Experimental Medicine*, 207(6), 1247–1260. <https://doi.org/10.1084/JEM.20092140>

- Jun, J. il, & Lau, L. F. (2020). CCN1 is an opsonin for bacterial clearance and a direct activator of Toll-like receptor signaling. *Nature Communications* 2020 11:1, 11(1), 1–15. <https://doi.org/10.1038/s41467-020-15075-5>
- Kaech, S. M., Tan, J. T., Wherry, E. J., Konieczny, B. T., Surh, C. D., & Ahmed, R. (2003). Selective expression of the interleukin 7 receptor identifies effector CD8 T cells that give rise to long-lived memory cells. *Nature Immunology*, 4(12), 1191–1198. <https://doi.org/10.1038/NI1009>
- Kaji, T., Ishige, A., Hikida, M., Taka, J., Hijikata, A., Kubo, M., Nagashima, T., Takahashi, Y., Kurosaki, T., Okada, M., Ohara, O., Rajewsky, K., & Takemori, T. (2012). Distinct cellular pathways select germline-encoded and somatically mutated antibodies into immunological memory. *The Journal of Experimental Medicine*, 209(11), 2079. <https://doi.org/10.1084/JEM.20120127>
- Kaplan, M. H. (2013). Th9 cells: differentiation and disease. *Immunological Reviews*, 252(1), 104–115. <https://doi.org/10.1111/imr.12028>
- Kato, Y., Zaid, A., Davey, G. M., Mueller, S. N., Nutt, S. L., Zotos, D., Tarlinton, D. M., Shortman, K., Lahoud, M. H., Heath, W. R., & Caminschi, I. (2015). Targeting Antigen to Clec9A Primes Follicular Th Cell Memory Responses Capable of Robust Recall. *Journal of Immunology (Baltimore, Md.: 1950)*, 195(3), 1006–1014. <https://doi.org/10.4049/JIMMUNOL.1500767>
- Khaled, A. R., Li, W. Q., Huang, J., Fry, T. J., Khaled, A. S., Mackall, C. L., Muegge, K., Young, H. A., & Durum, S. K. (2002). Bax deficiency partially corrects interleukin-7 receptor alpha deficiency. *Immunity*, 17(5), 561–573. [https://doi.org/10.1016/S1074-7613\(02\)00450-8](https://doi.org/10.1016/S1074-7613(02)00450-8)
- Kitano, M., Moriyama, S., Ando, Y., Hikida, M., Mori, Y., Kurosaki, T., & Okada, T. (2011). Bcl6 Protein Expression Shapes Pre-Germinal Center B Cell Dynamics and Follicular Helper T Cell Heterogeneity. *Immunity*, 34(6), 961–972. <https://doi.org/10.1016/J.IMMUNI.2011.03.025>
- Klaus, G. G., & Humphrey, J. H. (1977). The generation of memory cells. I. The role of C3 in the generation of B memory cells. *Immunology*, 33(1), 31. [/pmc/articles/PMC1445413/?report=abstract](https://PMC1445413/?report=abstract)
- Koguchi, Y., Buenafe, A. C., Thauland, T. J., Gardell, J. L., Bivins-Smith, E. R., Jacoby, D. B., Slifka, M. K., & Parker, D. C. (2012). Preformed CD40L is stored in Th1, Th2, Th17, and T follicular helper cells as well as CD4+ 8- thymocytes and invariant NKT cells but not in Treg cells. *PloS One*, 7(2). <https://doi.org/10.1371/JOURNAL.PONE.0031296>
- Koguchi, Y., Thauland, T. J., Slifka, M. K., & Parker, D. C. (2007). Preformed CD40 ligand exists in secretory lysosomes in effector and memory CD4+ T cells and is quickly expressed on the cell surface in an antigen-specific manner. *Blood*, 110(7), 2520–2527. <https://doi.org/10.1182/BLOOD-2007-03-081299>

- Kolls, J. K., & Lindén, A. (2004). Interleukin-17 family members and inflammation. *Immunity*, 21(4), 467–476. <https://doi.org/10.1016/J.IMMUNI.2004.08.018>
- Komatsu, N., Okamoto, K., Sawa, S., Nakashima, T., Oh-Hora, M., Kodama, T., Tanaka, S., Bluestone, J. A., & Takayanagi, H. (2013). Pathogenic conversion of Foxp3+ T cells into TH17 cells in autoimmune arthritis. *Nature Medicine* 2013 20:1, 20(1), 62–68. <https://doi.org/10.1038/nm.3432>
- Kondrack, R. M., Harbertson, J., Tan, J. T., McBreen, M. E., Surh, C. D., & Bradley, L. M. (2003). Interleukin 7 Regulates the Survival and Generation of Memory CD4 Cells. *Journal of Experimental Medicine*, 198(12), 1797–1806. <https://doi.org/10.1084/JEM.20030735>
- Kong, K. F., Yokosuka, T., Canonigo-Balancio, A. J., Isakov, N., Saito, T., & Altman, A. (2011). A motif in the V3 domain of the kinase PKC-θ determines its localization in the immunological synapse and functions in T cells via association with CD28. *Nature Immunology*, 12(11), 1105–1112. <https://doi.org/10.1038/NI.2120>
- Koopman, G., Keehnen, R. M., Lindhout, E., Newman, W., Shimizu, Y., van Seventer, G. A., de Groot, C., & Pals, S. T. (1994). Adhesion through the LFA-1 (CD11a/CD18)-ICAM-1 (CD54) and the VLA-4 (CD49d)-VCAM-1 (CD106) pathways prevents apoptosis of germinal center B cells. *The Journal of Immunology*, 152(8).
- Kranich, J., Krautler, N. J., Heinen, E., Polymenidou, M., Bridel, C., Schildknecht, A., Huber, C., Kosco-Vilbois, M. H., Zinkernagel, R., Miele, G., & Aguzzi, A. (2008). Follicular dendritic cells control engulfment of apoptotic bodies by secreting Mfge8. *The Journal of Experimental Medicine*, 205(6), 1293–1302. <https://doi.org/10.1084/JEM.20071019>
- Krautler, N. J., Kana, V., Kranich, J., Tian, Y., Perera, D., Lemm, D., Schwarz, P., Armulik, A., Browning, J. L., Tallquist, M., Buch, T., Oliveira-Martins, J. B., Zhu, C., Hermann, M., Wagner, U., Brink, R., Heikenwalder, M., & Aguzzi, A. (2012). Follicular dendritic cells emerge from ubiquitous perivascular precursors. *Cell*, 150(1), 194–206. <https://doi.org/10.1016/J.CELL.2012.05.032>
- Kroenke, M. A., Eto, D., Locci, M., Cho, M., Davidson, T., Haddad, E. K., & Crotty, S. (2012). Bcl6 and Maf cooperate to instruct human follicular helper CD4 T cell differentiation. *Journal of Immunology (Baltimore, Md.: 1950)*, 188(8), 3734–3744. <https://doi.org/10.4049/JIMMUNOL.1103246>
- Kumar, H., Kawai, T., & Akira, S. (2009). Toll-like receptors and innate immunity. *Biochemical and Biophysical Research Communications*, 388(4), 621–625. <https://doi.org/10.1016/J.BBRC.2009.08.062>
- Kwok, W. W., Tan, V., Gillette, L., Littell, C. T., Soltis, M. A., LaFond, R. B., Yang, J., James, E. A., & DeLong, J. H. (2012). Frequency of epitope-specific naive CD4(+) T cells correlates with immunodominance in the human memory repertoire. *Journal of*

Immunology (Baltimore, Md.: 1950), 188(6), 2537–2544.

<https://doi.org/10.4049/JIMMUNOL.1102190>

Ladle, B. H., Li, K. P., Phillips, M. J., Pucsek, A. B., Haile, A., Powell, J. D., Jaffee, E. M., Hildeman, D. A., & Gamper, C. J. (2016). De novo DNA methylation by DNA methyltransferase 3a controls early effector CD8+ T-cell fate decisions following activation. *Proceedings of the National Academy of Sciences of the United States of America, 113*(38), 10631–10636.
https://doi.org/10.1073/PNAS.1524490113/SUPPL_FILE/PNAS.1524490113.SD04.XLSX

Langrish, C. L., Chen, Y., Blumenschein, W. M., Mattson, J., Basham, B., Sedgwick, J. D., McClanahan, T., Kastlein, R. A., & Cua, D. J. (2005). IL-23 drives a pathogenic T cell population that induces autoimmune inflammation. *The Journal of Experimental Medicine, 201*(2), 233–240. <https://doi.org/10.1084/JEM.20041257>

Lanzavecchia, A., & Sallusto, F. (2002). Progressive differentiation and selection of the fittest in the immune response. *Nature Reviews. Immunology, 2*(12), 982–987.
<https://doi.org/10.1038/NRI959>

Leal Rojas, I. M., Mok, W. H., Pearson, F. E., Minoda, Y., Kenna, T. J., Barnard, R. T., & Radford, K. J. (2017). Human Blood CD1c + Dendritic Cells Promote Th1 and Th17 Effector Function in Memory CD4 + T Cells. *Frontiers in Immunology, 8*(AUG).
<https://doi.org/10.3389/FIMMU.2017.00971>

Lebre, M. C., van der Aar, A. M. G., van Baarsen, L., van Capel, T. M. M., Schuitemaker, J. H. N., Kapsenberg, M. L., & de Jong, E. C. (2007). Human Keratinocytes Express Functional Toll-Like Receptor 3, 4, 5, and 9. *Journal of Investigative Dermatology, 127*(2), 331–341. <https://doi.org/10.1038/SJ.JID.5700530>

le Grand, R., Dereuddre-Bosquet, N., Dispineri, S., Gosse, L., Desjardins, D., Shen, X., Tolazzi, M., Ochsenbauer, C., Saidi, H., Tomaras, G., Prague, M., Barnett, S. W., Thiebaut, R., Cope, A., Scarlatti, G., & Shattock, R. J. (2016). Superior Efficacy of a Human Immunodeficiency Virus Vaccine Combined with Antiretroviral Prevention in Simian-Human Immunodeficiency Virus-Challenged Nonhuman Primates. *Journal of Virology, 90*(11), 5315–5328. <https://doi.org/10.1128/JVI.00230-16>

Lemaitre, B., Nicolas, E., Michaut, L., Reichhart, J. M., & Hoffmann, J. A. (1996). The dorsoventral regulatory gene cassette spätzle/Toll/cactus controls the potent antifungal response in *Drosophila* adults. *Cell, 86*(6), 973–983.
[https://doi.org/10.1016/S0092-8674\(00\)80172-5](https://doi.org/10.1016/S0092-8674(00)80172-5)

Lexberg, M. H., Taubner, A., Förster, A., Albrecht, I., Richter, A., Kamradt, T., Radbruch, A., & Chang, H. D. (2008). Th memory for interleukin-17 expression is stable in vivo. *European Journal of Immunology, 38*(10), 2654–2664.
<https://doi.org/10.1002/EJI.200838541>

- L, G., E, L., Y, J., Z, P., CM, P., MF, Q., JR, A., E, G., Z, Y., C, C., E, W., DC, D., DA, P., CH, J., FM, M., M, R., & NP, R. (2011). A human memory T cell subset with stem cell-like properties. *Nature Medicine*, 17(10), 1290–1297. <https://doi.org/10.1038/NM.2446>
- Liao, W., Hua, Z., Liu, C., Lin, L., Chen, R., & Hou, B. (2017a). Characterization of T-Dependent and T-Independent B Cell Responses to a Virus-like Particle. *The Journal of Immunology*, 198(10), 3846–3856.
<https://doi.org/10.4049/JIMMUNOL.1601852/-/DCSUPPLEMENTAL>
- Liao, W., Hua, Z., Liu, C., Lin, L., Chen, R., & Hou, B. (2017b). Characterization of T-Dependent and T-Independent B Cell Responses to a Virus-like Particle. *The Journal of Immunology*, 198(10), 3846–3856.
<https://doi.org/10.4049/jimmunol.1601852>
- Liard, C., Munier, S., Joulin-Giet, A., Bonduelle, O., Hadam, S., Duffy, D., Vogt, A., Verrier, B., & Combadière, B. (2012). Intradermal immunization triggers epidermal Langerhans cell mobilization required for CD8 T-cell immune responses. *The Journal of Investigative Dermatology*, 132(3 Pt 1), 615–625.
<https://doi.org/10.1038/JID.2011.346>
- Li, D., & Wu, M. (2021). Pattern recognition receptors in health and diseases. *Signal Transduction and Targeted Therapy* 2021 6:1, 6(1), 1–24.
<https://doi.org/10.1038/s41392-021-00687-0>
- Li, G., Cheng, L., & Su, L. (2021). Phenotypic and Functional Study of Human Plasmacytoid Dendritic Cells. *Current Protocols*, 1(4), e50.
<https://doi.org/10.1002/CPZ1.50>
- Lighvani, A. A., Frucht, D. M., Jankovic, D., Yamane, H., Aliberti, J., Hissong, B. D., Nguyen, B. v., Gadina, M., Sher, A., Paul, W. E., & O'Shea, J. J. (2001). T-bet is rapidly induced by interferon- γ in lymphoid and myeloid cells. *Proceedings of the National Academy of Sciences of the United States of America*, 98(26), 15137–15142.
<https://doi.org/10.1073/PNAS.261570598>
- Li, J., Ahmet, F., Sullivan, L. C., Brooks, A. G., Kent, S. J., de Rose, R., Salazar, A. M., Reis e Sousa, C., Shortman, K., Lahoud, M. H., Heath, W. R., & Caminschi, I. (2015). Antibodies targeting Clec9A promote strong humoral immunity without adjuvant in mice and non-human primates. *European Journal of Immunology*, 45(3), 854–864. <https://doi.org/10.1002/EJI.201445127>
- Li, J. C., Huston, G., & Swain, S. L. (2003). IL-7 Promotes the Transition of CD4 Effectors to Persistent Memory Cells. *Journal of Experimental Medicine*, 198(12), 1807–1815.
<https://doi.org/10.1084/JEM.20030725>
- Lindsey, N. P., Horiuchi, K. A., Fulton, C., Panella, A. J., Kosoy, O. I., Velez, J. O., Krow-Lucal, E. R., Fischer, M., & Staples, J. E. (2018). Persistence of yellow fever virus-specific neutralizing antibodies after vaccination among US travellers. *Journal of Travel Medicine*, 25(1), 1–6. <https://doi.org/10.1093/JTM/TAY108>

- Li, S., Roush, N., Duraisingham, S., Romero-Steiner, S., Presnell, S., Davis, C., Schmidt, D. S., Johnson, S. E., Milton, A., Rajam, G., Kasturi, S., Carlone, G. M., Quinn, C., Chaussabel, D., Palucka, A. K., Mulligan, M. J., Ahmed, R., Stephens, D. S., Nakaya, H. I., & Pulendran, B. (2014). Molecular signatures of antibody responses derived from a systems biology study of five human vaccines. *Nature Immunology*, 15(2), 195–204. <https://doi.org/10.1038/ni.2789>
- Liu, X., Zhao, Y., & Qi, H. (2022). T-independent antigen induces humoral memory through germinal centers. *Journal of Experimental Medicine*, 219(3). <https://doi.org/10.1084/JEM.20210527/212958>
- Locci, M., Havenar-Daughton, C., Landais, E., Wu, J., Kroenke, M. A., Arlehamn, C. L., Su, L. F., Cubas, R., Davis, M. M., Sette, A., Haddad, E. K., Poignard, P., & Crotty, S. (2013). Human circulating PD-1+CXCR3-CXCR5+ memory Tfh cells are highly functional and correlate with broadly neutralizing HIV antibody responses. *Immunity*, 39(4), 758–769. <https://doi.org/10.1016/J.IMMUNI.2013.08.031>
- Loebbermann, J., Thornton, H., Durant, L., Sparwasser, T., Webster, K. E., Sprent, J., Culley, F. J., Johansson, C., & Openshaw, P. J. (2012). Regulatory T cells expressing granzyme B play a critical role in controlling lung inflammation during acute viral infection. *Mucosal Immunology* 2012 5:2, 5(2), 161–172. <https://doi.org/10.1038/mi.2011.62>
- Io Kien Wei Siah Chi Heem Wong, A. W., Lo, A. W., Wei Siah, K., & Heem Wong, C. (2020). *Estimating Probabilities of Success of Vaccine and Other Anti-Infective Therapeutic Development Programs*. <https://doi.org/10.3386/W27176>
- Luckheeram, R. V., Zhou, R., Verma, A. D., & Xia, B. (2012). CD4⁺T cells: differentiation and functions. *Clinical & Developmental Immunology*, 2012. <https://doi.org/10.1155/2012/925135>
- Lugo-Villarino, G., Maldonado-López, R., Possemato, R., Peñaranda, C., & Glimcher, L. H. (2003). T-bet is required for optimal production of IFN-γ and antigen-specific T cell activation by dendritic cells. *Proceedings of the National Academy of Sciences of the United States of America*, 100(13), 7749–7754. <https://doi.org/10.1073/PNAS.1332767100>
- Lu, K. T., Kanno, Y., Cannons, J. L., Handon, R., Bible, P., Elkahloun, A. G., Anderson, S. M., Wei, L., Sun, H., O'Shea, J. J., & Schwartzberg, P. L. (2011). Functional and epigenetic studies reveal multistep differentiation and plasticity of in vitro-generated and in vivo-derived follicular T helper cells. *Immunity*, 35(4), 622–632. <https://doi.org/10.1016/J.IMMUNI.2011.07.015>
- Luther, S. A., Tang, H. L., Hyman, P. L., Farr, A. G., & Cyster, J. G. (2000). Coexpression of the chemokines ELC and SLC by T zone stromal cells and deletion of the ELC gene in the plt=plt mouse. *Proceedings of the National Academy of Sciences of the United States of America*, 97(23), 12694–12699. <https://doi.org/10.1073/PNAS.97.23.12694>

- Mackay, F., & Browning, J. L. (2002). BAFF: A fundamental survival factor for B cells. *Nature Reviews Immunology*, 2(7), 465–475. <https://doi.org/10.1038/nri844>
- Mackay, F., Majeau, G. R., Lawton, P., Hochman, P. S., & Browning, J. L. (1997). Lymphotoxin but not tumor necrosis factor functions to maintain splenic architecture and humoral responsiveness in adult mice. *European Journal of Immunology*, 27(8), 2033–2042. <https://doi.org/10.1002/EJI.1830270830>
- MacLeod, M. K. L., Kappler, J. W., & Marrack, P. (2010). Memory CD4 T cells: generation, reactivation and re-assignment. *Immunology*, 130(1), 10–15. <https://doi.org/10.1111/J.1365-2567.2010.03260.X>
- MacLeod, M., Kwakkenbos, M. J., Crawford, A., Brown, S., Stockinger, B., Schepers, K., Schumacher, T., & Gray, D. (2006). CD4 memory T cells survive and proliferate but fail to differentiate in the absence of CD40. *The Journal of Experimental Medicine*, 203(4), 897–906. <https://doi.org/10.1084/JEM.20050711>
- Martinez-Sanchez, M. E., Huerta, L., Alvarez-Buylla, E. R., & Luján, C. V. (2018). Role of cytokine combinations on CD4+ T cell differentiation, partial polarization, and plasticity: Continuous network modeling approach. *Frontiers in Physiology*, 9(AUG), 877. <https://doi.org/10.3389/FPHYS.2018.00877/BIBTEX>
- Martín-Gayo, E., Sierra-Filardi, E., Corbí, A. L., & Toribio, M. L. (2010). Plasmacytoid dendritic cells resident in human thymus drive natural Treg cell development. *Blood*, 115(26), 5366–5375. <https://doi.org/10.1182/BLOOD-2009-10-248260>
- Masopust, D., & Schenkel, J. M. (2013). The integration of T cell migration, differentiation and function. *Nature Reviews Immunology*, 13(5), 309–320. <https://doi.org/10.1038/nri3442>
- Mateus, J., Grifoni, A., Tarke, A., Sidney, J., Ramirez, S. I., Dan, J. M., Burger, Z. C., Rawlings, S. A., Smith, D. M., Phillips, E., Mallal, S., Lammers, M., Rubiro, P., Quiambao, L., Sutherland, A., Yu, E. D., da Silva Antunes, R., Greenbaum, J., Frazier, A., ... Weiskopf, D. (2020). Selective and cross-reactive SARS-CoV-2 T cell epitopes in unexposed humans. *Science (New York, N.Y.)*, 370(6512). <https://doi.org/10.1126/SCIENCE.ABD3871>
- Matos, T. R., Gehad, A., Teague, J. E., Dyring-Andersen, B., Benezeder, T., Dowlatshahi, M., Crouch, J., Watanabe, Y., O'Malley, J. T., Kupper, T. S., Yang, C., Watanabe, R., & Clark, R. A. (2022). Central memory T cells are the most effective precursors of resident memory T cells in human skin. *Science Immunology*, 7(70). https://doi.org/10.1126/SCIIMMUNOL.ABN1889/SUPPL_FILE/SCIIMMUNOL.ABN1889_MDAR
- McBride, J. M., Jung, T., de Vries, J. E., & Aversa, G. (2002). IL-10 alters DC function via modulation of cell surface molecules resulting in impaired T-cell responses.

Cellular Immunology, 215(2), 162–172. [https://doi.org/10.1016/S0008-8749\(02\)00007-2](https://doi.org/10.1016/S0008-8749(02)00007-2)

- McGeachy, M. J., Bak-Jensen, K. S., Chen, Y., Tato, C. M., Blumenschein, W., McClanahan, T., & Cua, D. J. (2007). TGF-beta and IL-6 drive the production of IL-17 and IL-10 by T cells and restrain T(H)-17 cell-mediated pathology. *Nature Immunology*, 8(12), 1390–1397. <https://doi.org/10.1038/NI1539>
- McKinstry, K. K., Strutt, T. M., Bautista, B., Zhang, W., Kuang, Y., Cooper, A. M., & Swain, S. L. (2014). Effector CD4 T-cell transition to memory requires late cognate interactions that induce autocrine IL-2. *Nature Communications* 2014 5:1, 5(1), 1–12. <https://doi.org/10.1038/ncomms6377>
- Meitei, H. T., & Lal, G. (2022). T cell receptor signaling in the differentiation and plasticity of CD4+ T cells. *Cytokine & Growth Factor Reviews*. <https://doi.org/10.1016/J.CYTOGFR.2022.08.001>
- Mercado, R., Vijh, S., Allen, S. E., Kerksiek, K., Pilip, I. M., & Pamer, E. G. (2000). Early programming of T cell populations responding to bacterial infection. *Journal of Immunology (Baltimore, Md.: 1950)*, 165(12), 6833–6839. <https://doi.org/10.4049/JIMMUNOL.165.12.6833>
- Messi, M., Giacchettto, I., Nagata, K., Lanzavecchia, A., Natoli, G., & Sallusto, F. (2003). Memory and flexibility of cytokine gene expression as separable properties of human T(H)1 and T(H)2 lymphocytes. *Nature Immunology*, 4(1), 78–86. <https://doi.org/10.1038/NI872>
- Mikhak, Z., Fukui, M., Farsidjani, A., Medoff, B. D., Tager, A. M., & Luster, A. D. (2009). Contribution of CCR4 and CCR8 to antigen-specific Th2 cell trafficking in allergic pulmonary inflammation. *The Journal of Allergy and Clinical Immunology*, 123(1), 67. <https://doi.org/10.1016/J.JACI.2008.09.049>
- Monath, T. P. (2001). Yellow fever: An update. In *Lancet Infectious Diseases* (Vol. 1, Issue 1, pp. 11–20). [https://doi.org/10.1016/S1473-3099\(01\)00016-0](https://doi.org/10.1016/S1473-3099(01)00016-0)
- Monath, T. P., Fowler, E., Johnson, C. T., Balser, J., Morin, M. J., Sisti, M., & Trent, D. W. (2011). An inactivated cell-culture vaccine against yellow fever. *New England Journal of Medicine*, 364(14), 1326–1333. <https://doi.org/10.1056/NEJMoa1009303>
- Monath, T. P., Lee, C. K., Julander, J. G., Brown, A., Beasley, D. W., Watts, D. M., Hayman, E., Guertin, P., Makowiecki, J., Crowell, J., Levesque, P., Bowick, G. C., Morin, M., Fowler, E., & Trent, D. W. (2010). Inactivated yellow fever 17D vaccine: Development and nonclinical safety, immunogenicity and protective activity. *Vaccine*, 28(22), 3827–3840. <https://doi.org/10.1016/j.vaccine.2010.03.023>
- Monks, C. R. F., Freiberg, B. A., Kupfer, H., Sciaky, N., & Kupfer, A. (1998). Three-dimensional segregation of supramolecular activation clusters in T cells. *Nature* 1998 395:6697, 395(6697), 82–86. <https://doi.org/10.1038/25764>

- Moon, J. J., Chu, H. H., Pepper, M., McSorley, S. J., Jameson, S. C., Kedl, R. M. M., & Jenkins, M. K. (2007). Naive CD4(+) T cell frequency varies for different epitopes and predicts repertoire diversity and response magnitude. *Immunity*, 27(2), 203–213. <https://doi.org/10.1016/J.IMMUNI.2007.07.007>
- Moreno, E. S., Spinola, R., Tengan, C. H., Brasil, R. A., Siciliano, M. M., Coimbra, T. L. M., Silveira, V. R., Rocco, I. M., Bisordi, I., de Souza, R. P., Petrella, S., Pereira, L. E., Maeda, A. Y., da Silva, F. G., & Suzuki, A. (2013). Yellow fever epizootics in non-human primates, São Paulo state, Brazil, 2008-2009. *Revista Do Instituto de Medicina Tropical de Sao Paulo*, 55(1), 45–50. <https://doi.org/10.1590/S0036-46652013000100008>
- Morita, R., Schmitt, N., Bentebibel, S. E., Ranganathan, R., Bourdery, L., Zurawski, G., Foucat, E., Dullaers, M., Oh, S. K., Sabzghabaei, N., Lavecchia, E. M., Punaro, M., Pascual, V., Banchereau, J., & Ueno, H. (2011). Human blood CXCR5(+)CD4(+) T cells are counterparts of T follicular cells and contain specific subsets that differentially support antibody secretion. *Immunity*, 34(1), 108–121. <https://doi.org/10.1016/J.IMMUNI.2010.12.012>
- Mueller, S. N., & Mackay, L. K. (2015). Tissue-resident memory T cells: local specialists in immune defence. *Nature Reviews Immunology* 2015 16:2, 16(2), 79–89. <https://doi.org/10.1038/nri.2015.3>
- Murphy, T. L., Grajales-Reyes, G. E., Wu, X., Tussiwand, R., Briseño, C. G., Iwata, A., Kretzer, N. M., Durai, V., & Murphy, K. M. (2016). Transcriptional Control of Dendritic Cell Development. *Annual Review of Immunology*, 34, 93–119. <https://doi.org/10.1146/ANNUREV-IMMUNOL-032713-120204>
- Nagai, S., & Azuma, M. (2019). The CD28-B7 Family of Co-signaling Molecules. *Advances in Experimental Medicine and Biology*, 1189, 25–51. https://doi.org/10.1007/978-981-32-9717-3_2
- Nakaya, H. I., Clutterbuck, E., Kazmin, D., Wang, L., Cortese, M., Bosinger, S. E., Patel, N. B., Zak, D. E., Aderem, A., Dong, T., del Giudice, G., Rappuoli, R., Cerundolo, V., Pollard, A. J., Pulendran, B., & Siegrist, C. A. (2016). Systems biology of immunity to MF59-adjuvanted versus nonadjuvanted trivalent seasonal influenza vaccines in early childhood. *Proceedings of the National Academy of Sciences of the United States of America*, 113(7), 1853–1858. <https://doi.org/10.1073/PNAS.1519690113/-DCSUPPLEMENTAL>
- Nakayamada, S., Kanno, Y., Takahashi, H., Jankovic, D., Lu, K. T., Johnson, T. A., Sun, H. wei, Vahedi, G., Hakim, O., Handon, R., Schwartzberg, P. L., Hager, G. L., & O’Shea, J. J. (2011). Early Th1 cell differentiation is marked by a Tfh cell-like transition. *Immunity*, 35(6), 919–931. <https://doi.org/10.1016/J.IMMUNI.2011.11.012>
- Nayak, J. L., Fitzgerald, T. F., Richards, K. A., Yang, H., Treanor, J. J., & Sant, A. J. (2013). CD4+ T-cell expansion predicts neutralizing antibody responses to monovalent, inactivated 2009 pandemic influenza A(H1N1) virus subtype H1N1 vaccine. *The*

Journal of Infectious Diseases, 207(2), 297–305.

<https://doi.org/10.1093/INFDIS/JIS684>

Ndeupen, S., Bouteau, A., Herbst, C., Qin, Z., Jacobsen, S., Powers, N. E., Hutchins, Z., Kurup, D., Diba, L. Z., Watson, M., Ramage, H., & Igyártó, B. Z. (2022). Langerhans cells and cDC1s play redundant roles in mRNA-LNP induced protective anti-influenza and anti-SARS-CoV-2 immune responses. *PLOS Pathogens*, 18(1), e1010255. <https://doi.org/10.1371/JOURNAL.PPAT.1010255>

Netea, M. G., Schlitzer, A., Placek, K., Joosten, L. A. B., & Schultze, J. L. (2019). Innate and Adaptive Immune Memory: an Evolutionary Continuum in the Host's Response to Pathogens. In *Cell Host and Microbe* (Vol. 25, Issue 1, pp. 13–26). Cell Press. <https://doi.org/10.1016/j.chom.2018.12.006>

Ngo, V. N., Korner, H., Gunn, M. D., Schmidt, K. N., Riminton, D. S., Cooper, M. D., Browning, J. L., Sedgwick, J. D., & Cyster, J. G. (1999). Lymphotoxin alpha/beta and tumor necrosis factor are required for stromal cell expression of homing chemokines in B and T cell areas of the spleen. *The Journal of Experimental Medicine*, 189(2), 403–412. <https://doi.org/10.1084/JEM.189.2.403>

Nienen, M., Stervbo, U., Mölder, F., Kaliszczyk, S., Kuchenbecker, L., Gayova, L., Schweiger, B., Jürchott, K., Hecht, J., Neumann, A. U., Rahmann, S., Westhoff, T., Reinke, P., Thiel, A., & Babel, N. (2019). The role of pre-existing cross-reactive central memory CD4 T-cells in vaccination with previously unseen influenza strains. *Frontiers in Immunology*, 10(APR), 593. [https://doi.org/10.3389/FIMMU.2019.00593/BIBTEX](https://doi.org/10.3389/FIMMU.2019.00593)

Nizzoli, G., Krietsch, J., Weick, A., Steinfelder, S., Facciotti, F., Gruarin, P., Bianco, A., Steckel, B., Moro, M., Crosti, M., Romagnani, C., Stölzel, K., Torretta, S., Pignataro, L., Scheibenbogen, C., Neddermann, P., de Francesco, R., Abrignani, S., & Geginat, J. (2013). Human CD1c+ dendritic cells secrete high levels of IL-12 and potently prime cytotoxic T-cell responses. *Blood*, 122(6), 932–942. <https://doi.org/10.1182/BLOOD-2013-04-495424>

Nizzoli, G., Larghi, P., Paroni, M., Crosti, M. C., Moro, M., Neddermann, P., Caprioli, F., Pagani, M., de Francesco, R., Abrignani, S., & Geginat, J. (2016). IL-10 promotes homeostatic proliferation of human CD8(+) memory T cells and, when produced by CD1c(+) DCs, shapes naive CD8(+) T-cell priming. *European Journal of Immunology*, 46(7), 1622–1632. <https://doi.org/10.1002/EJI.201546136>

Nolz, J. C., & Harty, J. T. (2014). IL-15 regulates memory CD8+ T cell O-glycan synthesis and affects trafficking. *The Journal of Clinical Investigation*, 124(3), 1013. <https://doi.org/10.1172/JCI72039>

Obst, R., van Santen, H. M., Mathis, D., & Benoist, C. (2005). Antigen persistence is required throughout the expansion phase of a CD4+ T cell response. *The Journal of Experimental Medicine*, 201(10), 1555. <https://doi.org/10.1084/JEM.20042521>

- O'Connor, B. P., Raman, V. S., Erickson, L. D., Cook, W. J., Weaver, L. K., Ahonen, C., Lin, L., Mantchev, G. T., Bram, R. J., & Noelle, R. J. (2004). BCMA Is Essential for the Survival of Long-lived Bone Marrow Plasma Cells. *The Journal of Experimental Medicine*, 199(1), 91. <https://doi.org/10.1084/JEM.20031330>
- Ogawa, L. M., & Vallender, E. J. (2014). Genetic substructure in cynomolgus macaques (*Macaca fascicularis*) on the island of Mauritius. *BMC Genomics*, 15(1), 1–14. <https://doi.org/10.1186/1471-2164-15-748/TABLES/2>
- O'Hagan, D. T., Ott, G. S., De Gregorio, E., & Seubert, A. (2012). The mechanism of action of MF59 – An innately attractive adjuvant formulation. *Vaccine*, 30(29), 4341–4348. <https://doi.org/10.1016/j.vaccine.2011.09.061>
- Ohl, L., Mohaupt, M., Czeloth, N., Hintzen, G., Kiafard, Z., Zwirner, J., Blankenstein, T., Henning, G., & Förster, R. (2004). CCR7 Governs Skin Dendritic Cell Migration under Inflammatory and Steady-State Conditions. *Immunity*, 21(2), 279–288. <https://doi.org/10.1016/j.immuni.2004.06.014>
- Okada, T., Ise, W., Shiroguchi, K., Kurosaki, T., Takeda, K., Kawakami, E., Ito, A., Suzuki, K., Kometani, K., Fujii, K., & Yamashita, K. (2018). T Follicular Helper Cell-Germinal Center B Cell Interaction Strength Regulates Entry into Plasma Cell or Recycling Germinal Center Cell Fate. *Immunity*, 48(4), 702–715.e4. <https://doi.org/10.1016/j.immuni.2018.03.027>
- Okhrimenko, A., Grün, J. R., Westendorf, K., Fang, Z., Reinke, S., von Roth, P., Wassilew, G., Kühl, A. A., Kudernatsch, R., Demski, S., Scheibenbogen, C., Tokoyoda, K., McGrath, M. A., Raftery, M. J., Schönrich, G., Serra, A., Chang, H. D., Radbruch, A., & Dong, J. (2014). Human memory T cells from the bone marrow are resting and maintain long-lasting systemic memory. *Proceedings of the National Academy of Sciences of the United States of America*, 111(25), 9229–9234. <https://doi.org/10.1073/PNAS.1318731111/-/DCSUPPLEMENTAL>
- Ols, S., Yang, L., Thompson, E. A., Pushparaj, P., Tran, K., Liang, F., Lin, A., Eriksson, B., Karlsson Hedestam, G. B., Wyatt, R. T., & Loré, K. (2020). Route of Vaccine Administration Alters Antigen Trafficking but Not Innate or Adaptive Immunity. *Cell Reports*, 30(12), 3964–3971.e7. <https://doi.org/10.1016/j.celrep.2020.02.111>
- Onodera, K., Fujiwara, T., Onishi, Y., Itoh-Nakadai, A., Okitsu, Y., Fukuhara, N., Ishizawa, K., Shimizu, R., Yamamoto, M., & Harigae, H. (2016). GATA2 regulates dendritic cell differentiation. *Blood*, 128(4), 508. <https://doi.org/10.1182/BLOOD-2016-02-698118>
- Ornatsky, O., Bandura, D., Baranov, V., Nitz, M., Winnik, M. A., & Tanner, S. (2010). Highly multiparametric analysis by mass cytometry. In *Journal of Immunological Methods*. <https://doi.org/10.1016/j.jim.2010.07.002>
- Padhan, K., Moysi, E., Noto, A., Chassiakos, A., Ghneim, K., Perra, M. M., Shah, S., Papaioannou, V., Fabozzi, G., Ambrozak, D. R., Poultysi, A., Ioannou, M., Fenwick,

C., Darko, S., Douek, D. C., Sekaly, R. P., Pantaleo, G., Koup, R. A., & Petrovas, C. (2021). Acquisition of optimal TFH cell function is defined by specific molecular, positional, and TCR dynamic signatures. *Proceedings of the National Academy of Sciences of the United States of America*, 118(18), e2016855118.
https://doi.org/10.1073/PNAS.2016855118/SUPPL_FILE/PNAS.2016855118.SM06.AVI

Pagán, A. J., Pepper, M., Chu, H. H., Green, J. M., & Jenkins, M. K. (2012). CD28 Promotes CD4+ T Cell Clonal Expansion During infection Independently of its YMNM and PYAP Motifs. *Journal of Immunology (Baltimore, Md.: 1950)*, 189(6), 2909.
<https://doi.org/10.4049/JIMMUNOL.1103231>

Palgen, J. L., Tchitchek, N., Elhmouzi-Younes, J., Delandre, S., Namet, I., Rosenbaum, P., Dereuddre-Bosquet, N., Martinon, F., Cosma, A., Lévy, Y., Le Grand, R., & Beignon, A. S. (2018). Prime and Boost Vaccination Elicit a Distinct Innate Myeloid Cell Immune Response. *Scientific Reports*, 8(1). <https://doi.org/10.1038/s41598-018-21222-2>

Palgen, J. L., Tchitchek, N., Rodriguez-Pozo, A., Jouhault, Q., Abdelhouahab, H., Dereuddre-Bosquet, N., Contreras, V., Martinon, F., Cosma, A., Lévy, Y., Le Grand, R., & Beignon, A. S. (2020). Innate and secondary humoral responses are improved by increasing the time between MVA vaccine immunizations. *Npj Vaccines*, 5(1).
<https://doi.org/10.1038/s41541-020-0175-8>

Palgen, J., Tchitchek, N., Huot, N., Elhmouzi-Younes, J., Lefebvre, C., Rosenbaum, P., Dereuddre-Bosquet, N., Martinon, F., Hocini, H., Cosma, A., Müller-Trutwin, M., Lévy, Y., Grand, R., & Beignon, A. (2019). NK cell immune responses differ after prime and boost vaccination. *Journal of Leukocyte Biology*, 105(5), 1055–1073.
<https://doi.org/10.1002/JLB.4A1018-391RR>

Park, C. O., Fu, X., Jiang, X., Pan, Y., Teague, J. E., Collins, N., Tian, T., O'Malley, J. T., Emerson, R. O., Kim, J. H., Jung, Y., Watanabe, R., Fuhlbrigge, R. C., Carbone, F. R., Gebhardt, T., Clark, R. A., Lin, C. P., & Kupper, T. S. (2017). Staged development of long-lived T-cell receptor $\alpha\beta$ T_H17 resident memory T-cell population to *Candida albicans* after skin infection. *The Journal of Allergy and Clinical Immunology*, 142(2), 647–662. <https://doi.org/10.1016/J.JACI.2017.09.042>

Park, H., Li, Z., Yang, X. O., Chang, S. H., Nurieva, R., Wang, Y. H., Wang, Y., Hood, L., Zhu, Z., Tian, Q., & Dong, C. (2005). A distinct lineage of CD4 T cells regulates tissue inflammation by producing interleukin 17. *Nature Immunology*, 6(11), 1133–1141.
<https://doi.org/10.1038/NI1261>

Park, S. M., Brooks, A. E. S., Chen, C. J. J., Sheppard, H. M., Loef, E. J., McIntosh, J. D., Angel, C. E., Mansell, C. J., Bartlett, A., Cebon, J., Birch, N. P., & Dunbar, P. R. (2021). Migratory cues controlling B-lymphocyte trafficking in human lymph nodes. *Immunology and Cell Biology*, 99(1), 49–64. <https://doi.org/10.1111/IMCB.12386>

- Parry, R. v., Rumbley, C. A., Vandenbergh, L. H., June, C. H., & Riley, J. L. (2003). CD28 and inducible costimulatory protein Src homology 2 binding domains show distinct regulation of phosphatidylinositol 3-kinase, Bcl-xL, and IL-2 expression in primary human CD4 T lymphocytes. *Journal of Immunology (Baltimore, Md.: 1950)*, 171(1), 166–174. <https://doi.org/10.4049/JIMMUNOL.171.1.166>
- Paul, W. E., & Seder, R. A. (1994). Lymphocyte responses and cytokines. *Cell*, 76(2), 241–251. [https://doi.org/10.1016/0092-8674\(94\)90332-8](https://doi.org/10.1016/0092-8674(94)90332-8)
- Paus, D., Tri, G. P., Chan, T. D., Gardam, S., Basten, A., & Brink, R. (2006). Antigen recognition strength regulates the choice between extrafollicular plasma cell and germinal center B cell differentiation. *The Journal of Experimental Medicine*, 203(4), 1081–1091. <https://doi.org/10.1084/JEM.20060087>
- Pauthner, M., Havenar-Daughton, C., Sok, D., Nkolola, J. P., Bastidas, R., Boopathy, A. v., Carnathan, D. G., Chandrashekhar, A., Cirelli, K. M., Cottrell, C. A., Eroshkin, A. M., Guenaga, J., Kaushik, K., Kulp, D. W., Liu, J., McCoy, L. E., Oom, A. L., Ozorowski, G., Post, K. W., ... Burton, D. R. (2017). Elicitation of Robust Tier 2 Neutralizing Antibody Responses in Nonhuman Primates by HIV Envelope Trimer Immunization Using Optimized Approaches. *Immunity*, 46(6), 1073–1088.e6. <https://doi.org/10.1016/j.jimmuni.2017.05.007>
- Péguet-Navarro, J., Furio, L., Briotet, I., Journeaux, A., & Billard, H. (2010). Human Langerhans Cells Are More Efficient Than CD14–CD1c+ Dermal Dendritic Cells at Priming Naive CD4+ T Cells. *Journal of Investigative Dermatology*, 130(5), 1345–1354. <https://doi.org/10.1038/JID.2009.424>
- Pentcheva-Hoang, T., Egen, J. G., Wojnoonski, K., & Allison, J. P. (2004). B7-1 and B7-2 selectively recruit CTLA-4 and CD28 to the immunological synapse. *Immunity*, 21(3), 401–413. <https://doi.org/10.1016/J.IMMUNI.2004.06.017>
- Pepper, M., Pagán, A. J., Iggyártó, B. Z., Taylor, J. J., & Jenkins, M. K. (2011). Opposing signals from the Bcl6 transcription factor and the interleukin-2 receptor generate T helper 1 central and effector memory cells. *Immunity*, 35(4), 583–595. <https://doi.org/10.1016/J.IMMUNI.2011.09.009>
- Pfeiffer, C., Stein, J., Southwood, S., Ketelaar, H., Sette, A., & Bottomly, K. (1995). Altered peptide ligands can control CD4 T lymphocyte differentiation in vivo. *The Journal of Experimental Medicine*, 181(4), 1569–1574. <https://doi.org/10.1084/JEM.181.4.1569>
- Pierson, T. C., & Diamond, M. S. (2020). The continued threat of emerging flaviviruses. *Nature Microbiology* 2020 5:6, 5(6), 796–812. <https://doi.org/10.1038/s41564-020-0714-0>
- Plantinga, M., Guilliams, M., Vanheerswyngels, M., Deswarte, K., Branco-Madeira, F., Toussaint, W., Vanhoutte, L., Neyt, K., Killeen, N., Malissen, B., Hammad, H., & Lambrecht, B. N. (2013). Conventional and monocyte-derived CD11b(+) dendritic

- cells initiate and maintain T helper 2 cell-mediated immunity to house dust mite allergen. *Immunity*, 38(2), 322–335. <https://doi.org/10.1016/J.IMMUNI.2012.10.016>
- Platon, L., Pejoski, D., Gautreau, G., Targat, B., le Grand, R., Beignon, A. S., & Tchitchev, N. (2018). A computational approach for phenotypic comparisons of cell populations in high-dimensional cytometry data. *Methods (San Diego, Calif.)*, 132, 66–75. <https://doi.org/10.1016/J.YMETHOD.2017.09.005>
- Plotkin, S. A., Orenstein, W. A., Offit, P. A., & Kathryn M. Edwards. (2017). *Plotkin's vaccines: Vol. 7th Edition.*
- Pogorelyy, M. v., Minervina, A. A., Touzel, M. P., Sycheva, A. L., Komech, E. A., Kovalenko, E. I., Karganova, G. G., Egorov, E. S., Komkov, A. Y., Chudakov, D. M., Mamedov, I. Z., Mora, T., Walczak, A. M., & Lebedev, Y. B. (2018). Precise tracking of vaccine-responding T cell clones reveals convergent and personalized response in identical twins. *Proceedings of the National Academy of Sciences of the United States of America*, 115(50), 12704–12709.
https://doi.org/10.1073/PNAS.1809642115/SUPPL_FILE/PNAS.1809642115.SD02.TX
- Poland, G. A., Ovsyannikova, I. G., Jacobson, R. M., & Smith, D. I. (2007). Heterogeneity in vaccine immune response: The role of immunogenetics and the emerging field of vaccinomics. *Clinical Pharmacology and Therapeutics*, 82(6), 653–664.
<https://doi.org/10.1038/SJ.CLPT.6100415>
- Polonsky, M., Rimer, J., Kern-Perets, A., Zaretsky, I., Miller, S., Bornstein, C., David, E., Kopelman, N. M., Stelzer, G., Porat, Z., Chain, B., & Friedman, N. (2018). Induction of CD4 T cell memory by local cellular collectivity. *Science*, 360(6394).
https://doi.org/10.1126/SCIENCE.AAJ1853/SUPPL_FILE/AAJ1853S1.MOV
- Principles of Virology, 4th Edition, 2 Vol set by S. Jane Flint, Lynn W. Enquist, Vincent R. Racaniello, Glenn F. Rall, Anna Marie Skalka: Free Download, Borrow, and Streaming: Internet Archive.* (n.d.). Retrieved September 22, 2022, from https://archive.org/details/Principles_of_Virology_4th_Edition_2_Vol_set_by_S._Jane_Flnt_Lynn_W._Enquist_Vi/page/n535/mode/2up
- Puel, A., Cypowij, S., Bustamante, J., Wright, J. F., Liu, L., Lim, H. K., Migaud, M., Israel, L., Chrabieh, M., Audry, M., Gumbleton, M., Toulon, A., Bodemer, C., El-Baghdadi, J., Whitters, M., Paradis, T., Brooks, J., Collins, M., Wolfman, N. M., ... Casanova, J. L. (2011). Chronic mucocutaneous candidiasis in humans with inborn errors of interleukin-17 immunity. *Science (New York, N.Y.)*, 332(6025), 65–68.
<https://doi.org/10.1126/SCIENCE.1200439>
- Purwar, R., Schlapbach, C., Xiao, S., Kang, H. S., Elyaman, W., Jiang, X., Jetten, A. M., Khoury, S. J., Fuhlbrigge, R. C., Kuchroo, V. K., Clark, R. A., & Kupper, T. S. (2012). Robust tumor immunity to melanoma mediated by interleukin-9-producing T cells. *Nature Medicine*, 18(8), 1248–1253. <https://doi.org/10.1038/NM.2856>

- Qin, D., Wu, J., Vora, K. A., Ravetch, J. v., Szakal, A. K., Manser, T., & Tew, J. G. (2000). Fcγ Receptor IIb on Follicular Dendritic Cells Regulates the B Cell Recall Response. *The Journal of Immunology*, 164(12), 6268–6275.
<https://doi.org/10.4049/JIMMUNOL.164.12.6268>
- Querec, T., Bennouna, S., Alkan, S., Laouar, Y., Gorden, K., Flavell, R., Akira, S., Ahmed, R., & Pulendran, B. (2006). Yellow fever vaccine YF-17D activates multiple dendritic cell subsets via TLR2, 7, 8, and 9 to stimulate polyvalent immunity. *Journal of Experimental Medicine*, 203(2), 413–424. <https://doi.org/10.1084/JEM.20051720>
- Querec, T. D., Akondy, R. S., Lee, E. K., Cao, W., Nakaya, H. I., Teuwen, D., Pirani, A., Gernert, K., Deng, J., Marzolf, B., Kennedy, K., Wu, H., Bennouna, S., Oluoch, H., Miller, J., Vencio, R. Z., Mulligan, M., Aderem, A., Ahmed, R., & Pulendran, B. (2009). Systems biology approach predicts immunogenicity of the yellow fever vaccine in humans. *Nature Immunology*, 10(1), 116–125. <https://doi.org/10.1038/ni.1688>
- Raeber, M. E., Zurbuchen, Y., Impellizzieri, D., & Boyman, O. (2018). The role of cytokines in T-cell memory in health and disease. *Immunological Reviews*, 283(1), 176–193.
<https://doi.org/10.1111/IMR.12644>
- Rahmberg, A. R., Markowitz, T. E., Mudd, J. C., Hirsch, V., & Brenchley, J. M. (2022). Epigenetic Reprogramming Leads to Downregulation of CD4 and Functional Changes in African Green Monkey Memory CD4+ T Cells. *The Journal of Immunology*, 209(2), 337–345. <https://doi.org/10.4049/JIMMUNOL.2200109>
- Ravetch, J. v., & Nussenzweig, M. (2007). Killing some to make way for others. *Nature Immunology*, 8(4), 337–340.
<https://go.gale.com/ps/i.do?p=HRCA&sw=w&issn=15292908&v=2.1&it=r&id=GALE%7CA197365050&sid=googleScholar&linkaccess=fulltext>
- Rehwinkel, J., & Gack, M. U. (2020). RIG-I-like receptors: their regulation and roles in RNA sensing. *Nature Reviews Immunology* 20:9, 20(9), 537–551.
<https://doi.org/10.1038/s41577-020-0288-3>
- Richer, M. J., Nolz, J. C., & Harty, J. T. (2013). Pathogen-specific inflammatory milieux tune the antigen sensitivity of CD8+ T cells by enhancing T cell receptor signaling. *Immunity*, 38(1), 140. <https://doi.org/10.1016/J.IMMUNI.2012.09.017>
- Roozendaal, R., & Carroll, M. C. (2007). Complement receptors CD21 and CD35 in humoral immunity. *Immunological Reviews*, 219(1), 157–166.
<https://doi.org/10.1111/J.1600-065X.2007.00556.X>
- Rosenbaum, P., Tchitchev, N., Joly, C., Rodriguez Pozo, A., Stimmer, L., Langlois, S., Hocini, H., Gosse, L., Pejoski, D., Cosma, A., Beignon, A.-S., Dereuddre-Bosquet, N., Levy, Y., le Grand, R., & Martinon, F. (2020). Vaccine Inoculation Route Modulates Early Immunity and Consequently Antigen-Specific Immune Response. *SSRN Electronic Journal*. <https://doi.org/10.2139/ssrn.3535877>

- Sadegh-Nasseri, S., Dalai, S. K., Korb Ferris, L. C., & Mirshahidi, S. (2010). Suboptimal engagement of the T-cell receptor by a variety of peptide–MHC ligands triggers T-cell anergy. *Immunology*, 129(1), 1–7. <https://doi.org/10.1111/J.1365-2567.2009.03206.X>
- Sallusto, F., Geginat, J., & Lanzavecchia, A. (2004). Central memory and effector memory T cell subsets: function, generation, and maintenance. *Annual Review of Immunology*, 22, 745–763.
<https://doi.org/10.1146/ANNUREV.IMMUNOL.22.012703.104702>
- Sanders, R. W., & Moore, J. P. (2017). Native-like Env trimers as a platform for HIV-1 vaccine design. In *Immunological Reviews*. <https://doi.org/10.1111/imr.12481>
- Sathaliyawala, T., Kubota, M., Yudanin, N., Turner, D., Camp, P., Thome, J. J. C., Bickham, K. L., Lerner, H., Goldstein, M., Sykes, M., Kato, T., & Farber, D. L. (2013). Distribution and compartmentalization of human circulating and tissue-resident memory T cell subsets. *Immunity*, 38(1), 187–197. <https://doi.org/10.1016/J.IMMUNI.2012.09.020>
- Schadendorf, D., Ugurel, S., Schuler-Thurner, B., Nestles, F. O., Enk, A., Bröcker, E. B., Grabbe, S., Rittgen, W., Sucker, A., Zimpfer-Rechner, C., Berger, T., Kamarashev, J., Burg, G., Jonuleit, H., Tüttenberg, A., Becker, J. C., Keikavoussi, P., Kämpgen, E., & Schuler, G. (2006). Dacarbazine (DTIC) versus vaccination with autologous peptide-pulsed dendritic cells (DC) in first-line treatment of patients with metastatic melanoma: a randomized phase III trial of the DC study group of the DeCOG. *Annals of Oncology: Official Journal of the European Society for Medical Oncology*, 17(4), 563–570. <https://doi.org/10.1093/ANNONC/MDJ138>
- Schenkel, J. M., & Masopust, D. (2014). Tissue-resident memory T cells. *Immunity*, 41(6), 886–897. <https://doi.org/10.1016/J.IMMUNI.2014.12.007>
- Schiemann, B., Gommerman, J. L., Vora, K., Cachero, T. G., Shutga-Morskaya, S., Dobles, M., Frew, E., & Scott, M. L. (2001). An essential role for BAFF in the normal development of B cells through a BCMA-independent pathway. *Science (New York, N.Y.)*, 293(5537), 2111–2114. <https://doi.org/10.1126/SCIENCE.1061964>
- Schlitzer, A., McGovern, N., Teo, P., Zelante, T., Atarashi, K., Low, D., Ho, A. W. S., See, P., Shin, A., Wasan, P. S., Hoeffel, G., Malleret, B., Heiseke, A., Chew, S., Jardine, L., Purvis, H. A., Hilkens, C. M. U., Tam, J., Poidinger, M., ... Ginhoux, F. (2013). IRF4 Transcription Factor-Dependent CD11b+ Dendritic Cells in Human and Mouse Control Mucosal IL-17 Cytokine Responses. *Immunity*, 38(5), 970–983.
<https://doi.org/10.1016/J.IMMUNI.2013.04.011>
- Schmitt, N., Bentebibel, S. E., & Ueno, H. (2014). Phenotype and Functions of Memory Tfh cells in Human Blood. *Trends in Immunology*, 35(9), 436.
<https://doi.org/10.1016/J.IT.2014.06.002>
- Schreibelt, G., Klinkenberg, L. J. J., Cruz, L. J., Tacken, P. J., Tel, J., Kreutz, M., Adema, G. J., Brown, G. D., Figdor, C. G., & de Vries, I. J. M. (2012). The C-type lectin receptor

CLEC9A mediates antigen uptake and (cross-)presentation by human blood BDCA3+ myeloid dendritic cells. *Blood*, 119(10), 2284–2292.
<https://doi.org/10.1182/BLOOD-2011-08-373944>

Schuler, G., & Steinman, R. M. (1985). Murine epidermal Langerhans cells mature into potent immunostimulatory dendritic cells in vitro. *The Journal of Experimental Medicine*, 161(3), 526. <https://doi.org/10.1084/JEM.161.3.526>

Schwickert, T. A., Victora, G. D., Fooksman, D. R., Kamphorst, A. O., Mugnier, M. R., Gitlin, A. D., & Nussenzweig, M. L. D. (2011). A dynamic T cell-limited checkpoint regulates affinity-dependent B cell entry into the germinal center. *The Journal of Experimental Medicine*, 208(6), 1243. <https://doi.org/10.1084/JEM.20102477>

Segura, E., Durand, M., & Amigorena, S. (2013). Similar antigen cross-presentation capacity and phagocytic functions in all freshly isolated human lymphoid organ-resident dendritic cells. *The Journal of Experimental Medicine*, 210(5), 1035–1047. <https://doi.org/10.1084/JEM.20121103>

Segura, E., Touzot, M., Bohineust, A., Cappuccio, A., Chiocchia, G., Hosmalin, A., Dalod, M., Soumelis, V., & Amigorena, S. (2013). Human Inflammatory Dendritic Cells Induce Th17 Cell Differentiation. *Immunity*, 38(2), 336–348. <https://doi.org/10.1016/j.immuni.2012.10.018>

Seneschal, J., Clark, R. A., Gehad, A., Baecher-Allan, C. M., & Kupper, T. S. (2012). Human epidermal Langerhans cells maintain immune homeostasis in skin by activating skin resident regulatory T cells. *Immunity*, 36(5), 873–884. <https://doi.org/10.1016/J.IMMUNI.2012.03.018>

Shaw, J., Wang, Y. H., Ito, T., Arima, K., & Liu, Y. J. (2010). Plasmacytoid dendritic cells regulate B-cell growth and differentiation via CD70. *Blood*, 115(15), 3051–3057. <https://doi.org/10.1182/BLOOD-2009-08-239145>

Shin, J. S., & Greer, A. M. (2015). The role of Fc ϵ RI expressed in dendritic cells and monocytes. *Cellular and Molecular Life Sciences: CMLS*, 72(12), 2349–2360. <https://doi.org/10.1007/S00018-015-1870-X>

Shiow, L. R., Rosen, D. B., Brdičková, N., Xu, Y., An, J., Lanier, L. L., Cyster, J. G., & Matloubian, M. (2006). CD69 acts downstream of interferon- α/β to inhibit S1P 1 and lymphocyte egress from lymphoid organs. *Nature*, 440(7083), 540–544. <https://doi.org/10.1038/nature04606>

Shulman, Z., Gitlin, A. D., Targ, S., Jankovic, M., Pasqual, G., Nussenzweig, M. C., & Victora, G. D. (2013). T Follicular Helper Cell Dynamics in Germinal Centers. *Science (New York, N.Y.)*, 341(6146), 673. <https://doi.org/10.1126/SCIENCE.1241680>

Sirvent, S., Vallejo, A. F., Davies, J., Clayton, K., Wu, Z., Woo, J., Riddell, J., Chaudhri, V. K., Stumpf, P., Nazlamova, L. A., Wheway, G., Rose-Zerilli, M., West, J., Pujato, M., Chen, X., Woelk, C. H., MacArthur, B., Ardern-Jones, M., Friedmann, P. S., ... Polak, M. E. (2020). Genomic programming of IRF4-expressing human Langerhans cells.

Nature Communications 2020 11:1, 11(1), 1–12. <https://doi.org/10.1038/s41467-019-14125-x>

Sittig, S. P., Bakdash, G., Weiden, J., Sköld, A. E., Tel, J., Figdor, C. G., de Vries, I. J. M., & Schreibelt, G. (2016). A Comparative Study of the T Cell Stimulatory and Polarizing Capacity of Human Primary Blood Dendritic Cell Subsets. *Mediators of Inflammation*, 2016. <https://doi.org/10.1155/2016/3605643>

Sliepen, K., Han, B. W., Bontjer, I., Mooij, P., Garces, F., Behrens, A. J., Rantalainen, K., Kumar, S., Sarkar, A., Brouwer, P. J. M., Hua, Y., Tolazzi, M., Schermer, E., Torres, J. L., Ozorowski, G., van der Woude, P., de la Peña, A. T., van Breemen, M. J., Camacho-Sánchez, J. M., ... Sanders, R. W. (2019). Structure and immunogenicity of a stabilized HIV-1 envelope trimer based on a group-M consensus sequence. *Nature Communications*, 10(1). <https://doi.org/10.1038/S41467-019-10262-5>

Small, E. J., Schellhammer, P. F., Higano, C. S., Redfern, C. H., Nemunaitis, J. J., Valone, F. H., Verjee, S. S., Jones, L. A., & Hershberg, R. M. (2006). Placebo-controlled phase III trial of immunologic therapy with sipuleucel-T (APC8015) in patients with metastatic, asymptomatic hormone refractory prostate cancer. *Journal of Clinical Oncology: Official Journal of the American Society of Clinical Oncology*, 24(19), 3089–3094. <https://doi.org/10.1200/JCO.2005.04.5252>

Snook, J. P., Kim, C., & Williams, M. A. (2018). TCR signal strength controls the differentiation of CD4+ effector and memory T cells. *Science Immunology*, 3(25). https://doi.org/10.1126/SCIIMMUNOL.AAS9103/SUPPL_FILE/AAS9103_TABLE_S2.XLSX

Solouki, S., Huang, W., Elmore, J., Limper, C., Huang, F., & August, A. (2020). TCR Signal Strength and Antigen Affinity Regulate CD8 + Memory T Cells . *The Journal of Immunology*, 205(5), 1217–1227. <https://doi.org/10.4049/JIMMUNOL.1901167/-DCSUPPLEMENTAL>

Song, N., Sengupta, S., Khoruzhenko, S., Welsh, R. A., Kim, A. R., Kumar, M. R., Sønder, S. U., Sidhom, J. W., Zhang, H., Jie, C., Siliciano, R. F., & Sadegh-Nasseri, S. (2020). Multiple genetic programs contribute to CD4 T cell memory differentiation and longevity by maintaining T cell quiescence. *Cellular Immunology*, 357, 104210. <https://doi.org/10.1016/J.CELLIMM.2020.104210>

Staudt, V., Bothur, E., Klein, M., Lingnau, K., Reuter, S., Grebe, N., Gerlitzki, B., Hoffmann, M., Ulges, A., Taube, C., Dehzad, N., Becker, M., Stassen, M., Steinborn, A., Lohhoff, M., Schild, H., Schmitt, E., & Bopp, T. (2010). Interferon-regulatory factor 4 is essential for the developmental program of T helper 9 cells. *Immunity*, 33(2), 192–202. <https://doi.org/10.1016/J.IMMUNI.2010.07.014>

Steinman, R. M., & Cohn, Z. A. (1973). IDENTIFICATION OF A NOVEL CELL TYPE IN PERIPHERAL LYMPHOID ORGANS OF MICE I. MORPHOLOGY, QUANTITATION, TISSUE DISTRIBUTION. *Journal of Experimental Medicine*, 137(5), 1142–1162. <https://doi.org/10.1084/JEM.137.5.1142>

- Stemberger, C., Huster, K. M., Koffler, M., Anderl, F., Schiemann, M., Wagner, H., & Busch, D. H. (2007). A Single Naive CD8+ T Cell Precursor Can Develop into Diverse Effector and Memory Subsets. *Immunity*, 27(6), 985–997.
<https://doi.org/10.1016/j.jimmuni.2007.10.012>
- Stritesky, G. L., Yeh, N., & Kaplan, M. H. (2008). IL-23 promotes maintenance but not commitment to the Th17 lineage. *Journal of Immunology (Baltimore, Md.: 1950)*, 181(9), 5948–5955. <https://doi.org/10.4049/JIMMUNOL.181.9.5948>
- Su, L. F., & Davis, M. M. (2013). Antiviral memory phenotype T cells in unexposed adults. *Immunological Reviews*, 255(1), 95–109. <https://doi.org/10.1111/IMR.12095>
- Su, L. F., Kidd, B. A., Han, A., Kotzin, J. J., & Davis, M. M. (2013). Virus-Specific CD4+ Memory-Phenotype T Cells Are Abundant in Unexposed Adults. *Immunity*, 38(2), 373–383. <https://doi.org/10.1016/J.IMMUNI.2012.10.021>
- Suloway, C., Pulokas, J., Fellmann, D., Cheng, A., Guerra, F., Quispe, J., Stagg, S., Potter, C. S., & Carragher, B. (2005). Automated molecular microscopy: The new Leginon system. *Journal of Structural Biology*, 151(1), 41–60.
<https://doi.org/10.1016/j.jsb.2005.03.010>
- Sun, B., Liu, M., Cui, M., & Li, T. (2020). Granzyme B-expressing treg cells are enriched in colorectal cancer and present the potential to eliminate autologous T conventional cells. *Immunology Letters*, 217, 7–14. <https://doi.org/10.1016/J.IMLET.2019.10.007>
- Swain, S. L., Weinberg, A. D., English, M., & Huston, G. (1990). IL-4 directs the development of Th2-like helper effectors. *The Journal of Immunology*, 145(11).
- Szabo, S. J., Sullivan, B. M., Peng, S. L., & Glimcher, L. H. (2003). Molecular mechanisms regulating Th1 immune responses. *Annual Review of Immunology*, 21, 713–758.
<https://doi.org/10.1146/ANNUREV.IMMUNOL.21.120601.140942>
- Tai, Y., Wang, Q., Korner, H., Zhang, L., & Wei, W. (2018). Molecular Mechanisms of T Cells Activation by Dendritic Cells in Autoimmune Diseases. *Frontiers in Pharmacology*, 9(JUN). <https://doi.org/10.3389/FPHAR.2018.00642>
- Tamura, T., Kurotaki, D., & Koizumi, S. ichi. (2015). Regulation of myelopoiesis by the transcription factor IRF8. *International Journal of Hematology*, 101(4), 342–351.
<https://doi.org/10.1007/S12185-015-1761-9/FIGURES/4>
- Tan, C., Aziz, M. K., Lovaas, J. D., Vistica, B. P., Shi, G., Wawrousek, E. F., & Gery, I. (2010). Antigen-specific Th9 cells exhibit uniqueness in their kinetics of cytokine production and short retention at the inflammatory site. *Journal of Immunology (Baltimore, Md.: 1950)*, 185(11), 6795–6801.
<https://doi.org/10.4049/JIMMUNOL.1001676>
- Tang, Y., Li, H., Li, J., Liu, Y., Li, Y., Zhou, J., Zhou, J., Lu, X., Zhao, W., Hou, J., Wang, X. Y., Chen, Z., & Zuo, D. (2018). Macrophage scavenger receptor 1 contributes to pathogenesis of fulminant hepatitis via neutrophil-mediated complement

activation. *Journal of Hepatology*, 68(4), 733.

<https://doi.org/10.1016/J.JHEP.2017.11.010>

Tan, J. T., Ernst, B., Kieper, W. C., LeRoy, E., Sprent, J., & Surh, C. D. (2002). Interleukin (IL)-15 and IL-7 jointly regulate homeostatic proliferation of memory phenotype CD8+ cells but are not required for memory phenotype CD4+ cells. *The Journal of Experimental Medicine*, 195(12), 1523–1532. <https://doi.org/10.1084/JEM.20020066>

Taylor, J. J., Pape, K. A., & Jenkins, M. K. (2012). A germinal center-independent pathway generates unswitched memory B cells early in the primary response. *The Journal of Experimental Medicine*, 209(3), 597–606. <https://doi.org/10.1084/JEM.20111696>

Taylor, P. R., Tsoni, S. V., Willment, J. A., Dennehy, K. M., Rosas, M., Findon, H., Haynes, K., Steele, C., Botto, M., Gordon, S., & Brown, G. D. (2007). Dectin-1 is required for beta-glucan recognition and control of fungal infection. *Nature Immunology*, 8(1), 31–38. <https://doi.org/10.1038/NI1408>

Theiler, M., & Smith, H. H. (1937). THE USE OF YELLOW FEVER VIRUS MODIFIED BY IN VITRO CULTIVATION FOR HUMAN IMMUNIZATION. *The Journal of Experimental Medicine*, 65(6), 787–800. <https://doi.org/10.1084/JEM.65.6.787>

Tian, Y., Babor, M., Lane, J., Schulten, V., Patil, V. S., Seumois, G., Rosales, S. L., Fu, Z., Picarda, G., Burel, J., Zapardiel-Gonzalo, J., Tennekoon, R. N., de Silva, A. D., Premawansa, S., Premawansa, G., Wijewickrama, A., Greenbaum, J. A., Vijayanand, P., Weiskopf, D., ... Peters, B. (2017). Unique phenotypes and clonal expansions of human CD4 effector memory T cells re-expressing CD45RA. *Nature Communications* 2017 8:1, 8(1), 1–13. <https://doi.org/10.1038/s41467-017-01728-5>

Tilbeurgh, M. van, Lemdani, K., Beignon, A.-S., Chapon, C., Tchitchek, N., Cheraitia, L., Lopez, E. M., Pascal, Q., le Grand, R., Maisonnasse, P., Manet, C., Isagulants, G., & Burt, F. J. (2021). Predictive Markers of Immunogenicity and Efficacy for Human Vaccines. *Vaccines* 2021, Vol. 9, Page 579, 9(6), 579. <https://doi.org/10.3390/vaccines9060579>

Tilbeurgh, M. van, Maisonnasse, P., Palgen, J.-L., Tolazzi, M., Aldon, Y., Dereuddre-Bosquet, N., Cavarelli, M., Beignon, A.-S., Marcos-Lopez, E., Gallouet, A.-S., Gilson, E., Ozorowski, G., Ward, A. B., Bontjer, I., McKay, P. F., Shattock, R. J., Scarlatti, G., Sanders, R. W., & Grand, R. le. (2022). Innate cell markers that predict anti-HIV neutralizing antibody titers in vaccinated macaques. *Cell Reports Medicine*, 0(0), 100751. <https://doi.org/10.1016/J.XCRM.2022.100751>

Tirapu, I., Giquel, B., Alexopoulou, L., Uematsu, S., Flavell, R., Akira, S., & Diebold, S. S. (2009). PolyI:C-induced reduction in uptake of soluble antigen is independent of dendritic cell activation. *International Immunology*, 21(7), 871–879. <https://doi.org/10.1093/INTIMM/DXP053>

Toor, J., Echeverria-Londono, S., Li, X., Abbas, K., Carter, E. D., Clapham, H. E., Clark, A., de Villiers, M. J., Eilertson, K., Ferrari, M., Gamkrelidze, I., Hallett, T. B., Hinsley, W. R.,

- Hogan, D., Huber, J. H., Jackson, M. L., Jean, K., Jit, M., Karachaliou, A., ... Gaythorpe, K. A. (2021). Lives saved with vaccination for 10 pathogens across 112 countries in a pre-COVID-19 world. *ELife*, 10. <https://doi.org/10.7554/ELIFE.67635>
- Trifari, S., Kaplan, C. D., Tran, E. H., Crellin, N. K., & Spits, H. (2009). Identification of a human helper T cell population that has abundant production of interleukin 22 and is distinct from T(H)-17, T(H)1 and T(H)2 cells. *Nature Immunology*, 10(8), 864–871. <https://doi.org/10.1038/NI.1770>
- Trinchieri, G., Pflanz, S., & Kastlein, R. A. (2003). The IL-12 Family of Heterodimeric Cytokines: New Players in the Regulation of T Cell Responses. *Immunity*, 19(5), 641–644. [https://doi.org/10.1016/S1074-7613\(03\)00296-6](https://doi.org/10.1016/S1074-7613(03)00296-6)
- Tripp, C. H., Chang-Rodriguez, S., Stoitzner, P., Holzmann, S., Stössel, H., Douillard, P., Saeland, S., Koch, F., Elbe-Bürger, A., & Romani, N. (2004). Ontogeny of Langerin/CD207 expression in the epidermis of mice. *The Journal of Investigative Dermatology*, 122(3), 670–672. <https://doi.org/10.1111/J.0022-202X.2004.22337.X>
- Tsang, J. S., Schwartzberg, P. L., Kotliarov, Y., Biancotto, A., Xie, Z., Germain, R. N., Wang, E., Olnes, M. J., Narayanan, M., Golding, H., Moir, S., Dickler, H. B., Perl, S., & Cheung, F. (2014). Global Analyses of Human Immune Variation Reveal Baseline Predictors of Postvaccination Responses. *Cell*, 157(2), 499–513. <https://doi.org/10.1016/J.CELL.2014.03.031>
- Tsuji, M., Komatsu, N., Kawamoto, S., Suzuki, K., Kanagawa, O., Honjo, T., Hori, S., & Fagarasan, S. (2009). Preferential generation of follicular B helper T cells from Foxp3+ T cells in gut Peyer's patches. *Science (New York, N.Y.)*, 323(5920), 1488–1492. <https://doi.org/10.1126/SCIENCE.1169152>
- Turner, D. L., Cauley, L. S., Khanna, K. M., & Lefrançois, L. (2007). Persistent Antigen Presentation after Acute Vesicular Stomatitis Virus Infection. *Journal of Virology*, 81(4), 2039–2046. <https://doi.org/10.1128/JVI.02167-06/ASSET/027BF74A-68BA-40F0-A064-69BFB222A1B3/ASSETS/GRAPHIC/ZJV0040787740004.JPG>
- Turner, M. S., Kane, L. P., & Morel, P. A. (2009). Dominant role of antigen dose in CD4+Foxp3+ regulatory T cell induction and expansion. *Journal of Immunology (Baltimore, Md.: 1950)*, 183(8), 4895–4903. <https://doi.org/10.4049/JIMMUNOL.0901459>
- Tuttle, A. H., Rankin, M. M., Teta, M., Sartori, D. J., Stein, G. M., Kim, G. J., Virgilio, C., Granger, A., Zhou, D., Long, S. H., Schiffman, A. B., & Kushner, J. A. (2010). Immunofluorescent Detection of Two Thymidine Analogues (Cl^dU and Id^dU) in Primary Tissue. *JoVE (Journal of Visualized Experiments)*, 46(46), e2166. <https://doi.org/10.3791/2166>
- Usui, T., Nishikomori, R., Kitani, A., & Strober, W. (2003). GATA-3 Suppresses Th1 Development by Downregulation of Stat4 and Not through Effects on IL-12R β 2

Chain or T-bet. *Immunity*, 18(3), 415–428. [https://doi.org/10.1016/S1074-7613\(03\)00057-8](https://doi.org/10.1016/S1074-7613(03)00057-8)

Vaccari, M., Fourati, S., Gordon, S. N., Brown, D. R., Bissa, M., Schifanella, L., Silva De Castro, I., Doster, M. N., Galli, V., Omsland, M., Fujikawa, D., Gorini, G., Liyanage, N. P. M., Trinh, H. v., McKinnon, K. M., Foulds, K. E., Keele, B. F., Roederer, M., Koup, R. A., ... Franchini, G. (2018). HIV vaccine candidate activation of hypoxia and the inflammasome in CD14+ monocytes is associated with a decreased risk of SIVmac251 acquisition. *Nature Medicine* 2018 24:6, 24(6), 847–856. <https://doi.org/10.1038/s41591-018-0025-7>

vander Lugt, B., Khan, A. A., Hackney, J. A., Agrawal, S., Lesch, J., Zhou, M., Lee, W. P., Park, S., Xu, M., Devoss, J., Spooner, C. J., Chalouni, C., Delamarre, L., Mellman, I., & Singh, H. (2014). Transcriptional programming of dendritic cells for enhanced MHC class II antigen presentation. *Nature Immunology*, 15(2), 161–167. <https://doi.org/10.1038/NI.2795>

van der Poel, C. E., Bajic, G., Macaulay, C. W., van den Broek, T., Ellson, C. D., Bouma, G., Victora, G. D., Degn, S. E., & Carroll, M. C. (2019). Follicular Dendritic Cells Modulate Germinal Center B Cell Diversity through FcγRIIB. *Cell Reports*, 29(9), 2745–2755.e4. <https://doi.org/10.1016/J.CELREP.2019.10.086>

van Oosterwijk, M. F., Juwana, H., Arens, R., Tesselaar, K., van Oers, M. H. J., Eldering, E., & van Lier, R. A. W. (2007). CD27-CD70 interactions sensitise naive CD4+ T cells for IL-12-induced Th1 cell development. *International Immunology*, 19(6), 713–718. <https://doi.org/10.1093/INTIMM/DXM033>

VanPanhuis, N., Klauschen, F., & Germain, R. N. (2014). T-Cell-Receptor-Dependent Signal Intensity Dominantly Controls CD4+ T Cell Polarization In Vivo. *Immunity*, 41(1), 63–74. <https://doi.org/10.1016/J.IMMUNI.2014.06.003>

Veldhoen, M., Uyttenhove, C., van Snick, J., Helmby, H., Westendorf, A., Buer, J., Martin, B., Wilhelm, C., & Stockinger, B. (2008). Transforming growth factor-beta “reprograms” the differentiation of T helper 2 cells and promotes an interleukin 9-producing subset. *Nature Immunology*, 9(12), 1341–1346. <https://doi.org/10.1038/NI.1659>

Villadangos, J. A., & Young, L. (2008). Antigen-presentation properties of plasmacytoid dendritic cells. *Immunity*, 29(3), 352–361. <https://doi.org/10.1016/J.IMMUNI.2008.09.002>

Villani, A. C., Satija, R., Reynolds, G., Sarkizova, S., Shekhar, K., Fletcher, J., Griesbeck, M., Butler, A., Zheng, S., Lazo, S., Jardine, L., Dixon, D., Stephenson, E., Nilsson, E., Grundberg, I., McDonald, D., Filby, A., Li, W., de Jager, P. L., ... Hacohen, N. (2017). Single-cell RNA-seq reveals new types of human blood dendritic cells, monocytes, and progenitors. *Science (New York, N.Y.)*, 356(6335). <https://doi.org/10.1126/SCIENCE.AAH4573>

- Vogel, I., Kasran, A., Cremer, J., Kim, Y. J., Boon, L., van Gool, S. W., & Ceuppens, J. L. (2015). CD28/CTLA-4/B7 costimulatory pathway blockade affects regulatory T-cell function in autoimmunity. *European Journal of Immunology*, 45(6), 1832–1841. <https://doi.org/10.1002/EJI.201445190>
- Vogelzang, A., McGuire, H. M., Yu, D., Sprent, J., Mackay, C. R., & King, C. (2008). A Fundamental Role for Interleukin-21 in the Generation of T Follicular Helper Cells. *Immunity*, 29(1), 127–137. <https://doi.org/10.1016/J.IMMUNI.2008.06.001>
- Voutouri, C., Nikmaneshi, M. R., Corey Hardin, C., Patel, A. B., Verma, A., Khandekar, M. J., Dutta, S., Stylianopoulos, T., Munn, L. L., & Jain, R. K. (2021). In silico dynamics of COVID-19 phenotypes for optimizing clinical management. *Proceedings of the National Academy of Sciences of the United States of America*, 118(3), e2021642118. https://doi.org/10.1073/PNAS.2021642118/SUPPL_FILE/PNAS.2021642118.SAPP.PDF
- Wang, C., Hillsamer, P., & Kim, C. H. (2011). Phenotype, effector function, and tissue localization of PD-1-expressing human follicular helper T cell subsets. *BMC Immunology*, 12(1), 1–15. <https://doi.org/10.1186/1471-2172-12-53/FIGURES/8>
- Wang, R., & Huang, K. (2020). CCL11 increases the proportion of CD4+CD25+Foxp3+ Treg cells and the production of IL-2 and TGF- β by CD4+ T cells via the STAT5 signaling pathway. *Molecular Medicine Reports*, 21(6), 2522–2532. <https://doi.org/10.3892/MMR.2020.11049/HTML>
- Watanabe, S., Yamada, Y., & Murakami, H. (2020). Expression of Th1/Th2 cell-related chemokine receptors on CD4+ lymphocytes under physiological conditions. *International Journal of Laboratory Hematology*, 42(1), 68–76. <https://doi.org/10.1111/IJLH.13141>
- Watson, A. M., & Klimstra, W. B. (2017). T Cell-Mediated Immunity towards Yellow Fever Virus and Useful Animal Models. *Viruses 2017, Vol. 9, Page 77*, 9(4), 77. <https://doi.org/10.3390/V9040077>
- Weiskopf, D., Bangs, D. J., Sidney, J., Kolla, R. v., de Silva, A. D., de Silva, A. M., Crotty, S., Peters, B., & Sette, A. (2015). Dengue virus infection elicits highly polarized CX3CR1+ cytotoxic CD4+ T cells associated with protective immunity. *Proceedings of the National Academy of Sciences of the United States of America*, 112(31), E4256–E4263. <https://doi.org/10.1073/PNAS.1505956112>
- Weiss, J. M., Bilate, A. M., Gobert, M., Ding, Y., de Lafaille, M. A. C., Parkhurst, C. N., Xiong, H., Dolpady, J., Frey, A. B., Ruocco, M. G., Yang, Y., Floess, S., Huehn, J., Oh, S., Li, M. O., Niec, R. E., Rudensky, A. Y., Dustin, M. L., Littman, D. R., & Lafaille, J. J. (2012). Neuropilin 1 is expressed on thymus-derived natural regulatory T cells, but not mucosa-generated induced Foxp3+ T reg cells. *The Journal of Experimental Medicine*, 209(10), 1723. <https://doi.org/10.1084/JEM.20120914>

- Whitmire, J. K., Benning, N., Eam, B., & Whitton, J. L. (2008). Increasing the CD4+ T Cell Precursor Frequency Leads to Competition for IFN- γ Thereby Degrading Memory Cell Quantity and Quality. *The Journal of Immunology*, 180(10), 6777–6785. <https://doi.org/10.4049/JIMMUNOL.180.10.6777>
- Williams, J. W., Tjota, M. Y., Clay, B. S., vander Lugt, B., Bandukwala, H. S., Hrusch, C. L., Decker, D. C., Blaine, K. M., Fixsen, B. R., Singh, H., Sciammas, R., & Sperling, A. I. (2013). Transcription factor IRF4 drives dendritic cells to promote Th2 differentiation. *Nature Communications*, 4. <https://doi.org/10.1038/NCOMMS3990>
- Williams, M. A., Ravkov, E. v., & Bevan, M. J. (2008). Rapid culling of the CD4+ T cell repertoire in the transition from effector to memory. *Immunity*, 28(4), 533–545. <https://doi.org/10.1016/J.IMMUNI.2008.02.014>
- Wong, M. T., Chen, J., Narayanan, S., Lin, W., Anicete, R., Kiaang, H. T. K., de Lafaille, M. A. C., Poidinger, M., & Newell, E. W. (2015). Mapping the Diversity of Follicular Helper T Cells in Human Blood and Tonsils Using High-Dimensional Mass Cytometry Analysis. *Cell Reports*, 11(11), 1822–1833. <https://doi.org/10.1016/j.celrep.2015.05.022>
- Worbs, T., Mempel, T. R., Böltner, J., von Andrian, U. H., & Förster, R. (2007). CCR7 ligands stimulate the intranodal motility of T lymphocytes in vivo. *Journal of Experimental Medicine*, 204(3), 489–495. <https://doi.org/10.1084/JEM.20061706/VIDEO-6>
- Xu, L., Kitani, A., Fuss, I., & Strober, W. (2007). Cutting Edge: Regulatory T Cells Induce CD4+CD25–Foxp3– T Cells or Are Self-Induced to Become Th17 Cells in the Absence of Exogenous TGF- β . *The Journal of Immunology*, 178(11), 6725–6729. <https://doi.org/10.4049/JIMMUNOL.178.11.6725>
- Yadav, M., Louvet, C., Davini, D., Gardner, J. M., Martinez-Llordella, M., Bailey-Bucktrout, S., Anthony, B. A., Sverdrup, F. M., Head, R., Kuster, D. J., Ruminski, P., Weiss, D., von Schack, D., & Bluestone, J. A. (2012). Neuropilin-1 distinguishes natural and inducible regulatory T cells among regulatory T cell subsets in vivo. *The Journal of Experimental Medicine*, 209(10), 1713–1722. <https://doi.org/10.1084/JEM.20120822>
- Yamane, H., & Paul, W. E. (2013). Early signaling events that underlie fate decisions of naive CD4(+) T cells toward distinct T-helper cell subsets. *Immunological Reviews*, 252(1), 12–23. <https://doi.org/10.1111/IMR.12032>
- Yamashita, M., Shinnakasu, R., Nigo, Y., Kimura, M., Hasegawa, A., Taniguchi, M., & Nakayama, T. (2004). Interleukin (IL)-4-independent maintenance of histone modification of the IL-4 gene loci in memory Th2 cells. *The Journal of Biological Chemistry*, 279(38), 39454–39464. <https://doi.org/10.1074/JBC.M405989200>
- Yao, W., Tepper, R. S., & Kaplan, M. H. (2011). Predisposition to the development of IL-9-secreting T cells in atopic infants. *The Journal of Allergy and Clinical Immunology*, 128(6), 1357. <https://doi.org/10.1016/J.JACI.2011.06.019>

- Yin, X., Yu, H., Jin, X., Li, J., Guo, H., Shi, Q., Yin, Z., Xu, Y., Wang, X., Liu, R., Wang, S., & Zhang, L. (2017). Human Blood CD1c+ Dendritic Cells Encompass CD5high and CD5low Subsets That Differ Significantly in Phenotype, Gene Expression, and Functions. *Journal of Immunology (Baltimore, Md.: 1950)*, 198(4), 1553–1564. <https://doi.org/10.4049/JIMMUNOL.1600193>
- Yoshida, K., Berg, T. K. van den, & Dijkstra, C. D. (1993). Two functionally different follicular dendritic cells in secondary lymphoid follicles of mouse spleen, as revealed by CR1/2 and FcR gamma II-mediated immune-complex trapping. *Immunology*, 80(1), 34. [./pmc/articles/PMC1422113/?report=abstract](https://pmc/articles/PMC1422113/?report=abstract)
- Youngblood, B., Hale, J. S., Kissick, H. T., Ahn, E., Xu, X., Wieland, A., Araki, K., West, E. E., Ghoneim, H. E., Fan, Y., Dogra, P., Davis, C. W., Konieczny, B. T., Antia, R., Cheng, X., & Ahmed, R. (2017). Effector CD8 T cells dedifferentiate into long-lived memory cells. *Nature* 2017 552:7685, 552(7685), 404–409. <https://doi.org/10.1038/nature25144>
- Yurova, K. A., Khaziakhmatova, O. G., Todosenko, N. M., & Litvinova, L. S. (2020). The Role of γC Cytokines (IL-2, IL-7, and IL-15) in Regulation of Activation-Induced Cell Death of Memory T Cells. *Cell and Tissue Biology* 2020 14:6, 14(6), 419–426. <https://doi.org/10.1134/S1990519X20060115>
- Zammit, D. J., Turner, D. L., Klonowski, K. D., Lefrançois, L., & Cauley, L. S. (2006). Residual antigen presentation after influenza virus infection affects CD8 T cell activation and migration. *Immunity*, 24(4), 439–449. <https://doi.org/10.1016/J.IMMUNI.2006.01.015>
- Zaric, M., Lyubomska, O., Poux, C., Hanna, M. L., McCrudden, M. T., Malissen, B., Ingram, R. J., Power, U. F., Scott, C. J., Donnelly, R. F., & Kisselkell, A. (2015). Dissolving microneedle delivery of nanoparticle-encapsulated antigen elicits efficient cross-priming and Th1 immune responses by murine Langerhans cells. *The Journal of Investigative Dermatology*, 135(2), 425–434. <https://doi.org/10.1038/JID.2014.415>
- Zhang, J. G., Czabotar, P. E., Policheni, A. N., Caminschi, I., San Wan, S., Kitsoulis, S., Tullett, K. M., Robin, A. Y., Brammananth, R., van Delft, M. F., Lu, J., O'Reilly, L. A., Josefsson, E. C., Kile, B. T., Chin, W. J., Mintern, J. D., Olshina, M. A., Wong, W., Baum, J., ... Lahoud, M. H. (2012). The dendritic cell receptor Clec9A binds damaged cells via exposed actin filaments. *Immunity*, 36(4), 646–657. <https://doi.org/10.1016/J.IMMUNI.2012.03.009>
- Zhang, P., Liu, X., & Cao, X. (2015). Extracellular pattern recognition molecules in health and diseases. *Cellular and Molecular Immunology*, 12(3), 255. <https://doi.org/10.1038/CMI.2014.81>
- Zhang, X., Sun, S., Hwang, I., Tough, D. F., & Sprent, J. (1998). Potent and selective stimulation of memory-phenotype CD8+ T cells in vivo by IL-15. *Immunity*, 8(5), 591–599. [https://doi.org/10.1016/S1074-7613\(00\)80564-6](https://doi.org/10.1016/S1074-7613(00)80564-6)

- Zhang, Y., Joe, G., Hexner, E., Zhu, J., & Emerson, S. G. (2005). Host-reactive CD8+ memory stem cells in graft-versus-host disease. *Nature Medicine*, 11(12), 1299–1305. <https://doi.org/10.1038/NM1326>
- Zheng, W. P., & Flavell, R. A. (1997). The transcription factor GATA-3 is necessary and sufficient for Th2 cytokine gene expression in CD4 T cells. *Cell*, 89(4), 587–596. [https://doi.org/10.1016/S0092-8674\(00\)80240-8](https://doi.org/10.1016/S0092-8674(00)80240-8)
- Zhou, L., Ivanov, I. I., Spolski, R., Min, R., Shenderov, K., Egawa, T., Levy, D. E., Leonard, W. J., & Littman, D. R. (2007). IL-6 programs T(H)-17 cell differentiation by promoting sequential engagement of the IL-21 and IL-23 pathways. *Nature Immunology*, 8(9), 967–974. <https://doi.org/10.1038/NI1488>
- Zhu, J., Cote-Sierra, J., Guo, L., & Paul, W. E. (2003). Stat5 Activation Plays a Critical Role in Th2 Differentiation. *Immunity*, 19(5), 739–748. [https://doi.org/10.1016/S1074-7613\(03\)00292-9](https://doi.org/10.1016/S1074-7613(03)00292-9)
- Zhu, J., & Paul, W. E. (2008). CD4 T cells: fates, functions, and faults. *Blood*, 112(5), 1557–1569. <https://doi.org/10.1182/BLOOD-2008-05-078154>

ANNEXE

La revue présenté ci-après a été publiée dans MDPI Vaccines (Van Tilbeurgh et al., 2021) et a pour objectif de mettre en avant la pertinence de la vaccinologie des systèmes pour approfondir notre compréhension des mécanismes de la réponse vaccinale. Nous avons pour cela abordé l'intérêt de combiner l'études des réponses vaccinales à différentes échelles et des outils d'analyses bio statistiques pour identifier des signatures et des biomarqueurs prédictifs dans le but ultime d'améliorer le design de vaccins efficace.



Review

Predictive Markers of Immunogenicity and Efficacy for Human Vaccines

Matthieu Van Tilbeurgh ¹, Katia Lemdani ¹, Anne-Sophie Beignon ¹, Catherine Chapon ¹ , Nicolas Tchitcheck ² , Lina Cheraitia ¹, Ernesto Marcos Lopez ¹, Quentin Pascal ¹, Roger Le Grand ¹ , Pauline Maisonnasse ¹ and Caroline Manet ^{1,*}

¹ Immunology of Viral Infections and Autoimmune Diseases (IMVA), IDMIT Department, Institut de Biologie François-Jacob (IBJF), University Paris-Sud—INSERM U1184, CEA, 92265 Fontenay-Aux-Roses, France; matthieu.van-tilbeurgh@cea.fr (M.V.T.); lemdani.katia@gmail.com (K.L.); anne-sophie.beignon@cea.fr (A.-S.B.); catherine.chapon@cea.fr (C.C.); lina.cheraitia@yahoo.com (L.C.); ernesto.marcos-lopez@cea.fr (E.M.L.); quentin.pascal@cea.fr (Q.P.); roger.le-grand@cea.fr (R.L.G.); pauline.maisonnasse@cea.fr (P.M.)

² Unité de Recherche i3, Inserm UMR-S 959, Bâtiment CERVI, Hôpital de la Pitié-Salpêtrière, 75013 Paris, France; nicolas.tchitcheck@sorbonne-universite.fr

* Correspondence: caroline.manet@cea.fr; Tel.: +33-01-46-54-94-77



Citation: Van Tilbeurgh, M.; Lemdani, K.; Beignon, A.-S.; Chapon, C.; Tchitcheck, N.; Cheraitia, L.; Marcos Lopez, E.; Pascal, Q.; Le Grand, R.; Maisonnasse, P.; et al. Predictive Markers of Immunogenicity and Efficacy for Human Vaccines. *Vaccines* **2021**, *9*, 579. <https://doi.org/10.3390/vaccines9060579>

Academic Editors: Maria G. Isagulants and Felicity Jane Burt

Received: 30 April 2021

Accepted: 24 May 2021

Published: 1 June 2021

Publisher's Note: MDPI stays neutral with regard to jurisdictional claims in published maps and institutional affiliations.



Copyright: © 2021 by the authors. Licensee MDPI, Basel, Switzerland. This article is an open access article distributed under the terms and conditions of the Creative Commons Attribution (CC BY) license (<https://creativecommons.org/licenses/by/4.0/>).

Abstract: Vaccines represent one of the major advances of modern medicine. Despite the many successes of vaccination, continuous efforts to design new vaccines are needed to fight “old” pandemics, such as tuberculosis and malaria, as well as emerging pathogens, such as Zika virus and severe acute respiratory syndrome coronavirus 2 (SARS-CoV-2). Vaccination aims at reaching sterilizing immunity, however assessing vaccine efficacy is still challenging and underscores the need for a better understanding of immune protective responses. Identifying reliable predictive markers of immunogenicity can help to select and develop promising vaccine candidates during early preclinical studies and can lead to improved, personalized, vaccination strategies. A systems biology approach is increasingly being adopted to address these major challenges using multiple high-dimensional technologies combined with in silico models. Although the goal is to develop predictive models of vaccine efficacy in humans, applying this approach to animal models empowers basic and translational vaccine research. In this review, we provide an overview of vaccine immune signatures in preclinical models, as well as in target human populations. We also discuss high-throughput technologies used to probe vaccine-induced responses, along with data analysis and computational methodologies applied to the predictive modeling of vaccine efficacy.

Keywords: vaccines; systems immunology; predictive biomarkers; vaccine signatures; preclinical models; high-throughput technologies; in vivo imaging; unsupervised analyses; machine learning

1. Introduction

Vaccines are the most effective preventive measure ever developed in the fight against diseases. They have led to the eradication of smallpox and to a major reduction in the incidence of diseases such as diphtheria, tetanus or poliomyelitis. Nevertheless, the need for new vaccines has never been so critical as demonstrated by the recent SARS-CoV-2 pandemic. Novel vaccines are also required to fight against “old” diseases like malaria and tuberculosis [1], which are still responsible for millions of new infections and hundreds of thousands of deaths each year [2]. Improving existing vaccines is also important to increase disease control and prevent outbreaks of re-emerging pathogens [3]. For example, despite its high efficacy, the live-attenuated yellow fever (YF) vaccine cannot be safely administrated to immunocompromised individuals, and its slow production can lead to vaccine shortage and subsequent inadequate control of YF epidemics [4].

One of the main goals in vaccinology is to identify factors that reflect vaccine-induced immune responses and thus provide biomarkers of vaccine immunogenicity and efficacy.

A biomarker can be defined as “a characteristic that is objectively measured and evaluated as an indicator of normal biological processes, pathogenic processes, or pharmacological responses to a therapeutic intervention” [5]. By extension, a vaccine signature can be defined as a set of biomarkers that statistically differ between vaccinated and non-vaccinated individuals and are indicative of vaccine-induced biological responses.

The emerging field of systems vaccinology aims to identify biomarkers and immune signatures that correlate with vaccine efficacy to decipher protective immune mechanisms. A correlate of protection is defined as a biomarker or an immune mechanism that is “statistically related to and responsible for protection” [6,7]. Thus, the possibility to predict vaccine efficacy is tightly intertwined with the notion of correlates of protection which can be characterized by various types of biomarkers.

High-throughput technologies have rapidly expanded over the last several years and have been frequently employed in systems vaccinology studies, making it possible to extend the range of biomarkers included in vaccine signatures [8–12]. New approaches in data analysis methodologies and computational modeling take vaccine signatures a step further by giving rise to the possibility of identifying immune responses that correlate and/or predict vaccine efficacy.

Although systems vaccinology ultimately aims to develop predictive models of vaccine efficacy in human populations, applying the same approach to animal models, which allow the use of a wide range of tools in controlled study designs, empowers vaccine research and improves preclinical studies. Notably, high-throughput imaging technologies can be used in preclinical models to characterize immune responses at the whole-body and tissue levels [13,14] and to define more comprehensive vaccine signatures. In addition, using systems vaccinology in models such as non-human primates (NHPs), which are highly predictive of the human immune and vaccine responses, will increase the translation of discoveries from animal studies to human clinics.

Here, we review approaches to identify biomarkers and signatures of vaccine responses in preclinical models and humans. We provide an overview of high-throughput technologies used to probe vaccine-induced responses, including *in vivo* and *ex vivo* imaging technologies. We also present data analysis and computational methodologies used to define signatures that correlate with and potentially predict vaccine efficacy.

2. Identification of Biomarkers and Signatures of Vaccine Responses

One of the main goals in systems vaccinology is to identify a strong and reliable vaccine signature that statistically differs between immunized and non-immunized individuals that can be easily measured in the blood and at a reasonable cost.

However, protection conferred by vaccination results from complex interactions between innate and adaptive immunity and there are considerable differences between individuals in the response to immunization. Such variation, mediated by both host factors and vaccine properties, precludes the description of a universal marker of vaccine efficacy (Figure 1).

Indeed, many studies have demonstrated the effects of sex on vaccine responses [15–17], as well as the preexistent immunological background and non-immunological co-factors. Host genetic background also modulates immune responses to vaccines, for example, several studies [8,18] demonstrated that different signatures of the yellow fever 17D strain (YF-17D) vaccine can be found between human cohorts and Pogorelyy et al. [11] even found differences between monozygotic twins. In the past years, the influence of host genetic factors has been investigated more precisely through vaccinomics [19,20]. Genome wide association studies (GWAS) have identified several polymorphisms in the human leukocyte antigen (HLA) gene associated to a poor or non-response to the hepatitis B virus (HBV) [21–24] and to the measles, mumps, and rubella (MMR) [25] (REF) vaccines. Other genes encoding various cytokines, Toll-like-receptors (TLR) and their signaling molecules have been associated to increased or decreased HBV and MMR vaccine efficacy, as reviewed extensively by Omersel and Kuzelicki [19].

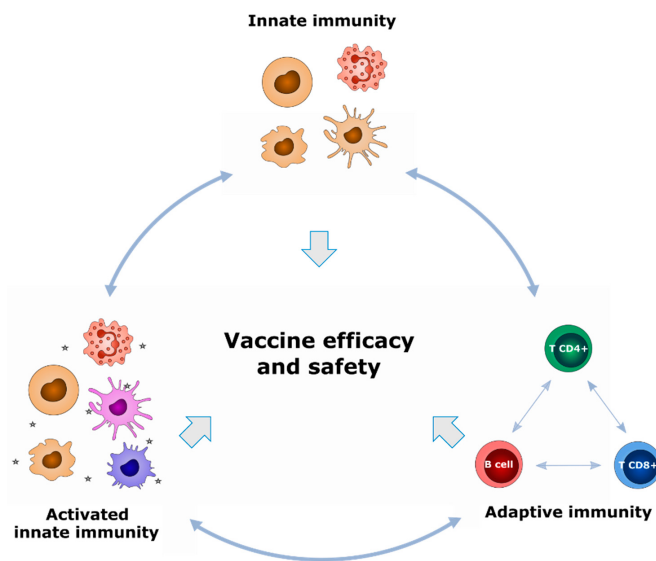


Figure 1. Vaccine efficacy and safety are determined by interactions between innate and adaptive immunity. These interactions are shaped by host factors and can be oriented by vaccine properties.

Similarly, vaccine composition influences the dynamics of immune parameters, such as immune-cell migration to the injection site or the immune-cell transcriptional profile [26,27]. In addition, Li et al. demonstrated that the vaccine signature differs depending on the type of immunogen, similarly to pathogens targeting cells and tissues through various mechanisms [27].

Consequently, host- and vaccine-related factors, extensively reviewed by Zimmermann and Curtis [28], may influence and shape biomarker expression by affecting immune responses and, subsequently, vaccine signatures.

The characterization of extensive vaccine signatures is further influenced by the different types and sources of biomarkers, as discussed hereafter.

2.1. What Types of Biomarkers Can Be Used to Define Vaccine Signatures?

Antibody responses are widely used to assess vaccine responses [29]. However, they may not always represent the best biomarkers of vaccine efficacy, especially when vaccine-induced protection is mediated by cellular immunity. In addition, effective neutralizing antibody responses may take months or years to be induced, such as for broadly human immunodeficiency virus (HIV)-neutralizing antibodies, and can jeopardize the use of antibodies as early biomarkers of vaccine-induced protection [30]. Moreover, effective antibody responses can also be induced through T-cell independent pathways, suggesting that unconventional or unknown biomarkers could correlate with and predict such responses [31]. Indeed, Chaudhury et al. showed that the sole use of such analysis is too reductive to identify differences between immune responses. Indeed, their predictive model of the malaria vaccine-induced immune response also integrates other immune parameters, such as IL-4 and IL-6 levels, which are variables of importance in different tissues such as blood or liver [32].

Years of immune system screening have demonstrated that immune responses to pathogens and vaccines are highly multifactorial and involve numerous diverse actors. Historically, the quality of the vaccine response has been closely related to adaptive lymphoid cell populations, including effector responses of CD8⁺ T cells and CD4⁺ T helper cells, as well as immune memory. However, the role of innate cell populations has been recently re-evaluated to consider their influence in initiating and orienting the adaptive response. Consequently, innate cells are increasingly being studied as early biomarkers of vaccine efficacy. Notably, several studies have shown that innate myeloid cells, such as neutrophils, monocytes, and innate lymphoid cells (ILCs), such as natural killer (NK) cells, are of interest in defining vaccine signatures [33–36]. The diverse innate and adaptive

immune-cell subsets, including unconventional subsets such as T γ δ lymphocytes and ILCs, represent a large source of potential biomarkers that could be used to define signatures of vaccine response. Furthermore, it has also been shown that the route of immunization can orient vaccine responses, suggesting that non-immunological cells within target tissues could broaden the list of potential biomarkers of vaccine responses [26,37].

Until now, systems vaccinology studies have mainly used transcriptomic techniques to investigate vaccine responses and identify biomarkers to define vaccine signatures [8,11,27]. However, the multitude of chain reactions induced by vaccine injection may affect cellular activity at different levels, such as epigenetic modifications, protein levels, or enzyme activity, which may also constitute a large reservoir of potential biomarkers [6,38]. Other factors, such as cytokines or growth factors should not be excluded from the list of candidate biomarkers of vaccine responses [32,39]. Finally, variations in the composition of the gut microbiota have been shown to influence vaccine-induced responses, thus further increasing the spectrum of possible immune biomarkers [40].

Thus, a biomarker can be based on the detection of gene transcripts, proteins, and metabolites at the single cell or cell population level. Furthermore, data provided by histology, tissue imaging, and even clinical metadata are still poorly represented in the emerging field of systems vaccinology but would also empower holistic approaches aiming to define comprehensive signatures of vaccine efficacy (Figure 2).

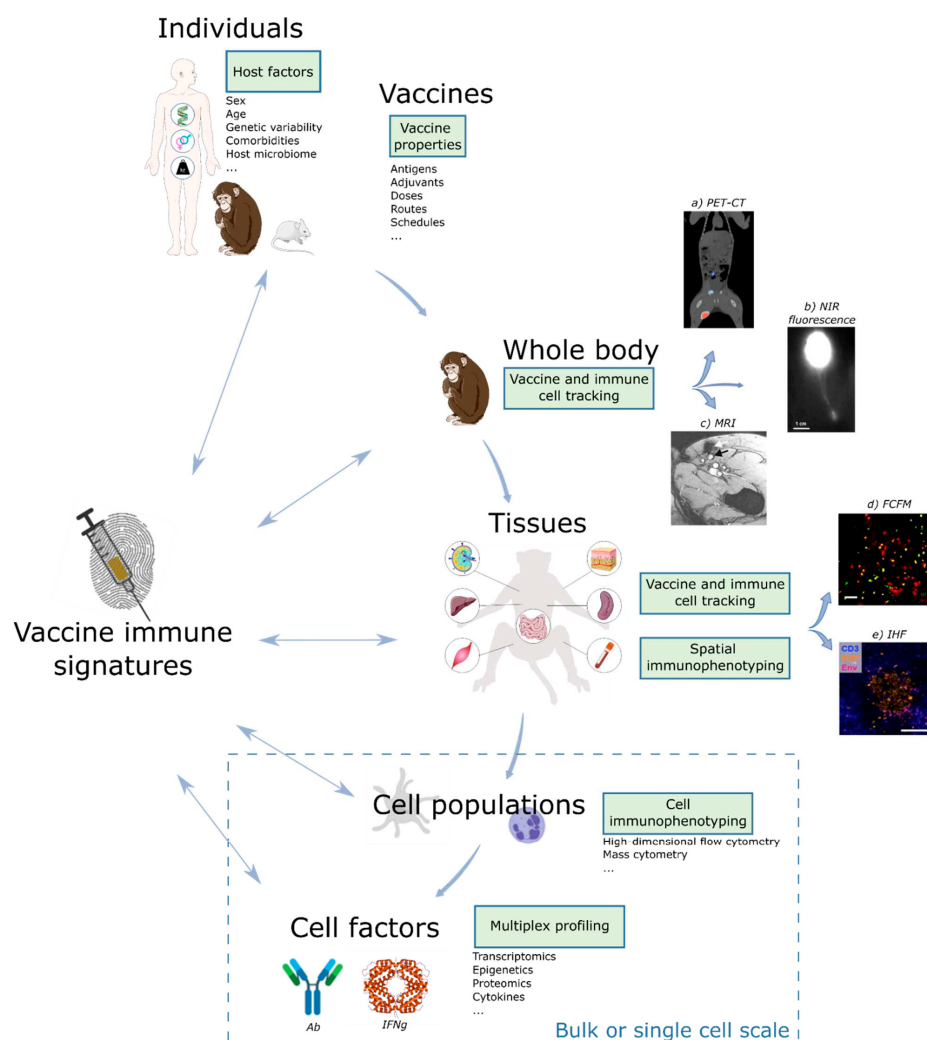


Figure 2. From individuals to single cells: integrating multi-level data into comprehensive vaccine signatures. Host factors and vaccine properties are important determinants of immune responses.

Variations of these determinants, such as genetic polymorphisms, age, host microbiome or immunization procedure, thus condition the definition of vaccine signatures. Systems immunology enables the identification of biomarkers of vaccine responses at multiple scales, from whole-body to cellular factors. Diverse high-throughput technologies, including *in vivo* imaging, allow the characterization of vaccine immune signatures through various applications, such as immune-cell tracking, cell immunophenotyping, and multiplex profiling. Combining and integrating data at different scales will be of great value in identifying extensive vaccine immune signatures. (a) Positron emission tomography-computed tomography (PET-CT) imaging of the YF preM mRNA vaccine in NHPs [41]. (b) Near-infrared fluorescence (NIR) imaging to follow an anti-Langerin-HIVGag fusion vaccine from the injection site to the draining lymph node [42]. (c) Magnetic resonance imaging (MRI) of a DC-based vaccine in the lymph node [43]. (d) *In vivo* tracking of Langerhans cells within the skin by fibered confocal fluorescence microscopy (FCFM) [44]. (e) Tracking of fluorescently labeled HIV-1 envelope glycoprotein trimers in lymph nodes by immunohistofluorescence (IHF) [45].

2.2. From What Samples Can We Identify Vaccine Response Biomarkers?

In terms of where to look, the search for immune biomarkers is not only oriented by the factors to be identified per se and existing knowledge on the immunological processes involved but is also further constrained by practical aspects, including technical feasibility, as well as ethical and financial restrictions. Given such limitations, **blood** constitutes the main source of biomarkers, as it is the most accessible sample in humans, allowing the study of circulating cells, soluble factors (plasma), and antibodies (serum). The diversity and functionality of circulating immune cells have been extensively investigated, especially since the rise of high-throughput technologies [46,47], providing a good snapshot of the global immune state. Furthermore, peripheral blood mononuclear cells (PBMCs) may also reflect immune activity in other tissues, as shown by DeGottardi et al. for circulatory CXCR5⁺ CD4⁺ T cells and lymph node T follicular helper (TFH) activity [48]. Others have also used blood samples to identify correlates of protection for several vaccines, such as cell-mediated immunity for varicella-zoster virus (VZV) or humoral response for smallpox [49–51]. Finally, predictive models have also been developed from PBMC samples, such as that described by Querec et al., predicting the YF-17D CD8⁺ T cell response with high accuracy [52].

However, immune responses imply cell mobilization and maturation processes within various tissues, including lymphoid (lymph nodes, bone marrow) and non-lymphoid organs (liver, skin, muscles, etc.). Contrary to peripheral blood, other human tissues are not easy to access without invasive procedures or advanced imaging techniques and have rarely been included in large-scale studies (see Section 4). However, certain tissues may be accessible by performing small biopsies, such as fine-needle aspiration, commonly used for tumor biopsies or skin explants [53], although the size of such samples may limit the use of techniques that require large numbers of cells. On the other hand, preclinical models allow much wider access to all organs and thus the identification of relevant biomarkers that reflect tissue-based immune mechanisms.

Moreover, differences in immune-cell colonization between tissues have been demonstrated and must be considered when searching for vaccine biomarkers [37,46]. Indeed, the injection site may be used to identify early biomarkers, such as antigen uptake [42,45], whereas biomarkers of immune memory can be detected in lymph nodes and/or bone marrow [54,55]. Deep characterization of vaccine responses may also need to account for pathogen tropism for the identification of biomarkers. For example, liver or spleen could be a source of biomarkers in the case of YF-17D vaccination [56].

Furthermore, mucosal immunity can be crucial in the protection conferred by certain vaccines. Darrah et al. demonstrated that intravenous immunization of Rhesus macaques with bacille Calmette-Guérin (BCG) vaccine (Danish Strain 1331, Statens Serum Institute, Copenhagen, Denmark) induced a higher CD4⁺ and CD8⁺ T cell responses in cells from bronchoalveolar lavages than by other immunization routes [57]. Pattyn et al. reviewed studies in which human papillomavirus (HPV)-specific antibodies were measured in

cervicovaginal secretions in response to HPV vaccine [58], which implies that, similarly to tissues, biological fluids may also represent a potential source of biomarkers.

In conclusion, various types of biological samples reflect different aspects of the immune response and influence the biomarkers that can be identified. Thus, investigating diverse types of samples leads to deeper characterization of vaccine responses and allows unravelling of the vaccine biomarkers involved in various immune processes.

2.3. At What Time Should We Identify Vaccine Response Biomarkers?

Temporality is another important dimension to consider when identifying biomarkers to define vaccine signatures, as they would vary in parallel with the stages of the immune response, from the baseline to effector and memory stages.

Recently, a study aiming to better understand the impact of early innate parameters on the adaptive response against modified vaccinia Ankara (MVA) identified cellular and molecular events specifically activated by MVA immunization as early as six hours post-vaccination [36]. Other studies have also shown that early time points, within 24 h post-immunization, are of interest, as early innate biomarkers correlated with the adaptive responses to the vaccine [8,33]. Furthermore, innate immune biomarkers can be detected as late as two months after vaccination, as observed for granulocytes, monocytes, and dendritic cells (DCs) from NHPs immunized with MVA [35]. Apart from innate immunity, certain biomarkers may need weeks to appear, in particular those associated with adaptive responses and maturation processes that lead to vaccine memory. In addition, the identification of immune parameters that correlate with long-term memory induced by vaccines may require searching for biomarkers several months after immunization. For example, Bhaumik et al. investigated the long-term persistence of immune memory following one- or two-dose inactivated poliovirus vaccine schedules. They showed that memory B cells can be induced by both vaccine regimens, although this cell subset declined by five months after a single immunization, whereas it persisted for more than one year with the two-dose strategy [59]. Additionally, identifying predictive biomarkers at baseline, i.e., before vaccination, has drawn interest from researchers who reported proof-of-concept results on influenza [60,61], yellow fever [62], and hepatitis B [63] vaccines. Thus, the identification of biomarkers will be highly dependent on the time of sampling.

However, sampling is not the only temporal component that influences vaccine signatures. Indeed, several studies have highlighted the impact of the vaccine schedule on the distribution of cell populations or antibody production [33,64]. Thus, differential post-prime and post-boost vaccine signatures could be identified and characterized, which could provide useful insights to the design of new vaccination strategies for human populations.

Temporal considerations thus represent an important source of biomarker variation that need to be thoroughly investigated to fully understand the impact of time on the immune responses and biomarker dynamics following vaccine injection.

Beyond considerations of nature, distribution and time, the identification of vaccine signatures is also conditioned by the technologies used to measure immune-related biomarkers, as discussed in the following sections.

3. Conventional High-Throughput Technologies to Assess Vaccine Responses

3.1. High-Dimensional Flow and Mass Cytometry

Technologies for single cell analysis have become crucial in the field of vaccinology. The advances in cytometric technologies over the last several years have allowed researchers to obtain a comprehensive understanding of heterogeneity among immune cells, cell function, cellular differentiation, and signaling pathways [65] and to apply this knowledge to the discovery of biomarkers of vaccine responses [66].

Traditional fluorescent flow cytometry relies on fluorescent markers as a reporter. The emission spectra overlap of the various fluorophores, auto-fluorescence, and compensation-related issues limit the number of markers that can be simultaneously measured. On the other hand, spectral flow cytometry is based on many of the fundamental aspects of

conventional flow cytometry but has unique optical collection and analytical capabilities, doubling the number of markers that can be simultaneously measured [67].

A format for flow cytometry has been developed that takes advantage of the precision of mass spectrometry. This fusion of the two technologies, called mass cytometry, enables the simultaneous measurement of up to 50 cellular features at single-cell resolution, significantly augmenting the ability of cytometry to evaluate complex cellular systems and processes [68,69]. These characteristics enable the investigation of complex and coordinated cellular systems by observing the diversity of cellular phenotypes and behaviors in a single sample [68]. This technology opens new possibilities in vaccinology, providing a tool capable of simultaneously capturing diverse aspects of cellular behavior in millions of individual immune cells.

Indeed, mass cytometry has since shown that there are hundreds of phenotypically distinct cell types in the peripheral blood of humans and animal models [36,70,71]. The ability to discriminate between these cell types is crucial to our understanding of cellular immunity and vaccine responses, and mass cytometry has become a powerful tool for this purpose. This can be illustrated by recent human and preclinical vaccine studies, which provide evidence of the phenotypic diversity of both lymphoid and myeloid cells [46].

For example, Palgen et al. characterized qualitative and quantitative differences in the recruitment of innate myeloid cells following MVA prime-boost immunization of NHPs [35]. Moreover, longitudinal mass cytometry analysis of NK cells after MVA vaccination revealed key features of cell phenotype, suggesting that the innate response to the boost is more highly coordinated between NK cells and innate myeloid cells than the response to the prime [34]. Another study highlighted the phenotypic heterogeneity of vaccine-altered circulating B cells of NHPs immunized twice with MVA, two months apart [72].

Mass cytometry has also been used to identify novel influenza vaccine-specific CD4⁺ T-cell subsets in humans [73]. In this study, the authors identified two cell clusters that responded either to influenza peptide stimulation or influenza vaccination. One cluster corresponded to pre-existing influenza virus-specific cells that presumably persisted from previous vaccination(s) or infection(s), whereas the second cluster reflected CD4⁺ T cells responding to influenza vaccination but not the specific peptides used for stimulation. Both clusters appeared to be effector memory subsets with low CCR7 and CD45RA expression and their cytokine expression profiles were distinct, as the first showed high IL-2, TNF- α , and IFN- γ expression, whereas the second mainly expressed IL-17. These detailed analyses underscore the role of CD4⁺ memory T-cell subsets in influenza virus infection and highlight the huge potential of mass cytometry to distinguish and characterize very specific cell subsets [73].

In a unique study, the ontogeny of various subsets of YF-17D-specific circulatory CXCR5⁺ CD4⁺ T cells was accessed by unsupervised analysis of mass cytometry data. The authors observed that YF virus-specific CXCR5⁺ T cells existed in multiple phenotypic clusters and that one key population was mainly ICOS⁺ PD1⁺ CD38⁺. This population most resembled germinal center T follicular helper (GC-TFH) cells, based on surface marker expression, and exhibited delayed accumulation in the periphery, implying that these T cells could be emigrants from lymph node germinal centers (GCs). The relative kinetics of their emergence following vaccination suggests that these triple positive CXCR5⁺ cells transition to become CD38⁺ ICOS⁻ PD1⁺ and then CD38⁻ ICOS⁻ PD1⁺ cells before accumulating in the periphery as CD38⁻ ICOS⁻ PD1⁻ CCR7⁺ cells. Overall, these results imply that most antigen-specific CXCR5⁺ T cells are derived from pre-TFH, and/or TFH cells [48].

Mass cytometry was also applied to comprehensively characterize the circulating immune-cell populations in elderly individuals, both before and after administration of an investigational adjuvanted protein vaccine against respiratory syncytial virus (RSV) in a Phase 1a trial. Here, mass cytometry was used to characterize the cellular response profile of enzyme-linked immunospot (ELISPOT) responders and non-responders. Principal component analysis revealed baseline differences in activated (HLA-DR⁺) CD4⁺ and CD8⁺ T cells, which were more numerous in non-responders than responders. Higher expression

of HLA-DR, CCR7, CD127, and CD69 was also found in non-responders than responders using a viSNE algorithm to analyze RSV-responsive CD4⁺ and CD8⁺ T cells [74].

These studies demonstrate the potential of mass cytometry as a powerful technology to enable comprehensive profiling of immune components, thus allowing the prediction of responses to vaccines.

3.2. Cytokine Profiling

Immune-based assays are widely used to assess vaccine responses and since the rise of systems vaccinology, numerous studies have shown correlations between transcriptomic and cytokine signatures to various vaccines. Various technologies are currently available, from single-plex to multiplex analysis, allowing the identification of soluble vaccine biomarkers. Some have been reviewed by D. Furman and MM. Davis [75].

Most immunoassays are based on enzyme-linked immunosorbent assays (ELISAs), widely used for the robust and reliable detection of soluble components at low concentration (ng to pg/mL) by the measurement of absorbance. ELISPOT and fluoro-immunospot (FLUOROSPOT) are very sensitive ELISA-derived techniques designed to study the cytokine production capacity of cells upon specific stimulation. Contrary to ELISA, FLUOROSPOT allows the identification of poly-secreting cells by the simultaneous detection of up to four analytes using fluorescent antibodies. Despite their sensitivity, these techniques are restricted to a small number of analytes and multiplying tests to increase soluble factor detection requires larger sample volumes and is time consuming.

Therefore, multiplex immunoassays have been developed that allow rapid simultaneous quantification of a wide diversity of soluble proteins combined with high sensitivity (down to pg/mL and even fg/mL for SIMOA®, Quanterix, Billerica, MA, USA) with very small biological samples (down to 1 µL). ELISA-based multiplexing technologies, such as Quantibody® microarrays (MSD) or xMAP® Technology (Luminex®, Austin, TX, USA), are commonly used for cytokine profiling and immunological studies. For example, multiplex profiling of 24 cytokines/chemokines was performed on healthy individuals and tuberculosis patients and identified seven differentially expressed biomarkers between the two groups [76]. Such techniques might also reveal biomarkers in vaccine studies. These techniques rely on capture antibodies coated on slides with a spatial specificity (MSD, Quantibody® microarrays) or on microbeads in suspension (xMAP® Technology, Luminex® assays), with a detection method related to flow cytometry. Another high-throughput multiplexing immunoassay with a sensitive detection method, based on quantitative polymerase chain reaction (qPCR) amplification of DNA oligonucleotides coupled to antibodies, has been developed: the proximity extension assay (PEA, Olink®, Uppsala, Sweden). PEA has demonstrated a robust ability in proteomic profiling in various diseases, including SARS-CoV-2 infection [77], and is yet another powerful tool to explore biomarkers of vaccine responses.

Cytokine measurement can also be performed using flow or mass-cytometry by intracellular cytokine staining (ICS). This method allows characterization of the cell secretion profile after their potential stimulation, along with their surface phenotype. However, despite precise identification of the producing cells, the sensitivity of ICS is generally lower than that of other immunoassays [78].

Systems vaccinology studies have embedded multiplexing technologies in the identification of soluble biomarkers of vaccine responses. Huttner et al. defined an Ebola vaccine (recombinant vesicular stomatitis virus-vectored Zaire Ebola vaccine, rVSV-ZEBOV) cytokine signature associated with biological and clinical outcomes [79]. An early IP-10 signature correlating with the antibody response was also identified after immunization with rVSV-ZEBOV [12]. More recently, several soluble factors, including IP-10, were identified using a 27-plex assay and shown to be important biomarkers of immune responses to tularemia vaccines [39].

Large-scale profiling techniques of soluble factors are thus appropriate for the deep characterization of cell secretion in response to immunogens.

3.3. OMICS Technologies

In addition to immune-cell phenotyping using multiparameter cytometry (flow or mass) and immunoproteomics, gene expression is widely used to identify signatures and predictors of vaccine-induced specific antibody and T-cell responses. Furthermore, transcriptomic and genomic data (using next-generation sequencing) allow to capture the diversity of the immune repertoire induced by vaccines [80], with a comprehensive quantification of full-length T cell receptor (TCR) and B cell receptor (BCR) variable region sequences [81]. Additional layers of information, including epigenomic (using ChIP-Seq or ATAC-Seq), metabolomic (using nuclear magnetic resonance spectroscopy and mass spectrometry), and that from the microbiome (using 16S rRNA or shotgun metagenomic sequencing) can be used to further characterize vaccine responses, as appropriate technologies are becoming available [38,82].

Transcriptomics (using RNA microarrays or RNA-Seq) analyzes sets of RNA transcripts. Microarrays are based on a fixed probe technology, whereas RNA-Seq quantifies the abundance of all transcripts (any sequence). Epigenomics studies the set of chemical modifications of the DNA and histone proteins, of which the type and position determine the chromatin structure and accessibility to the transcriptional machinery. These are key for the regulation of gene expression. Metabolomics studies the set of metabolites present in biofluids, cells, and tissues. Metabolites can be the substrates or products of metabolism. They can also originate from microorganisms, xenobiotic exposure, or the diet. The microbiome refers to the genomes of all microorganisms in our body (gut, skin, lungs, and other epithelial surfaces). The microbiota modulates host immune responses locally and globally.

Transcriptomes and chromatin states can also be studied at the single-cell level and even simultaneously. Bulk measurements, such as whole blood or PBMC RNA-Seq, are indeed sensitive to changes in the most abundant cell subsets (changes in gene expression and/or cell composition), but do not capture changes in rare cell populations. Recently, single-cell -omics technologies have been used successfully to study the immune cell responses triggered by BCG [57], HIV [83] and SARS-CoV2 [84] vaccines. Similarly, TCR and BCR sequencing have been applied at the single-cell level to characterize the immune repertoire of human individuals immunized with YF-17D [85], and influenza [86,87] vaccines and in HIV-vaccinated Rhesus macaques [88]. Similarly, Waickman et al. used single-cell RNA-Seq in combination with longitudinal TCR clonotype analysis to study T cell immunity in response to immunization with a recombinant, tetravalent dengue virus (DENV) vaccine [89]. Precisely, they were able to identify a set of biomarkers which characterize the most persistent vaccine-reactive memory CD8⁺ T cells. These studies illustrate how single-cell transcriptomic analyses can provide insights into the molecular mechanisms implicated in the regulation of immune memory and more generally, in immune responses to vaccines.

However, there are many challenges associated to the use of -omics technologies. The sample size for both discovery and validation cohorts needs to be sufficient to overcome the risk of high type 1 and 2 errors due to the large number of markers that are measured using omics technologies and the low contributing effect size of individual markers. Moreover, the integration of multi-omics data is far from being straightforward (see Section 5).

In addition to these high-throughput technologies, conventionally used in systems vaccinology studies, preclinical models offer the possibility to enrich vaccine signatures with imaging data.

4. Imaging Technologies to Refine and Expand Vaccine Signatures

4.1. In Vivo Imaging of Vaccine Trafficking and the Immune Response

The monitoring of vaccine components and the assessment of immune-cell dynamics at injection sites and lymph nodes allows better understanding of the immune response to vaccines. A variety of in vivo imaging modalities, including optical imaging (fluorescence and bioluminescence), magnetic resonance imaging (MRI), and nuclear imaging (positron emission tomography (PET), single photon emission computed tomography (SPECT)) can

be used to study such dynamics. Thus, *in vivo* non-invasive imaging techniques are widely used to visualize the location and distribution of molecules, antigens, and inflammatory immune cells. The advantages, limitations, and applications of these imaging modalities have been well reviewed in the literature [90–92].

4.1.1. Whole Body Imaging of Vaccine Distribution and the Immune Response

Fluorescence imaging allows the *in vivo* visualization of the dynamics of vaccines and their interaction with immune cells in real time, facilitating the understanding of vaccine-induced immune-response mechanisms in preclinical models. For example, Romain et al. assessed the migration kinetics of a vaccine based on DCs expressing HIV-Gag protein from the injection site to draining lymph nodes (DLNs) in macaques by NIR (near infrared) fluorescence imaging [93]. Furthermore, Salabert et al. studied the development of *in vivo* and *in vivo* approaches to track vaccine-targeted Langerhans cells (LCs) following intradermal injection in NHPs [42].

Magnetic resonance imaging (MRI), widely used in clinical practice, makes it possible to obtain high whole-body anatomical resolution and is particularly suited for the analysis of both vaccine biodistribution and the associated immune response. This is achieved using various contrast agents and probes to label the vaccines and cells for MRI tracking [94]. For example, the *in vivo* longitudinal biodistribution of a vaccine labeled with superparamagnetic iron oxide (SPIO) was assessed in a mouse HPV16 tumor model and showed the presence of the antigen for several weeks post-vaccination in the DLNs [95]. The efficacy of DC-based vaccines is limited in patients and may be due to insufficient delivery of the vaccine to the lymph nodes. The tracking of iron nanoparticle-labelled DCs to the lymph nodes by MRI is possible in mice [96] and can be safely performed in patients [43], allowing the improvement of vaccine design.

The ability to directly image myeloid and lymphoid cells, and changes in their distribution *in vivo* is crucial to achieving a better understanding of the processes of the immune response. Several studies have demonstrated the ability to track and visualize immune cells by *in vivo* imaging (e.g., MRI and PET imaging) in various applications following either the reinjection of previously *ex vivo* labeled cells or the direct *in vivo* administration of specific labeled ligands [92].

The labeling of macrophages for the evaluation of inflammatory processes by MRI has been performed directly *in situ* after the phagocytosis of injected iron oxide contrast agents. This method has been shown to allow the visualization of tumor-associated macrophages (TAMs) or monocyte infiltration in various animal models [97–100]. Tremblay et al. [101] evaluated whether MRI can be used to track immune-cell populations in response to a lipid-based vaccine immunotherapy in a mouse model of human papillomavirus-based cervical cancer. They were able to track the increased recruitment of SPIO labeled CD8⁺ cytotoxic T cells and the decreased recruitment of myeloid-derived suppressor cells and regulatory T cells to the tumor with hypo-intensities due to the clearing of iron-labeled cells. However, the sensitivity of MRI is relatively low, limiting the possible detection of a low number of cells.

Nuclear imaging, PET, and SPECT are highly sensitive imaging modalities used in the clinic, based on the biodistribution of radiotracers within the body. SPECT imaging was proposed to investigate the biodistribution and kinetics of reinjected [¹¹¹In] adiolabeled NK cell-based vaccines in patients with renal carcinoma. The authors observed the accumulation of 50% of the activity in the lesions, but a high level of circulating activity was also observed, caused by the released Indium-111 [102].

PET is mainly used in oncology for the visualization of sites of inflammation [90]. To date, only a few studies describing the use of PET for the tracking of vaccines have been published. Among them, Yuki et al. developed a PET imaging approach associated with MRI or CT (computed tomography) to study the biodistribution of an intranasal botulism antigen vaccine (Bo-Hc/A) labelled with [¹⁸F] in mice and NHPs [103]. In addition, Lindsay et al. developed an innovative dual radionuclide-near-infrared probe that allowed

the longitudinal monitoring of an mRNA vaccine at the injection site and the lymph nodes, as well as its uptake by the immune cells, by PET and NIR fluorescence in macaques [41].

The visualization of inflammatory processes by PET imaging is an approach applicable to the monitoring of vaccine responses. Several studies have shown cell activation in lymphoid tissues, such as lymph nodes, by [¹⁸F]-FDG PET imaging after the administration of vaccines in mice [104] and humans [105]. Darrah et al. [57] described the use of [¹⁸F]-FDG, 2-deoxy-2-[fluorine-18]fluoro-D-glucose to track granuloma formation after Mycobacterium tuberculosis infection, as a correlate of active disease after BCG immunization. [¹⁸F]-FDG PET imaging can also be used for the monitoring of the inflammation related to vaccination, such as that induced by influenza vaccines [106–108].

Aarntzen et al. [109] showed the interest of using a radiolabeled thymidine analog, [¹⁸F]-labeled 3'-fluoro-3'-deoxy-thymidine ([¹⁸F]-FLT), to assess the proliferative immune cell response in lymph nodes after vaccination with an antigen-loaded DC vaccine. The authors showed a better correlation of [¹⁸F]-FLT than [¹⁸F]-FDG PET imaging with immune reactivity. However, these imaging methods, lack the specificity and discriminatory power that antibodies or their fragments provide to specifically target immune cells *in vivo* [14,110–112].

Several studies aiming to track immune cells have used *ex vivo* *v* cell labeling to visualize them by nuclear imaging [113,114]. PET-CT imaging allowed the visualization of adoptively-infused NK cells, previously labeled with [⁸⁹Zr]-oxine, in rhesus macaques.

Ex vivo cell labeling shows certain drawbacks, such as the need of autologous transfer, especially in the case of clinical applications, or the potential loss of cell properties by *ex vivo* manipulation. Thus, other strategies have been used to directly label cells *in vivo*. Certain strategies have been recently developed to specifically target, track, and visualize disease-specific antigens, as well as immune-cell subsets, after injection of the antibody or derived fragments coupled with metal chelators, such as [⁶⁴Cu], [⁶⁸Ga], or [⁸⁹Zr] [115,116] for PET (so called immuno-PET) or coupled with MRI contrast agents [117] or fluorophores for *in vivo* optical imaging [44,118].

Full-sized antibodies have been widely and successfully used for immuno-PET imaging [119–121]. However, the size and the long half-life of intact antibodies can be a limitation for their use as imaging agents. Many of these issues have been addressed by the use of smaller antibody fragments (Fabs, diabodies, single-domain antibody fragments (nanobodies), etc.) [112,116,122].

Among the strategies for imaging innate myeloid inflammatory cells, entire anti-CD11b, anti-class II major histocompatibility complex (MHC), and anti-macrophage mannose receptor antibodies or antibody fragments have been widely used to characterize inflammation by immuno-PET, mainly in mice [14,111,119,123,124]. For example, Cao et al. [119] developed the radiotracer [⁶⁴Cu]-labeled anti-CD11b for longitudinal monitoring of the mobilization of CD11b⁺ myeloid cells from the bone marrow to the spleen and to local inflammatory lesions in mice.

Imaging of macrophages has already been performed in various applications to study inflammatory processes by targeting folate receptors [125] with radioligands. The macrophage mannose receptor has largely been used to track macrophages, especially with nanobodies specifically developed for SPECT and PET imaging to target the receptor in various preclinical models [123,126,127].

The presence of CD8⁺ T cells has also been monitored by immunoPET in preclinical tumor models, specifically in the context of immunotherapies using checkpoint-blockade inhibitors against the PD-1/PD-L1 and CTLA-4 axes [111]. Strategies can vary according to the injected radiolabeled antibody fragment [14,128–131]. An even higher specificity can be achieved by targeting and visualizing antigen-specific T cells *in vivo* [132].

Thus, whole-body immunoPET combines the sensitivity of PET with the high specificity and affinity of monoclonal antibodies. Furthermore, the use of antibody-derived fragments allows better tissue penetration, a lower background, and a smaller radiation burden for the patient.

4.1.2. In Vivo Microscopic Imaging of the Interactions between Vaccines and Immune Cells

The complexity of the immune system, particularly when vaccines are involved, requires real-time, high-resolution imaging to visualize immune-cell interactions at the microscopic level. Intravital microscopy (fibered confocal fluorescence microscopy (FCFM), two-photon imaging) provides the detailed visualization of vaccines and their behaviors in the injection sites or lymph nodes.

Fibered confocal fluorescence microscopy (FCFM) was limited to preclinical applications due to the lack of human validated fluorescent tracers. FCFM is developed notably for the visualization of tumor growth and angiogenesis [133,134], as well as the tracking of vaccines and immune cell behavior. For example, Mahe et al. tracked percutaneous injected MVA expressing green-fluorescent protein (eGFP) in mice, its uptake by antigen presenting cells (APCs), and their transport to lymph nodes using FCFM [135]. Later, Rosenbaum et al. evaluated the kinetics of the arrival of MVA-eGFP-expressing cells in the skin by repeated *in vivo* imaging using FCFM (CellVizio Dualband®, Mauna Kea Technologies, France) in NHPs [36]. FCFM has also been used to study the *in vivo* effect of electroporation on antigen expression and APC behavior after intradermal injection of DNA-SIV vaccine expressing eGFP in macaques [118].

Two-photon microscopy (2PM) has been adopted to study single-cell dynamics at high spatial resolution at a depth of several hundred microns [136]. The available adapted 2PM devices allow *ex vivo* studies of tissue and *in vivo* studies in small animals. After vaccination, Rattanapack et al. studied the kinetics of *in vivo* uptake of a peptide antigen delivered within a lipid nanosystem by dermal DCs over time in mice [137]. It is also possible to track T- and B-cell motility in isolated lymph nodes from mice following antigen stimulation [138]. Bousso et al. used 2PM to directly examine the cellular dynamics of fluorescently labeled CD8⁺ T cells and DCs *in vivo* in the lymph node before and during antigen recognition in mice [139]. Although this approach is only limited to preclinical studies, intravital microscopy of the skin or surgically exposed internal organs offers excellent resolution for studying individual cells or even subcellular structures and microorganisms [140,141].

4.2. *Ex Vivo Multiparametric Analyses*

To provide the most advanced technologies for characterization of the complexity of the immune response to vaccination in relevant tissues, it is necessary to complement and strengthen *in vivo* imaging methods with state-of-the-art technologies for *in situ* multiplexed characterization of cellular and subcellular markers of the immune response. Despite the considerable advantages of available imaging techniques, one of the main drawbacks is the small number of parameters that can be simultaneously analyzed.

Immunohistochemistry (IHC) and immunohistofluorescence (IHF) are currently the most common and suitable techniques to gain insights on changes in the spatial immune phenotype in various tissues. Immunofluorescence is widely used to detect multiple immune and inflammatory cell populations, as well as pathogens or vaccines in *ex-vivo* samples. It allows the assessment of innate and adaptive immune responses, especially their effectors in lymphoid organs or infected sites after pathogen challenge or immunization. For example, Darrah and al. [57] observed differences in immune-cell activation in the lungs of rhesus macaques depending on the route of BCG immunization.

Epifluorescence and confocal microscopy allow the observation of cellular and subcellular compartments. However, the number of observable markers is limited using such devices due to fluorophore spectra overlap. This can be partially resolved by the use of white laser confocal microscopy, spectral imaging, or cyclic immunofluorescence [142].

Tissue clearing, by reducing light-scattering and light-absorbing components, overcomes the limits of light penetration and thus allows deep imaging [143]. Three-dimensional imaging can then be performed by confocal, super-resolution confocal, multiphoton, and light-sheet microscopy [144]. For example, Li et al. [145] showed the interest of this method in characterizing the distribution of fluorescent vaccine constructs and the structural com-

position of tissues using an endothelial marker (CD31), T (CD8) and B (B220) lymphocyte markers. Although multiplex analyses can be performed at high spatial resolution using IHF approaches, the revelation of the diversity of the visualized markers can be limited.

Mass spectrometry imaging (MSI), the combination of molecular mass analysis and spatial information, can provide information on the spatial distribution of endogenous and exogenous species in tissue sections, without the need to disrupt sample integrity [146,147]. It enables both untargeted and direct targeted investigations for the discovery of disease or host immune response-related biomarkers, although the sensitivity for intact macromolecules, such as proteins, is still limited [148,149]. Matrix-assisted laser desorption/ionization (MALDI) is the most popular ionization technique for MSI due to its ability to image a wide range of molecular weights and molecular species (e.g., metabolites and proteins). To further analyze tissue specimens, multimodal studies combining MRI, 3D-MALDI-MSI, and histology [150] allow rapid correlation between molecular information and anatomical annotation. Combining MSI with liquid chromatography coupled to tandem mass spectrometry (LC-MS/MS) has also allowed the multiparametric analysis of proteins, lipids, metabolites, and mRNA to explore early immune events following vaccination [53]. The combination of MSI and histology is of particular interest for providing a snapshot of the tissue microenvironment and enables the correlation of drugs, metabolites, lipids, peptides, and proteins with histological/pathological features [151,152].

One of the major recent advances of MSI is associated with the introduction of mass cytometry imaging (MCI), a label-based MSI technique to follow protein markers at the cellular and subcellular level that combines mass cytometry and immunocytochemistry (ICC), IHC or IHF techniques, a high-resolution laser ablation system, and a low-dispersion laser ablation chamber [153,154]. MCI is a multiplex method for tissue phenotyping, signaling pathway imaging, and cell marker assessment at sub-cellular resolution (1 μm) that allows up to 40 parameters to be visualized in a single tissue section [155]. They offer the opportunity to investigate the heterogeneity of tissues and to understand disease development using disease-related probes [153,156,157]. MCI is currently more compatible with common sample preservation methods (formalin fixation or embedding in optimal cutting temperature compound (OCT)) [158]. It is being extensively used for the analysis of immune-cell composition, interactions, and localization in tissues. For example, this method allowed mapping of the anatomical location of myeloid cell subsets in human tonsil tissue [159] and the spatiotemporal relationship between memory B cells and the marginal zone [156].

Progress in the development of these high-multiplex techniques has allowed the identification of various cell populations that comprise the immune system, but they still present certain limitations. Gerner et al. developed an approach, histocytometry, which associates the spatial information that can be obtained using histology with the phenotypic data provided by flow cytometry [160]. They showed that the positioning of DC subsets within lymph nodes defines different levels of T-cell activation in response to vaccination [161]. Histochemical analysis of human lymph nodes during HIV infection led to the identification of potent CD8 T cells within the germinal center, which could be considered as an effective component for the development of HIV cures [162]. Nevertheless, the non-uniform distribution of cells in the organ and the low density of certain populations compromise this analysis, performed on individual tissue sections. To overcome these limitations, Li et al. proposed methods to enable quantitative visualization of cells in their microenvironment within large tissue volumes, allowing better exploration of cellular relationships in various tissues [145,163]. Recent automation has allowed high-throughput image analysis, making histocytometry more useful for immunology applications [164].

High multiplexing methods have prompted the need for the development of image processing and analysis tools using complex machine-learning algorithms.

5. Bioinformatics and Statistical Tools to Build Predictive Models of Vaccine Responses

5.1. Analysis of High-Dimensional Biological Data

The ability to efficiently use or design analytical pipelines for interpreting -omics data has emerged as a critical element for modern vaccinology research. Such analytical pipelines are generally developed using one or more programming languages (usually including R or Python). Their aim is to handle a large panel of analytical steps, ranging from data preprocessing to data integration. Proper analytical pipelines should be sufficiently flexible to tackle various studies but also sufficiently focused on certain methods to answer immunological questions specific to each study. Bioinformatics pipelines used to interpret high-dimensional immunological data should follow the FAIR principles (that is to say that data collected and handled within these pipelines must be findable, accessible, interoperable, and reusable) [165]. The use of paradigms derived from computer science, such as code versioning and the writing of extended documentation, are fundamental when developing pipelines, as it allows them to be reusable over time. Machine-learning methods and algorithms that comprise analysis pipelines can generally be classified into unsupervised or supervised approaches. Unsupervised algorithms aim to analyze datasets without major *a priori* assumptions, especially in terms of the biological conditions to which the samples belong. The most commonly used unsupervised algorithms are clustering (kmeans, hierarchical clustering), dimensionality reduction (principal component analysis (PCA), multidimensional scaling (MDS)), and association rules learning (*a priori* algorithm). On the other hand, supervised algorithms aim to analyze datasets with direct consideration of the metainformation available for each sample. The most commonly used supervised algorithms are discriminant analyses, decision trees with random forests, and, more generally, all classification or regression approaches. Although supervised analyses are critical for identifying biomarkers for an immunization, unsupervised analyses are critical for revealing unexpected characteristics of a dataset (such as subgroups of responders/non-responders and the heterogeneity of the conditions). Both unsupervised and supervised approaches are extremely complementary when analyzing -omics responses to vaccines and immunizations.

Due to its development in the early 21st century, transcriptomics analysis now benefits from an outstanding variety of algorithms, methods, software, and dedicated databases. Despite the large set of available data analysis approaches, differential expression analysis is still the gold-standard for interpreting transcriptomic profiles [166]. Differential expression analysis aims to identify genes or transcripts that are significantly differentially expressed between conditions to identify biomarkers of the immune response. Volcano-plot representations are informative graphs used to visualize the magnitude (quantified using the relative fold-change of expression) and statistical significance (quantified using *p*-values) of differentially expressed genes. Once identified, the ability of one or multiple gene signatures to segregate the biological conditions of interest is tested using multivariate representations. Among them, heatmaps combined with dendrograms show the relative levels of gene expression for the gene signature in all samples using unsupervised hierarchical clustering at both the gene and sample level. Dimensionality reduction methods, such as PCA and MDS, are also useful in determining the quality of a signature and its ability to separate conditions in a multivariate manner. Venn diagrams are common representations that show the amount of overlap between multiple gene signatures. Due to their length (generally ranging from a few hundred to a few thousand genes), gene signatures cannot be interpreted manually, gene by gene, in relation to the literature and must be interpreted using specific methods. Functional enrichment analysis gathers a large set of methods and databases and aims to identify over-represented biological functions or pathways in a gene signature of interest. Statistical tests, generally based on Fisher's exact test, make it possible to determine which pathways are significantly over-represented. The most widely used databases for functional enrichment analysis are Gene Ontology [167], KEGG, and WikiPathways. Other databases, such the Human Gene Atlas database [168], are of in-

terest in systems immunology as they aim to deconvolute transcriptomic profiles from PBMCs or whole blood samples into the cell populations that comprise them. The EnrichR database [169] is a meta-database for functional enrichment analysis that is composed of more than 170 different databases of pathways, function, and biological properties. Such a large spectrum of covered databases is useful for the discovery of functions associated with identified gene signatures. Gene co-expression networks, created by algorithms such as WGCNA [170], can be used to identify sets of genes with similar expression patterns in the datasets to complement the analysis of transcriptomic profiles. In such networks, each dot corresponds to a gene and genes are linked if there is a significant correlation between their expression profiles in the dataset. Such approaches are especially useful when integrating transcriptomics data with other -omics or clinical information.

The development of algorithms for analyzing cytometry profiles is still an active area of research. Although automatic gating approaches mimic cytometry experts by positioning gates in cytogram plots (two-dimension (2D) representations in which each axis corresponds to the expression of one cell parameter), automatic cell clustering algorithms identify groups of cells that have similar phenotypes (also called cell clusters). SPADE [171] and FlowSOM [172] were among the first widely adopted automatic cell clustering algorithms. Dimensionality reduction methods combined with unsupervised clustering are now commonly used, especially the tSNE [173] and UMAP [174] algorithms, which generate 2D representations of cytometry profiles and have become increasingly popular in recent years in immunology and vaccinology. In such 2D representations, each dot corresponds to a cell and cells are positioned based on their similarity of expression for selected markers. Once generated, UMAP or tSNE representations can be overlaid with the expression of specific markers using a color gradient to annotate cells and define sets of cell subpopulations. Clustering algorithms can be used to automatically identify these groups of cells. Such algorithms are essential, as they can identify complex phenotypes of cell populations that cannot be characterized using regular manual gating approaches. Importantly, these algorithms can also identify cell populations that have distinct phenotypes, as well as those that show continuous differences in marker expression (especially important in the context of cell differentiation and activation states). Once cellular clusters have been determined, the aim of subsequent analyses is to identify clusters that are statistically differentially abundant between conditions. Topological data analysis algorithms are currently used to unravel the characteristics of cell differentiation or kinetics to a stimulus. The annotation of determined cell clusters (also called cell cluster labeling) is currently a major challenge. The aim of such approaches is to annotate the cell clusters based on their levels of marker expression and existing knowledge about the cell populations. The exact classification of cell populations into a well-defined nomenclature does not yet exist and represents a major limitation for applying these annotation algorithms. In addition, the complexity and heterogeneity of the cell populations involved in vaccination are yet to be fully explored.

Single cell sequencing will have for sure a pivotal role in modern biology to decipher both molecular and cellular events involved in vaccination. Thanks to this technique, key internal mechanisms responsible for cell activation, proliferation, and differentiation will be characterized at unprecedented level of detail allowing more rational when designing vaccines. While most of the recent efforts have been done for applying this technique on transcriptomics, the characterization of B and T cell repertoires at the single cell levels is of great interest. The analysis challenge for single cell sequencing data is important as methods created for the analysis of bulk transcriptomics and high dimensional cytometry must be combined for handling them. The Cell Ranger suite developed by 10X Genomics allow bioinformaticians a straightforward way to analyze single cell sequencing data, especially regarding the preprocessing steps. The first analysis step consists of the alignment of sequenced reads of a reference genome. The filtering of cell events with abnormal number of mapped transcripts or associated with aberrant mitochondrial activities is done at this step. Once the reads have been aligned on the reference and transcript expressions are

quantified for each cell of each sample, an analysis step consisting in a dimensionality reduction is done. As for cytometry data, tSNE or UMAP algorithm are commonly used for that purpose. Of note, the Loupe browser also developed by 10X Genomics offers the possibility to graphically handle UMAP and tSNE representation for a processed dataset. Different R packages or approaches, such as Seurat [175] are complementary to cell ranger and Loupe browser for interpreting these data. Efforts are now done to create methods and algorithms able to integrate events of different structure together, allowing then a holistic characterization at a single cell resolution.

5.2. Machine Learning and In Silico Models

Machine learning is “the study of computer algorithms that improve automatically through experience”, as defined by Tom Mitchell [176], by learning from the data to make predictions about the data. Machine learning is widely used in various applications in biology. It allows the solving of complex problems using observations or data. Machine-learning algorithms can be classified into three types: supervised learning, unsupervised learning, and reinforcement learning. Various supervised machine-learning algorithms can be used to predict the immunogenicity, efficacy, or reactogenicity of vaccines, either by performing classification, which is a predictive modeling approach in which the output of data is composed of class labels (discrete values), or by performing regression, which is also a predictive modeling approach, but the output is in the form of quantities (continuous values). There are a large number of algorithms available that can be used to predict biomarkers of vaccine responses. However, choosing one over another can be challenging, as the choice depends on various considerations, such as the amount of data, its interpretability and accuracy, training time, number and type of features, and many other factors. Thus, to conduct a scientific study using machine-learning algorithms, one must prioritize the considerations that are the most relevant to the study and questions addressed and proceed by implementing the most pertinent algorithms and comparing them. Importantly, before using any machine-learning algorithm for prediction, a process of data cleaning and processing and feature selection is required. This is a key step but is not the focus of this review. However, this topic has been recently reviewed elsewhere [177]. Table 1 summarizes the principles of several machine learning methods and their respective pros and cons (Table 1).

Several vaccines have been studied with the goal to identify predictors of immunogenicity after delineating signatures that correlate with immunogenicity, mainly in healthy adults (Table 2). In most cases, it consists of predicting the magnitude of the antibody response, which is often a correlate of protection, with early predictors induced within the first week following immunization. However, certain studies have aimed to find pre-existing predictors before immunization [60,62,178,179], or predictors of the intensity of specific T-cell responses [52,180], protection after experimental human challenge infection [181], or reactogenicity [182,183]. Most studies identified predictive genes or gene sets (from PBMC/whole microarray or RNA-Seq). However, more recent studies have used additional molecular data, such as metabolite clusters and cytokines, as well as cell populations, in addition to gene transcripts to predict the antibody and T-cell responses to the live-attenuated VZV vaccine for example [180]. Variables appeared to be highly connected or even overlapping in the so-called multiscale, multifactorial response network (MMRN) that was constructed to integrate the multi-omics data. The authors proposed that the MMRN approach increases the statistical prediction beyond linear models by network connections that accommodate indirect steps and temporal developments.

Table 1. Principle, advantages and drawbacks of common machine learning algorithms.

Machine Learning Algorithm	Principle	Advantages	Drawbacks
Linear regression	<p>It assumes a linear relationship between input variables and output and thus, attempts to model this relationship by fitting a linear equation to the observed data</p> <p>There are several implementations of this model, of which the most commonly used is ordinary least squares, which tends to minimize the residual sum of the squares between the observed and predicted targets.</p>	<ul style="list-style-type: none"> • Simplicity • Ease of implementation 	<ul style="list-style-type: none"> • It assumes that the input variables are independent • It risks generating biased models due to oversimplification
Linear discriminant analysis (LDA)	<p>It is used to identify to which class samples belong, certain statistical properties of the data are first calculated and then substituted into the LDA equation. The statistical properties consist of the mean and variance for the case of a single input and the means and covariance matrix for multiple inputs.</p>	<ul style="list-style-type: none"> • Simplicity • Robust and interpretable classification results 	<ul style="list-style-type: none"> • Does not perform well when the discriminant information is not present in the mean • It cannot be applied to non-linear problems
Random Forest	<p>It builds a number of decision trees on bootstrapped training sets and considers a random sample of m predictors to be split candidates from the full set of p predictors to overcome the problem of high variance. Therefore, on average, the strong predictor is not considered and other predictors have a better chance. This process can be thought of as decorrelating of the trees, thereby making the average of the resulting trees less variable and hence more accurate and reliable.</p>	<ul style="list-style-type: none"> • Reduced variation. • Accurate and reliable • It works well for both classification and regression problems 	<ul style="list-style-type: none"> • It requires considerable computational power and time for training • It suffers from interpretability
Support vector machine	<p>It converts a non-linear separable problem by transforming it onto another higher dimensional space and thus, the problem becomes linearly separable. This is accomplished using various types of so-called kernel functions. Then, classification is performed by finding the hyperplane that well separates the classes of samples.</p>	<ul style="list-style-type: none"> • It can solve any complex problem with the appropriate kernel function • Less risk of overfitting 	<ul style="list-style-type: none"> • Choosing the appropriate kernel function is not easy • It does not work well with large or noisy datasets
Discriminant analysis via mixed integer programming (DAMIP)	<p>It is a classification model based on a very powerful supervised-learning approach used primarily in the biomedical field. It is a discrete support vector machine coupled with a powerful embedded feature-selection module [176].</p>	<ul style="list-style-type: none"> • It reduces noise and errors. • It applies constraints that result in superior classification accuracy • Universally consistent. • Handles well imbalanced data 	<ul style="list-style-type: none"> • This algorithm is mainly used in the biomedical field, little is known about its drawbacks in literature

Table 2. Machine learning methods to predict vaccine immunogenicity and efficacy. Different machine learning algorithms can be used. The quality of the model needs to be evaluated, and there are different metrics to assess a model performance, such as accuracy (defined as the number of correct predictions divided by the total number of input data), Area Under the Receiver Operator Characteristic curve (AUROC) or Root Mean Squared Error for regressions. It depends on the machine learning method itself. (Ab, antibody; ClaNc, classification to nearest centroid; DAMIP, discriminant analysis via mixed integer programming; HAI, hemagglutination-inhibition; CHMI, Controlled Human Malaria Infection; * accuracy except otherwise mentioned).

Vaccine	Vaccinees	Predicted Responses	Predictors	Machine Learning Method	Performance *	Reference
Yellow fever vaccine (YF-17D)	Healthy adults	The magnitude of the activated CD8+ T cell and neutralizing Ab responses	Early blood transcriptional signatures	ClaNc and DAMIP	Up to 90% and 100% respectively	[52]
Seasonal Trivalent Inactivated influenza Vaccine (TIV)	Patients 50–89 years old suffering from multiple chronic medical conditions	The magnitude of plasma HAI Ab response	Baseline signatures among 26 input continuous or categorical variables inc. previous vaccination, low grade chronic inflammation, chronic infections, blood cell counts	Neural network (multilayer perceptron (MLP), radial-basis function network (RBFN) and probabilistic network (PNN)) and Logistic regression	72.5% of average hit rate across 10 samples	[184]
Seasonal Trivalent Inactivated influenza Vaccine (TIV)	Healthy adults	The magnitude of plasma HAI Ab response	Early blood transcriptional signatures	DAMIP	Up to 90%	[185]
Seasonal Trivalent Inactivated influenza Vaccine (TIV)	Healthy adults, inc. young (20–30 years) and older subjects (60 to 89 years)	The magnitude of plasma HAI Ab response	Baseline blood transcriptional, cytokines and cell populations signatures	Logistic regression	84%	[178]
Seasonal Trivalent Inactivated influenza Vaccine (TIV) and pandemic H1N1 (pH1N1) vaccine	Healthy adults	The magnitude of the Ab response	Baseline HAI titer, blood cell populations, transcripts and pathways signatures	Diagonal linear discriminant analysis (for cell frequency data and when cell frequency and pathway status were combined); or partial least square (for data dimension reduction due to the large number of genes) followed by linear discriminant analysis (PLS-LDA) for transcript data alone	0.86 of AUROC	[60]
Seasonal Trivalent Inactivated influenza Vaccine (TIV) over 5 seasons	Human adults, inc. elderlies (>65 years)	The magnitude of plasma HAI Ab response	Early blood transcriptional signatures	DAMIP and artificial neural network classifier	>80%	[10]
Seasonal Trivalent Inactivated influenza Vaccine (TIV)	Healthy adults (50 to 74 years)	The magnitude of the B-cell ELISPOT and plasma HAI Ab responses	Early blood cell composition, mRNA-Seq, and DNA methylation signatures	The ensemble learner (inc. Generalized linear models, Recursive Partitioning, and Regression Trees), and random forest models	0.64–0.79 of AUROC	[186]
Seasonal Trivalent Inactivated influenza Vaccine (TIV)	Healthy adults	The magnitude of plasma HAI Ab response	Baseline HAI titer and blood transcriptional signatures	Gaussian Mixture Model (GMM)	R ² = 0.64 for the correlation between observed and predicted data	[187]
Seasonal Trivalent Inactivated influenza Vaccine (TIV)	Healthy adults	The magnitude of the Ab response	Early blood transcriptional signatures	Logistic Multiple Network-constrained Regression	69%	[188]
Seasonal Trivalent Inactivated influenza Vaccine (TIV) over 8 seasons	Healthy adults	The magnitude of the specific Ab response	Baseline blood cell populations signatures	128 machine learning algorithms suitable for classification using Sequential Iterative Modeling “OverNight” (SIMON), inc. Diagonal Discriminant Analysis, Partial Least Squares, Linear Discriminant Analysis, Logic Regression, Neural Network, Random Forest	Up to 0.92 of AUROC	[179]

Table 2. Cont.

Vaccine	Vaccinees	Predicted Responses	Predictors	Machine Learning Method	Performance *	Reference
Seasonal Trivalent Inactivated influenza Vaccine (TIV) given transcutaneously, intradermally or intramuscularly	Healthy adults	The magnitude of the specific T CD8+ and Ab responses	Early blood transcriptional and serum cytokines signatures	Logistic regression	0.93 to 0.96 of AUROC	[189]
Seasonal Trivalent Inactivated influenza Vaccine (TIV) and 23-valent pneumococcal polysaccharide vaccine	Old patients (>65 years) with chronic kidney disease with or without non-dialysis	The magnitude of the HAI Ab and anti-PnPS IgG responses	Baseline signatures among 30 input continuous or categorical variables inc. previous vaccinations, low grade chronic inflammation, chronic infections, blood cell counts	Multivariable linear regression model	<i>p</i> < 0.05	[190]
RTS,S malaria vaccine	Healthy adults	The protection against CHMI	Early blood transcriptional signatures	DAMIP	>80%	[181]
Candidate malaria vaccine composed of a Self-Assembling Protein Nanoparticles presenting the malarial circumsporozoite protein (CSP) adjuvanted with three different liposomal formulations: liposome plus Alum, liposome plus QS21, or both	Rhesus macaques	Adjuvant condition	Vaccine-induced immune response signatures among many variables inc. serology, fluorospot, ICS from blood, liver, LN and spleen	Random forest followed by Linear regression analysis	92%	[32]
Live-attenuated varicella zoster virus (VZV) vaccine	Healthy adults, inc. younger (25–40 years) and older (60–79 years)	The magnitude of the specific T and IgG responses	Early blood transcriptional, metabolite clusters, cytokines, and cell populations signatures	Multivariate regression model (Partial least square)	<i>p</i> < 0.05	[180]
Monovalent oral polio vaccine type 3 (mOPV3)	Infants aged 6–11 months	Seroconversion or shedding of vaccine virus as a marker of vaccine “take”	Baseline enteric pathogens blood cell populations, and plasma cytokines signatures	Random forest	58%	[191]
Two distinct live attenuated Tularemia vaccine administered by scarification	Healthy humans	The magnitude of the specific Ab and activated CD4 and CD8 T cell responses	Early blood transcriptional signatures	Logistic regression	26% of mean misclassification error	[39]
rVSV-ZEBOV	Healthy adults	The magnitude of the Ab response	Early blood transcriptional, plasma cytokine and cell populations signatures	Sparse partial least-squares followed by multivariable linear regression	0.77 of root square residuals leave-one-out explaining 55% of the variability	[12]
DNA/rAd5 HIV-1 preventive candidate vaccine	Healthy adults	HIV infection	Magnitude and quality of CD4 and CD8 T cells	PCA followed by Cox proportional hazards regression model, and Logistic regression with lasso	Up to 0.75 of AUROC	[192]
Seven preventive HIV-1 vaccine regimens (inc. DNA, NYVAC, ALVAC, MVA, AIDSVAX)	Healthy adults	The magnitude of long-term immune responses	Baseline demographic variables and peak immune responses	Regularized random forest and linear regression models	R = 0.91 for the correlation between observed and predicted data	[193]
41 different vaccine vectors all expressing the same antigen	Mice	The quality of late T-cell responses	Early transcriptome of dendritic cells	Random forest	Up to 98%	[194]

The most popular vaccine models for immunologists include the YF-17D and flu vaccines. YF-17D represents an ideal vaccine to understand and mimic because it induces life-long protection after a single injection. There are two major types of influenza vaccine: a live attenuated vaccine, which is delivered intranasally, and an inactivated vaccine, which is injected intramuscularly, both providing protection through distinct mechanisms. Adjuvanted versions or higher doses are also available for specific populations, such as the elderly, and thus represent the first personalized vaccines. However, these traditional seasonal flu vaccines do not provide long lasting and broad protection. They are based on yearly predictions of the circulating viruses, and they confer protection only when strains do match the circulating viruses. A key challenge is to develop pan-influenza viruses vaccines targeting conserved regions that would protect against seasonal, future drifted and pandemic strains. Anyway, not surprisingly, YF-17D and seasonal trivalent inactivated influenza vaccines (TIVs), likely because of practical reasons (annual immunizations of adults with a safe, albeit imperfect vaccine and identified immune correlate of protection), are over-represented among studies to define predictors of immunogenicity. Of note, predictors of the antibody and T-cell responses [52,180] and baseline and early predictors [60,185] of a given vaccine and study differ. Among the genes present in the various DAMIP gene signatures predictive of the antibody response to vaccination with TIV and YF-17D, seven are shared [52,185]. Finally, the predictive signatures have also differed for TIVs, depending on the season, the age and health status of those vaccinated, and the machine-learning method.

It is expected that predictors of vaccine-induced antibodies could be clinically useful by predicting suboptimal immune responses to certain vaccines to stratify them, for example those requiring a booster. However, the robustness and predictive accuracy depend on the sample size and the identification of solid predictors requires extensive validation in multiple clinical trials. A cost-effective PCR-based ‘vaccine chip’ that focused on a set of predictive genes was successfully developed for flu vaccines [185]. It is admittedly more challenging [195], but predictors can also provide insight about key players (molecules or cells) and uncover new mechanisms to target to more rationally improve vaccines. Several studies to identify predictors of vaccine immunogenicity included or were followed by mouse studies to evaluate the mechanistic relevance of the predictors, including *Camk4* [185] and apoptosis [178] for flu vaccines and *Gcn2* (also known as *Eif2ka4*) for YF-17D [196].

The purpose of mechanistic mathematical modeling differs from that of machine learning. It aims to mimic biological mechanisms through observations of and assumptions about the phenomenon of interest. This type of modeling uses mathematical formulations that seek to identify a mechanistic relationship between inputs and outputs of the phenomenon of interest [197,198]. These approaches are complementary to machine-learning approaches, which seek to establish statistical relationships and correlations between inputs and outputs. Due to the oversimplified assumptions and extremely specific nature of mechanistic mathematical models, they are limited to establishing universal predictions, which are achievable by machine learning. However, mechanistic modelling may be more suitable for studying certain phenomena than machine-learning approaches, depending on the research objectives. Therefore, these two approaches should not be considered as competing with each other but rather as complementary [199].

6. Vaccine Signatures in Preclinical Models to Improve Human Vaccination Strategies

Although reducing and refining animal experiments require permanent efforts from the scientific community, assessing vaccine responses in animal models is still, for now, a necessary step in the vaccine registration process [200]. Currently, preclinical trials often provide key decisional points to pursue vaccine development [201], as it has been the case for SARS-CoV-2 vaccine candidates [202]. Indeed, they allow to design robust, controlled studies with a wider range of tools and samplings than the ones available in clinical

trials. Plus, some models, such as NHPs, are highly predictive of the human immune and vaccine responses.

Applying systems vaccinology approaches to animal models assuredly provides a way to improve preclinical studies, accelerate vaccine development, and increase our knowledge of vaccine-induced protective responses, as discussed below.

6.1. Defining New Correlates of Protection

Through the use of diverse high-throughput technologies, systems immunology can lead to the identification of multiple biomarkers, combined into complex signatures that can be used to build predictive models of vaccine-induced responses. Being able to predict the efficacy of a vaccine with the identification of early biomarkers could considerably facilitate preclinical and clinical trials. Currently, vaccine development starts with an exploratory phase that addresses basic scientific questions and ideally leads to proof-of-concept studies that validate the efficacy of the vaccine in experimental—usually small animal—models. Translational research then follows with immunogenicity and efficacy studies in preclinical models, which guide subsequent clinical trials in humans [203].

The evaluation of vaccine efficacy can be challenging and partially relies on the possibility to define reliable correlates of protection. According to Plotkin and Gilbert, a correlate of protection can be defined as a marker of immune function that statistically correlates with protection after vaccination [204]. As mentioned previously, antibody titers have been used as correlates of protection for many vaccines. For example, a protective level of antibody measured by ELISA has been defined for vaccines against hepatitis A virus (HAV) and HBV [205]. For other vaccines, such as rabies or YF vaccines, neutralization titers have been linked to protection [206,207]. While antibodies can be considered as reliable correlates of protection for genetically stable pathogens, they cannot be properly used in the case of viruses with high mutational capacities and that can escape humoral responses, as we observe in the still on-going SARS-CoV-2 pandemic [208]. In addition, well-defined correlates of protection are still lacking for multiple vaccines, including those against malaria and tuberculosis [209], and serological measurements are probably not the only or relevant immune correlates.

Defining accurate correlates of protection is pivotal in the vaccine development process, as it allows the rapid assessment of vaccine efficacy. Hence, applying systems immunology approaches to clinical trials has been proposed to accelerate the discovery of early predictive markers of vaccine efficacy [210]. Additionally, systems vaccinology could be integrated into preclinical studies and further empower translational vaccine research. Cellular immunity will need to be explored thoroughly to enable better prediction of vaccine immunogenicity. As already discussed, local cellular events shape subsequent protective responses [36,211–213]. Thus, their characterization can provide a way to rapidly assess the quality of vaccine-induced immunity. In-depth studies of immune cells involved at the site of vaccination, such as skin DCs or LCs, is achievable in preclinical models due to the use of multiple and complementary exploratory approaches (Figure 2) and can provide very early predictive markers of vaccine immunogenicity. Elsewhere, in addition to antibody responses, exploring T cell responses will certainly provide key biomarkers of efficacy for vaccines targeting mutating pathogens. For example, T lymphocytes seem to play a key role after SARS-CoV-2 infection and vaccination [214,215]. Precisely, a study on Rhesus macaques showed a strong decrease of the protection induced by natural immunization after depletion of CD8+ T cells thus indicating that CD8+ T cell responses could be used to define more accurate correlates of protection for SARS-CoV-2 infection [216]. Additionally, preclinical models are often instrumental in appraising long-term immune memory, as longitudinal studies can be initiated and conducted more easily and rapidly than in human populations. For example, NHPs have been successfully used to study memory responses induced by vaccines against SIV, tuberculosis, and/or polio [59,217–219]. Implementing systems vaccinology techniques in prolonged longitudinal preclinical studies [72] could link initial and long-term responses and generate early signatures of immune memory.

Applying these approaches to human studies could therefore provide a way to reduce the time and cost of vaccine efficacy trials.

6.2. Stepping up Personalized Vaccinology

Presently, validated correlates of protection are generally based on results obtained from cohorts of vaccinated healthy adults, whereas target human populations are often highly heterogeneous, and defining a universal response to vaccination is probably impossible [220]. Indeed, many host-related factors can modulate immune responses to vaccination, including age, gender, infectious history, comorbidities, genetic background, and microbiota composition (Figure 2) [28].

In vulnerable populations, such as infants and young children, pregnant women, and elderly and immunocompromised individuals, immune responses to vaccination are often under characterized and assessing vaccine efficacy in these specific populations remains a major challenge. Preclinical models are well-suited for in-depth studies on population subsets with specific attributes, especially animal models with the most predictive value for human vaccine efficacy studies, such as NHPs. Although systems vaccinology approaches have already been used in human cohorts of aged individuals [63,221,222], high-throughput characterization of vaccine-induced responses in children are still rare [9,223] and awaited for newborns [224]. Importantly, NHPs provide a highly relevant pediatric model to test vaccine efficacy, as they share many similarities with humans in terms of immune system development [225–228].

Infant NHPs have been frequently used in studies to evaluate vaccines against *Mycobacterium tuberculosis* [229–231] and HIV [232–234]. Recently, Han et al. used high-throughput technologies, including single-cell RNA sequencing of PBMCs, to perform an in-depth comparison of neonatal and adult immune responses to HIV immunization in macaques [235]. More specifically, they were able to show higher activated circulating TFH cell frequencies in Env-immunized neonatal macaques than in adults. This study also revealed distinct post-immunization transcriptome profiles between infant and adult macaques, with elevated B-cell lymphoma 2 (*BCL2*) transcript levels in T cells and lower interleukin-10 (*IL-10*) receptor alpha (*IL10RA*) transcript levels in T, B, and NK cells and monocytes of macaque neonates. This study illustrates how systems vaccinology in preclinical models can guide and help human vaccine efficacy trials. Moreover, identifying vaccine signatures in preclinical models of vulnerable populations would allow investigation of the influence of host factors on responses to immunization.

Pharmacogenomics and vaccinomics also contribute to improve personalized medicine and vaccination, respectively [19,20]. Indeed, identifying genetic polymorphisms associated to increased or decreased vaccine efficacy before administration of the vaccine may allow to adapt the vaccination strategy to particular individuals or to sub-groups of different ethnic ancestry. However, human GWASs require large cohorts of thousands of individuals to detect true genotype-phenotype associations [236] and are thus limited to the retrospective study of licensed vaccines. Vaccinomic studies in preclinical models could provide a way to rapidly assess the influence of host genetic factors on the efficacy of newly developed vaccines. For ethical and financial reasons, vaccine preclinical studies in NHPs commonly use limited numbers of individuals and are thus not powered for genetic association studies. However, alternative models such as genetically diverse mouse populations are well-suited for this application. For example, the Collaborative Cross constitutes a new experimental platform to investigate the influence of host genetic factors in the susceptibility to infectious diseases [237] and starts to be used to study vaccine-induced responses [148].

Consequently, the various approaches of systems vaccinology empower personalized vaccination strategies, which should improve efficient vaccination coverage in target populations.

6.3. Improving Vaccine Formulation and Administration

Another way to increase global vaccine efficacy in highly diverse human populations is to improve vaccine formulation with adjuvants and refine administration routes and schedules. Systems immunology offers powerful tools to investigate the effects of adjuvants and vaccine regimens on human immune responses [9,181] and can lead to reference signatures to which new vaccine candidates can be compared. Additionally, preclinical models are still highly valuable for the development and evaluation of innovative adjuvants, new administration routes, and various vaccine regimens.

As previously stated, applying systems biology technologies in this context will further improve preclinical studies and enhance innovation and progress in the field of vaccinology. For example, transcriptomics was first used in mouse models to characterize the molecular and cellular signatures of clinically tested human vaccine adjuvants [26,238]. These studies provided new insights about the modes of action of vaccine adjuvants by identifying both common transcriptional differences and adjuvant-specific responses associated with either germinal-center reactions or the orientation of helper T cell responses [26,238]. Systems vaccinology studies performed in NHP preclinical models can further guide the rational development of vaccine adjuvants for clinical use. Kasturi et al. studied the capacity of TLR agonists to promote durable protective immunity against SIV [239], whereas Thompson et al. investigated the effect of such TLR-based adjuvants on immune responses induced by a vaccine against *Plasmodium falciparum* [240]. In a huge leap forward, Chaudhury et al. combined extensive immuno-profiling of three adjuvant formulations in Rhesus macaques with multivariate analysis and machine learning [32]. This study identified adjuvant-specific immune “fingerprints” that could be used as rudiments to define correlates of protection and immunogenicity in human vaccine trials.

The mode of vaccine administration is another important parameter that modulates immune responses, as illustrated in a recent study of Cirelli et al. on the effect of slow delivery of HIV antigens in Rhesus macaques [88]. They showed that slow-delivery immunization improves neutralizing antibody production and leads to increased frequencies of antigen-specific GC-TFH cells using a combination of high dimensional techniques, such as scRNA sequencing, BCR sequencing, and whole lymph node imaging. In another study, Adam et al. investigated the early mechanisms that occur in the skin after intradermal injection and electroporation of SIV immunogens in Cynomolgus macaques. They used flow cytometry, cytokine profiling, and transcriptomics of skin cells to demonstrate that electroporation has a strong adjuvant effect mediated by inflammatory cell recruitment and LC mobilization [212]. Finally, studying how the vaccine regimen influences immune signatures could be critical to improving vaccination strategies in human populations. For example, mass cytometry was used to perform in-depth phenotyping of innate immune cell populations differentially induced by MVA vaccine prime and boost immunizations [34,35]. Similarly, multi-parameter flow or mass cytometry were successfully used to study the effects of heterologous prime-boost combinations of tuberculosis vaccination in mice [241], and the influence of the interval between MVA immunizations in Cynomolgus monkeys [33].

Overall, these results illustrate how systems vaccinology can strengthen preclinical findings on vaccine formulation and administration, and thus support vaccine development processes.

6.4. Deciphering Mechanisms That Underly Immune Protective Responses

Finally, the use of systems vaccinology in preclinical models will provide mechanistic insights on immune responses triggered by vaccines. Because of the constraints on collecting tissue samples in human clinical trials, most studies have strived to define signatures of myeloid and lymphoid responses in the blood [8,10,61,62,142,189]. However, immune processes are highly orchestrated in time and space and thus occur in multiple tissues and organs of the body (Figure 2).

As mentioned previously, early local events in the skin following immunization can shape subsequent immune responses and vaccine efficacy [36,211–213]. In other respects, the acquisition of immune memory characterizes adaptive responses and is of critical importance for vaccines to confer long-lasting protection. Specifically, activated B and CD4⁺ T cells differentiate into memory cells within lymph nodes and spleen GCs, and then migrate to the bone marrow, which represents their main homing site [242,243]. Thus, a major challenge for human vaccine studies is to identify signatures in the blood that would truly reflect the magnitude and persistence of tissue-specific immune events. Recent efforts have been undertaken to investigate vaccine-induced immune events in human skin explants [53] or in human lymph node fine-needle aspirates [86,244]. However, preclinical models are still instrumental to comprehensively studying the mechanisms of vaccine-induced immune responses at the tissue and whole-body levels (Figure 2). For example, immunogens slow delivery administration, described by Cirelli et al., triggered higher frequencies of HIV-specific GC B cells and altered their BCR repertoire compared to conventional bolus immunization [88]. In another recent study, Eslamizar et al. examined NHP lymph node-derived cells after immunization with HIV Env protein encoded either by a plasmid DNA, a recombinant MVA, or a recombinant VSV vector [245]. They demonstrated that recombinant MVA was the most potent vector to induce GC-TFH cells expressing high levels of ICOS (inducible T cell co-stimulator), a key receptor of TFH help to GC B cells. The investigation of how mucosal immunity is modulated by immunization and contributes to vaccine-induced protection is another field of research in vaccinology that warrants the exploration of tissue-based immune processes. For example, systems immunology approaches have been used to characterize the molecular signatures of vaginal tissues of macaques immunized with a TLR-adjuvanted SIV vaccine [239] and to show that vaginal HIV Env-specific antibody and cellular responses presumably confer auxiliary mechanisms of protection against viral challenge in NHPs [83].

In addition, animal models are also particularly appropriate for assessing and dissecting immune responses to a combination of vaccines and/or pathogens. Indeed, exposition to pathogens and the vaccination history of animals are strictly monitored and recorded in laboratory settings. Such controlled experimental conditions facilitate the study of interactions between antigenically unrelated pathogens or immunogens. Recently, much attention has been given to the importance of non-specific effects of vaccines with a growing body of evidence suggesting that live-attenuated vaccines such as BGC, measles and oral polio vaccines overall improve childhood health [246]. Indeed, several randomized trials and population-based cohort studies led in young children revealed a significant decrease in infectious disease mortality rate in BGC-vaccinated newborns in low-income regions and a reduction of the risk of admissions for infectious diseases in BGC-vaccinated babies in high-income settings [246]. Several hypotheses have been formulated to explain the underlying mechanisms, including cross-protection conferred by heterologous T cell responses and the development of a kind of innate immune memory now referred to as “trained immunity” [247–249]. However, much remains to be done to fully understand the precise mechanisms underpinning non-specific effects of vaccines. To this end, preclinical models can greatly contribute to increasing our knowledge on trained immunity processes, as recently reviewed by Palgen et al. [250], and systems vaccinology will also endorse such studies.

Finally, although NHPs most likely provide the best model of human vaccine responses in terms of prediction, small animal models can be used to further investigate the functional mechanisms underlying predictive biomarkers identified in preclinical and clinical studies. Notably, transgenic mice have been instrumental in elucidating the functions of genes implicated in immune responses to pathogens or vaccines [251,252]. For example, Querec et al. identified general control non-derepressible 2 kinase (GCN2) as a biomarker that correlates with CD8⁺ T-cell responses to YF-17D vaccination in one of the earliest systems vaccinology studies [52]. They used mice carrying constitutional or conditional knock-out deletion of *Gcn2* to demonstrate that GCN2 leads to increased autophagy and antigen presentation in DCs in response to YF-17D immunization and thus

revealed a connection between a vaccine-induced stress response in DCs and adaptive immune responses [253].

To conclude, preclinical models are invaluable for expanding our knowledge of immune mechanisms underlying vaccine protection and for improving rational vaccine development.

7. Conclusions

Systems immunology approaches used in preclinical studies and clinical trials are invaluable in vaccine biomarker discovery through the analysis and statistical modeling of large datasets.

Despite the outstanding development of high-throughput technologies and computational methodologies, many challenges still remain to be tackled to realize the full promise of systems vaccinology. Indeed, most recent studies in the field of vaccinology have restricted their findings to a description of vaccine biomarkers without further exploring the correlative, predictive, or explanatory aspects of these signatures. Furthermore, being able to discriminate between markers of immunogenicity and protection is not an easy task as illustrated by many clinical trials of HIV vaccines [254]. The application of systems immunology, in particular systems serology, to preclinical and clinical trials of HIV vaccines offers a means to specify new correlates of protection, though we are still at the beginning of this process [29].

In this review, we highlighted numerous technological and biological aspects useful to study vaccine responses and to the development of future vaccines. Nevertheless, limitations inherent to research techniques or to animal models question the methods currently employed in vaccine studies. First, the inherent differences in data formats generated by immunophenotyping platforms are a major impediment to the integration of large data sets. For instance, mRNA expression levels do not always represent intracellular protein expression levels and may not either reflect extracellular marker expression detected by cytometry [255]. Second, the measurement of diverse immunological parameters usually implicates multiple platforms and/or laboratories, standardization efforts are thus required to reduce technical and analytical variability and improve the robustness of predictive models [256,257]. Third, collaborations between vaccinologists and researchers with expertise in bioinformatics and computational and mathematical modeling also need to be strengthened to create predictive algorithms that are transposable to clinical applications.

Although human clinical trials of vaccine efficacy increasingly rely on systems immunology approaches, preclinical studies are lagging behind. Nonetheless, preclinical models harbor rare assets to explore vaccine-induced responses, including the possibility to investigate immune processes in tissues and the whole organism. The future of defining comprehensive vaccine signatures will likely rely on extended data analyses, including data obtained through imaging technologies, similarly to what has already been implemented in the field of cancerology [258,259]. In the near future, we believe that it will be possible to optimize and standardize several high-dimensional technologies so that they can be used conjointly on a regular basis in preclinical and clinical trials. For example, mass cytometry and imaging mass cytometry employ the same reagents, rely on the same detection method and generate datasets which can be analyzed with the same bioinformatic pipelines while providing complementary biological information on vaccine responses. Finally, applying high-throughput technologies to preclinical studies will expand our knowledge of the immune processes induced by vaccines in experimental models and hopefully improve the rate of translation of discoveries from animal studies to human trials [219].

Overall, application of systems biology concepts to preclinical and clinical studies promises great advancements in our understanding of vaccine-induced immune protective responses and provides unprecedented opportunities for the development of new vaccines.

Author Contributions: Writing—original draft preparation, M.V.T., K.L., A.-S.B., C.C., N.T., L.C., E.M.L., Q.P., C.M.; writing—review and editing, M.V.T., K.L., A.-S.B., C.C., N.T., P.M., R.L.G., C.M.; supervision, P.M., R.L.G., C.M.; funding acquisition, R.L.G. All authors have read and agreed to the published version of the manuscript.

Funding: The Infectious Disease Models and Innovative Therapies (IDMIT) research infrastructure is supported by the ‘Programme Investissements d’Avenir’, managed by the ANR (ANR-11-INBS-0008). The Fondation Bettencourt Schueller and the Region Ile-de-France contributed to the implementation of IDMIT’s facilities and imaging technologies.

Institutional Review Board Statement: Not applicable.

Informed Consent Statement: Not applicable.

Data Availability Statement: Not applicable.

Acknowledgments: The authors thank all the members in the laboratory for their contributions.

Conflicts of Interest: A.-S.B. is the recipient of Sanofi Innovation Award (iAward program), Europe 2020, on Trained Immunity-Inducing Vaccines. The remaining authors declare no conflict of interest. The funders had no role in the writing of the manuscript.

References

1. Heaton, P.M. Challenges of Developing Novel Vaccines With Particular Global Health Importance. *Front. Immunol.* **2020**, *11*, 517290. [[CrossRef](#)]
2. World Health Organization (WHO). Global Vaccine Action Plan 2011–2020. Available online: <https://www.who.int/publications/i/item/global-vaccine-action-plan-2011--2020> (accessed on 20 May 2021).
3. Trovato, M.; Sartorius, R.; D’Apice, L.; Manco, R.; De Berardinis, P. Viral Emerging Diseases: Challenges in Developing Vaccination Strategies. *Front. Immunol.* **2020**, *11*, 2130. [[CrossRef](#)] [[PubMed](#)]
4. Montalvo Zurbia-Flores, G.; Rollier, C.S.; Reyes-Sandoval, A. Re-thinking yellow fever vaccines: Fighting old foes with new generation vaccines. *Hum. Vaccines Immunother.* **2021**, *1*–9. [[CrossRef](#)] [[PubMed](#)]
5. Group, B.D.W. Biomarkers and surrogate endpoints: Preferred definitions and conceptual framework. *Clin. Pharm.* **2001**, *69*, 89–95. [[CrossRef](#)]
6. Galassie, A.C.; Link, A.J. Proteomic contributions to our understanding of vaccine and immune responses. *Proteom. Clin. Appl.* **2015**, *9*, 972–989. [[CrossRef](#)]
7. Plotkin, S.A. Correlates of protection induced by vaccination. *Clin. Vaccine Immunol.* **2010**, *17*, 1055–1065. [[CrossRef](#)] [[PubMed](#)]
8. Hou, J.; Wang, S.; Jia, M.; Li, D.; Liu, Y.; Li, Z.; Zhu, H.; Xu, H.; Sun, M.; Lu, L.; et al. A Systems Vaccinology Approach Reveals Temporal Transcriptomic Changes of Immune Responses to the Yellow Fever 17D Vaccine. *J. Immunol.* **2017**, *199*, 1476–1489. [[CrossRef](#)] [[PubMed](#)]
9. Nakaya, H.I.; Clutterbuck, E.; Kazmin, D.; Wang, L.; Cortese, M.; Bosinger, S.E.; Patel, N.B.; Zak, D.E.; Aderem, A.; Dong, T.; et al. Systems biology of immunity to MF59-adjuvanted versus nonadjuvanted trivalent seasonal influenza vaccines in early childhood. *Proc. Natl. Acad. Sci. USA* **2016**, *113*, 1853–1858. [[CrossRef](#)]
10. Nakaya, H.I.; Hagan, T.; Duraisingham, S.S.; Lee, E.K.; Kwissa, M.; Rouphael, N.; Frasca, D.; Gersten, M.; Mehta, A.K.; Gaujoux, R.; et al. Systems Analysis of Immunity to Influenza Vaccination across Multiple Years and in Diverse Populations Reveals Shared Molecular Signatures. *Immunity* **2015**, *43*, 1186–1198. [[CrossRef](#)] [[PubMed](#)]
11. Pogorelyy, M.V.; Minervina, A.A.; Touzel, M.P.; Sycheva, A.L.; Komech, E.A.; Kovalenko, E.I.; Karganova, G.G.; Egorov, E.S.; Komkov, A.Y.; Chudakov, D.M.; et al. Precise tracking of vaccine-responding T cell clones reveals convergent and personalized response in identical twins. *Proc. Natl. Acad. Sci. USA* **2018**, *115*, 12704–12709. [[CrossRef](#)]
12. Rechtien, A.; Richert, L.; Lorenzo, H.; Martrus, G.; Hejblum, B.; Dahlke, C.; Kasonta, R.; Zinser, M.; Stubbe, H.; Matschl, U.; et al. Systems Vaccinology Identifies an Early Innate Immune Signature as a Correlate of Antibody Responses to the Ebola Vaccine rVSV-ZEBOV. *Cell Rep.* **2017**, *20*, 2251–2261. [[CrossRef](#)] [[PubMed](#)]
13. McCarthy, C.E.; White, J.M.; Viola, N.T.; Gibson, H.M. In vivo Imaging Technologies to Monitor the Immune System. *Front. Immunol.* **2020**, *11*, 1067. [[CrossRef](#)] [[PubMed](#)]
14. Rashidian, M.; Keliher, E.J.; Bilate, A.M.; Duarte, J.N.; Wojtkiewicz, G.R.; Jacobsen, J.T.; Cragnolini, J.; Swee, L.K.; Victora, G.D.; Weissleder, R.; et al. Noninvasive imaging of immune responses. *Proc. Natl. Acad. Sci. USA* **2015**, *112*, 6146–6151. [[CrossRef](#)] [[PubMed](#)]
15. Klein, S.L.; Poland, G.A. Personalized vaccinology: One size and dose might not fit both sexes. *Vaccine* **2013**, *31*, 2599–2600. [[CrossRef](#)]
16. Kennedy, R.B.; Ovsyannikova, I.G.; Pankratz, V.S.; Vierkant, R.A.; Jacobson, R.M.; Ryan, M.A.; Poland, G.A. Gender effects on humoral immune responses to smallpox vaccine. *Vaccine* **2009**, *27*, 3319–3323. [[CrossRef](#)]
17. Klein, S.L.; Hodgson, A.; Robinson, D.P. Mechanisms of sex disparities in influenza pathogenesis. *J. Leukoc. Biol.* **2012**, *92*, 67–73. [[CrossRef](#)] [[PubMed](#)]
18. Muyanja, E.; Ssemaganda, A.; Ngauv, P.; Cubas, R.; Perrin, H.; Srinivasan, D.; Canderan, G.; Lawson, B.; Kopycinski, J.; Graham, A.S.; et al. Immune activation alters cellular and humoral responses to yellow fever 17D vaccine. *J. Clin. Investig.* **2014**, *124*, 3147–3158. [[CrossRef](#)]
19. Omersel, J.; Karas Kuželički, N. Vaccinomics and Adversomics in the Era of Precision Medicine: A Review Based on HBV, MMR, HPV, and COVID-19 Vaccines. *J. Clin. Med.* **2020**, *9*, 3561. [[CrossRef](#)]

20. Poland, G.A.; Ovsyannikova, I.G.; Jacobson, R.M. Application of pharmacogenomics to vaccines. *Pharmacogenomics* **2009**, *10*, 837–852. [[CrossRef](#)]
21. Davila, S.; Froeling, F.E.; Tan, A.; Bonnard, C.; Boland, G.J.; Snippe, H.; Hibberd, M.L.; Seielstad, M. New genetic associations detected in a host response study to hepatitis B vaccine. *Genes Immun.* **2010**, *11*, 232–238. [[CrossRef](#)] [[PubMed](#)]
22. Pan, L.; Zhang, L.; Zhang, W.; Wu, X.; Li, Y.; Yan, B.; Zhu, X.; Liu, X.; Yang, C.; Xu, J.; et al. A genome-wide association study identifies polymorphisms in the HLA-DR region associated with non-response to hepatitis B vaccination in Chinese Han populations. *Hum. Mol. Genet.* **2014**, *23*, 2210–2219. [[CrossRef](#)]
23. Wu, T.W.; Chen, C.F.; Lai, S.K.; Lin, H.H.; Chu, C.C.; Wang, L.Y. SNP rs7770370 in HLA-DPB1 loci as a major genetic determinant of response to booster hepatitis B vaccination: Results of a genome-wide association study. *J. Gastroenterol. Hepatol.* **2015**, *30*, 891–899. [[CrossRef](#)]
24. Nishida, N.; Sugiyama, M.; Sawai, H.; Nishina, S.; Sakai, A.; Ohashi, J.; Khor, S.S.; Kakisaka, K.; Tsuchiura, T.; Hino, K.; et al. Key HLA-DRB1-DQB1 haplotypes and role of the BTNL2 gene for response to a hepatitis B vaccine. *Hepatology* **2018**, *68*, 848–858. [[CrossRef](#)]
25. Scepanovic, P.; Alanio, C.; Hammer, C.; Hodel, F.; Bergstedt, J.; Patin, E.; Thorball, C.W.; Chaturvedi, N.; Charbit, B.; Abel, L.; et al. Human genetic variants and age are the strongest predictors of humoral immune responses to common pathogens and vaccines. *Genome Med.* **2018**, *10*, 59. [[CrossRef](#)]
26. Mosca, F.; Tritto, E.; Muzzi, A.; Monaci, E.; Bagnoli, F.; Iavarone, C.; O'Hagan, D.; Rappuoli, R.; De Gregorio, E. Molecular and cellular signatures of human vaccine adjuvants. *Proc. Natl. Acad. Sci. USA* **2008**, *105*, 10501–10506. [[CrossRef](#)]
27. Li, S.; Rouphael, N.; Duraisingham, S.; Romero-Steiner, S.; Presnell, S.; Davis, C.; Schmidt, D.S.; Johnson, S.E.; Milton, A.; Rajam, G.; et al. Molecular signatures of antibody responses derived from a systems biology study of five human vaccines. *Nat. Immunol.* **2014**, *15*, 195–204. [[CrossRef](#)] [[PubMed](#)]
28. Zimmermann, P.; Curtis, N. Factors That Influence the Immune Response to Vaccination. *Clin. Microbiol. Rev.* **2019**, *32*, e00084-18. [[CrossRef](#)] [[PubMed](#)]
29. Ackerman, M.E.; Barouch, D.H.; Alter, G. Systems serology for evaluation of HIV vaccine trials. *Immunol. Rev.* **2017**, *275*, 262–270. [[CrossRef](#)]
30. Van Gils, M.J.; Sanders, R.W. Broadly neutralizing antibodies against HIV-1: Templates for a vaccine. *Virology* **2013**, *435*, 46–56. [[CrossRef](#)] [[PubMed](#)]
31. Liao, W.; Hua, Z.; Liu, C.; Lin, L.; Chen, R.; Hou, B. Characterization of T-Dependent and T-Independent B Cell Responses to a Virus-like Particle. *J. Immunol.* **2017**, *198*, 3846–3856. [[CrossRef](#)]
32. Chaudhury, S.; Duncan, E.H.; Atre, T.; Storme, C.K.; Beck, K.; Kaba, S.A.; Lanar, D.E.; Bergmann-Leitner, E.S. Identification of Immune Signatures of Novel Adjuvant Formulations Using Machine Learning. *Sci. Rep.* **2018**, *8*, 17508. [[CrossRef](#)]
33. Palgen, J.L.; Tchitchek, N.; Rodriguez-Pozo, A.; Jouhault, Q.; Abdelhouahab, H.; Dereuddre-Bosquet, N.; Contreras, V.; Martinon, F.; Cosma, A.; Lévy, Y.; et al. Innate and secondary humoral responses are improved by increasing the time between MVA vaccine immunizations. *NPJ Vaccines* **2020**, *5*, 24. [[CrossRef](#)]
34. Palgen, J.L.; Tchitchek, N.; Huot, N.; Elhmouzi-Younes, J.; Lefebvre, C.; Rosenbaum, P.; Dereuddre-Bosquet, N.; Martinon, F.; Hocini, H.; Cosma, A.; et al. NK cell immune responses differ after prime and boost vaccination. *J. Leukoc. Biol.* **2019**, *105*, 1055–1073. [[CrossRef](#)]
35. Palgen, J.L.; Tchitchek, N.; Elhmouzi-Younes, J.; Delandre, S.; Namet, I.; Rosenbaum, P.; Dereuddre-Bosquet, N.; Martinon, F.; Cosma, A.; Lévy, Y.; et al. Prime and Boost Vaccination Elicit a Distinct Innate Myeloid Cell Immune Response. *Sci. Rep.* **2018**, *8*, 3087. [[CrossRef](#)] [[PubMed](#)]
36. Rosenbaum, P.; Tchitchek, N.; Joly, C.; Stimmer, L.; Hocini, H.; Dereuddre-Bosquet, N.; Beignon, A.S.; Chapon, C.; Levy, Y.; Le Grand, R.; et al. Molecular and Cellular Dynamics in the Skin, the Lymph Nodes, and the Blood of the Immune Response to Intradermal Injection of Modified Vaccinia Ankara Vaccine. *Front. Immunol.* **2018**, *9*, 870. [[CrossRef](#)]
37. Rosenbaum, P.; Tchitchek, N.; Joly, C.; Rodriguez Pozo, A.; Stimmer, L.; Langlois, S.; Hocini, H.; Gosse, L.; Pejoski, D.; Cosma, A.; et al. Vaccine Inoculation Route Modulates Early Immunity and Consequently Antigen-Specific Immune Response. *Front. Immunol.* **2021**, *12*, 1362. [[CrossRef](#)]
38. Wimmers, F.; Pulendran, B. Emerging technologies for systems vaccinology—Multi-omics integration and single-cell (epi)genomic profiling. *Curr. Opin. Immunol.* **2020**, *65*, 57–64. [[CrossRef](#)]
39. Natrajan, M.S.; Rouphael, N.; Lai, L.; Kazmin, D.; Jensen, T.L.; Weiss, D.S.; Ibegbu, C.; Sztein, M.B.; Hooper, W.F.; Hill, H.; et al. Systems Vaccinology for a Live Attenuated Tularemia Vaccine Reveals Unique Transcriptional Signatures That Predict Humoral and Cellular Immune Responses. *Vaccines* **2019**, *8*, 4. [[CrossRef](#)] [[PubMed](#)]
40. Hagan, T.; Cortese, M.; Rouphael, N.; Boudreau, C.; Linde, C.; Maddur, M.S.; Das, J.; Wang, H.; Guthmiller, J.; Zheng, N.Y.; et al. Antibiotics-Driven Gut Microbiome Perturbation Alters Immunity to Vaccines in Humans. *Cell* **2019**, *178*, 1313–1328.e1313. [[CrossRef](#)]
41. Lindsay, K.E.; Bhosle, S.M.; Zurla, C.; Beyersdorf, J.; Rogers, K.A.; Vanover, D.; Xiao, P.; Araínga, M.; Shirreff, L.M.; Pitard, B.; et al. Visualization of early events in mRNA vaccine delivery in non-human primates via PET-CT and near-infrared imaging. *Nat. Biomed. Eng.* **2019**, *3*, 371–380. [[CrossRef](#)] [[PubMed](#)]
42. Salabert, N.; Todorova, B.; Martinon, F.; Boisgard, R.; Zurawski, G.; Zurawski, S.; Dereuddre-Bosquet, N.; Cosma, A.; Kortulewski, T.; Banchereau, J.; et al. Intradermal injection of an anti-Langerin-HIVGag fusion vaccine targets epidermal Langerhans cells in nonhuman primates and can be tracked in vivo. *Eur. J. Immunol.* **2016**, *46*, 689–700. [[CrossRef](#)] [[PubMed](#)]

43. de Vries, I.J.; Lesterhuis, W.J.; Barentsz, J.O.; Verdijk, P.; van Krieken, J.H.; Boerman, O.C.; Oyen, W.J.; Bonenkamp, J.J.; Boezeman, J.B.; Adema, G.J.; et al. Magnetic resonance tracking of dendritic cells in melanoma patients for monitoring of cellular therapy. *Nat. Biotechnol.* **2005**, *23*, 1407–1413. [[CrossRef](#)] [[PubMed](#)]
44. Todorova, B.; Salabert, N.; Tricot, S.; Boisgard, R.; Rathaux, M.; Le Grand, R.; Chapon, C. Fibered Confocal Fluorescence Microscopy for the Noninvasive Imaging of Langerhans Cells in Macaques. *Contrast Media Mol. Imaging* **2017**, *2017*, 3127908. [[CrossRef](#)]
45. Ols, S.; Yang, L.; Thompson, E.A.; Pushparaj, P.; Tran, K.; Liang, F.; Lin, A.; Eriksson, B.; Karlsson Hedestam, G.B.; Wyatt, R.T.; et al. Route of Vaccine Administration Alters Antigen Trafficking but Not Innate or Adaptive Immunity. *Cell Rep.* **2020**, *30*, 3964–3971.e3967. [[CrossRef](#)]
46. Wong, M.T.; Ong, D.E.; Lim, F.S.; Teng, K.W.; McGovern, N.; Narayanan, S.; Ho, W.Q.; Cerny, D.; Tan, H.K.; Anicete, R.; et al. A High-Dimensional Atlas of Human T Cell Diversity Reveals Tissue-Specific Trafficking and Cytokine Signatures. *Immunity* **2016**, *45*, 442–456. [[CrossRef](#)] [[PubMed](#)]
47. Chen, Z.; Ji, C.; Shen, Q.; Liu, W.; Qin, F.X.; Wu, A. Tissue-specific deconvolution of immune cell composition by integrating bulk and single-cell transcriptomes. *Bioinformatics* **2020**, *36*, 819–827. [[CrossRef](#)]
48. DeGottardi, Q.; Gates, T.J.; Yang, J.; James, E.A.; Malhotra, U.; Chow, I.T.; Simoni, Y.; Fehlings, M.; Newell, E.W.; DeBerg, H.A.; et al. Ontogeny of different subsets of yellow fever virus-specific circulatory CXCR5⁺ CD4⁺ T cells after yellow fever vaccination. *Sci. Rep.* **2020**, *10*, 15686. [[CrossRef](#)] [[PubMed](#)]
49. Weinberg, A.; Zhang, J.H.; Oxman, M.N.; Johnson, G.R.; Hayward, A.R.; Caulfield, M.J.; Irwin, M.R.; Clair, J.; Smith, J.G.; Stanley, H.; et al. Varicella-zoster virus-specific immune responses to herpes zoster in elderly participants in a trial of a clinically effective zoster vaccine. *J. Infect. Dis.* **2009**, *200*, 1068–1077. [[CrossRef](#)] [[PubMed](#)]
50. Panchanathan, V.; Chaudhri, G.; Karupiah, G. Protective immunity against secondary poxvirus infection is dependent on antibody but not on CD4 or CD8 T-cell function. *J. Virol.* **2006**, *80*, 6333–6338. [[CrossRef](#)] [[PubMed](#)]
51. Moss, B. Smallpox vaccines: Targets of protective immunity. *Immunol. Rev.* **2011**, *239*, 8–26. [[CrossRef](#)]
52. Querec, T.D.; Akondy, R.S.; Lee, E.K.; Cao, W.; Nakaya, H.I.; Teuwen, D.; Pirani, A.; Gernert, K.; Deng, J.; Marzolf, B.; et al. Systems biology approach predicts immunogenicity of the yellow fever vaccine in humans. *Nat. Immunol.* **2009**, *10*, 116–125. [[CrossRef](#)]
53. Gonnet, J.; Poncelet, L.; Meriaux, C.; Gonçalves, E.; Weiss, L.; Tchitchek, N.; Pedruzzi, E.; Soria, A.; Boccaro, D.; Vogt, A.; et al. Mechanisms of innate events during skin reaction following intradermal injection of seasonal influenza vaccine. *J. Proteom.* **2020**, *216*, 103670. [[CrossRef](#)]
54. Gourley, T.S.; Wherry, E.J.; Masopust, D.; Ahmed, R. Generation and maintenance of immunological memory. *Semin Immunol.* **2004**, *16*, 323–333. [[CrossRef](#)] [[PubMed](#)]
55. Shinoda, K.; Tokoyoda, K.; Hanazawa, A.; Hayashizaki, K.; Zehentmeier, S.; Hosokawa, H.; Iwamura, C.; Koseki, H.; Tumes, D.J.; Radbruch, A.; et al. Type II membrane protein CD69 regulates the formation of resting T-helper memory. *Proc. Natl. Acad. Sci. USA* **2012**, *109*, 7409–7414. [[CrossRef](#)] [[PubMed](#)]
56. Monath, T.P. Yellow fever: An update. *Lancet Infect. Dis.* **2001**, *1*, 11–20. [[CrossRef](#)]
57. Darrah, P.A.; Zeppa, J.J.; Maiello, P.; Hackney, J.A.; Wadsworth, M.H., 2nd; Hughes, T.K.; Pokkali, S.; Swanson, P.A., 2nd; Grant, N.L.; Rodgers, M.A.; et al. Prevention of tuberculosis in macaques after intravenous BCG immunization. *Nature* **2020**, *577*, 95–102. [[CrossRef](#)] [[PubMed](#)]
58. Pattyn, J.; Van Keer, S.; Tjalma, W.; Matheeussen, V.; Van Damme, P.; Vorsters, A. Infection and vaccine-induced HPV-specific antibodies in cervicovaginal secretions. A review of the literature. *Papillomavirus Res.* **2019**, *8*, 100185. [[CrossRef](#)] [[PubMed](#)]
59. Bhaumik, S.K.; Kulkarni, R.R.; Weldon, W.C.; Silveira, E.L.V.; Ahmed, H.; Gunisetty, S.; Chandele, A.; Antia, R.; Verma, H.; Sutter, R.; et al. Immune Priming and Long-term Persistence of Memory B Cells After Inactivated Poliovirus Vaccine in Macaque Models: Support for at least 2 Doses. *Clin. Infect. Dis.* **2018**, *67*, S66–S77. [[CrossRef](#)]
60. Tsang, J.S.; Schwartzberg, P.L.; Kotliarov, Y.; Biancotto, A.; Xie, Z.; Germain, R.N.; Wang, E.; Olnes, M.J.; Narayanan, M.; Golding, H.; et al. Global analyses of human immune variation reveal baseline predictors of postvaccination responses. *Cell* **2014**, *157*, 499–513. [[CrossRef](#)]
61. Human Immunology Project Consortium—Center for Human Immunology (HIPC-CHI) Signatures Project Team and HIPC-I Consortium. Multicohort analysis reveals baseline transcriptional predictors of influenza vaccination responses. *Sci. Immunol.* **2017**, *2*, eaal4656. [[CrossRef](#)]
62. Kotliarov, Y.; Sparks, R.; Martins, A.J.; Mulè, M.P.; Lu, Y.; Goswami, M.; Kardava, L.; Banchereau, R.; Pascual, V.; Biancotto, A.; et al. Broad immune activation underlies shared set point signatures for vaccine responsiveness in healthy individuals and disease activity in patients with lupus. *Nat. Med.* **2020**, *26*, 618–629. [[CrossRef](#)]
63. Fourati, S.; Cristescu, R.; Loboda, A.; Talla, A.; Filali, A.; Railkar, R.; Schaeffer, A.K.; Favre, D.; Gagnon, D.; Peretz, Y.; et al. Pre-vaccination inflammation and B-cell signalling predict age-related hyporesponse to hepatitis B vaccination. *Nat. Commun.* **2016**, *7*, 10369. [[CrossRef](#)]
64. Pauthner, M.; Havenar-Daughton, C.; Sok, D.; Nkolola, J.P.; Bastidas, R.; Boopathy, A.V.; Carnathan, D.G.; Chandrashekhar, A.; Cirelli, K.M.; Cottrell, C.A.; et al. Elicitation of Robust Tier 2 Neutralizing Antibody Responses in Nonhuman Primates by HIV Envelope Trimer Immunization Using Optimized Approaches. *Immunity* **2017**, *46*, 1073–1088.e1076. [[CrossRef](#)]
65. Mahnke, Y.D.; Roederer, M. Optimizing a multicolor immunophenotyping assay. *Clin. Lab. Med.* **2007**, *27*, 469–485. [[CrossRef](#)]
66. Reeves, P.M.; Sluder, A.E.; Paul, S.R.; Scholzen, A.; Kashiwagi, S.; Poznansky, M.C. Application and utility of mass cytometry in vaccine development. *FASEB J.* **2018**, *32*, 5–15. [[CrossRef](#)]

67. Futamura, K.; Sekino, M.; Hata, A.; Ikebuchi, R.; Nakanishi, Y.; Egawa, G.; Kabashima, K.; Watanabe, T.; Furuki, M.; Tomura, M. Novel full-spectral flow cytometry with multiple spectrally-adjacent fluorescent proteins and fluorochromes and visualization of in vivo cellular movement. *Cytom. A* **2015**, *87*, 830–842. [CrossRef] [PubMed]
68. Spitzer, M.H.; Nolan, G.P. Mass Cytometry: Single Cells, Many Features. *Cell* **2016**, *165*, 780–791. [CrossRef] [PubMed]
69. Olsen, L.R.; Leipold, M.D.; Pedersen, C.B.; Maecker, H.T. The anatomy of single cell mass cytometry data. *Cytom. A* **2019**, *95*, 156–172. [CrossRef]
70. De Rosa, S.C.; Roederer, M. Eleven-color flow cytometry. A powerful tool for elucidation of the complex immune system. *Clin. Lab. Med.* **2001**, *21*, 697–712. [PubMed]
71. Boesch, M.; Cosma, A.; Sopper, S. Flow Cytometry: To Dump or Not To Dump. *J. Immunol.* **2018**, *201*, 1813–1815. [CrossRef]
72. Pejoski, D.; Tchitchek, N.; Rodriguez Pozo, A.; Elhmouzi-Younes, J.; Yousfi-Bogniaho, R.; Rogez-Kreuz, C.; Clayette, P.; Dereuddre-Bosquet, N.; Lévy, Y.; Cosma, A.; et al. Identification of Vaccine-Altered Circulating B Cell Phenotypes Using Mass Cytometry and a Two-Step Clustering Analysis. *J. Immunol.* **2016**, *196*, 4814–4831. [CrossRef]
73. Subrahmanyam, P.B.; Holmes, T.H.; Lin, D.; Su, L.F.; Obermoser, G.; Banchereau, J.; Pascual, V.; García-Sastre, A.; Albrecht, R.A.; Palucka, K.; et al. Mass Cytometry Defines Virus-Specific CD4⁺ T Cells in Influenza Vaccination. *Immunohorizons* **2020**, *4*, 774–788. [CrossRef]
74. Lingblom, C.M.D.; Kowli, S.; Swaminathan, N.; Maecker, H.T.; Lambert, S.L. Baseline immune profile by CyTOF can predict response to an investigational adjuvanted vaccine in elderly adults. *J. Transl. Med.* **2018**, *16*, 153. [CrossRef] [PubMed]
75. Furman, D.; Davis, M.M. New approaches to understanding the immune response to vaccination and infection. *Vaccine* **2015**, *33*, 5271–5281. [CrossRef] [PubMed]
76. Anbarasu, D.; Raja, C.P.; Raja, A. Multiplex analysis of cytokines/chemokines as biomarkers that differentiate healthy contacts from tuberculosis patients in high endemic settings. *Cytokine* **2013**, *61*, 747–754. [CrossRef] [PubMed]
77. Patel, H.; Ashton, N.J.; Dobson, R.J.B.; Andersson, L.M.; Yilmaz, A.; Blennow, K.; Gisslen, M.; Zetterberg, H. Proteomic blood profiling in mild, severe and critical COVID-19 patients. *Sci. Rep.* **2021**, *11*, 6357. [CrossRef] [PubMed]
78. Chauvat, A.; Benhamouda, N.; Gey, A.; Lemoine, F.M.; Paulie, S.; Carrat, F.; Gougeon, M.L.; Rozenberg, F.; Krivine, A.; Cherai, M.; et al. Clinical validation of IFN γ /IL-10 and IFN γ /IL-2 FluoroSpot assays for the detection of Tr1 T cells and influenza vaccine monitoring in humans. *Hum. Vaccines Immunother.* **2014**, *10*, 104–113. [CrossRef] [PubMed]
79. Huttner, A.; Combescure, C.; Grillet, S.; Haks, M.C.; Quinten, E.; Modoux, C.; Agnandji, S.T.; Brosnahan, J.; Dayer, J.A.; Harandi, A.M.; et al. A dose-dependent plasma signature of the safety and immunogenicity of the rVSV-Ebola vaccine in Europe and Africa. *Sci. Transl. Med.* **2017**, *9*, eaaj1701. [CrossRef] [PubMed]
80. Galson, J.D.; Pollard, A.J.; Trück, J.; Kelly, D.F. Studying the antibody repertoire after vaccination: Practical applications. *Trends Immunol.* **2014**, *35*, 319–331. [CrossRef]
81. Teraguchi, S.; Saputri, D.S.; Llamas-Covarrubias, M.A.; Davila, A.; Diez, D.; Nazlica, S.A.; Rozewicki, J.; Ismanto, H.S.; Wilamowski, J.; Xie, J.; et al. Methods for sequence and structural analysis of B and T cell receptor repertoires. *Comput. Struct. Biotechnol. J.* **2020**, *18*, 2000–2011. [CrossRef]
82. Cotugno, N.; Ruggiero, A.; Santilli, V.; Manno, E.C.; Rocca, S.; Zicari, S.; Amadio, D.; Colucci, M.; Rossi, P.; Levy, O.; et al. OMIC Technologies and Vaccine Development: From the Identification of Vulnerable Individuals to the Formulation of Invulnerable Vaccines. *J. Immunol. Res.* **2019**, *2019*, 8732191. [CrossRef]
83. Arunachalam, P.S.; Charles, T.P.; Joag, V.; Bollimpelli, V.S.; Scott, M.K.D.; Wimmers, F.; Burton, S.L.; Labranche, C.C.; Petitdemange, C.; Gangadhara, S.; et al. T cell-inducing vaccine durably prevents mucosal SHIV infection even with lower neutralizing antibody titers. *Nat. Med.* **2020**, *26*, 932–940. [CrossRef]
84. Routhu, N.K.; Cheedarla, N.; Gangadhara, S.; Bollimpelli, V.S.; Boddapati, A.K.; Shiferaw, A.; Rahman, S.A.; Sahoo, A.; Edara, V.V.; Lai, L.; et al. A modified vaccinia Ankara vector-based vaccine protects macaques from SARS-CoV-2 infection, immune pathology, and dysfunction in the lungs. *Immunity* **2021**, *54*, 542–556.e549. [CrossRef]
85. Afik, S.; Yates, K.B.; Bi, K.; Darko, S.; Godec, J.; Gerdemann, U.; Swadling, L.; Douek, D.C.; Klenerman, P.; Barnes, E.J.; et al. Targeted reconstruction of T cell receptor sequence from single cell RNA-seq links CDR3 length to T cell differentiation state. *Nucleic Acids Res.* **2017**, *45*, e148. [CrossRef] [PubMed]
86. Turner, J.S.; Zhou, J.Q.; Han, J.; Schmitz, A.J.; Rizk, A.A.; Alsoussi, W.B.; Lei, T.; Amor, M.; McIntire, K.M.; Meade, P.; et al. Human germinal centres engage memory and naive B cells after influenza vaccination. *Nature* **2020**, *586*, 127–132. [CrossRef]
87. Horns, F.; Dekker, C.L.; Quake, S.R. Memory B Cell Activation, Broad Anti-influenza Antibodies, and Bystander Activation Revealed by Single-Cell Transcriptomics. *Cell Rep.* **2020**, *30*, 905–913.e906. [CrossRef]
88. Cirelli, K.M.; Carnathan, D.G.; Nogal, B.; Martin, J.T.; Rodriguez, O.L.; Upadhyay, A.A.; Enemuo, C.A.; Gebru, E.H.; Choe, Y.; Viviano, F.; et al. Slow Delivery Immunization Enhances HIV Neutralizing Antibody and Germinal Center Responses via Modulation of Immunodominance. *Cell* **2020**, *180*, 206. [CrossRef] [PubMed]
89. Waickman, A.T.; Victor, K.; Li, T.; Hatch, K.; Rutvisuttinunt, W.; Medin, C.; Gabriel, B.; Jarman, R.G.; Friberg, H.; Currier, J.R. Dissecting the heterogeneity of DENV vaccine-elicited cellular immunity using single-cell RNA sequencing and metabolic profiling. *Nat. Commun.* **2019**, *10*, 3666. [CrossRef]
90. James, M.L.; Gambhir, S.S. A molecular imaging primer: Modalities, imaging agents, and applications. *Physiol. Rev.* **2012**, *92*, 897–965. [CrossRef] [PubMed]

91. Gabrielson, K.; Maronpot, R.; Monette, S.; Mlynarczyk, C.; Ramot, Y.; Nyska, A.; Sysa-Shah, P. In Vivo Imaging With Confirmation by Histopathology for Increased Rigor and Reproducibility in Translational Research: A Review of Examples, Options, and Resources. *Ilar J.* **2018**, *59*, 80–98. [CrossRef]
92. Ottobrini, L.; Martelli, C.; Trabattoni, D.L.; Clerici, M.; Lucignani, G. In vivo imaging of immune cell trafficking in cancer. *Eur. J. Nucl. Med. Mol. Imaging* **2011**, *38*, 949–968. [CrossRef]
93. Romain, G.; van Gulck, E.; Epaulard, O.; Oh, S.; Li, D.; Zurawski, G.; Zurawski, S.; Cosma, A.; Adam, L.; Chapon, C.; et al. CD34-derived dendritic cells transfected ex vivo with HIV-Gag mRNA induce polyfunctional T-cell responses in nonhuman primates. *Eur. J. Immunol.* **2012**, *42*, 2019–2030. [CrossRef]
94. Ahrens, E.T.; Bulte, J.W. Tracking immune cells in vivo using magnetic resonance imaging. *Nat. Rev. Immunol.* **2013**, *13*, 755–763. [CrossRef] [PubMed]
95. Brewer, K.D.; Lake, K.; Pelot, N.; Stanford, M.M.; DeBay, D.R.; Penwell, A.; Weir, G.M.; Karkada, M.; Mansour, M.; Bowen, C.V. Clearance of depot vaccine SPIO-labeled antigen and substrate visualized using MRI. *Vaccine* **2014**, *32*, 6956–6962. [CrossRef]
96. Ferguson, P.M.; Slocumbe, A.; Tilley, R.D.; Hermans, I.F. Using magnetic resonance imaging to evaluate dendritic cell-based vaccination. *PLoS ONE* **2013**, *8*, e65318. [CrossRef] [PubMed]
97. Daldrup-Link, H.E.; Golovko, D.; Ruffell, B.; Denardo, D.G.; Castaneda, R.; Ansari, C.; Rao, J.; Tikhomirov, G.A.; Wendland, M.F.; Corot, C.; et al. MRI of tumor-associated macrophages with clinically applicable iron oxide nanoparticles. *Clin. Cancer Res.* **2011**, *17*, 5695–5704. [CrossRef] [PubMed]
98. Makela, A.V.; Gaudet, J.M.; Foster, P.J. Quantifying tumor associated macrophages in breast cancer: A comparison of iron and fluorine-based MRI cell tracking. *Sci. Rep.* **2017**, *7*, 42109. [CrossRef] [PubMed]
99. Floris, S.; Blezer, E.L.; Schreiber, G.; Döpp, E.; van der Pol, S.M.; Schadée-Eestermans, I.L.; Nicolay, K.; Dijkstra, C.D.; de Vries, H.E. Blood-brain barrier permeability and monocyte infiltration in experimental allergic encephalomyelitis: A quantitative MRI study. *Brain* **2004**, *127*, 616–627. [CrossRef]
100. Zhang, Y.; Wells, J.; Buist, R.; Peeling, J.; Yong, V.W.; Mitchell, J.R. Active inflammation increases the heterogeneity of MRI texture in mice with relapsing experimental allergic encephalomyelitis. *Magn. Reson. Imaging* **2014**, *32*, 168–174. [CrossRef]
101. Tremblay, M.L.; Davis, C.; Bowen, C.V.; Stanley, O.; Parsons, C.; Weir, G.; Karkada, M.; Stanford, M.M.; Brewer, K.D. Using MRI cell tracking to monitor immune cell recruitment in response to a peptide-based cancer vaccine. *Magn. Reson. Med.* **2018**, *80*, 304–316. [CrossRef] [PubMed]
102. Meller, B.; Frohn, C.; Brand, J.M.; Lauer, I.; Schelper, L.F.; von Hof, K.; Kirchner, H.; Richter, E.; Baehre, M. Monitoring of a new approach of immunotherapy with allogenic (111)In-labelled NK cells in patients with renal cell carcinoma. *Eur. J. Nucl. Med. Mol. Imaging* **2004**, *31*, 403–407. [CrossRef]
103. Yuki, Y.; Nochi, T.; Harada, N.; Katakai, Y.; Shibata, H.; Mejima, M.; Kohda, T.; Tokuhara, D.; Kurokawa, S.; Takahashi, Y.; et al. In vivo molecular imaging analysis of a nasal vaccine that induces protective immunity against botulism in nonhuman primates. *J. Immunol.* **2010**, *185*, 5436–5443. [CrossRef]
104. Pektor, S.; Hilscher, L.; Walzer, K.C.; Miederer, I.; Bausbacher, N.; Loquai, C.; Schreckenberger, M.; Sahin, U.; Diken, M.; Miederer, M. In vivo imaging of the immune response upon systemic RNA cancer vaccination by FDG-PET. *EJNMMI Res.* **2018**, *8*, 80. [CrossRef]
105. Coates, E.E.; Costner, P.J.; Nason, M.C.; Herrin, D.M.; Conant, S.; Herscovitch, P.; Sarwar, U.N.; Holman, L.; Mitchell, J.; Yamshchikov, G.; et al. Lymph Node Activation by PET/CT Following Vaccination With Licensed Vaccines for Human Papillomavirus. *Clin. Nucl. Med.* **2017**, *42*, 329–334. [CrossRef]
106. Vadalà, M.; Cistaro, A.; Quartuccio, N.; Calcagni, M.L.; Fania, P.; Margotti, S.; Schiera, I.G.; Laurino, C.; Palmieri, B. 18F-FDG-PET brain imaging may highlight brain metabolic alterations in dysautonomic syndrome after human papilloma virus vaccination. *Nucl. Med. Commun.* **2020**, *41*, 1275–1282. [CrossRef]
107. Mingos, M.; Howard, S.; Giacalone, N.; Kozono, D.; Jacene, H. Systemic Immune Response to Vaccination on FDG-PET/CT. *Nucl. Med. Mol. Imaging* **2016**, *50*, 358–361. [CrossRef]
108. Shirone, N.; Shinkai, T.; Yamane, T.; Uto, F.; Yoshimura, H.; Tamai, H.; Imai, T.; Inoue, M.; Kitano, S.; Kichikawa, K.; et al. Axillary lymph node accumulation on FDG-PET/CT after influenza vaccination. *Ann. Nucl. Med.* **2012**, *26*, 248–252. [CrossRef] [PubMed]
109. Aarntzen, E.H.; Srinivas, M.; De Wilt, J.H.; Jacobs, J.F.; Lesterhuis, W.J.; Windhorst, A.D.; Troost, E.G.; Bonenkamp, J.J.; van Rossum, M.M.; Blokx, W.A.; et al. Early identification of antigen-specific immune responses in vivo by [18F]-labeled 3'-fluoro-3'-deoxy-thymidine ([18F]FLT) PET imaging. *Proc. Natl. Acad. Sci. USA* **2011**, *108*, 18396–18399. [CrossRef]
110. Wu, C.; Li, F.; Niu, G.; Chen, X. PET imaging of inflammation biomarkers. *Theranostics* **2013**, *3*, 448–466. [CrossRef]
111. Rashidian, M.; LaFleur, M.W.; Verschoor, V.L.; Dongre, A.; Zhang, Y.; Nguyen, T.H.; Kolifrath, S.; Aref, A.R.; Lau, C.J.; Paweletz, C.P.; et al. Immuno-PET identifies the myeloid compartment as a key contributor to the outcome of the antitumor response under PD-1 blockade. *Proc. Natl. Acad. Sci. USA* **2019**, *116*, 16971–16980. [CrossRef]
112. Freise, A.C.; Wu, A.M. In vivo imaging with antibodies and engineered fragments. *Mol. Immunol.* **2015**, *67*, 142–152. [CrossRef]
113. Peters, A.M.; Saverymuttu, S.H.; Reavy, H.J.; Danpure, H.J.; Osman, S.; Lavender, J.P. Imaging of inflammation with indium-111 tropolonate labeled leukocytes. *J. Nucl. Med.* **1983**, *24*, 39–44.
114. Watson, H.A.; Durairaj, R.R.P.; Ohme, J.; Alatsatianos, M.; Almutairi, H.; Mohammed, R.N.; Vigar, M.; Reed, S.G.; Paisey, S.J.; Marshall, C.; et al. L-Selectin Enhanced T Cells Improve the Efficacy of Cancer Immunotherapy. *Front. Immunol.* **2019**, *10*, 1321. [CrossRef] [PubMed]

115. Heskamp, S.; Raavé, R.; Boerman, O.; Rijpkema, M.; Goncalves, V.; Denat, F. (89)Zr-Immuno-Positron Emission Tomography in Oncology: State-of-the-Art (89)Zr Radiochemistry. *Bioconjug. Chem.* **2017**, *28*, 2211–2223. [CrossRef] [PubMed]
116. Fu, R.; Carroll, L.; Yahioglu, G.; Aboagye, E.O.; Miller, P.W. Antibody Fragment and Affibody ImmunoPET Imaging Agents: Radiolabelling Strategies and Applications. *Chem. Med. Chem.* **2018**, *13*, 2466–2478. [CrossRef]
117. Cruz, L.J.; Tacken, P.J.; Bonetto, F.; Buschow, S.I.; Croes, H.J.; Wijers, M.; de Vries, I.J.; Figdor, C.G. Multimodal imaging of nanovaccine carriers targeted to human dendritic cells. *Mol. Pharm.* **2011**, *8*, 520–531. [CrossRef] [PubMed]
118. Todorova, B.; Adam, L.; Culina, S.; Boisgard, R.; Martinon, F.; Cosma, A.; Ustav, M.; Kortulewski, T.; Le Grand, R.; Chapon, C. Electroporation as a vaccine delivery system and a natural adjuvant to intradermal administration of plasmid DNA in macaques. *Sci. Rep.* **2017**, *7*, 4122. [CrossRef]
119. Cao, Q.; Huang, Q.; Mohan, C.; Li, C. Small-Animal PET/CT Imaging of Local and Systemic Immune Response Using (64)Cu- α CD11b. *J. Nucl. Med.* **2019**, *60*, 1317–1324. [CrossRef]
120. Nigam, S.; McCarl, L.; Kumar, R.; Edinger, R.S.; Kurland, B.F.; Anderson, C.J.; Panigrahy, A.; Kohanbash, G.; Edwards, W.B. Preclinical ImmunoPET Imaging of Glioblastoma-Infiltrating Myeloid Cells Using Zirconium-89 Labeled Anti-CD11b Antibody. *Mol. Imaging Biol.* **2020**, *22*, 685–694. [CrossRef]
121. Warram, J.M.; de Boer, E.; Sorace, A.G.; Chung, T.K.; Kim, H.; Pleijhuis, R.G.; van Dam, G.M.; Rosenthal, E.L. Antibody-based imaging strategies for cancer. *Cancer Metastasis Rev.* **2014**, *33*, 809–822. [CrossRef]
122. Chanier, T.; Chames, P. Nanobody Engineering: Toward Next Generation Immunotherapies and Immunoimaging of Cancer. *Antibodies* **2019**, *8*, 13. [CrossRef] [PubMed]
123. Blykers, A.; Schoonooghe, S.; Xavier, C.; D’Hoe, K.; Laoui, D.; D’Huyvetter, M.; Vaneycken, I.; Cleeren, F.; Bormans, G.; Heemskerk, J.; et al. PET Imaging of Macrophage Mannose Receptor-Expressing Macrophages in Tumor Stroma Using 18F-Radiolabeled Camelid Single-Domain Antibody Fragments. *J. Nucl. Med.* **2015**, *56*, 1265–1271. [CrossRef]
124. Van Elssen, C.; Rashidian, M.; Vrbanac, V.; Wucherpfennig, K.W.; Habre, Z.E.; Sticht, J.; Freund, C.; Jacobsen, J.T.; Cagnolini, J.; Ingram, J.; et al. Noninvasive Imaging of Human Immune Responses in a Human Xenograft Model of Graft-Versus-Host Disease. *J. Nucl. Med.* **2017**, *58*, 1003–1008. [CrossRef]
125. Chandrupatla, D.; Molthoff, C.F.M.; Lammertsma, A.A.; van der Laken, C.J.; Jansen, G. The folate receptor β as a macrophage-mediated imaging and therapeutic target in rheumatoid arthritis. *Drug Deliv. Transl. Res.* **2019**, *9*, 366–378. [CrossRef]
126. Varasteh, Z.; Mohanta, S.; Li, Y.; López Armbruster, N.; Braeuer, M.; Nekolla, S.G.; Habenicht, A.; Sager, H.B.; Raes, G.; Weber, W.; et al. Targeting mannose receptor expression on macrophages in atherosclerotic plaques of apolipoprotein E-knockout mice using (68)Ga-NOTA-anti-MMR nanobody: Non-invasive imaging of atherosclerotic plaques. *EJNMMI Res.* **2019**, *9*, 5. [CrossRef]
127. Movahedi, K.; Schoonooghe, S.; Laoui, D.; Houbraken, I.; Waelput, W.; Breckpot, K.; Bouwens, L.; Lahoutte, T.; De Baetselier, P.; Raes, G.; et al. Nanobody-based targeting of the macrophage mannose receptor for effective in vivo imaging of tumor-associated macrophages. *Cancer Res.* **2012**, *72*, 4165–4177. [CrossRef]
128. Mall, S.; Yusufi, N.; Wagner, R.; Klar, R.; Bianchi, H.; Steiger, K.; Straub, M.; Audehm, S.; Laitinen, I.; Aichler, M.; et al. Immuno-PET Imaging of Engineered Human T Cells in Tumors. *Cancer Res.* **2016**, *76*, 4113–4123. [CrossRef]
129. Tavaré, R.; McCracken, M.N.; Zettlitz, K.A.; Knowles, S.M.; Salazar, F.B.; Olafsen, T.; Witte, O.N.; Wu, A.M. Engineered antibody fragments for immuno-PET imaging of endogenous CD8 $^{+}$ T cells in vivo. *Proc. Natl. Acad. Sci. USA* **2014**, *111*, 1108–1113. [CrossRef]
130. Tavaré, R.; Escuin-Ordinas, H.; Mok, S.; McCracken, M.N.; Zettlitz, K.A.; Salazar, F.B.; Witte, O.N.; Ribas, A.; Wu, A.M. An Effective Immuno-PET Imaging Method to Monitor CD8-Dependent Responses to Immunotherapy. *Cancer Res.* **2016**, *76*, 73–82. [CrossRef]
131. Rashidian, M.; Ingram, J.R.; Dougan, M.; Dongre, A.; Whang, K.A.; LeGall, C.; Cagnolini, J.J.; Bierie, B.; Gostissa, M.; Gorman, J.; et al. Predicting the response to CTLA-4 blockade by longitudinal noninvasive monitoring of CD8 T cells. *J. Exp. Med.* **2017**, *214*, 2243–2255. [CrossRef]
132. Woodham, A.W.; Zeigler, S.H.; Zeyang, E.L.; Kolifrath, S.C.; Cheloha, R.W.; Rashidian, M.; Chaparro, R.J.; Seidel, R.D.; Garforth, S.J.; Dearling, J.L.; et al. In vivo detection of antigen-specific CD8 $^{+}$ T cells by immuno-positron emission tomography. *Nat. Methods* **2020**, *17*, 1025–1032. [CrossRef]
133. Faye, N.; Fournier, L.; Balvay, D.; Wilhelm, C.; Broqueres-You, D.; Bruneval, P.; Clément, O. Antitumoral Effect of Mural Cells Assessed With High-Resolution MRI and Fluorescence Microscopy. *AJR Am. J. Roentgenol.* **2015**, *205*, W11–W18. [CrossRef]
134. Al-Gubory, K.H. Shedding light on fibered confocal fluorescence microscopy: Applications in biomedical imaging and therapies. *J. Biophotonics* **2019**, *12*, e201900146. [CrossRef]
135. Mahe, B.; Vogt, A.; Liard, C.; Duffy, D.; Abadie, V.; Bonduelle, O.; Boissonnas, A.; Sterry, W.; Verrier, B.; Blume-Peytavi, U.; et al. Nanoparticle-based targeting of vaccine compounds to skin antigen-presenting cells by hair follicles and their transport in mice. *J. Investig. Derm.* **2009**, *129*, 1156–1164. [CrossRef] [PubMed]
136. Helmchen, F.; Denk, W. Deep tissue two-photon microscopy. *Nat. Methods* **2005**, *2*, 932–940. [CrossRef]
137. Rattanapak, T.; Birchall, J.C.; Young, K.; Kubo, A.; Fujimori, S.; Ishii, M.; Hook, S. Dynamic visualization of dendritic cell-antigen interactions in the skin following transcutaneous immunization. *PLoS ONE* **2014**, *9*, e89503. [CrossRef]
138. Miller, M.J.; Wei, S.H.; Parker, I.; Cahalan, M.D. Two-photon imaging of lymphocyte motility and antigen response in intact lymph node. *Science* **2002**, *296*, 1869–1873. [CrossRef]
139. Bousso, P.; Robey, E. Dynamics of CD8 $^{+}$ T cell priming by dendritic cells in intact lymph nodes. *Nat. Immunol.* **2003**, *4*, 579–585. [CrossRef]
140. Deguine, J.; Bousso, P. Dynamics of NK cell interactions in vivo. *Immunol. Rev.* **2013**, *251*, 154–159. [CrossRef]

141. Boussou, P.; Bhakta, N.R.; Lewis, R.S.; Robey, E. Dynamics of thymocyte-stromal cell interactions visualized by two-photon microscopy. *Science* **2002**, *296*, 1876–1880. [[CrossRef](#)]
142. Tan, W.C.C.; Nerurkar, S.N.; Cai, H.Y.; Ng, H.H.M.; Wu, D.; Wee, Y.T.F.; Lim, J.C.T.; Yeong, J.; Lim, T.K.H. Overview of multiplex immunohistochemistry/immunofluorescence techniques in the era of cancer immunotherapy. *Cancer Commun.* **2020**, *40*, 135–153. [[CrossRef](#)]
143. Muntifering, M.; Castranova, D.; Gibson, G.A.; Meyer, E.; Kofron, M.; Watson, A.M. Clearing for Deep Tissue Imaging. *Curr. Protoc. Cytom.* **2018**, *86*, e38. [[CrossRef](#)] [[PubMed](#)]
144. Dekkers, J.F.; Alieva, M.; Wellens, L.M.; Ariese, H.C.R.; Jamieson, P.R.; Vonk, A.M.; Amatngalim, G.D.; Hu, H.; Oost, K.C.; Snippert, H.J.G.; et al. High-resolution 3D imaging of fixed and cleared organoids. *Nat. Protoc.* **2019**, *14*, 1756–1771. [[CrossRef](#)] [[PubMed](#)]
145. Li, W.; Germain, R.N.; Gerner, M.Y. Multiplex, quantitative cellular analysis in large tissue volumes with clearing-enhanced 3D microscopy (Ce3D). *Proc. Natl. Acad. Sci. USA* **2017**, *114*, E7321–E7330. [[CrossRef](#)] [[PubMed](#)]
146. Walch, A.; Rauscher, S.; Deininger, S.O.; Höfler, H. MALDI imaging mass spectrometry for direct tissue analysis: A new frontier for molecular histology. *Histochem. Cell Biol.* **2008**, *130*, 421–434. [[CrossRef](#)] [[PubMed](#)]
147. Caprioli, R.M.; Farmer, T.B.; Gile, J. Molecular imaging of biological samples: Localization of peptides and proteins using MALDI-TOF MS. *Anal. Chem.* **1997**, *69*, 4751–4760. [[CrossRef](#)] [[PubMed](#)]
148. Ryan, N.M.; Hess, J.A.; de Villena, F.P.; Leiby, B.E.; Shimada, A.; Yu, L.; Yarmahmoodi, A.; Petrovsky, N.; Zhan, B.; Bottazzi, M.E.; et al. Onchocerca volvulus bivalent subunit vaccine induces protective immunity in genetically diverse collaborative cross recombinant inbred intercross mice. *NPJ Vaccines* **2021**, *6*, 17. [[CrossRef](#)]
149. Yagnik, G.; Liu, Z.; Rothschild, K.J.; Lim, M.J. Highly Multiplexed Immunohistochemical MALDI-MS Imaging of Biomarkers in Tissues. *J. Am. Soc. Mass Spectrom.* **2021**, *32*, 977–988. [[CrossRef](#)]
150. Oetjen, J.; Aichler, M.; Trede, D.; Strehlow, J.; Berger, J.; Heldmann, S.; Becker, M.; Gottschalk, M.; Kobarg, J.H.; Wirtz, S.; et al. MRI-compatible pipeline for three-dimensional MALDI imaging mass spectrometry using PAXgene fixation. *J. Proteom.* **2013**, *90*, 52–60. [[CrossRef](#)]
151. Kriegsmann, K.; Longuespée, R.; Hundemer, M.; Zgorzelski, C.; Casadonte, R.; Schwamborn, K.; Weichert, W.; Schirmacher, P.; Harms, A.; Kazdal, D.; et al. Combined Immunohistochemistry after Mass Spectrometry Imaging for Superior Spatial Information. *Proteom. Clin. Appl.* **2019**, *13*, e1800035. [[CrossRef](#)]
152. Porta Siegel, T.; Hamm, G.; Bunch, J.; Cappell, J.; Fletcher, J.S.; Schwamborn, K. Mass Spectrometry Imaging and Integration with Other Imaging Modalities for Greater Molecular Understanding of Biological Tissues. *Mol. Imaging Biol.* **2018**, *20*, 888–901. [[CrossRef](#)] [[PubMed](#)]
153. Giesen, C.; Wang, H.A.; Schapiro, D.; Zivanovic, N.; Jacobs, A.; Hattendorf, B.; Schüffler, P.J.; Grolimund, D.; Buhmann, J.M.; Brandt, S.; et al. Highly multiplexed imaging of tumor tissues with subcellular resolution by mass cytometry. *Nat. Methods* **2014**, *11*, 417–422. [[CrossRef](#)] [[PubMed](#)]
154. Bandura, D.R.; Baranov, V.I.; Ornatsky, O.I.; Antonov, A.; Kinach, R.; Lou, X.; Pavlov, S.; Vorobiev, S.; Dick, J.E.; Tanner, S.D. Mass cytometry: Technique for real time single cell multitarget immunoassay based on inductively coupled plasma time-of-flight mass spectrometry. *Anal. Chem.* **2009**, *81*, 6813–6822. [[CrossRef](#)] [[PubMed](#)]
155. Baharloo, H.; Canete, N.P.; Cunningham, A.L.; Harman, A.N.; Patrick, E. Mass Cytometry Imaging for the Study of Human Diseases—Applications and Data Analysis Strategies. *Front. Immunol.* **2019**, *10*, 2657. [[CrossRef](#)]
156. Zhao, Y.; Uduman, M.; Siu, J.H.Y.; Tull, T.J.; Sanderson, J.D.; Wu, Y.B.; Zhou, J.Q.; Petrov, N.; Ellis, R.; Todd, K.; et al. Spatiotemporal segregation of human marginal zone and memory B cell populations in lymphoid tissue. *Nat. Commun.* **2018**, *9*, 3857. [[CrossRef](#)]
157. Diamond, N.; Engler, S.; Zanotelli, V.R.T.; Schapiro, D.; Wasserfall, C.H.; Kusmartseva, I.; Nick, H.S.; Thorel, F.; Herrera, P.L.; Atkinson, M.A.; et al. A Map of Human Type 1 Diabetes Progression by Imaging Mass Cytometry. *Cell Metab.* **2019**, *29*, 755–768.e755. [[CrossRef](#)]
158. Buchberger, A.R.; DeLaney, K.; Johnson, J.; Li, L. Mass Spectrometry Imaging: A Review of Emerging Advancements and Future Insights. *Anal. Chem.* **2018**, *90*, 240–265. [[CrossRef](#)]
159. Durand, M.; Walter, T.; Pirnay, T.; Naessens, T.; Gueguen, P.; Goudot, C.; Lameiras, S.; Chang, Q.; Talaei, N.; Ornatsky, O.; et al. Human lymphoid organ cDC2 and macrophages play complementary roles in T follicular helper responses. *J. Exp. Med.* **2019**, *216*, 1561–1581. [[CrossRef](#)]
160. Gerner, M.Y.; Kastenmuller, W.; Ifrim, I.; Kabat, J.; Germain, R.N. Histo-cytometry: A method for highly multiplex quantitative tissue imaging analysis applied to dendritic cell subset microanatomy in lymph nodes. *Immunity* **2012**, *37*, 364–376. [[CrossRef](#)]
161. Gerner, M.Y.; Torabi-Parizi, P.; Germain, R.N. Strategically localized dendritic cells promote rapid T cell responses to lymph-borne particulate antigens. *Immunity* **2015**, *42*, 172–185. [[CrossRef](#)]
162. Petrovas, C.; Ferrando-Martinez, S.; Gerner, M.Y.; Casazza, J.P.; Pegu, A.; Deleage, C.; Cooper, A.; Hataye, J.; Andrews, S.; Ambrozak, D.; et al. Follicular CD8 T cells accumulate in HIV infection and can kill infected cells in vitro via bispecific antibodies. *Sci. Transl. Med.* **2017**, *9*, eaag2285. [[CrossRef](#)]
163. Li, W.; Germain, R.N.; Gerner, M.Y. High-dimensional cell-level analysis of tissues with Ce3D multiplex volume imaging. *Nat. Protoc.* **2019**, *14*, 1708–1733. [[CrossRef](#)]
164. Kotov, D.I.; Pengo, T.; Mitchell, J.S.; Gastinger, M.J.; Jenkins, M.K. Chrysalis: A New Method for High-Throughput Histo-Cytometry Analysis of Images and Movies. *J. Immunol.* **2019**, *202*, 300–308. [[CrossRef](#)]

165. Wilkinson, M.D.; Dumontier, M.; Aalbersberg, I.J.; Appleton, G.; Axton, M.; Baak, A.; Blomberg, N.; Boiten, J.W.; da Silva Santos, L.B.; Bourne, P.E.; et al. The FAIR Guiding Principles for scientific data management and stewardship. *Sci. Data* **2016**, *3*, 160018. [\[CrossRef\]](#) [\[PubMed\]](#)
166. Costa-Silva, J.; Domingues, D.; Lopes, F.M. RNA-Seq differential expression analysis: An extended review and a software tool. *PLoS ONE* **2017**, *12*, e0190152. [\[CrossRef\]](#)
167. Gene Ontology Consortium. The Gene Ontology resource: Enriching a GOld mine. *Nucleic Acids Res.* **2021**, *49*, D325–D334. [\[CrossRef\]](#) [\[PubMed\]](#)
168. Su, A.I.; Wiltshire, T.; Batalov, S.; Lapp, H.; Ching, K.A.; Block, D.; Zhang, J.; Soden, R.; Hayakawa, M.; Kreiman, G.; et al. A gene atlas of the mouse and human protein-encoding transcriptomes. *Proc. Natl. Acad. Sci. USA* **2004**, *101*, 6062–6067. [\[CrossRef\]](#) [\[PubMed\]](#)
169. Chen, E.Y.; Tan, C.M.; Kou, Y.; Duan, Q.; Wang, Z.; Meirelles, G.V.; Clark, N.R.; Ma'ayan, A. Enrichr: Interactive and collaborative HTML5 gene list enrichment analysis tool. *BMC Bioinform.* **2013**, *14*, 128. [\[CrossRef\]](#) [\[PubMed\]](#)
170. Langfelder, P.; Horvath, S. WGCNA: An R package for weighted correlation network analysis. *BMC Bioinform.* **2008**, *9*, 559. [\[CrossRef\]](#)
171. Qiu, P.; Simonds, E.F.; Bendall, S.C.; Gibbs, K.D., Jr.; Bruggner, R.V.; Linderman, M.D.; Sachs, K.; Nolan, G.P.; Plevritis, S.K. Extracting a cellular hierarchy from high-dimensional cytometry data with SPADE. *Nat. Biotechnol.* **2011**, *29*, 886–891. [\[CrossRef\]](#)
172. Van Gassen, S.; Callebaut, B.; Van Helden, M.J.; Lambrecht, B.N.; Demeester, P.; Dhaene, T.; Saeys, Y. FlowSOM: Using self-organizing maps for visualization and interpretation of cytometry data. *Cytom. A* **2015**, *87*, 636–645. [\[CrossRef\]](#)
173. Amirel, A.D.; Davis, K.L.; Tadmor, M.D.; Simonds, E.F.; Levine, J.H.; Bendall, S.C.; Shenfeld, D.K.; Krishnaswamy, S.; Nolan, G.P.; Pe'er, D. t-SNE enables visualization of high dimensional single-cell data and reveals phenotypic heterogeneity of leukemia. *Nat. Biotechnol.* **2013**, *31*, 545–552. [\[CrossRef\]](#)
174. McInnes, L.; Healy, J.; Melville, J. UMAP: Uniform Manifold Approximation and Projection for Dimension Reduction. *arXiv* **2018**, arXiv:1802.03426.
175. Hao, Y.; Hao, S.; Andersen-Nissen, E.; Mauck, W.M.; Zheng, S.; Butler, A.; Lee, M.J.; Wilk, A.J.; Darby, C.; Zagar, M.; et al. Integrated analysis of multimodal single-cell data. *bioRxiv* **2020**. [\[CrossRef\]](#)
176. Mitchell, T.M. *Machine Learning*; McGraw-Hill, Inc.: New York, NY, USA, 1997.
177. Gonzalez-Dias, P.; Lee, E.K.; Sorgi, S.; de Lima, D.S.; Urbanski, A.H.; Silveira, E.L.; Nakaya, H.I. Methods for predicting vaccine immunogenicity and reactogenicity. *Hum. Vaccine Immunother.* **2020**, *16*, 269–276. [\[CrossRef\]](#) [\[PubMed\]](#)
178. Furman, D.; Jovic, V.; Kidd, B.; Shen-Orr, S.; Price, J.; Jarrell, J.; Tse, T.; Huang, H.; Lund, P.; Maecker, H.T.; et al. Apoptosis and other immune biomarkers predict influenza vaccine responsiveness. *Mol. Syst. Biol.* **2013**, *9*, 659. [\[CrossRef\]](#) [\[PubMed\]](#)
179. Tomic, A.; Tomic, I.; Rosenberg-Hasson, Y.; Dekker, C.L.; Maecker, H.T.; Davis, M.M. SIMON, an Automated Machine Learning System, Reveals Immune Signatures of Influenza Vaccine Responses. *J. Immunol.* **2019**, *203*, 749–759. [\[CrossRef\]](#) [\[PubMed\]](#)
180. Li, S.; Sullivan, N.L.; Rouphael, N.; Yu, T.; Banton, S.; Maddur, M.S.; McCausland, M.; Chiu, C.; Canniff, J.; Dubey, S.; et al. Metabolic Phenotypes of Response to Vaccination in Humans. *Cell* **2017**, *169*, 862–877.e817. [\[CrossRef\]](#) [\[PubMed\]](#)
181. Kazmin, D.; Nakaya, H.I.; Lee, E.K.; Johnson, M.J.; van der Most, R.; van den Berg, R.A.; Ballou, W.R.; Jongert, E.; Wille-Reece, U.; Ockenhouse, C.; et al. Systems analysis of protective immune responses to RTS,S malaria vaccination in humans. *Proc. Natl. Acad. Sci. USA* **2017**, *114*, 2425–2430. [\[CrossRef\]](#) [\[PubMed\]](#)
182. Lewis, D.J.; Lythgoe, M.P. Application of “Systems Vaccinology” to Evaluate Inflammation and Reactogenicity of Adjuvanted Preventative Vaccines. *J. Immunol. Res.* **2015**, *2015*, 909406. [\[CrossRef\]](#)
183. Campbell-Toft, J.; Vrahatis, A.; Josefson, K.; Mehlsen, J.; Winther, K. Investigating the aetiology of adverse events following HPV vaccination with systems vaccinology. *Cell Mol. Life Sci.* **2019**, *76*, 67–87. [\[CrossRef\]](#) [\[PubMed\]](#)
184. Trtica-Majnaric, L.; Zekic-Susac, M.; Sarlija, N.; Vitale, B. Prediction of influenza vaccination outcome by neural networks and logistic regression. *J. Biomed. Inf.* **2010**, *43*, 774–781. [\[CrossRef\]](#)
185. Nakaya, H.I.; Wrammert, J.; Lee, E.K.; Racioppi, L.; Marie-Kunze, S.; Haining, W.N.; Means, A.R.; Kasturi, S.P.; Khan, N.; Li, G.M.; et al. Systems biology of vaccination for seasonal influenza in humans. *Nat. Immunol.* **2011**, *12*, 786–795. [\[CrossRef\]](#) [\[PubMed\]](#)
186. Zimmermann, M.T.; Kennedy, R.B.; Grill, D.E.; Oberg, A.L.; Goergen, K.M.; Ovsyannikova, I.G.; Haralambieva, I.H.; Poland, G.A. Integration of Immune Cell Populations, mRNA-Seq, and CpG Methylation to Better Predict Humoral Immunity to Influenza Vaccination: Dependence of mRNA-Seq/CpG Methylation on Immune Cell Populations. *Front. Immunol.* **2017**, *8*, 445. [\[CrossRef\]](#) [\[PubMed\]](#)
187. Parvandeh, S.; Poland, G.A.; Kennedy, R.B.; McKinney, B.A. Multi-Level Model to Predict Antibody Response to Influenza Vaccine Using Gene Expression Interaction Network Feature Selection. *Microorganisms* **2019**, *7*, 79. [\[CrossRef\]](#) [\[PubMed\]](#)
188. Avey, S.; Mohanty, S.; Wilson, J.; Zapata, H.; Joshi, S.R.; Siconolfi, B.; Tsang, S.; Shaw, A.C.; Kleinstein, S.H. Multiple network-constrained regressions expand insights into influenza vaccination responses. *Bioinformatics* **2017**, *33*, i208–i216. [\[CrossRef\]](#)
189. Gonçalves, E.; Bonduelle, O.; Soria, A.; Loulergue, P.; Rousseau, A.; Cachanado, M.; Bonnabau, H.; Thiebaut, R.; Tchitchev, N.; Behillil, S.; et al. Innate gene signature distinguishes humoral versus cytotoxic responses to influenza vaccination. *J. Clin. Investig.* **2019**, *129*, 1960–1971. [\[CrossRef\]](#)
190. Wall, N.; Godlee, A.; Geh, D.; Jones, C.; Faustini, S.; Harvey, R.; Penn, R.; Chanouzas, D.; Nightingale, P.; O’Shea, M.; et al. Latent cytomegalovirus infection and previous capsular polysaccharide vaccination predict poor vaccine responses in older adults, independent of chronic kidney disease. *Clin. Infect. Dis.* **2021**. [\[CrossRef\]](#)
191. Babji, S.; Manickavasagam, P.; Chen, Y.H.; Jeyavelu, N.; Jose, N.V.; Praharaj, I.; Syed, C.; Kaliappan, S.P.; John, J.; Giri, S.; et al. Immune predictors of oral poliovirus vaccine immunogenicity among infants in South India. *NPJ Vaccines* **2020**, *5*, 27. [\[CrossRef\]](#) [\[PubMed\]](#)

192. Janes, H.E.; Cohen, K.W.; Frahm, N.; De Rosa, S.C.; Sanchez, B.; Hural, J.; Magaret, C.A.; Karuna, S.; Bentley, C.; Gottardo, R.; et al. Higher T-Cell Responses Induced by DNA/rAd5 HIV-1 Preventive Vaccine Are Associated With Lower HIV-1 Infection Risk in an Efficacy Trial. *J. Infect. Dis.* **2017**, *215*, 1376–1385. [[CrossRef](#)]
193. Huang, Y.; Zhang, L.; Janes, H.; Frahm, N.; Isaacs, A.; Kim, J.H.; Montefiori, D.; McElrath, M.J.; Tomaras, G.D.; Gilbert, P.B. Predictors of durable immune responses six months after the last vaccination in preventive HIV vaccine trials. *Vaccine* **2017**, *35*, 1184–1193. [[CrossRef](#)]
194. Dérian, N.; Bellier, B.; Pham, H.P.; Tsitoura, E.; Kazazi, D.; Huret, C.; Mavromara, P.; Klitzmann, D.; Six, A. Early Transcriptome Signatures from Immunized Mouse Dendritic Cells Predict Late Vaccine-Induced T-Cell Responses. *PLoS Comput. Biol.* **2016**, *12*, e1004801. [[CrossRef](#)]
195. Germain, R.N. Will Systems Biology Deliver Its Promise and Contribute to the Development of New or Improved Vaccines? What Really Constitutes the Study of “Systems Biology” and How Might Such an Approach Facilitate Vaccine Design. *Cold Spring Harb Perspect. Biol.* **2018**, *10*, a033308. [[CrossRef](#)]
196. Ravindran, R.; Loebbermann, J.; Nakaya, H.I.; Khan, N.; Ma, H.; Gama, L.; Machiah, D.K.; Lawson, B.; Hakimpour, P.; Wang, Y.C.; et al. The amino acid sensor GCN2 controls gut inflammation by inhibiting inflammasome activation. *Nature* **2016**, *531*, 523–527. [[CrossRef](#)] [[PubMed](#)]
197. Antia, R.; Ganusov, V.V.; Ahmed, R. The role of models in understanding CD8⁺ T-cell memory. *Nat. Rev. Immunol.* **2005**, *5*, 101–111. [[CrossRef](#)] [[PubMed](#)]
198. Le, D.; Miller, J.D.; Ganusov, V.V. Mathematical modeling provides kinetic details of the human immune response to vaccination. *Front. Cell Infect. Microbiol.* **2014**, *4*, 177. [[CrossRef](#)] [[PubMed](#)]
199. Baker, R.E.; Peña, J.M.; Jayamohan, J.; Jérusalem, A. Mechanistic models versus machine learning, a fight worth fighting for the biological community? *Biol. Lett.* **2018**, *14*, 20170660. [[CrossRef](#)]
200. Barré-Sinoussi, F.; Montagutelli, X. Animal models are essential to biological research: Issues and perspectives. *Future Sci. Oa* **2015**, *1*, Fso63. [[CrossRef](#)]
201. Kiros, T.G.; Levast, B.; Auray, G.; Strom, S.; van Kessel, J.; Gerdts, V. The Importance of Animal Models in the Development of Vaccines. In *Innovation in Vaccinology: From Design, through to Delivery and Testing*; Baschieri, S., Ed.; Springer: Dordrecht, The Netherlands, 2012; pp. 251–264.
202. Klasse, P.J.; Nixon, D.F.; Moore, J.P. Immunogenicity of clinically relevant SARS-CoV-2 vaccines in nonhuman primates and humans. *Sci. Adv.* **2021**, *7*, eabe8065. [[CrossRef](#)]
203. Rappuoli, R.; Black, S.; Bloom, D.E. Vaccines and global health: In search of a sustainable model for vaccine development and delivery. *Sci. Transl. Med.* **2019**, *11*, eaaw2888. [[CrossRef](#)]
204. Plotkin, S.A.; Gilbert, P.B. Nomenclature for immune correlates of protection after vaccination. *Clin. Infect. Dis.* **2012**, *54*, 1615–1617. [[CrossRef](#)]
205. Van Damme, P.; Van Herck, K. A review of the long-term protection after hepatitis A and B vaccination. *Travel Med. Infect. Dis.* **2007**, *5*, 79–84. [[CrossRef](#)] [[PubMed](#)]
206. Johnson, N.; Cunningham, A.F.; Fooks, A.R. The immune response to rabies virus infection and vaccination. *Vaccine* **2010**, *28*, 3896–3901. [[CrossRef](#)]
207. Wieter, R.W.; Jonker, E.F.; van Leeuwen, E.M.; Remmerswaal, E.B.; Ten Berge, I.J.; de Visser, A.W.; van Genderen, P.J.; Goorhuis, A.; Visser, L.G.; Grobusch, M.P.; et al. A Single 17D Yellow Fever Vaccination Provides Lifelong Immunity; Characterization of Yellow-Fever-Specific Neutralizing Antibody and T-Cell Responses after Vaccination. *PLoS ONE* **2016**, *11*, e0149871. [[CrossRef](#)]
208. Center for Viral Systems Biology CViSB. SARS-CoV-2 (hCoV-19) Mutation Situation Reports. Available online: <https://outbreak.info/situation-reports> (accessed on 28 April 2021).
209. Thakur, A.; Pedersen, L.E.; Jungersen, G. Immune markers and correlates of protection for vaccine induced immune responses. *Vaccine* **2012**, *30*, 4907–4920. [[CrossRef](#)] [[PubMed](#)]
210. Pulendran, B. Systems vaccinology: Probing humanity’s diverse immune systems with vaccines. *Proc. Natl. Acad. Sci. USA* **2014**, *111*, 12300–12306. [[CrossRef](#)] [[PubMed](#)]
211. Epaulard, O.; Adam, L.; Poux, C.; Zurawski, G.; Salabert, N.; Rosenbaum, P.; Dereuddre-Bosquet, N.; Zurawski, S.; Flamar, A.L.; Oh, S.; et al. Macrophage-and neutrophil-derived TNF- α instructs skin langerhans cells to prime antiviral immune responses. *J. Immunol.* **2014**, *193*, 2416–2426. [[CrossRef](#)]
212. Adam, L.; Tchitchek, N.; Todorova, B.; Rosenbaum, P.; Joly, C.; Poux, C.; Chapon, C.; Spetz, A.L.; Ustav, M.; Le Grand, R.; et al. Innate Molecular and Cellular Signature in the Skin Preceding Long-Lasting T Cell Responses after Electroporated DNA Vaccination. *J. Immunol.* **2020**, *204*, 3375–3388. [[CrossRef](#)]
213. Liard, C.; Munier, S.; Arias, M.; Joulin-Giet, A.; Bonduelle, O.; Duffy, D.; Shattock, R.J.; Verrier, B.; Combadière, B. Targeting of HIV-p24 particle-based vaccine into differential skin layers induces distinct arms of the immune responses. *Vaccine* **2011**, *29*, 6379–6391. [[CrossRef](#)]
214. Ewer, K.J.; Barrett, J.R.; Belij-Rammerstorfer, S.; Sharpe, H.; Makinson, R.; Morter, R.; Flaxman, A.; Wright, D.; Bellamy, D.; Bittaye, M.; et al. T cell and antibody responses induced by a single dose of ChAdOx1 nCoV-19 (AZD1222) vaccine in a phase 1/2 clinical trial. *Nat. Med.* **2021**, *27*, 270–278. [[CrossRef](#)]
215. Sahin, U.; Muik, A.; Derhovanessian, E.; Vogler, I.; Kranz, L.M.; Vormehr, M.; Baum, A.; Pascal, K.; Quandt, J.; Maurus, D.; et al. COVID-19 vaccine BNT162b1 elicits human antibody and T(H)1 T cell responses. *Nature* **2020**, *586*, 594–599. [[CrossRef](#)]

216. McMahan, K.; Yu, J.; Mercado, N.B.; Loos, C.; Tostanoski, L.H.; Chandrashekhar, A.; Liu, J.; Peter, L.; Atyeo, C.; Zhu, A.; et al. Correlates of protection against SARS-CoV-2 in rhesus macaques. *Nature* **2021**, *590*, 630–634. [[CrossRef](#)]
217. Arrode-Brusés, G.; Moussa, M.; Baccard-Longere, M.; Villinger, F.; Chebloune, Y. Long-term central and effector HIV-specific memory T cell responses elicited after a single immunization with a novel lentivector DNA vaccine. *PLoS ONE* **2014**, *9*, e110883. [[CrossRef](#)]
218. Hansen, S.G.; Zak, D.E.; Xu, G.; Ford, J.C.; Marshall, E.E.; Malouli, D.; Gilbride, R.M.; Hughes, C.M.; Ventura, A.B.; Ainslie, E.; et al. Prevention of tuberculosis in rhesus macaques by a cytomegalovirus-based vaccine. *Nat. Med.* **2018**, *24*, 130–143. [[CrossRef](#)]
219. Elhmouzi-Younes, J.; Palgen, J.L.; Tchitchek, N.; Delandre, S.; Namet, I.; Bodinham, C.L.; Pizzoferro, K.; Lewis, D.J.M.; Le Grand, R.; Cosma, A.; et al. In depth comparative phenotyping of blood innate myeloid leukocytes from healthy humans and macaques using mass cytometry. *Cytom. A* **2017**, *91*, 969–982. [[CrossRef](#)]
220. Mentzer, A.J.; O’Connor, D.; Pollard, A.J.; Hill, A.V. Searching for the human genetic factors standing in the way of universally effective vaccines. *Philos. Trans. R Soc. Lond. B Biol. Sci.* **2015**, *370*. [[CrossRef](#)]
221. Weinberg, A.; Pang, L.; Johnson, M.J.; Caldas, Y.; Cho, A.; Tovar-Salazar, A.; Canniff, J.; Schmader, K.E.; Popmihajlov, Z.; Levin, M.J. The Effect of Age on the Immunogenicity of the Live Attenuated Zoster Vaccine Is Predicted by Baseline Regulatory T Cells and Varicella-Zoster Virus-Specific T Cell Immunity. *J. Virol.* **2019**, *93*, e00305-19. [[CrossRef](#)] [[PubMed](#)]
222. van der Heiden, M.; Berbers, G.A.M.; Fuentes, S.; van Zelm, M.C.; Boots, A.M.H.; Buisman, A.M. An Explorative Biomarker Study for Vaccine Responsiveness after a Primary Meningococcal Vaccination in Middle-Aged Adults. *Front. Immunol.* **2017**, *8*, 1962. [[CrossRef](#)]
223. Alcorn, J.F.; Avula, R.; Chakka, A.B.; Schwarzmann, W.E.; Nowalk, M.P.; Lin, C.J.; Ortiz, M.A.; Horne, W.T.; Chandran, U.R.; Nagg, J.P.; et al. Differential gene expression in peripheral blood mononuclear cells from children immunized with inactivated influenza vaccine. *Hum. Vaccine Immunother.* **2020**, *16*, 1782–1790. [[CrossRef](#)]
224. Idoko, O.T.; Smolen, K.K.; Wariri, O.; Imam, A.; Shannon, C.P.; Dibassey, T.; Diray-Arce, J.; Darboe, A.; Strandmark, J.; Ben-Othman, R.; et al. Clinical Protocol for a Longitudinal Cohort Study Employing Systems Biology to Identify Markers of Vaccine Immunogenicity in Newborn Infants in The Gambia and Papua New Guinea. *Front. Pediatr.* **2020**, *8*, 197. [[CrossRef](#)]
225. Merino, K.M.; Slisarenko, N.; Taylor, J.M.; Falkenstein, K.P.; Gilbert, M.H.; Bohm, R.P.; Blanchard, J.L.; Ardeshir, A.; Didier, E.S.; Kim, W.K.; et al. Clinical and Immunological Metrics During Pediatric Rhesus Macaque Development. *Front. Pediatr.* **2020**, *8*, 388. [[CrossRef](#)]
226. Terao, K. Essentials for starting a pediatric clinical study (3): Dynamic changes in early development of immune system in macaque monkeys—the significance from standpoint of preclinical toxicity test using nonhuman primates. *J. Toxicol. Sci.* **2009**, *34* (Suppl. 2), SP321–SP325. [[CrossRef](#)]
227. Shen, C.; Xu, H.; Liu, D.; Veazey, R.S.; Wang, X. Development of serum antibodies during early infancy in rhesus macaques: Implications for humoral immune responses to vaccination at birth. *Vaccine* **2014**, *32*, 5337–5342. [[CrossRef](#)]
228. Levast, B.; Schulz, S.; Hurk, S.; Gerdts, V. Animal models for neonatal diseases in humans. *Vaccine* **2013**, *31*, 2489–2499. [[CrossRef](#)] [[PubMed](#)]
229. Ramos, L.; Lunney, J.K.; Gonzalez-Juarrero, M. Neonatal and infant immunity for tuberculosis vaccine development: Importance of age-matched animal models. *Dis. Model. Mech.* **2020**, *13*, dmm045740. [[CrossRef](#)]
230. Rosario, M.; Fulkerson, J.; Soneji, S.; Parker, J.; Im, E.J.; Borthwick, N.; Bridgeman, A.; Bourne, C.; Joseph, J.; Sadoff, J.C.; et al. Safety and immunogenicity of novel recombinant BCG and modified vaccinia virus Ankara vaccines in neonate rhesus macaques. *J. Virol.* **2010**, *84*, 7815–7821. [[CrossRef](#)] [[PubMed](#)]
231. Kesarwani, A.; Sahu, P.; Jain, K.; Sinha, P.; Mohan, K.V.; Nagpal, P.S.; Singh, S.; Zaidi, R.; Nagarajan, P.; Upadhyay, P. The safety and efficacy of BCG encapsulated alginate particle (BEAP) against M.tb H37Rv infection in Macaca mulatta: A pilot study. *Sci. Rep.* **2021**, *11*, 3049. [[CrossRef](#)] [[PubMed](#)]
232. Abel, K. The rhesus macaque pediatric SIV infection model—A valuable tool in understanding infant HIV-1 pathogenesis and for designing pediatric HIV-1 prevention strategies. *Curr. HIV Res.* **2009**, *7*, 2–11. [[CrossRef](#)] [[PubMed](#)]
233. Curtis, A.D., 2nd; Dennis, M.; Eudailey, J.; Walter, K.L.; Cronin, K.; Alam, S.M.; Choudhary, N.; Tuck, R.H.; Hudgens, M.; Kozlowski, P.A.; et al. HIV Env-Specific IgG Antibodies Induced by Vaccination of Neonatal Rhesus Macaques Persist and Can Be Augmented by a Late Booster Immunization in Infancy. *mSphere* **2020**, *5*, e00162-20. [[CrossRef](#)] [[PubMed](#)]
234. Bricker, K.M.; Obregon-Perko, V.; Uddin, F.; Williams, B.; Uffman, E.A.; Garrido, C.; Fouada, G.G.; Geleziunas, R.; Robb, M.; Michael, N.; et al. Therapeutic vaccination of SIV-infected, ART-treated infant rhesus macaques using Ad48/MVA in combination with TLR-7 stimulation. *PLoS Pathog.* **2020**, *16*, e1008954. [[CrossRef](#)] [[PubMed](#)]
235. Han, Q.; Bradley, T.; Williams, W.B.; Cain, D.W.; Montefiori, D.C.; Saunders, K.O.; Parks, R.J.; Edwards, R.W.; Ferrari, G.; Mueller, O.; et al. Neonatal Rhesus Macaques Have Distinct Immune Cell Transcriptional Profiles following HIV Envelope Immunization. *Cell Rep.* **2020**, *30*, 1553–1569.e1556. [[CrossRef](#)] [[PubMed](#)]
236. Chapman, S.J.; Hill, A.V. Human genetic susceptibility to infectious disease. *Nat. Rev. Genet.* **2012**, *13*, 175–188. [[CrossRef](#)] [[PubMed](#)]
237. Noll, K.E.; Ferris, M.T.; Heise, M.T. The Collaborative Cross: A Systems Genetics Resource for Studying Host-Pathogen Interactions. *Cell Host Microbe* **2019**, *25*, 484–498. [[CrossRef](#)]

238. Olafsdottir, T.A.; Lindqvist, M.; Nookae, I.; Andersen, P.; Maertzdorf, J.; Persson, J.; Christensen, D.; Zhang, Y.; Anderson, J.; Khoomrung, S.; et al. Comparative Systems Analyses Reveal Molecular Signatures of Clinically tested Vaccine Adjuvants. *Sci. Rep.* **2016**, *6*, 39097. [[CrossRef](#)]
239. Kasturi, S.P.; Kozlowski, P.A.; Nakaya, H.I.; Burger, M.C.; Russo, P.; Pham, M.; Kovalenkov, Y.; Silveira, E.L.V.; Havenar-Daughton, C.; Burton, S.L.; et al. Adjuvanting a Simian Immunodeficiency Virus Vaccine with Toll-Like Receptor Ligands Encapsulated in Nanoparticles Induces Persistent Antibody Responses and Enhanced Protection in TRIM5 α Restrictive Macaques. *J. Virol.* **2017**, *91*, e01844-16. [[CrossRef](#)]
240. Thompson, E.A.; Ols, S.; Miura, K.; Rausch, K.; Narum, D.L.; Spångberg, M.; Juraska, M.; Wille-Reece, U.; Weiner, A.; Howard, R.F.; et al. TLR-adjuvanted nanoparticle vaccines differentially influence the quality and longevity of responses to malaria antigen Pf525. *JCI Insight* **2018**, *3*, e120692. [[CrossRef](#)]
241. Ciabattini, A.; Pettini, E.; Fiorino, F.; Lucchesi, S.; Pastore, G.; Brunetti, J.; Santoro, F.; Andersen, P.; Bracci, L.; Pozzi, G.; et al. Heterologous Prime-Boost Combinations Highlight the Crucial Role of Adjuvant in Priming the Immune System. *Front. Immunol.* **2018**, *9*, 380. [[CrossRef](#)]
242. Elsner, R.A.; Shlomchik, M.J. Germinal Center and Extrafollicular B Cell Responses in Vaccination, Immunity, and Autoimmunity. *Immunity* **2020**, *53*, 1136–1150. [[CrossRef](#)] [[PubMed](#)]
243. Luo, W.; Yin, Q. B Cell Response to Vaccination. *Immunol. Investig.* **2021**, *1*–22. [[CrossRef](#)]
244. Ben-Othman, R.; Cai, B.; Liu, A.C.; Varankovich, N.; He, D.; Blimkie, T.M.; Lee, A.H.; Gill, E.E.; Novotny, M.; Aevermann, B.; et al. Systems Biology Methods Applied to Blood and Tissue for a Comprehensive Analysis of Immune Response to Hepatitis B Vaccine in Adults. *Front. Immunol.* **2020**, *11*, 580373. [[CrossRef](#)]
245. Eslamizar, L.; Petrovas, C.; Leggat, D.J.; Furr, K.; Lifton, M.L.; Levine, G.; Ma, S.; Fletez-Brant, C.; Hoyland, W.; Prabhakaran, M.; et al. Recombinant MVA-prime elicits neutralizing antibody responses by inducing antigen-specific B cells in the germinal center. *NPJ Vaccines* **2021**, *6*, 15. [[CrossRef](#)] [[PubMed](#)]
246. de Bree, L.C.J.; Koeken, V.; Joosten, L.A.B.; Aaby, P.; Benn, C.S.; van Crevel, R.; Netea, M.G. Non-specific effects of vaccines: Current evidence and potential implications. *Semin. Immunol.* **2018**, *39*, 35–43. [[CrossRef](#)] [[PubMed](#)]
247. Netea, M.G.; Joosten, L.A.; Latz, E.; Mills, K.H.; Natoli, G.; Stunnenberg, H.G.; O'Neill, L.A.; Xavier, R.J. Trained immunity: A program of innate immune memory in health and disease. *Science* **2016**, *352*, aaf1098. [[CrossRef](#)] [[PubMed](#)]
248. Covian, C.; Fernández-Fierro, A.; Retamal-Díaz, A.; Díaz, F.E.; Vasquez, A.E.; Lay, M.K.; Riedel, C.A.; González, P.A.; Bueno, S.M.; Kalergis, A.M. BCG-Induced Cross-Protection and Development of Trained Immunity: Implication for Vaccine Design. *Front. Immunol.* **2019**, *10*, 2806. [[CrossRef](#)]
249. O'Neill, L.A.J.; Netea, M.G. BCG-induced trained immunity: Can it offer protection against COVID-19? *Nat. Rev. Immunol.* **2020**, *20*, 335–337. [[CrossRef](#)]
250. Palgen, J.L.; Feraoun, Y.; Dzangué-Tchoupou, G.; Joly, C.; Martinon, F.; Le Grand, R.; Beignon, A.S. Optimize Prime/Boost Vaccine Strategies: Trained Immunity as a New Player in the Game. *Front. Immunol.* **2021**, *12*, 612747. [[CrossRef](#)]
251. Sarkar, S.; Heise, M.T. Mouse Models as Resources for Studying Infectious Diseases. *Clinthera* **2019**, *41*, 1912–1922. [[CrossRef](#)]
252. Ermann, J.; Glimcher, L.H. After GWAS: Mice to the rescue? *Curr. Opin Immunol.* **2012**, *24*, 564–570. [[CrossRef](#)]
253. Ravindran, R.; Khan, N.; Nakaya, H.I.; Li, S.; Loebbermann, J.; Maddur, M.S.; Park, Y.; Jones, D.P.; Chappert, P.; Davoust, J.; et al. Vaccine activation of the nutrient sensor GCN2 in dendritic cells enhances antigen presentation. *Science* **2014**, *343*, 313–317. [[CrossRef](#)]
254. Ng'uni, T.; Chasara, C.; Ndhlovu, Z.M. Major Scientific Hurdles in HIV Vaccine Development: Historical Perspective and Future Directions. *Front. Immunol.* **2020**, *11*, 590780. [[CrossRef](#)] [[PubMed](#)]
255. Wang, D.; Eraslan, B.; Wieland, T.; Hallström, B.; Hopf, T.; Zolg, D.P.; Zecha, J.; Asplund, A.; Li, L.H.; Meng, C.; et al. A deep proteome and transcriptome abundance atlas of 29 healthy human tissues. *Mol. Syst. Biol.* **2019**, *15*, e8503. [[CrossRef](#)]
256. Maecker, H.T.; McCoy, J.P.; Nussenblatt, R. Standardizing immunophenotyping for the Human Immunology Project. *Nat. Rev. Immunol.* **2012**, *12*, 191–200. [[CrossRef](#)] [[PubMed](#)]
257. Saeys, Y.; Van Gassen, S.; Lambrecht, B.N. Computational flow cytometry: Helping to make sense of high-dimensional immunology data. *Nat. Rev. Immunol.* **2016**, *16*, 449–462. [[CrossRef](#)]
258. Fruhwirth, G.O.; Kneilling, M.; de Vries, I.J.M.; Weigelin, B.; Srinivas, M.; Aarntzen, E. The Potential of In Vivo Imaging for Optimization of Molecular and Cellular Anti-cancer Immunotherapies. *Mol. Imaging Biol.* **2018**, *20*, 696–704. [[CrossRef](#)] [[PubMed](#)]
259. Torcellan, T.; Stolp, J.; Chtanova, T. In Vivo Imaging Sheds Light on Immune Cell Migration and Function in Cancer. *Front. Immunol.* **2017**, *8*, 309. [[CrossRef](#)] [[PubMed](#)]

Titre : Etudes des mécanismes associés à la qualité et la durabilité de la réponse vaccinale

Mots clés : Lymphocyte T, immunité innée, vaccin, mémoire, vaccinologie des systèmes, primate non-humain,

Résumé : Les vaccins représentent les produits de santé les plus efficaces dans la lutte contre les maladies infectieuses. Toutefois, certains pathogènes tel que le VIH, le paludisme ou la tuberculose, de même que les pathogènes émergents échappent encore à la vaccination. Le manque de connaissances des mécanismes déterminants une réponse vaccinale efficace sont à l'origine de nombreux échecs de développement de candidats vaccins. Dans cette thèse nous essayons de caractériser les réponses vaccinales précoces innée et adaptative, afin d'identifier leur implication dans la qualité et la persistance de la réponse anticorps. Nous avons employé deux modèles vaccinaux: un vaccin VIH administré selon différentes modalités et la fièvre jaune (YF), avec le vaccin commercial Stamaril et un vaccin inactivé. Nous avons caractérisé la réponse innée précoce induite par les vaccins VIH et identifié

des signatures cellulaires caractéristiques. Ces signatures ont par la suite été utilisé dans un modèle prédictif de la qualité de la réponse anticorps induite par les vaccins. A l'aide des vaccins YF nous avons pu mettre en évidence la capacité du Stamaril à induire une réponse neutralisante persistante comparé au vaccin inactivé. De plus, une forte mobilisation de lymphocytes T CD8+ et de cellules NK pour le Stamaril ainsi qu'une meilleure capacité des T CD4 du vaccin inactivé à répondre à une stimulation *in vitro* ont été observé. Cette étude a également pu identifier les lymphocytes T régulateurs et folliculaires comme étant des biomarqueurs potentiel de la persistance de la réponse neutralisante. Ces études mettent en évidence l'intérêt des modèles prédictifs dans l'accélération du développement de vaccins.

Title : Study of mechanisms associated with the quality and durability of vaccine immune responses

Keywords : T lymphocytes, innate immunity, vaccine, memory, system vaccinology, non-human primate

Abstract: Vaccines represent the most effective drugs to fight infectious diseases. However, emergent pathogens, HIV, malaria, and tuberculosis still evade vaccine immunity. Lack of knowledge on immune mechanisms driving the induction of an effective vaccine response are the source of numerous vaccine development failures. In this thesis, we characterized early innate and adaptive immune responses to specific vaccines, and identified their involvement in vaccine antibody response quality and persistence. Two vaccine models were employed: an HIV vaccine administered with different modalities, and the Yellow fever (YF) vaccine model with the commercial vaccine (Stamaril) and an inactivated vaccine.

We characterized early innate immune responses and identified cell signatures of HIV vaccines. These signatures were then include in a predictive model of the quality of the antibody response. With YF vaccines, we evidenced a higher ability of Stamaril to induce persistent neutralizing antibody response compare to the inactivated vaccine. Furthermore, a strong mobilization of NK and CD8 T cells was observed as well as greater ability of inactivated vaccine CD4+ T cells to respond to *in vitro* stimulation. This study also allowed the identification of regulatory T cells and follicular helper T cells as potential biomarkers of neutralizing antibody persistence. These studies demonstrate the usefulness of predictive models to improve vaccine design.